SYNTHESIS OF THERMALLY STABLE POLYUREAS AND POLY(UREA-IMIDE)S CONTAINING SCHIFF BASE METAL COMPLEXES

Miss Duangruthai Sridaeng

A Dissertation Submitted in Partial Fulfillment of the Requirements
for the Degree of Doctor of Philosophy Program in Petrochemistry
Faculty of Science
Chulalongkorn University
Academic Year 2008

การสังเคราะห์พอลิยูเรียและพอลิยูเรีย-อิมีดทนความร้อนที่มีสารประกอบโลหะเชิงซ้อนชิฟเบส

นางสาวดวงฤทัย ศรีแดง

วิทยานิพนธ์นี้เป็นส่วนหนึ่งของการศึกษาตามหลักสูตรปริญญาวิทยาศาสตรดุษฎีบัณฑิต
สาขาวิชาปิโตรเคมี
คณะวิทยาศาสตร์ จุฬาลงกรณ์มหาวิทยาลัย
ปีการศึกษา 2551

Thesis Title	SYNTHESIS OF THERMALLY STABLE POLYUREAS AND POLY(UREA-IMIDE)S CONTAINING SCHIFF BASE METAL COMPLEXES
By	Miss Duangruthai Sridaeng
Field of Study	Petrochemistry
Advisor	Associate Professor Nuanphun Chantarasiri, Ph.D.

Accepted by the Faculty of Science, Chulalongkorn University in Partial Fulfillment of the Requirements for the Doctor's Degree

…………………………………………Dean of the Faculty of Science
(Professor Supot Hannongbua, Dr.rer.nat)

THESIS COMMITTEE

………………………………………... Chairman
(Associate Professor Supawan Tantayanon, Ph.D.)

…………………………………….….…. Advisor
(Associate Professor Nuanphun Chantarasiri, Ph.D.)

………………………………...……… Examiner
(Assistant Professor Warinthorn Chavasiri, Ph.D.)

………………………………...……… Examiner
(Associate Professor Polkit Sangvanich, Ph.D.)

………………………………………... External Examiner
(Associate Professor Pranee Phinyocheep, Ph.D.)

ดวงฤทัย ศรีแดง : การสังเคราะห์พอลิยูเรียและพอลิยูเรีย-อิมีดทนความร้อนที่มีสารประกอบโลหะเชิงซ้อนชิฟเบส. (SYNTHESIS OF THERMALLY STABLE POLYUREAS AND POLY(UREA-IMIDE)S CONTAINING SCHIFF BASE METAL COMPLEXES) อ.ที่ปรึกษาวิทยานิพนธ์หลัก : รศ. ดร.นวลพรรณ จันทรศิริ, 177 หน้า.

งานวิจัยนี้ได้สังเคราะห์สารประกอบเฮกซะเดนเทตชิฟเบสของโลหะสังกะสีและโลหะนิกเกิลเพื่อใช้ในการสังเคราะห์พอลิเมอร์ที่มีโลหะอยู่ในโครงสร้าง พอลิยูเรียสังเคราะห์ได้จากปฏิกิริยาระหว่างเอ็มแนพไทรเอนกับไดไอโซไซยาเนตได้แก่ 4-4´-ไดเฟนิลมีเทนไดไอโซไซยาเนต (MDI) และไอโซเฟอโรนไดไอโซไซยาเนต (IPDI) โคพอลิยูเรียและพอลิยูรีเทน-ยูเรียสังเคราะห์จากเอ็มแนพไทรเอน/ไดไอโซไซยาเนต/ไดแอมีน และเอ็มแนพไทรเอน/ไดไอโซไซยาเนต/ไดแอลกอฮอล์ตามลำดับ โดยไดแอมีนที่ใช้คือ เมทาไซลิลีนไดแอมีน (*m*-XDA) และเฮกซะเมทิลีนไดแอมีน (HMDA) และไดแอลกอฮอล์ที่ใช้ได้แก่ 2,2-บิส4-ไฮดรอกซีเฟนิลโพรเพน (BPO) และ 1,6-เฮกซะเมทิลีนไดออล (HDO) พอลิยูเรียอิมีดสังเคราะห์ได้จากไอโซไซยาเนตเทอร์มิเนตเทตพอลิยูเรียพรีพอลิเมอร์ที่มีโลหะอยู่ในโครงสร้างซึ่งเตรียมมาจากปฏิริยาระหว่างเอ็มแนพไทรเอนและไดไอโซไซยาเนตปริมาณมากเกินพอซึ่งจะสามารถทำปฏิกิริยาต่อได้กับไดแอนไฮไดรด์ ซึ่งได้แก่ไพโรเมลิติกไดแอนไฮไดรด์ (PMDA) และ เบนโซฟีโนน 3,3´-4,4´-เททระคาร์บอกซิลิกไดแอนไฮไดรด์ (BTDA) จากนั้นพิสูจน์เอกลักษณ์ของพอลิเมอร์ที่มีโลหะในโครงสร้างโดยใช้เทคนิคอินฟราเรดสเปกโทรสโกปี โปรตอนเอ็นเอ็มอาร์สเปกโทรสโกปี วิเคราะห์ธาตุองค์ประกอบ เอกซเรย์ดิฟแฟรกชัน สมบัติการละลาย และความหนืด ศึกษาสมบัติทางความร้อนของพอลิเมอร์โดยใช้เทคนิคดิฟเฟอเรนเชียลสแกนนิงแคลอรีเมทรี และเทอร์โมกราวิเมท ริกอนาลิซิส จากการศึกษาพบว่าพอลิเมอร์ที่มีโลหะในโครงสร้างมีสมบัติทนต่อความร้อนได้ดีและมีการละลายที่ดี

สาขาวิชา ปิโตรเคมี ลายมือชื่อนิสิต

ปีการศึกษา 2551 ลายมือชื่ออ.ที่ปรึกษาวิทยานิพนธ์หลัก

4773812023 : MAJOR PETROCHEMISTRY
KEYWORDS : METAL-CONTAININNG POLYUREAS / METAL-CONTAININNG POLY(UREA-IMIDE)S

DUANGRUTHAI SRIDAENG : SYNTHESIS OF THERMALLY STABLE POLYUREAS AND POLY(UREA-IMIDE)S CONTAINING SCHIFF BASE METAL COMPLEXES. ADVISOR : ASSOC.PROF.NUANPHUN CHANTARASIRI,Ph.D. 177 pp.

Hexadentate Schiff base zinc and nickel complexes were synthesized and used for the synthesis of metal-containing polymers. Polyureas were synthesized by reacting $MNapth_2trien$ with diisocyanates, namely 4,4'-diphenylmethane diisocyanate (MDI) and isophorone diisocyanate (IPDI). Copolyureas and poly(urethane-urea)s were synthesized from $MNapth_2trien$/diisocyanates/diamines and $MNapth_2trien$/diisocyanates/dialcohols, respectively. The diamines and dialcohols employed were *m*-xylylenediamine, (*m*-XDA) and 1,6-hexamethylenediamine (HMDA), 2,2-bis(4-Hydroxyphenyl)propane (BPO) and 1,6-hexamethylenediol (HDO). Poly(urea-imide)s were obtained by synthesis of metal-containing isocyanate-terminated polyurea prepolymers from the reaction between $MNapth_2trien$ and excess diisocyanates, which could then undergo further reaction with different dianhydrides. The dianhydrides employed were pyromellitic dianhydride (PMDA) and benzophenone-3,3´,4,4´-tetracarboxylic dianhydride (BTDA). Metal-containing polymers were characterized by infrared spectroscopy (IR), proton nuclear magnetic resonance spectroscopy (^1H NMR), elemental analysis, X-ray diffraction (XRD), solubility and viscosity. Thermal properties of the polymers were investigated by differential scanning calorimetry (DSC), dynamic mechanical thermal analysis (DMTA) and thermogravimetric analysis (TGA). It was found that the metal-containing polymers showed good thermal stability and solubility.

Field of Study : Petrochemistry Student's Signature ....
Academic Year : 2008 Advisor's Signature ....

LIST OF SYMBOLS AND ABBREVIATIONS

BPO	2,2-Bis(4-Hydroxyphenyl)propane
BTDA	Benzophenone-3,3′,4,4′-tetracarboxylic dianhydride
DBTDL	Dibutyltin dilaurate
DMF	Dimethyl formamide
DMSO	Dimethyl sulphoxide
DMTA	Dynamic mechanical analysis
DSC	Differential scanning calorimetry
HDI	Hexamethylene diisocyanate
HDO	1,6-hexamethylenediol
HMDA	Hexamethylenediamine
HBHMPU	Hexamethylene bis[*N′*-(1-hydroxy-2-methyl-prop-2-yl)urea]
IDT	Initial decomposition temperature
IPDI	Isophorone diisocyanate
IPDI-BPO	IPDI and BPO
IPDI-BTDA	Polymer synthesized from IPDI and BTDA
IPDI-HDO	Polymer synthesized from IPDI and HDO
IPDI-HMDA	Polymer synthesized from IPDI and HMDA
IPDI-*m*-XDA	Polymer synthesized from IPDI and *m*-XDA
IPDI-PMDA	Polymer synthesized from IPDI and PMDA
KBr	Potassium bromide
MDI	4,4′-diphenylmethane diisocyanate
MDI-BPO	Polymer synthesized from MDI and BPO
MDI-BTDA	Polymer synthesized from MDI and BTDA
MDI-HDO	Polymer synthesized from MDI and HDO
MDI-HMDA	Polymer synthesized from MDI and HMDA
MDI-*m*-XDA	Polymer synthesized from MDI and *m*-XDA
MDI-PMDA	Polymer synthesized from MDI and PMDA
$M(HEEP)_2$	Mono (hydroxyethoxyethyl)phthalate
$M(HPP)_2$	mono(hydroxypentyl)phthalate
$MnNapth_2trien$	hexadentate Shiff base metal complexes

m-XDA	*m*-Xylylenediamine
M(HBH)$_2$,	Mono(hydroxybutyl)hexolate
NiNapth$_2$trien	hexadentate Shiff base zinc complexes
NiNapth$_2$trien-IPDI	Polymer synthesized from NiNapth$_2$trien and IPDI
NiNapth$_2$trien-IPDI-BPO	Polymer synthesized from NiNapth$_2$trien, IPDI and BPO
NiNapth$_2$trien-IPDI-BTDA	Polymer synthesized from NiNapth$_2$trien, IPDI and BTDA
NiNapth$_2$trien-IPDI-HDO	Polymer synthesized from NiNapth$_2$trien, IPDI and HDO
NiNapth$_2$trien-IPDI-HMDA	Polymer synthesized from NiNapth$_2$trien, IPDI and HMDA
NiNapth$_2$trien-IPDI-*m*-XDA	Polymer synthesized from NiNapth$_2$trien, IPDI and *m*-XDA
NiNapth$_2$trien-IPDI/PEG400-BTDA	Polymer synthesized from NiNapth$_2$trien, IPDI, PEG400 and BTDA
NiNapth$_2$trien-IPDI/PEG400-PMDA	Polymer synthesized from NiNapth$_2$trien, IPDI, PEG400 and PMDA
NiNapth$_2$trien-IPDI-PMDA	Polymer synthesized from NiNapth$_2$trien, IPDI and PMDA
NiNapth$_2$trien-MDI	Polymer synthesized from NiNapth$_2$trien and MDI
NiNapth$_2$trien-MDI-BPO	Polymer synthesized from NiNapth$_2$trien, MDI and BPO
NiNapth$_2$trien-MDI-BTDA	Polymer synthesized from NiNapth$_2$trien, MDI and BTDA
NiNapth$_2$trien-MDI-HDO	Polymer synthesized from NiNapth$_2$trien, MDI and HDO
NiNapth$_2$trien-MDI-HMDA	Polymer synthesized from NiNapth$_2$trien, MDI and HMDA
NiNapth$_2$trien-MDI-*m*-XDA	Polymer synthesized from NiNapth$_2$trien, MDI and *m*-XDA

NiNapth$_2$trien-MDI/PEG400-BTDA	Polymer synthesized from NiNapth$_2$trien, MDI, PEG400 and BTDA
NiNapth$_2$trien-MDI/PEG400-PMDA	Polymer synthesized from NiNapth$_2$trien, MDI, PEG400 and PMDA
NiNapth$_2$trien-MDI-PMDA	Polymer synthesized from NiNapth$_2$trien, MDI and PMDA
NMP	*N*-methyl-2-pyrrolidinone
PCL	polycaprolactone diol
PEG	polyethylene glycol (MW 400)
PMDA	Pyromellitic dianhydride
PTMO	polytetramethylene oxide
TBHMPU	toluene 2,4-bis[N'-(1-hydroxy-2-methyl-prop-2-yl)urea]
T_g	Glass transition temperature
TGA	Thermogravimetric analysis
XRD	X-ray diffraction
ZnNapth$_2$trien	Hexadentate Shiff base zinc complexes
ZnNapth$_2$trien-IPDI	Polymer synthesized from ZnNapth$_2$trien and IPDI
ZnNapth$_2$trien-IPDI-BPO	Polymer synthesized from ZnNapth$_2$trien, IPDI and BPO
ZnNapth$_2$trien-IPDI-BTDA	Polymer synthesized from ZnNapth$_2$trien, IPDI and BTDA
ZnNapth$_2$trien-IPDI-HDO	Polymer synthesized from ZnNapth$_2$trien, IPDI and HDO
ZnNapth$_2$trien-IPDI-HMDA	Polymer synthesized from ZnNapth$_2$trien, IPDI and HMDA
ZnNapth$_2$trien-IPDI-*m*-XDA	Polymer synthesized from ZnNapth$_2$trien, IPDI and *m*-XDA
ZnNapth$_2$trien-IPDI/PEG400-BTDA	Polymer synthesized from ZnNapth$_2$trien, IPDI, PEG400 and BTDA
ZnNapth$_2$trien-IPDI/PEG400-PMDA	Polymer synthesized from ZnNapth$_2$trien, IPDI, PEG400 and PMDA

$ZnNapth_2trien$-IPDI-PMDA	Polymer synthesized from $NiNapth_2trien$, IPDI and PMDA
$ZnNapth_2trien$-MDI	Polymer synthesized from $ZnNapth_2trien$ and MDI
$ZnNapth_2trien$-MDI-BPO	Polymer synthesized from $ZnNapth_2trien$, MDI and BPO
$ZnNapth_2trien$-MDI-BTDA	Polymer synthesized from $ZnNapth_2trien$, MDI and BTDA
$ZnNapth_2trien$-MDI-HDO	Polymer synthesized from $ZnNapth_2trien$, MDI and HDO
$ZnNapth_2trien$-MDI-HMDA	Polymer synthesized from $ZnNapth_2trien$, MDI and HMDA
$ZnNapth_2trien$-MDI-*m*-XDA	Polymer synthesized from $ZnNapth_2trien$, MDI and *m*-XDA
$ZnNapth_2trien$-MDI/PEG400-BTDA	Polymer synthesized from $ZnNapth_2trien$, MDI, PEG400 and BTDA
$ZnNapth_2trien$-MDI/PEG400-PMDA	Polymer synthesized from $ZnNapth_2trien$, MDI, PEG400 and PMDA
$ZnNapth_2trien$-MDI-PMDA	Polymer synthesized from $ZnNapth_2trien$, MDI and PMDA

CHAPTER I

INTRODUCTION

Polyureas are widely used to obtain a variety of products including industrial coating systems, elastomers, fibers, foams and adhesives. The improvement of thermal stability of the polymers is interesting in order to fulfill their applications. By the introduction of imide group, poly(urea-imide)s can be obtained and this type of polymer is thermally stable since polyimides are known as one of the materials for use in high-temperature applications. Introduction of urethane group into the polymer backbone is expected to improve the solubility of polymer without decreasing the thermal stability.

Generally, Polyureas and polyurethanes contain only covalent bonds in the polymer chain, and thus polyureas and polyurethanes having ionic bonds in the polymer backbone are less common. The other method that can improve the thermal property of polymer is the incorporation of metal complex into the polymer backbone. Metal-containing polymers are an important class of thermally stable or heat resistance polymers. The synthesis of metal-containing polymers has resulted in a tremendous variety because the polymers contain both organic and inorganic component, e.g. the flexibility of organic polymers coupled with the high thermal stability associated with inorganic species.

The aim of this work is to synthesize metal-containing polyureas, metal-containing copolyureas, metal-containing poly(urethane-urea)s and metal-containing poly(urea-imide)s in order to improve thermal stability of the polymers. Hexadentate Schiff base zinc and nickel complexes were synthesized and used for the synthesis of metal-containing polymers. Metal-containing polyureas were synthesized from the reaction between metal complexes and diisocyanates. Polymerization of metal complexes/diisocyanates/diamines, metal complexes/diisocyanates/dialcohols and metal complexes/diisocyanates/dianhydrides gave metal-containing copolyureas, poly(urethane-urea)s and poly(urea-imide)s, respectively. Different aliphatic and aromatic diamines, dialcohols and dianhydrides were employed to study the effect of structure on the polymer properties. Reference polymers without metal complexes were also synthesized for study the influence of metal on thermal property of the polymers. It was expected that the polymers would show good thermal stability together with good solubility in organic solvents and can be utilized in high temperature application.

CHAPTER II

THEORY AND LITERATURE REVIEW

Polyureas and their related polymers, polyurethane-ureas, are widely used to obtain a variety of products including fibers, elastomers, foams, coatings and adhesives. Poly(urethane-urea)s possess excellent mechanical and physical properties, high combustion resistance and high wear resistance. These polymers are widely applicable to a number of industrial products including elastomers, fibers, foams, adhesives, coatings and paints. The general structure of polyurea and polyurethane derived from diisocyanate and diamine or dialcohol can be presented as follows:

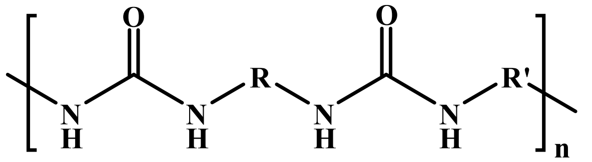

Polyurea

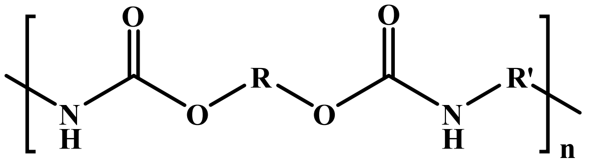

Polyurethane

Scheme 2.1 The general structure of polyurea and polyurethane

Copolymerization is used to modify the properties of polymer to specific needs, for example to reduce crystallinity, modify glass transition temperature or to improve solubility. Polyurethanes can also contain a urea linkage and these are formed when an isocyanate reacted with an amine resulting in a poly(urethane-urea)s. Polyurethane elastomers consist of elastomeric block copolymers containing alternating “hard” and “soft” segment. Poly(urethane-urea)s are a class of very important copolymers. It has both urea and urethane linkages in its backbone, which have wide range of applications.

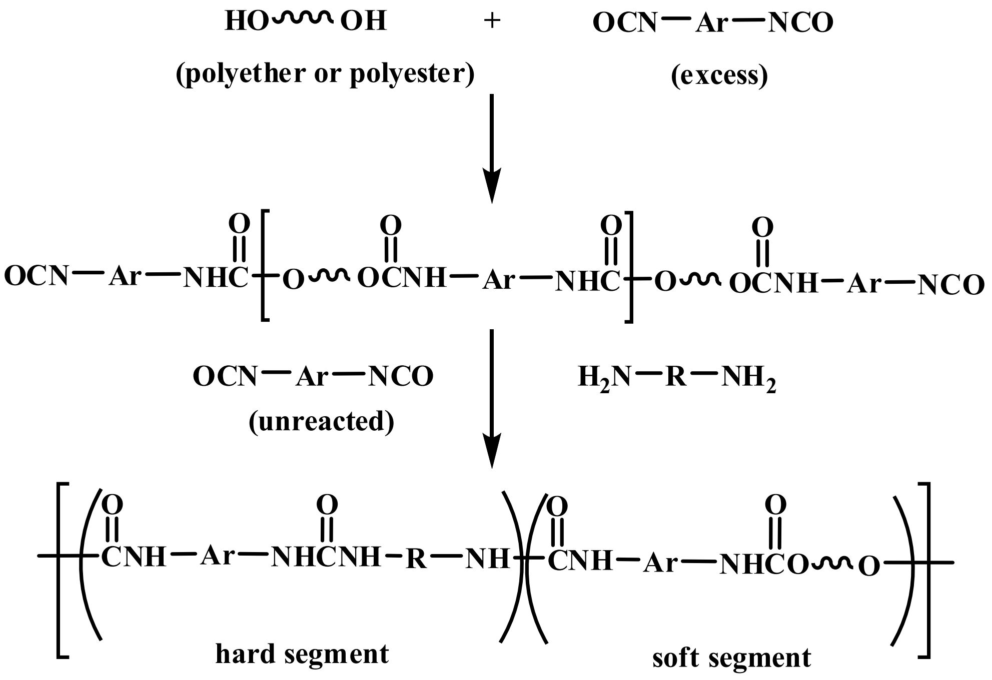

Scheme 2.2 Synthesis of an elastomeric polyurethane [1]

Schiff bases are widely used as ligands for synthesis of metal complexes. A large number of Schiff bases and their complexes have been studied because of their interesting properties and their good stability. Pentadentate and hexadentate complexes are obtained when polyamide are used in the synthesis of ligands. Metallo-polymers containing metal in the polymer chain have been investigated [2]. Aliphatic-aromatic poly(Schiff base)s containing 1,5-naphthyl or 1,4-phenyl was reported by Simionescu and coworker [3], these polymers showed starting weight loss higher than 369°C. The most common method for preparing imines is the reaction of amines with aldehydes or ketones (Scheme 2.3). This reaction was first discovered by Schiff [4] and imines are often called Schiff bases.

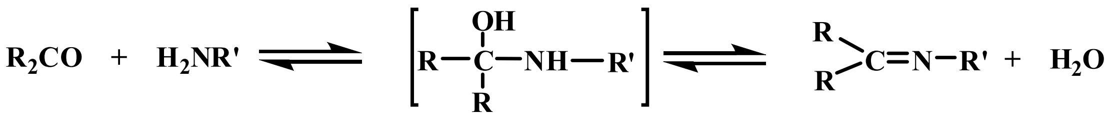

Scheme 2.3 Synthesis of imines

The incorporation of metal salts or metal complexes into the polymer backbone has led to wide applications [5-8] such as aqueous thickeners, coatings, textile seizers, adhesives, catalysts and additives. This is because the interaction between polymer with coordination group and metallic ions give them the numerous interesting properties such as the flexibility of organic polymers coupled with the high thermal stability associated with inorganic species.

The other way to improve thermal stability, fire retardancy, flexibility and solubility of polyurea and polyurethane is chemical modification in the polymer structure by introduction of functional groups which are thermally stable [9-10], for example, heterocyclic, aromatic groups [11-14] and imide groups. Aromatic heterocyclic polyimides are common for most commercial polyimides, such as Ultem from G.E. or Kapton from DuPont. These polymers have excellent mechanical and thermal properties. A modified method for the synthesis of poly(urea-imide)s was the reaction of isocyanate terminated polyurethane prepolymers with dianhydride to prepare polyurethane with imide group in the backbone.

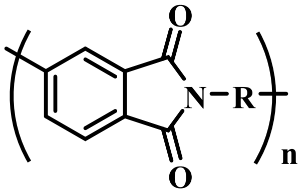

Scheme 2.4 Aromatic heterocyclic polyimide

Polyimides show excellent thermal stability with high temperature of thermal degradation. The reason for this type of behavior, in addition to the aromaticity in the chain structure, is due to a charge transfer complex in the polymer. For a charge transfer complex to exist there must be donor and acceptor electrons. The donor contains many electrons such as nitrogen atoms. The acceptor can pull electrons to it, the acceptors being the carbonyl groups (C=O) which draw the electron density from the nitrogen atoms. As seen in Scheme 2.5, there are parts of the polymer in which the carbonyl groups (C=O) draw electron density away from the acceptor units. The nitrogen atoms have high electron density than the carbonyl groups and lend it to the acceptor.

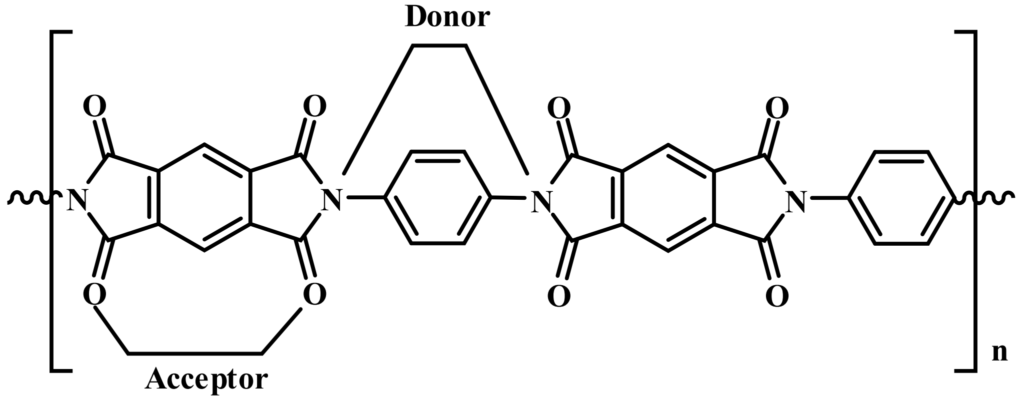

Scheme 2.5 Donor-Acceptor Charge Complex in a Polyimide

In addition to the donor-acceptor charge complex within the chain, it can also occur between adjacent units/chains (Scheme 2.6). The chains may stack together when the electron donors and acceptors interact. The stacking allows the carbonyls chemical units of the acceptor on one chain, to interact with the nitrogen atoms of the donor between the chains. Due to this interaction, the chains have less mobility in the whole material and this increases the strength of the polymer.

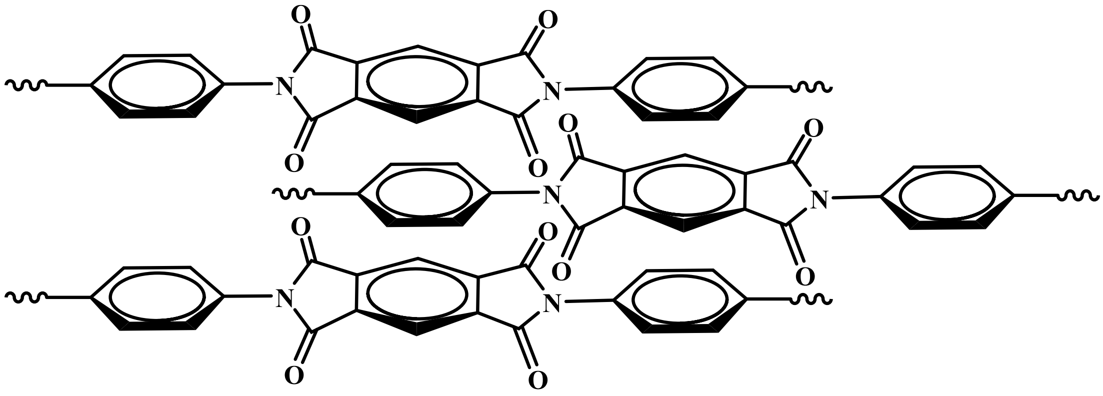

Scheme 2.6 Effect of charge complex between polymer chains

To improve the polymer properties for engineering applications such as high strength, solvent and chemical resistance, and especially high thermal stability, metal-containing polyureas, metal-containing polyurethanes [15], metal-containing poly(urethane-urea)s [16], poly(urethane-imide)s [17-22] and poly(urethane-urea-imide)s have been studied.

2.1 Literature review

The best method for polyurea synthesis [23] is to react diamines with diisocyanates. For example, Yuki and coworkers [24] prepared polyureas by the reaction of 2-anilino-4-aminoanilino-6-aminophenyl-l,3,5-triazines with diisocyanates (Scheme 2.7). These obtained polyureas have been demonstrated to possess high glass transition temperatures above 200°C and decomposition temperatures above 300°C with good solubility in organic solvents.

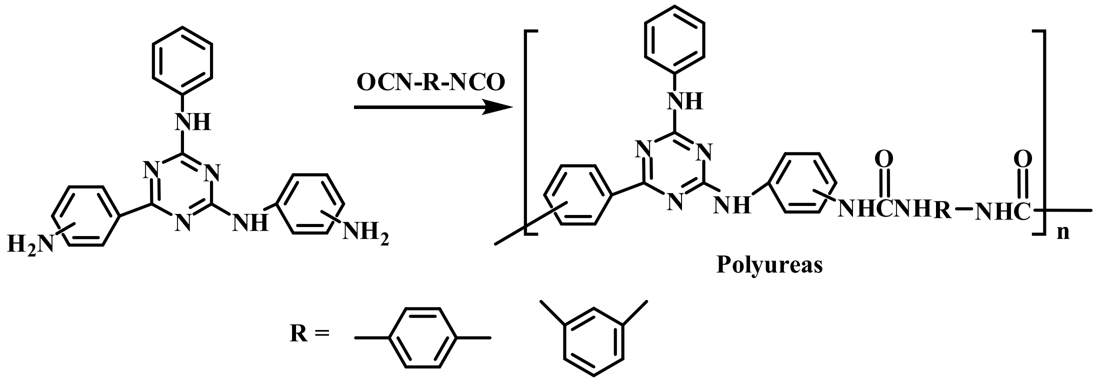

Scheme 2.7 Synthesis of polyureas from 2-anilino-4-aminoanilino-6-aminophenyl-l,3,5-triazines and diisocyanates.

Mallakpour and coworkers [25] prepared polyureas based on 4-(4′-aminophenyl)urazole and various diisocyanates (Scheme 2.8). All polymers showed 10% weight loss above 180°C.

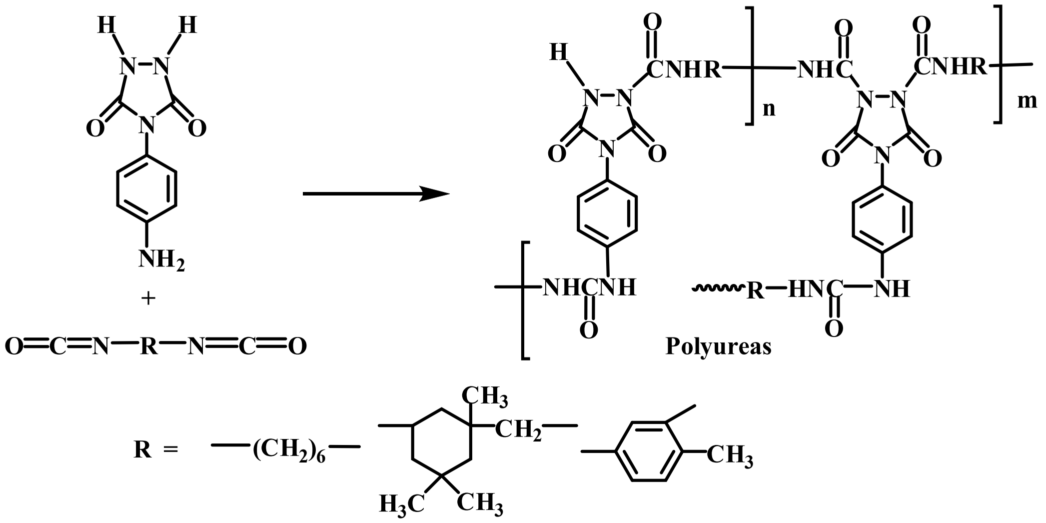

Scheme 2.8 Synthesis of polyureas based on 4-(4′-aminophenyl)urazole and various diisocyanates.

A number of research work concerning the preparation and physical properties of metal-containing polyureas, poly(urethane-urea)s and poly(urea-imide)s containing metal in the polymer backbone have been reported [26-28]. Modification of polymers by incorporating metal and functional groups are used extensively to improve various typically desired properties of materials, such as enhanced thermal stability, fire retardancy, flexibility and solubility. Wang and coworkers [29] prepared the polyureas from divalent metal salts of sulfanilic acid, 2,4-tolylene diisocyanate and 4,4′-diaminodiphenylmethane (Scheme 2.9). It was found that introduction of metal into the polyurea backbones increased their thermal stability.

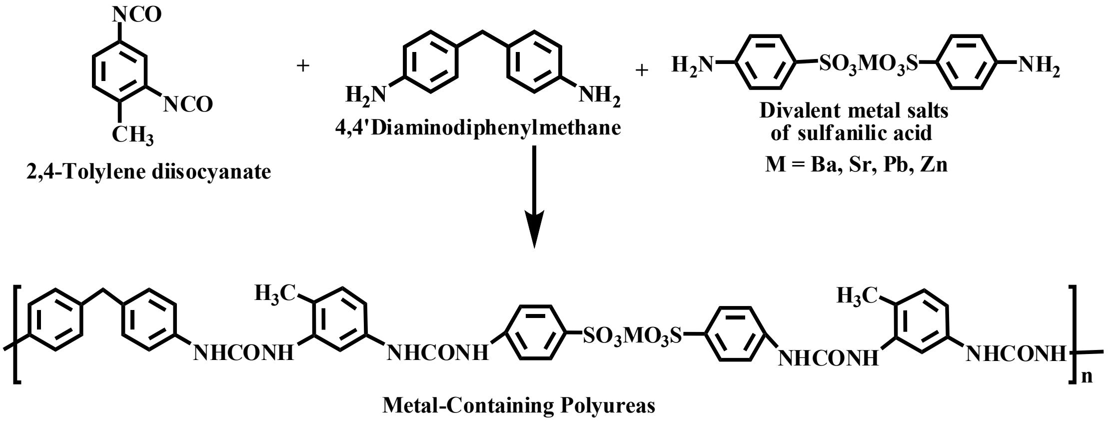

Scheme 2.9 Synthesis of metal-containing polyureas from divalent metal salts of sulfanilic acid, 2,4-tolylene diisocyanate and 4,4′-diaminodiphenylmethane.

Nanjundan and coworkers [30] synthesized metal-containing polyurethanes and poly(urethane-urea)s. Metal-containing polyurethanes were prepared by the solution polymerization of hexamethylene diisocyanate (HMDI) with the divalent metal salts of mono(hydroxybutyl)hexolate [$M(HBH)_2$, M = Ca^{2+}, Mn^{2+}, Pb^{2+}] as shown in Scheme 2.10.

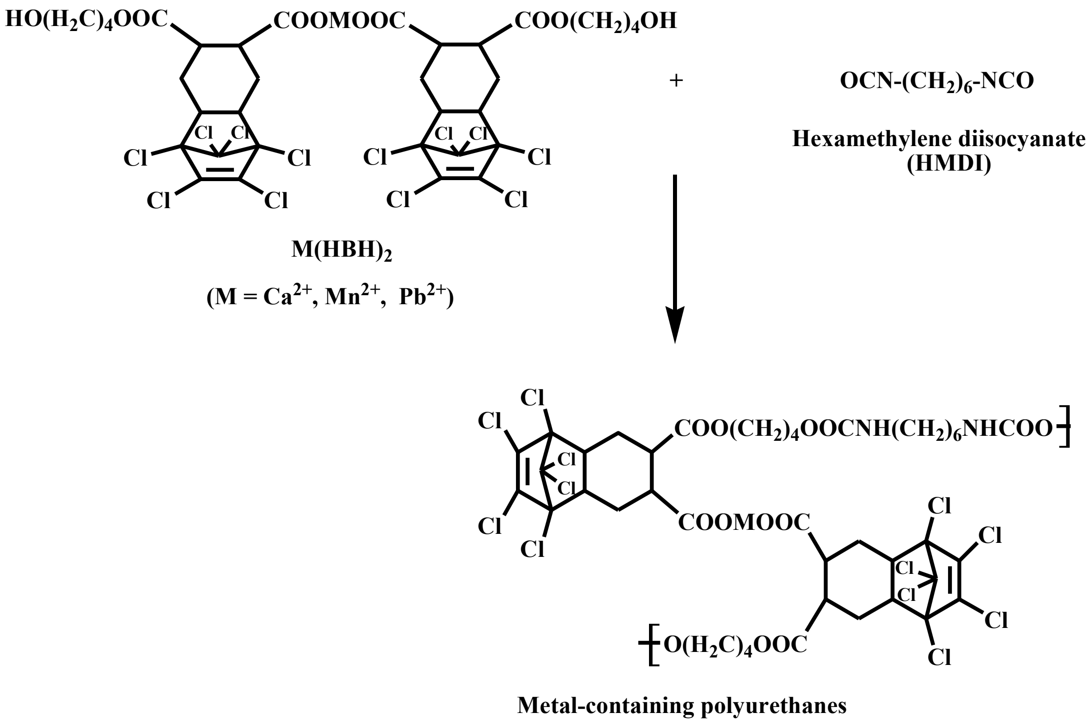

Scheme 2.10 Synthesis of metal-containing polyurethanes from M(HBH)$_2$ and HMDI

In addition, they synthesized poly(urethane-urea)s by the reaction of HMDI, M(HBH)$_2$ and hexamethylene bis[*N*′-(1-hydroxy-2-methyl-prop-2-yl)urea] (HBHMPU) or toluene 2,4-bis[*N*′-(1-hydroxy-2-methyl-prop-2-yl)urea] (TBHMPU) as shown in Scheme 2.11.

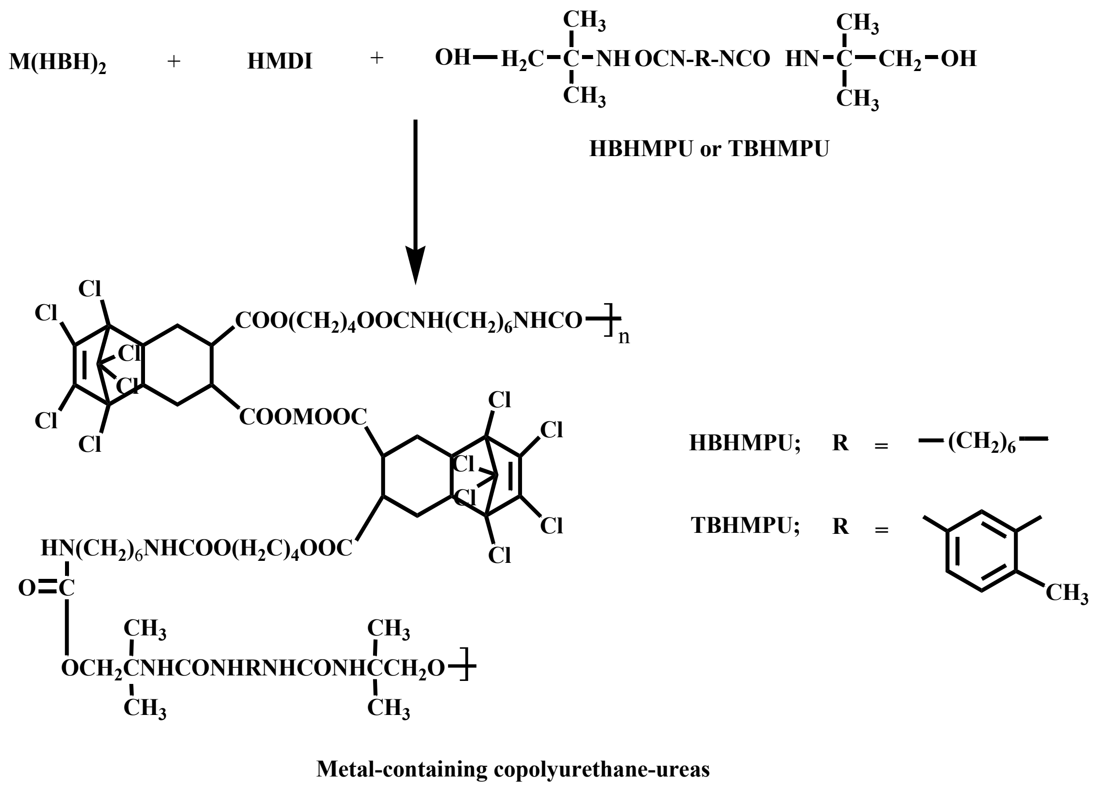

Scheme 2.11 Synthesis of metal-containing poly(urethane-urea)s from M(HBH)$_2$, HMDI and HBHMPU or TBHMPU

It was found that metal-containing polyurethanes more stable than metal-containing poly(urethane-urea)s. Among the poly(urethane-urea)s, TBHMPU-based poly(urethane-urea)s were slightly more stable than HBHMPU-based poly(urethane-urea)s due to the presence of aromatic ring in the polymer chain. The metal-containing polyurethanes showed higher flame retardancy than the corresponding metal-containing poly(urethane-urea)s. Similarly, Ca-containing poly(urethane-urea)s were prepared from HMDI or TDI and 1:1 mixture of calcium salt of mono(hydroxyetyloxyethyl)phthalate and bisureas by Jayakumar and coworker [31-33]. DSC studies showed that the poly(urethane-urea)s prepared from TDI-based bisureas have higher T_g values than those derived from HMDI-based bisureas due to flexible hexamethylene group. The XRD studies showed that the HMDI-based polymers were partially crystalline and TDI-based polymers were amorphous in nature.

Moreover, Jayakumar and Nanjundan [34-35] synthesized metal-containing copolyurethanes by the polyaddition reaction of diisocyanate with divalent metal salts of mono(hydroxyethoxyethyl)phthalate[M(HEEP)$_2$] or mono(hydroxypentyl)phthalate [M(HPP)$_2$] and diol. Examples of the metal-containing copolyurethanes are as follows:

Metal-containing copolyurethanes were synthesized by the polyaddition reaction of hexamethylene diisocyanate or tolylene 2,4-diisocyanate with 1:1 mixture of [M(HEEP)$_2$, M = Ca^{2+} and Zn^{2+}] and 1,5-pentane diol using DBTDL as a catalyst (Scheme 2.12).

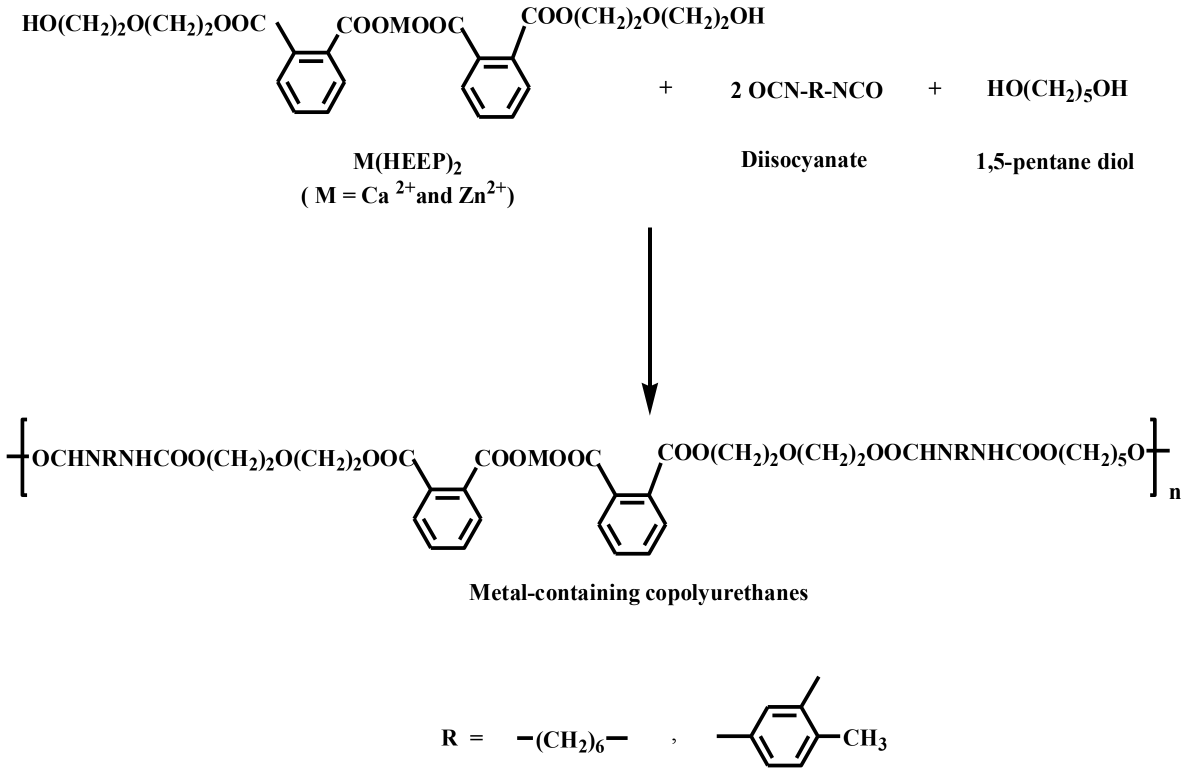

Schemes 2.12 Synthesis of metal-containing copolyurethanes from M(HEEP)$_2$, diisocyanates and 1,5-pentane diol

The result showed that these polymers were soluble in DMF, DMSO and DMAc. The initial decomposition temperatures (IDT) of the copolyurethanes were found to be in the range of 188-207 °C. HMDI-based copolymers showed lower IDT than the TDI-based copolymers. The reference polymers showed slightly higher IDT than metal-containing copolymers.

Another method used to improve the thermal stability of polyureas is copolymerization with thermally stable polymers such as the synthesis of poly(urea-imide)s [36]. Polyimides are known as one of the best materials for use at high temperature. Reaction of isocyanate-terminated polyimide prepolymers with diamines is one of the method used to introduce the urea function into the polyimides backbone. Another method for the synthesis of poly(urea-imide)s can be done by the reaction between acid dianhydrides and amines which contain urea groups. Polyimides themselves show poor solubility in common organic solvents. The introduction of urea group to yield poly(urea-imide)s copolymer improve solubility of the polymers.

Imai and coworkers [37] prepared poly(urea-imide)s by polyaddition of N,N′(-dimethyl-N,N′(-bis(aminophenyl) ureas to various aromatic tetracarboxylic dianhydrides to give poly(amic acid)s, followed by thermal cyclodehydration (Scheme 2.13). The introduction of urea group would be useful to produce soluble aromatic polyimides, which had problems in solubility and processability.

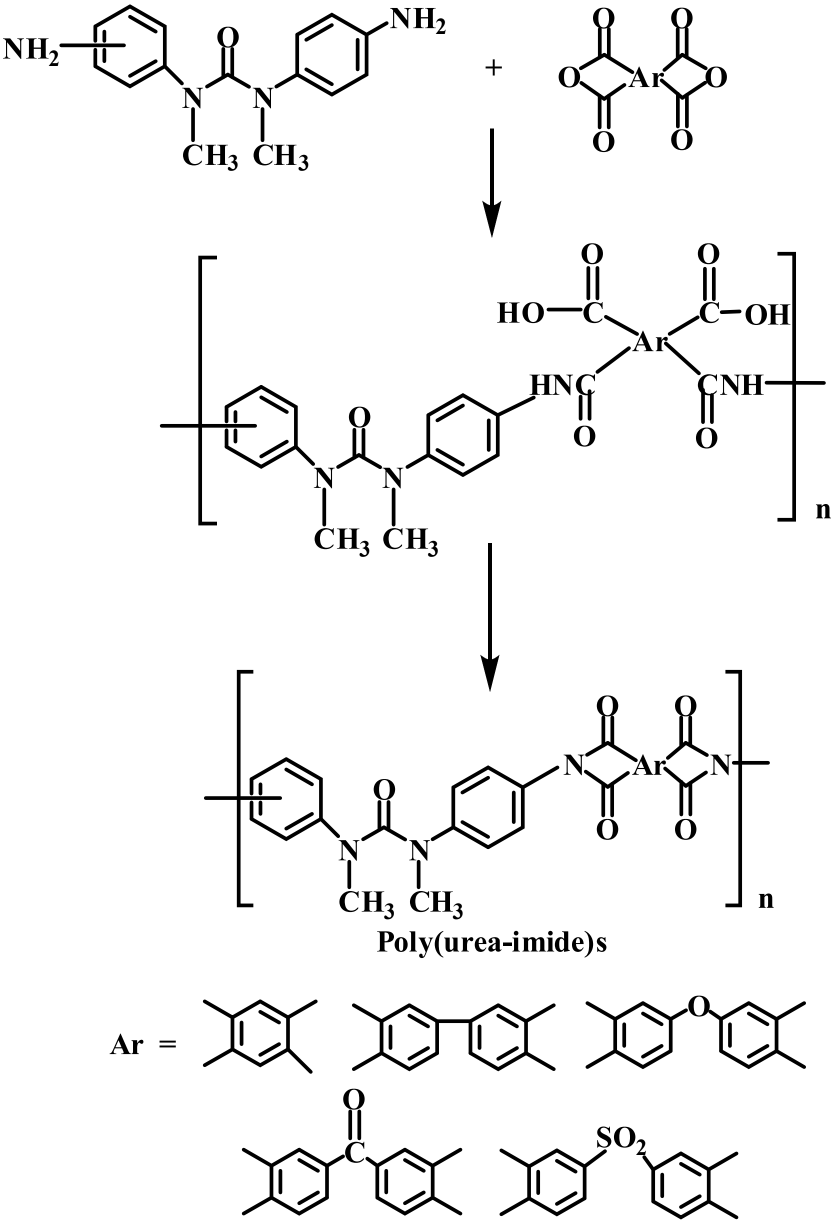

Scheme 2.13 Synthesis of poly(urea-imide)s from N,N′(-dimethyl-N,N′(-bis(aminophenyl) ureas and various aromatic tetracarboxylic dianhydrides.

Wang and coworkers [38-39] prepared poly(urea-imide)s by the reaction between diisocyanates, diamines and various dianhydrides (Scheme 2.14). The solubility of copolymers is in between those of polyimides and polyureas. It was found that the copolymers with high urea content showed good solubility.

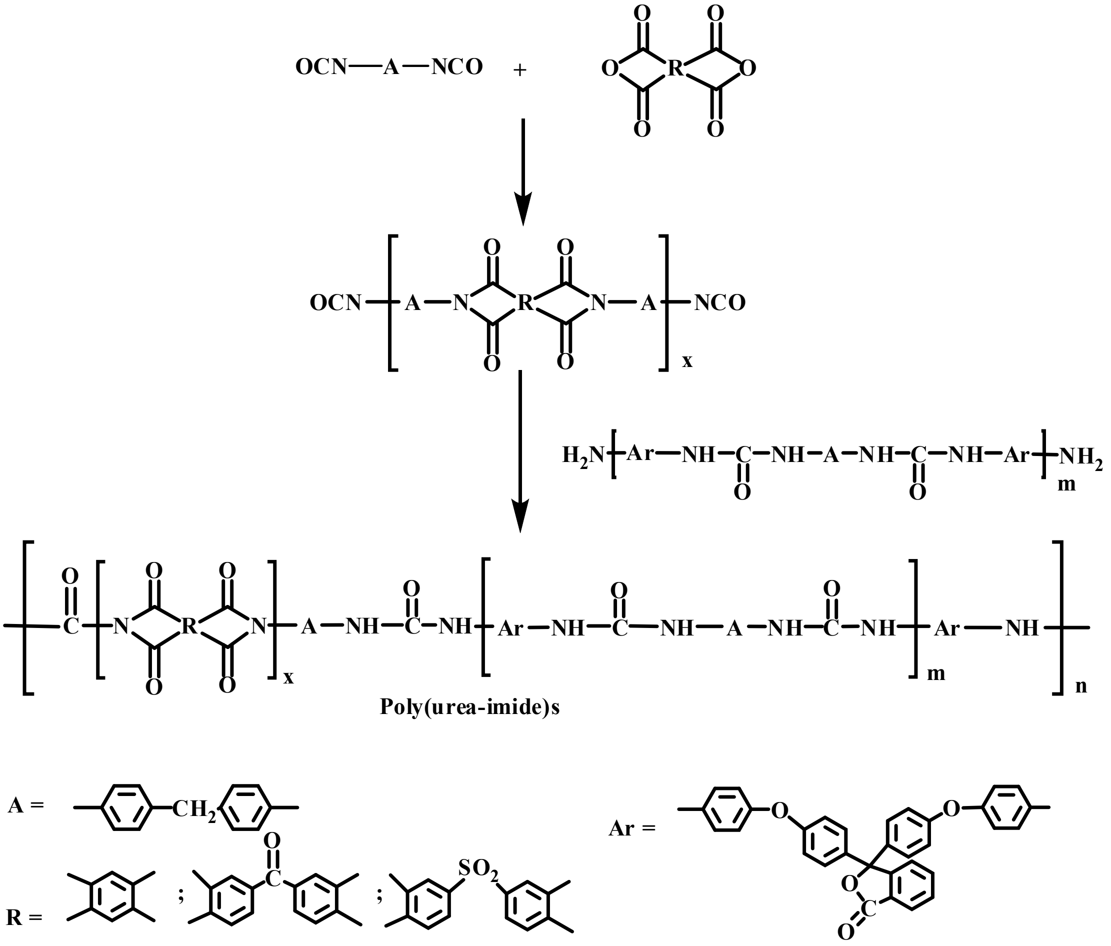

Scheme 2.14 Synthesis of poly(urea-imide)s from diisocyanates, diamines and various dianhydrides

Yeganeh and coworkers [40] synthesized poly(urethane-imide-imide) from the reaction of NCO-terminated polyurethane with 2,2′-pyromellitdiimidodisuccinic anhydride chain extender (Scheme 2.15).

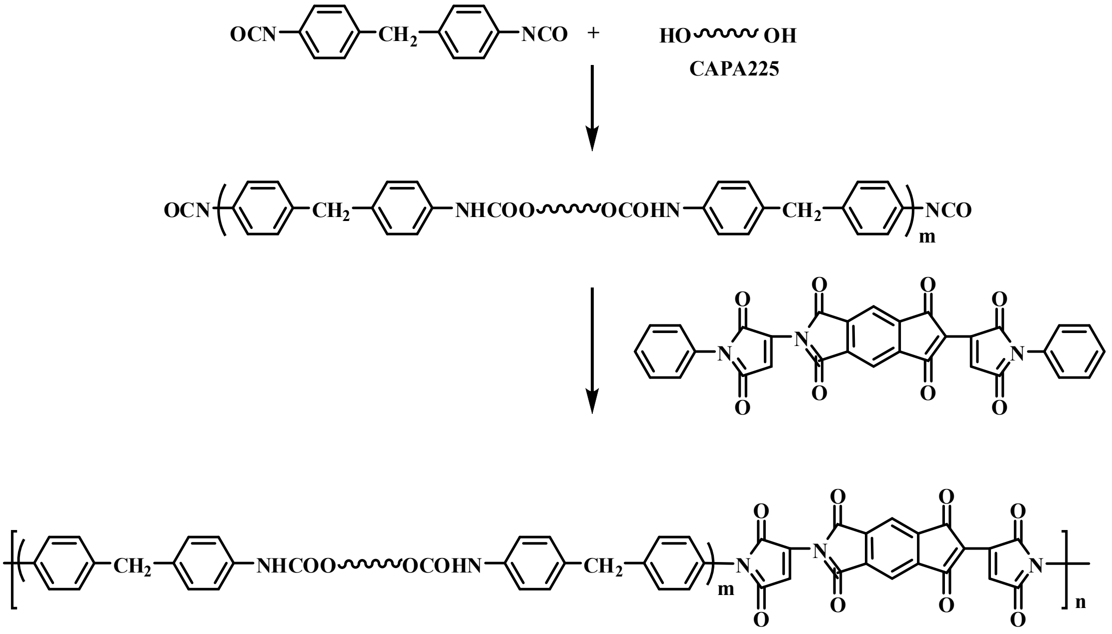

Scheme 2.15 Synthesis of poly(urethane-imide-imide)s

These polymers exhibited improved thermal stability as well as good solubility. Ten percent weight loss of polymers was in the range of 358-370°C. All polymers showed excellent solubility in polar aprotic solvent as well as chlorinated and polar solvents such as chloroform and tetrahydrofuran.

From the previous work in our research group, Chantarasiri and coworkers [41] prepared polyureas by the reaction of hexadentate Schiff base metal complexes with hexamethylene diisocyanate (HDI) or 4,4'-diphenylmethane diisocyanate (MDI) (Scheme 2.16). It was found from TGA study that the polymers are thermally stable.

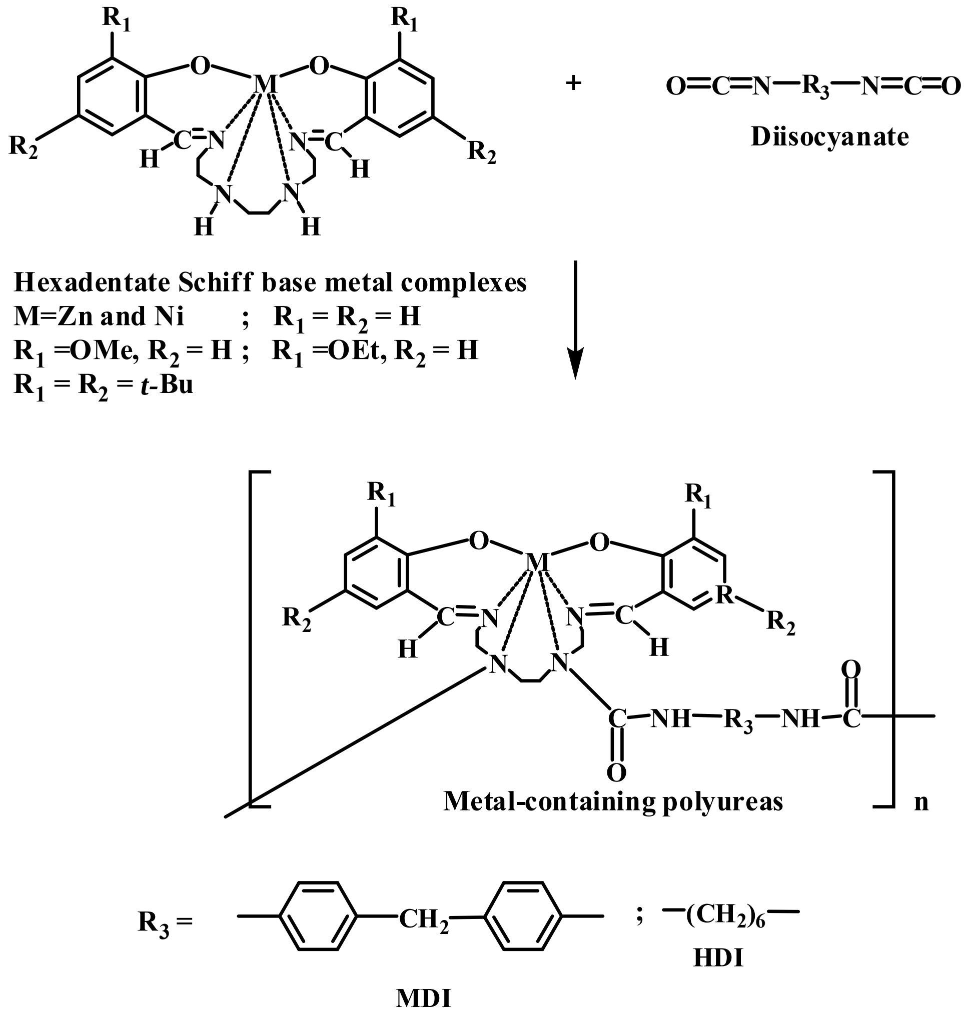

Scheme 2.16 Synthesis of polyureas from hexadentate Schiff base metal complexes and hexamethylene diisocyanate (HDI) or 4,4'-diphenylmethane diisocyanate (MDI)

In addition, they synthesized poly(urethane-urea)s by the reaction of hexadentate Schiff base metal complexes with MDI and polycaprolactone diol (PCL) or polytetramethylene oxide (PTMO)(Scheme 2.17) [42]. The metal-containing polymers had higher thermal stability than reference polymers synthesized without metal complexes.

Theses polymer showed IDT in the range 204-271°C, char yield of polymer were 18-32%. The thermal stability of polymer was increase when increased metal content.

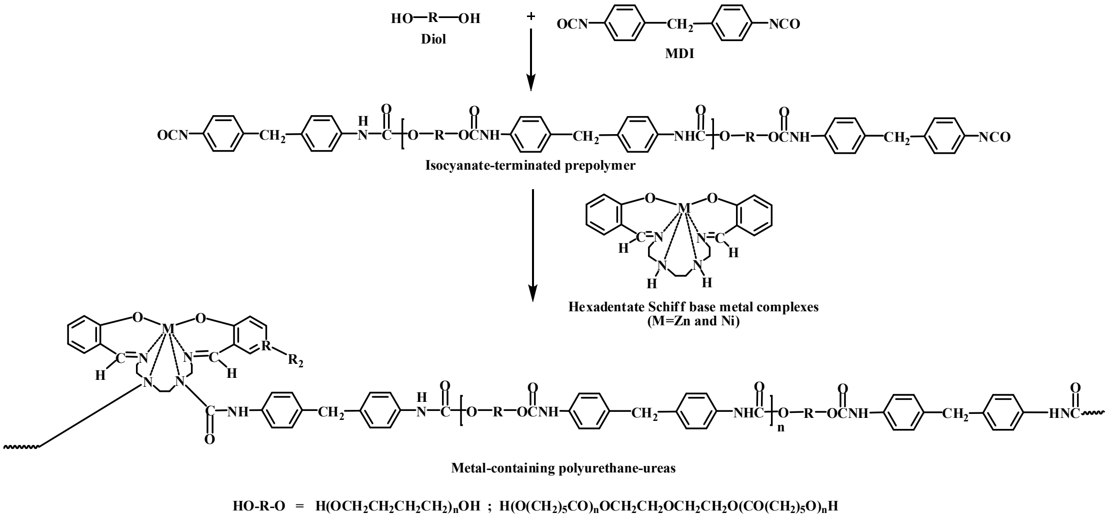

Scheme 2.17 Synthesis of metal-containing polyurethane-ureas from hexadentate Schiff base metal complexes, PCL or PTMO and MDI

2.2 Objectives and scope of the research

The target of this research is to synthesize hexadentate Shiff base metal complexes and their polymer which are metal-containing polyurea, metal-containing poly(urea-imide)s, metal-containing copolyurea, metal-containing poly(urea-imide)s and metal-containing poly(ureathane-urea-imide)s. It was expected that these metal-containing polymers would show good thermal stability, good solubility and can be utilized at high temperature application.

In the first step, hexadentate Shiff base metal complexes (MNapth$_2$trien, where M = Zn and Ni) were synthesized by a reaction between 2-hydroxy-1-naphthaldehyde, triethylenetetramine and metal acetate (Scheme 2.18).

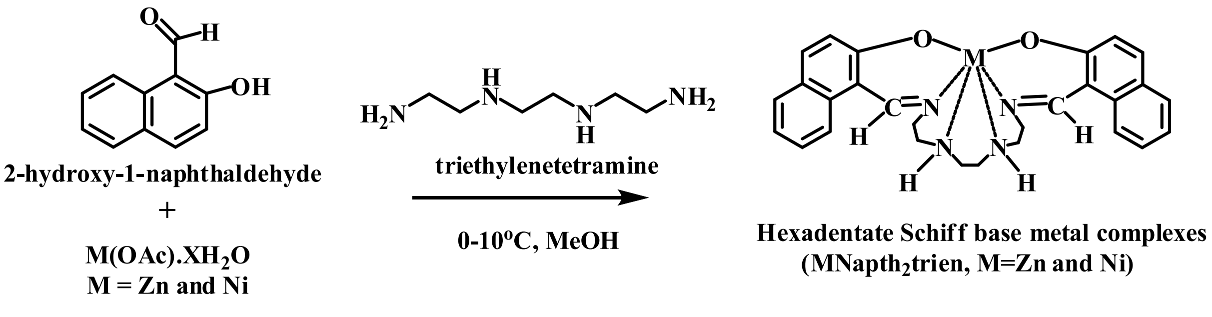

Scheme 2.18 Synthesis of hexadentate Shiff base metal complexes (MNapth$_2$trien)

In the next step, metal-containing polyurea were synthesized from the reaction between MNapth$_2$trien and 4,4′-diphenylmethane diisocyanate (MDI) or isophorone diisocyanate (IPDI) (Scheme 2.19).

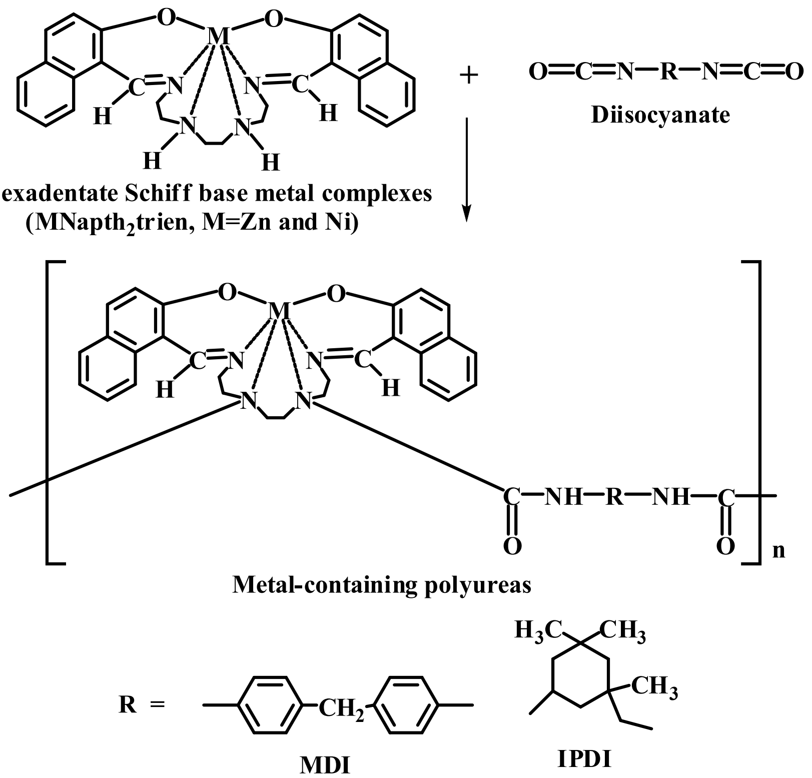

Scheme 2.19 Synthesis of metal-containing polyureas

Metal-containing copolyureas and copoly(urethane-urea)s were prepared in order to improve solubility of the polymers. The reaction between MNapth$_2$trien, diisocyanates and diamines, where the diamines were *m*-xylylenediamine (*m*-XDA) and 1,6-hexamethylenediamine (HMDA), gave metal-containing copolyureas (Scheme 2.20). Metal-containing poly(urethane-urea)s were prepared by the reaction between MNapth$_2$trien, diisocyanates and dialcohols. The dialcohols used were 2,2-Bis(4-Hydroxyphenyl)propane (BPO) and 1,6-hexamethylenediol (HDO) (Scheme 2.21). Different mole ratios of the starting materials were employed to investigate its effect on the polymer properties.

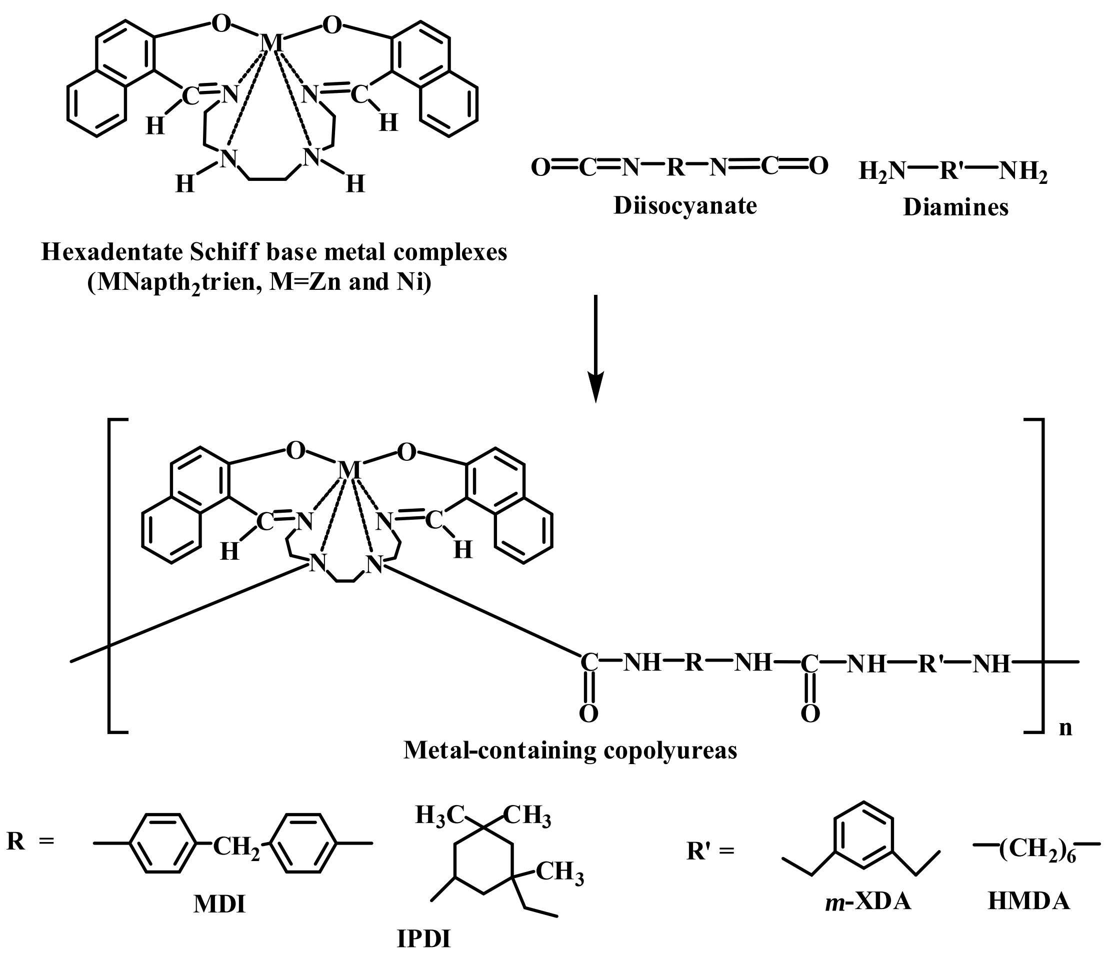

Scheme 2.20 Synthesis of metal-containing copolyureas

ZnNapth$_2$trien : MDI : *m*-XDA = 0.5:2:1.5	NiNapth$_2$trien: MDI : HMDA = 0.5:2:1.5
ZnNapth$_2$trien : MDI : *m*-XDA = 1:2:1	NiNapth$_2$trien : MDI : HMDA = 1:2:1
ZnNapth$_2$trien : MDI: *m*-XDA = 1.5:2:0.5	NiNapth$_2$trien : MDI :HMDA = 1.5:2:0.5
ZnNapth$_2$trien : IPDI : *m*-XDA = 0.5:2:1.5	NiNapth$_2$trien : IPDI : HMDA= 0.5:2:1.5
ZnNapth$_2$trien : IPDI : *m*-XDA = 1:2:1	NiNapth$_2$trien : IPDI : HMDA = 1:2:1
ZnNapth$_2$trien : IPDI: *m*-XDA = 1.5:2:0.5	NiNapth$_2$trien : IPDI : HMDA= 1.5:2:0.5

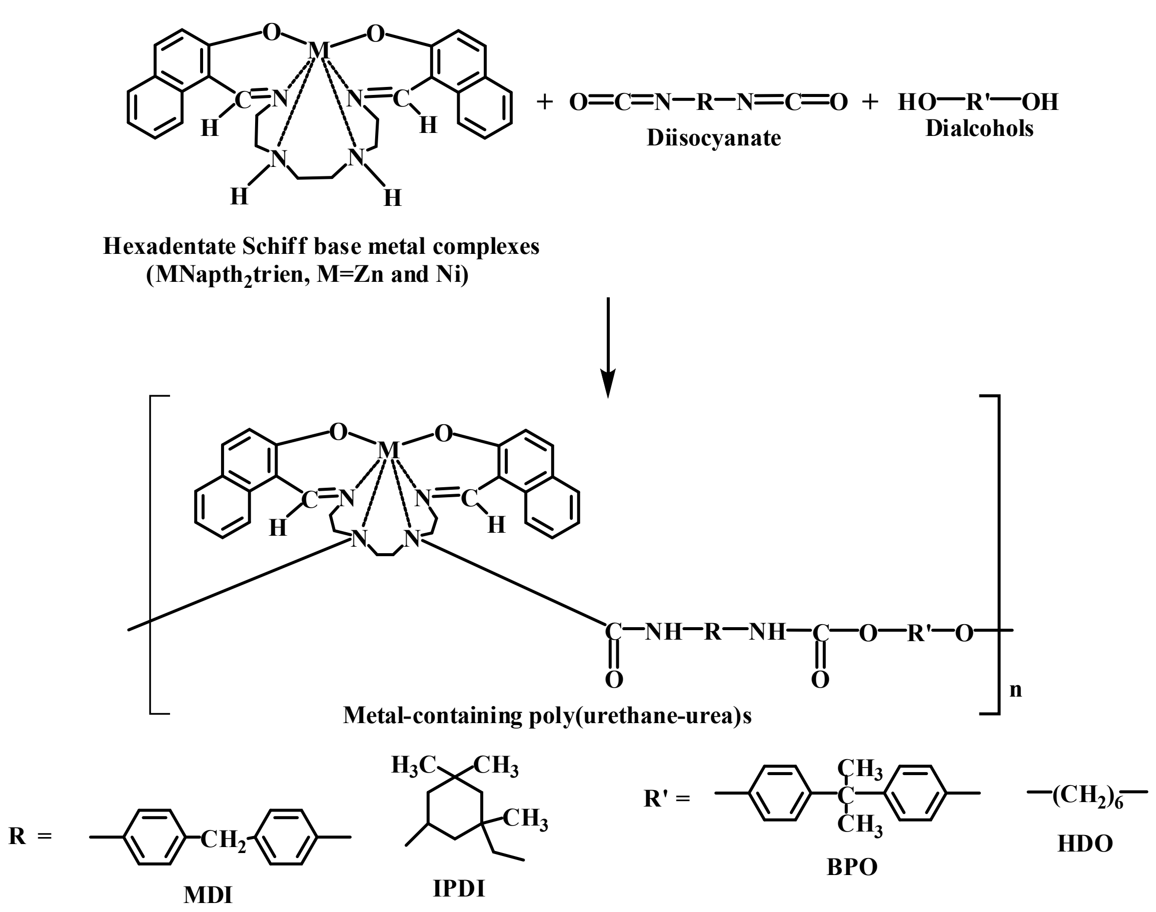

Scheme 2.21 Synthesis of metal-containing poly(urethane-urea)s

ZnNapth$_2$trien : MDI : BPO = 0.5:2:1.5
ZnNapth$_2$trien : MDI : BPO = 1:2:1
ZnNapth$_2$trien : MDI: BPO = 1.5:2:0.5
ZnNapth$_2$trien : IPDI : BPO = 0.5:2:1.5
ZnNapth$_2$trien : IPDI : BPO = 1:2:1
ZnNapth$_2$trien : IPDI: BPO = 1.5:2:0.5

NiNapth$_2$trien : MDI : HDO = 0.5:2:1.5
NiNapth$_2$trien : MDI : HDO = 1:2:1
NiNapth$_2$trien : MDI : HDO = 1.5:2:0.5
NiNapth$_2$trien : IPDI : HDO = 0.5:2:1.5
NiNapth$_2$trien : IPDI : HDO = 1:2:1
NiNapth$_2$trien : IPDI : HDO = 1.5:2:0.5

Metal-containing poly(urea-imide)s were synthesized in two steps by polyaddition of MNapth$_2$trien to 4,4′-diphenylmethane diisocyanate (MDI) or isophorone diisocyanate (IPDI) to give isocyanate terminated prepolymers. Then, these prepolymers were reacted with dianhydrides, namely pyromellitic dianhydride (PMDA) and benzophenone-3,3′,4,4′-tetracarboxylic dianhydride (BTDA), followed by thermal cyclodecarboxylation reaction (Scheme 2.22).

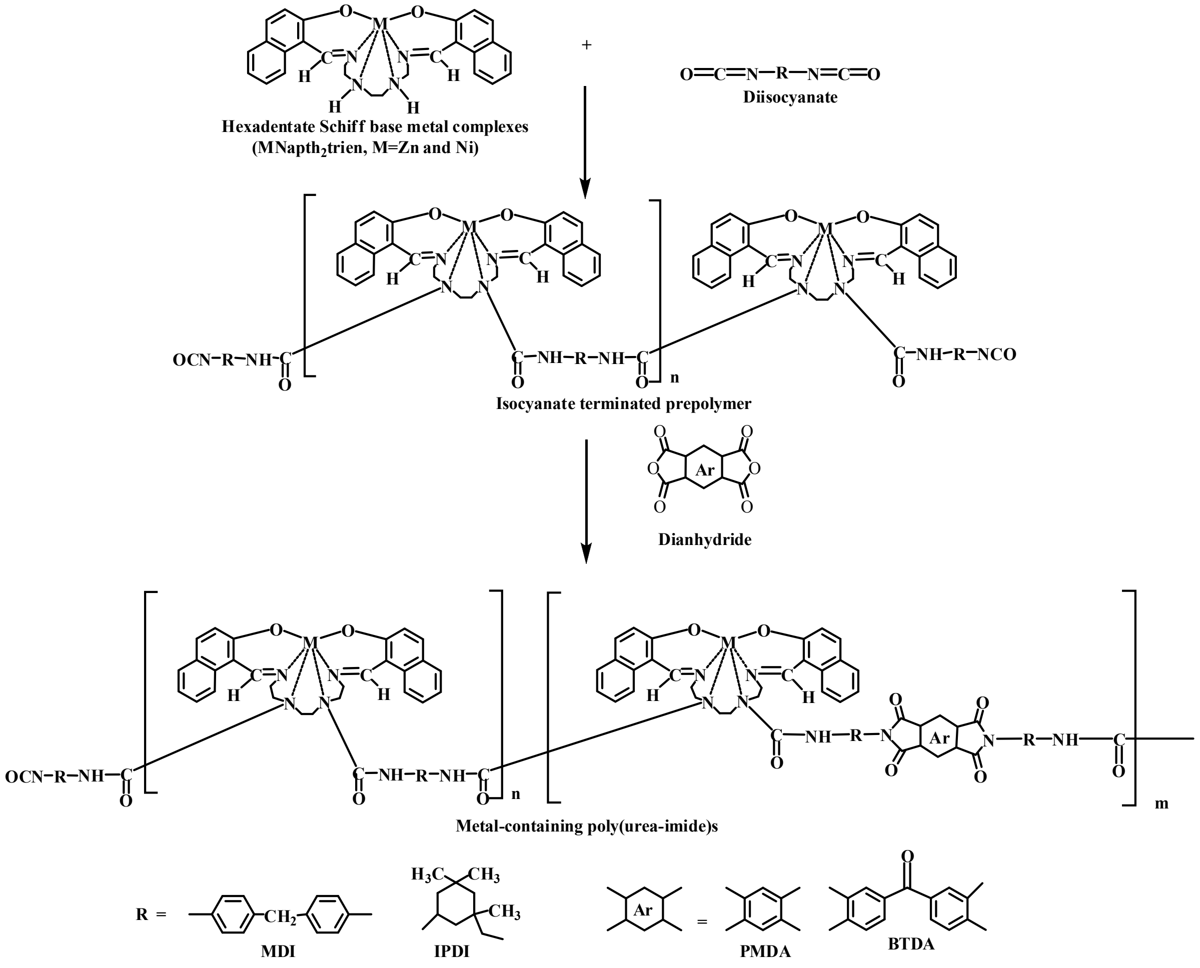

Scheme 2.22 Synthesis of metal-containing poly(urea-imide)s

ZnNapth$_2$trien : MDI : PMDA = 1:2:1
ZnNapth$_2$trien : MDI : PMDA = 1:2:0.5
ZnNapth$_2$trien : IPDI : PMDA = 1:2:1
ZnNapth$_2$trien : IPDI : PMDA = 1:2:0.5
ZnNapth$_2$trien : MDI : BTDA = 1:2:1
ZnNapth$_2$trien : MDI : BTDA = 1:2:0.5
ZnNapth$_2$trien : IPDI : BTDA = 1:2:1
ZnNapth$_2$trien : IPDI : BTDA = 1:2:0.5
NiNapth$_2$trien : MDI : PMDA = 1:2:1
NiNapth$_2$trien : MDI : PMDA = 1:2:0.5
NiNapth$_2$trien : IPDI : PMDA = 1:2:1
NiNapth$_2$trien : IPDI : PMDA = 1:2:0.5
NiNapth$_2$trien : MDI : BTDA = 1:2:1
NiNapth$_2$trien : MDI : BTDA = 1:2:0.5
NiNapth$_2$trien : IPDI : BTDA = 1:2:1
NiNapth$_2$trien : IPDI : BTDA = 1:2:0.5

Metal-containing poly(urethane-urea-imide)s were synthesized from the reaction between MNapth$_2$trien, diisocyanates, PEG400 and dianhydrides (Scheme 2.23). These polymers were prepared in order to improve solubility and processing properties of polymers.

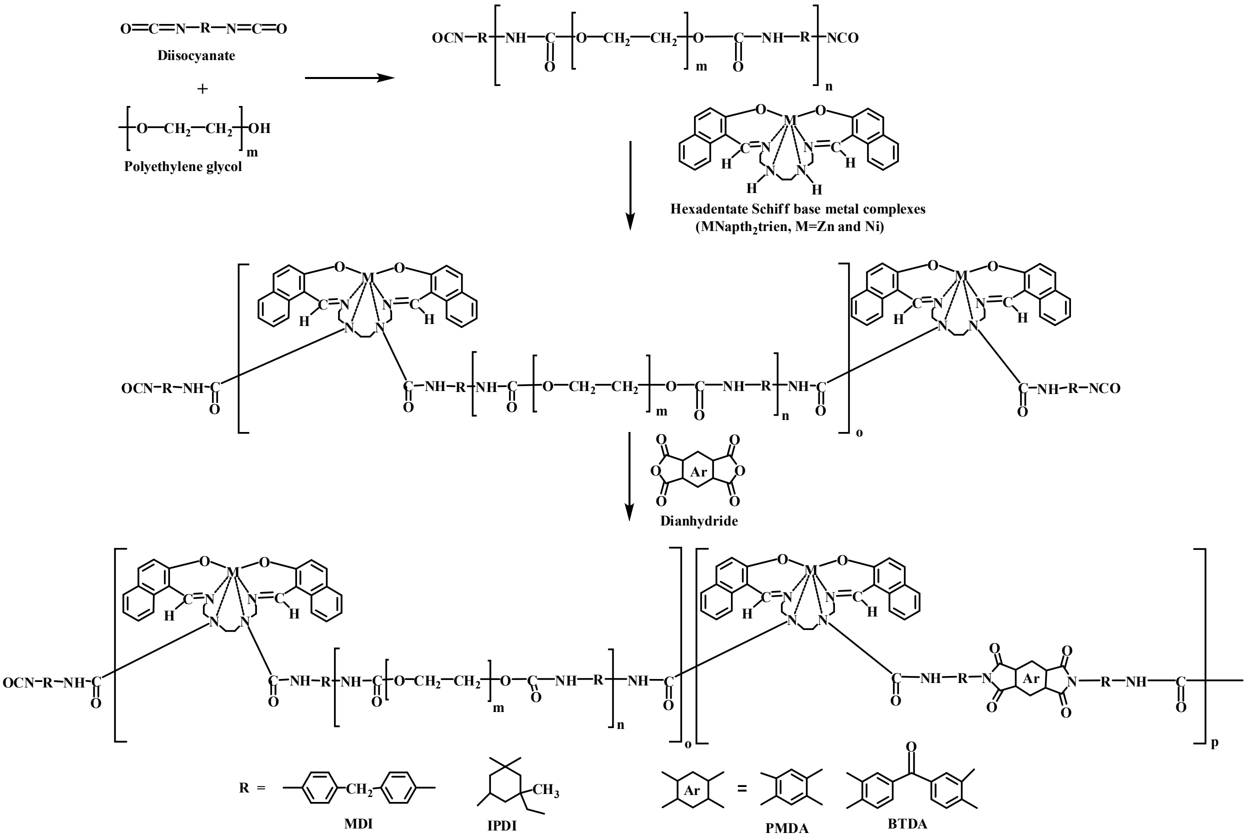

Scheme 2.23 Synthesis of metal-containing poly(urethane-urea-imide)s

ZnNapth$_2$trien : MDI/PEG400 : PMDA = 1:2:1

NiNapth$_2$trien : MDI/PEG400 : PMDA = 1:2:1

ZnNapth$_2$trien : IPDI/PEG400 : PMDA = 1:2:1

NiNapth$_2$trien : IPDI/PEG400 : PMDA = 1:2:1

ZnNapth$_2$trien : MDI/PEG400 : BTDA = 1:2:1

NiNapth$_2$trien : MDI/PEG400 : BTDA = 1:2:1

ZnNapth$_2$trien : IPDI/PEG400 : BTDA = 1:2:1

NiNapth$_2$trien : IPDI/PEG400 : BTDA = 1:2:1

Finally, metal-containing polymers were characterized by infrared spectroscopy (IR), proton nuclear magnetic resonance spectroscopy (^{1}H NMR), elemental analysis, X-ray diffraction (XRD), solubility and viscosity. Thermal properties of the polymers were investigated by differential scanning calorimetry (DSC), dynamic mechanical thermal analysis (DMTA) and thermogravimetric analysis (TGA).

CHAPTER III

EXPERIMENTAL

3.1 Materials

All reagents and solvents were of analytical grade quality. Dimethyl sulphoxide (DMSO) and dimethyl formamide (DMF) were purified by distillation under reduced pressure over calcium hydride and stored over molecular sieves. Zinc (II) acetate dihydrate, nickel (II) acetate tetrahydrate, 2-hydroxy-1-naphthaldehyde, triethylenetetramine, 4,4′-diphenylmethane diisocyanate (MDI), isophorone diisocyanate (IPDI), hexamethylenediamines (HMDA), *m*-Xylylenediamine (*m*-XDA), pyromellitic dianhydride (PMDA) and benzophenone-3,3′,4,4′-tetracarboxylic dianhydride (BTDA), 2,2-Bis(4-Hydroxyphenyl)propane (BPO), 1,6-hexamethylenediol (HDO), polyethylene glycol (PEG, MW=400) and dibutyltin dilaurate (DBTDL) were obtained from Fluka and Aldrich. All chemicals were used as received without any purification. The solvents were obtained from Lab-Scan.

3.2 Measurements

IR spectra of the samples were recorded on a Nicolet Impact 410 FTIR spectrophotometer at room temperature with potassium bromide (KBr) disk method. The samples were scanned over a range of 500-4000 cm^{-1} at a resolution of 16 cm^{-1} and the number of scan was 32. The measurement was controlled by Omnic Software. ^{1}H-NMR and ^{13}C-NMR spectra were recorded in DMSO-d_6 on a Varian Mercury-400 MHz and JEOL JNM-A 500 MHz NMR instruments. Chemical shifts are given in parts per million (ppm) using the proton residual as internal reference. Thermogravimetric analysis (TGA) was examined using a Netzsch STA 409C thermogravimetric analyzer at heating rate 20 °C/min under air atmosphere. All samples were held in the analyzer at 120 °C for 15 min and measured from temperature range 20 °C to 1000 °C. The result of thermal stability was reported in percentage weight residue of polymers. Initial decomposition temperature (IDT) was taken at the temperature where 5 wt% loss of the polymer occurred. Differential scanning calorimetric (DSC) analysis was carried out using a Netzsch DSC 204 F_1 phonic differential scanning calorimeter at heating rate of 10 °C/min under nitrogen atmosphere. Glass transition temperatures (T_g) were read at the middle of the transition in the heat capacity taken from the heating DSC traces. A sample was scanned from room temperature to 250 °C. All the samples were heated in DSC cell using a closed aluminum pan. Dynamic mechanical analysis (DMTA) was performed on a Netzsch DMA 242 thermal analyzer using penetration mode at a frequency of 0.5 Hz and a heating rate of 3°C/min over the temperature range of -50°C to 240°C in nitrogen atmosphere. The sample thickness was 3 mm. X-ray diffractometer (XRD) used in study was Bruker model D8 Discover with nickel filtered CuKα radiation (40kV, 40mA) at an angle of 2Θ range from 5 to 40°**.** The scan speed was 1.2 °/min and scan step was 0.02°. Elemental analyses were carried out using a Perkin Elmer 2400 CHN analyzer. MALDI-TOF mass spectra were obtained on a Bruker Bifex mass spectrometer using α-cyanocinnamic acid as a matrix. Solubility of polymer was tested in various polar and nonpolar solvents by placing 10 mg of samples to 2 mL of a solvent. Maximum solubility of polymers was tested in DMSO by addition of samples to 1 mL of DMSO. Inherent viscosity (η_{inh}) of the polymers was determined using a Cannon-Fenske viscometer at a concentration of 0.5 g/100 mL in DMSO at 40 ^{o}C according to ASTM D2270. Shore D hardness tests were performed using a Zwick 3100 durometer on a shore D acale according to ASTM D-2240. The polymer samples for DMTA and hardness testing were obtained by solution-cast from *N*-methyl-2-pyrrolidinone (NMP) solutions with heating in an oven at 100°C.

3.3 Synthetic Procedures

3.3.1 Synthesis of hexadentate Shiff base metal complexes ($ZnNapth_2trien$)

3.3.1.1 Synthesis of hexadentate Shiff base zinc complex ($ZnNapth_2trien$)

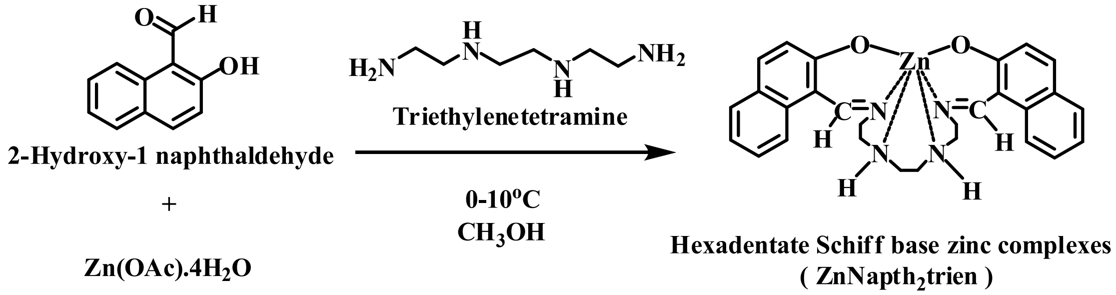

Scheme 3.1 Synthesis of hexadentate Shiff base zinc complex

The preparation of ZnNapth$_2$trien was performed according to the method reported in the literature [43]. The mixture of 2-hydroxy-1-naphthaldehyde (0.344 g, 2.0 mmol) and zinc (II) acetate dihydrate (0.220 g,1.0 mmol) was stirred in methanol (25 mL) and then cooled to (0 °C) for 10 minutes. A cool (0 °C) solution of triethylenetetramine (0.149 mL,1.0 mmol) in methanol (10 mL) was added dropwise to mixture over a period of 5 minutes. This mixture was stirred for 10 minutes and neutralized by adding a solution of 1 N sodium hydroxide (1.0 mL, 2.0 mmol) and stirred at 0 °C for 30 minutes. The yellow solution was allowed to stand at room temperature for 4 to 6 hours. ZnNapth$_2$trien crystallized from yellow solution and was subsequently isolated by filtration and was dried under vacuum to remove solvent. The yield of ZnNapth$_2$trien was obtained as a yellow crystal (0.363 g, 70%): IR (KBr,cm^{-1}); 3340 (NH), 3312, 3043, 2894, 2850, 1619 (C=N), 1533, 1500, 1463, 1171, 972, 828, 750, 649, 513. ^{1}H NMR (400 MHz, DMSO-*d$_6$*, ppm); δ 9.21 (2H, s, C**H**=N), 8.06 (2H, d, Ar-**H**, J = 8.8 Hz), 7.52 (2H, d, Ar-**H**, J = 7.2 Hz), 7.46 (2H, d, Ar-**H**, J = 9.2 Hz), 7.23-7.37 (2H, m, Ar-**H**), 7.02 (2H, t, Ar-**H**, J = 7.2 Hz), 6.62 (2H, d, Ar-**H**, J = 9.2 Hz), 3.83-3.93 (2H, m, C**H**$_2$), 3.60-3.69 (2H, m, C**H**$_2$), 3.12-3.26 (4H, m, N**H** and C**H**$_2$), 2.78-2.87 (2H, m, C**H**$_2$), 2.52-2.62 (2H, m, C**H**$_2$), 2.37-2.45 (2H, m, C**H**$_2$). ^{13}CNMR (125 MHz, DMSO-*d$_6$*, ppm); δ 172.60, 161.50, 135.98, 132.86, 128.40, 127.91, 126.46, 124.40, 119.60, 118.00, 107.44, 55.78, 46.16, 43.46. MAlDI-TOF MS (m/z) 518.78. Anal. Calcd. For $C_{28}H_{28}N_4O_2Zn.1/2H_2O$: C 63.81; H 5.55; N 10.63; found C 63.47; H 5.33; N 10.44.

3.3.1.2 Synthesis of hexadentate Shiff base nickel complex (NiNapth$_2$trien)

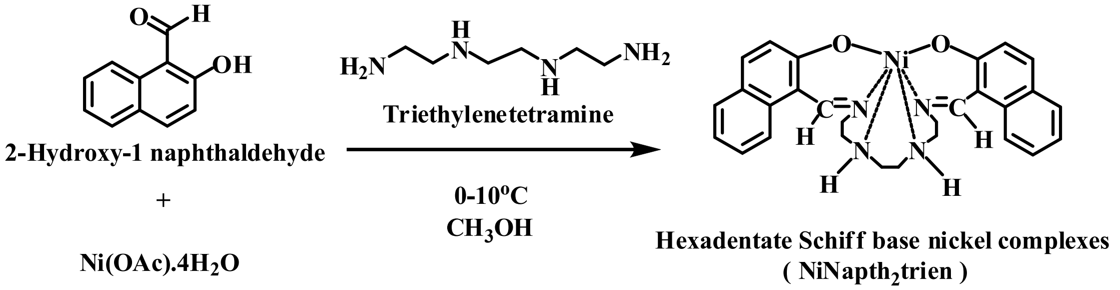

Scheme 3.2 Synthesis of hexadentate Shiff base nickel complex

The experiment was performed according to the proceduce described in experiment 3.3.1.1 employing nickel (II) acetate tetrahydrate (0.249 g, 1.0 mmol) instead of zinc (II) acetate dihydrate. The brown crystal of nickel complex (NiNapth$_2$trien) were filtered and dried *in vacuo* (0.35 g, 70%): (0.435 g, 85 %) IR (KBr, cm^{-1}); 3438 (NH), 3319, 3044, 2900, 2851, 1623 (C=N), 1533, 1500, 1463, 1175, 965, 828, 750, 649, 552. MAlDI-TOF MS (m/z) 511.14. Anal. Calcd. For $C_{28}H_{28}N_4O_2Ni.1/2H_2O$: C 64.64; H 5.63; N 10.77; found C 64.61; H 5.52; N 11.02.

3.3.2 Synthesis of metal-containing polymers

3.3.2.1 Synthesis of metal-containing polyureas from the reaction between MNapth$_2$trien and diisocyanates

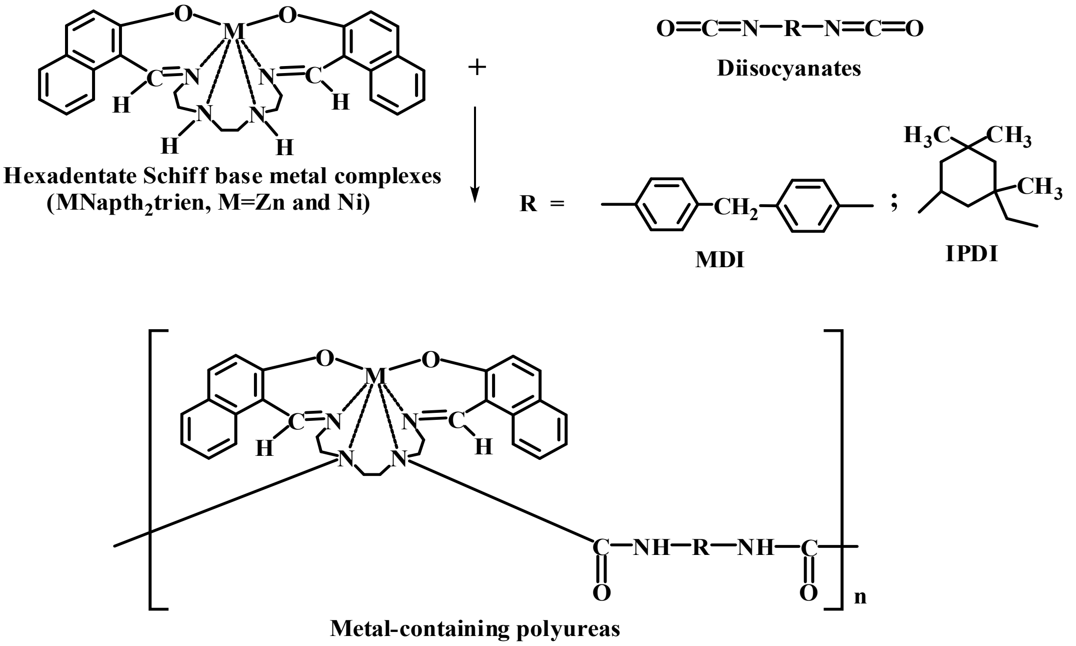

Scheme 3.3 Synthesis of metal-containing polyureas

Polyureas were synthesized from MNapth$_2$trien (where M = Zn and Ni) and diisocyanates. The diisocyanates used were 4,4′-diphenylmethane diisocyanate (MDI) and isophorone diisocyanate (IPDI) The mole ratio of MNapth$_2$trien : diisocyanate employed was 1:1. The general procedure for the synthesis of metal-containing polyureas was follows: A solution of diisocyanate (1.0 mmol) was added to the solution of MNapth$_2$trien (1.0 mmol) in dried methylene chloride (20 mL) under nitrogen atmosphere at room temperature. Dibutyltin dilaurate (0.04 mL, 0.067 mmol) was then added. The precipitated polyurea was filtered and dried in vacuo. The yields obtained for metal-containing polyureas were 53-85%.

Coding for various reactants is as follows: MNapth$_2$trien refers to metal complexes. MDI and IPDI represent 4,4′-diphenylmethane diisocyanate and isophorone diisocyanate.

Table 3.1 Composition of starting materials in the preparation of metal-containing polyureas

Polymer codes	**Weight. of ZnNapth$_2$trien (g)**	**Weights of composition (g)**			**Reaction Time (h)**	**Yield (%)**
		NiNapth$_2$trien	**MDI**	**IPDI**		
ZnNapth$_2$trien-MDI	0.500	-	0.242	0.202	4	85
ZnNapth$_2$trien-IPDI	0.500	-	-	-	24	65
NiNapth$_2$trien-MDI	-	0.500	0.245	0.205	4	82
NiNapth$_2$trien-IPDI	-	0.500	-	-	24	53

ZnNapth$_2$trien-MDI: IR (KBr, cm^{-1}); 3400 (NH), 3035, 2923, 1720 (C=O), 1616 (C=N), 1532, 1514, 1462, 1416, 1356, 1307, 1243, 1186, 965, 828, 749. ^{1}H NMR (400 MHz, DMSO-d_6, ppm) ; δ 9.09-9.28 (m, C**H**=N), 8.49-8.58 (m, N**H**), 7.91-8.19 (m, Ar-**H**), 7.57-7.66 (m, Ar-**H**), 7.42-7.48 (m, Ar-**H**), 7.22-7.42 (m, Ar-**H**), 6.93-7.21 (m, Ar-**H**), 6.80-6.87 (m, Ar-**H**), 6.66-6.80 (m, Ar-**H**), 6.58-6.64 (m, Ar-**H**), 6.42-6.52 (m, Ar-**H**), 4.82-4.87 (m, N**H**), 3.96-4.16 (m, C**H**$_2$), 3.83-3.94 (m, C**H**$_2$), 3.73-2.81 (m, C**H**$_2$), 3.44-3.71 (m, C**H**$_2$), 3.10-3.25 (m, C**H**$_2$), 2.77-2.86 (m, C**H**$_2$), 2.69-2.75 (m, C**H**$_2$), 2.38-2.45 (m, C**H**$_2$). Anal. Calcd. For $C_{43}H_{38}N_6O_4Zn$: C 67.23; H 4.99; N10.94; found C 65.87; H 5.54; N 10.54.

ZnNapth$_2$trien-IPDI: IR (KBr, cm^{-1}); 3360 (NH), 2941, 2923, 1692 (C=O), 1623 (C=N), 1543, 1463, 1434, 1394, 1358, 1304, 1245, 1189, 1040, 963, 831, 749. ^{1}HNMR (400 MHz, DMSO-*d$_6$,* ppm) 9.08 - 9.31 (m, C**H**=N), 7.99 - 8.16 (m, Ar-**H**), 7.54-7.65 (m, Ar-**H**), 7.49-7.54 (m, Ar-**H**), 7.43-7.48 (m, Ar-**H**), 7.26-7.41 (m, Ar-**H**), 7.04-7.16 (m, Ar-**H**),6.98-7.04 (m, Ar-**H**), 6.70-6.79 (m, Ar-**H**), 6.59-6.64 (m, Ar-**H**), 5.34-5.98 (m, N**H**), 3.73-3.94 (m, aliphatic-**H**), 3.46-3.73 (m, aliphatic-**H**), 3.11-3.24 (m, aliphatic-**H**), 2.55-2.91 (m, aliphatic-**H**), 0.65-1.82 (m, aliphatic-**H**). Anal. Calcd. For $C_{40}H_{46}N_6O_4Zn$: C 64.90; H 6.26; N11.35; found C 64.98; H 6.31; N 11.34.

NiNapth$_2$trien-MDI: IR (KBr, cm^{-1}); 3397 (NH), 3036, 2923, 1702 (C=O), 1618 (C=N), 1532, 1514, 1462, 1416,1356, 1307, 1243, 1186, 1085, 972, 945, 892, 828, 749. Anal. Calcd. For $C_{43}H_{38}N_6O_4Ni$: C 67.82; H 5.03; N11.04; found C 68.10; H 5.97; N 10.56.

NiNapth$_2$trien-IPDI: IR (KBr, cm^{-1}); 3378 (NH), 2924, 2855, 1699 (C=O), 1623 (C=N), 1547, 1457, 1436, 1400, 1357, 1314, 1250, 1197, 1124, 1028, 961, 827, 750. Anal. Calcd. For $C_{40}H_{46}N_6O_4Zn$: C 65.50; H 6.32; N11.46; found C 63.57; H 8.30; N 12.14.

3.3.2.2 Synthesis of metal-containing copolyureas from the reaction between MNapth$_2$trien, diisocyanates and diamines

Metal-containing copolyureas were synthesized from MNapth$_2$trien (where M = Zn and Ni), diisocyanates and diamines. The diisocyanates used were 4,4′-diphenylmethane diisocyanate (MDI) and isophorone diisocyanate (IPDI) and diamines used were *m*-xylylenediamine (*m*-XDA) and 1,6-hexamethylenediamine (HMDA). The mole ratios of MNapth$_2$trien : diisocyanate : diamine employed were 0.5:2:1.5, 1:2:1 and 1.5:2:0.5. MNapth$_2$trien and diamine were dissolved in 5 mL of dried DMSO in a 50 mL, two-necked round bottomed flask equipped with a nitrogen inlet. Then, diisocyanate was dissolved in DMSO (2 mL) and added to the solution. Dibutyltin dilaurate was used as a catalyst and the reaction was maintained at 90 °C for 36 hours.

Eventually, the hot solution was poured into distilled water to precipitate the polymer. The polymer was separated by filtration, washed with distilled methanol several times and dried in vacuo for 24 hours. Zinc-containing copolyureas were obtained as yellow powder in 55-88% yield and nickel-containing copolyureas were obtained as light brown powder in 63-94% yield. The compositions of starting materials in the preparation of polymers are shown in Tables 3.2 and 3.3.

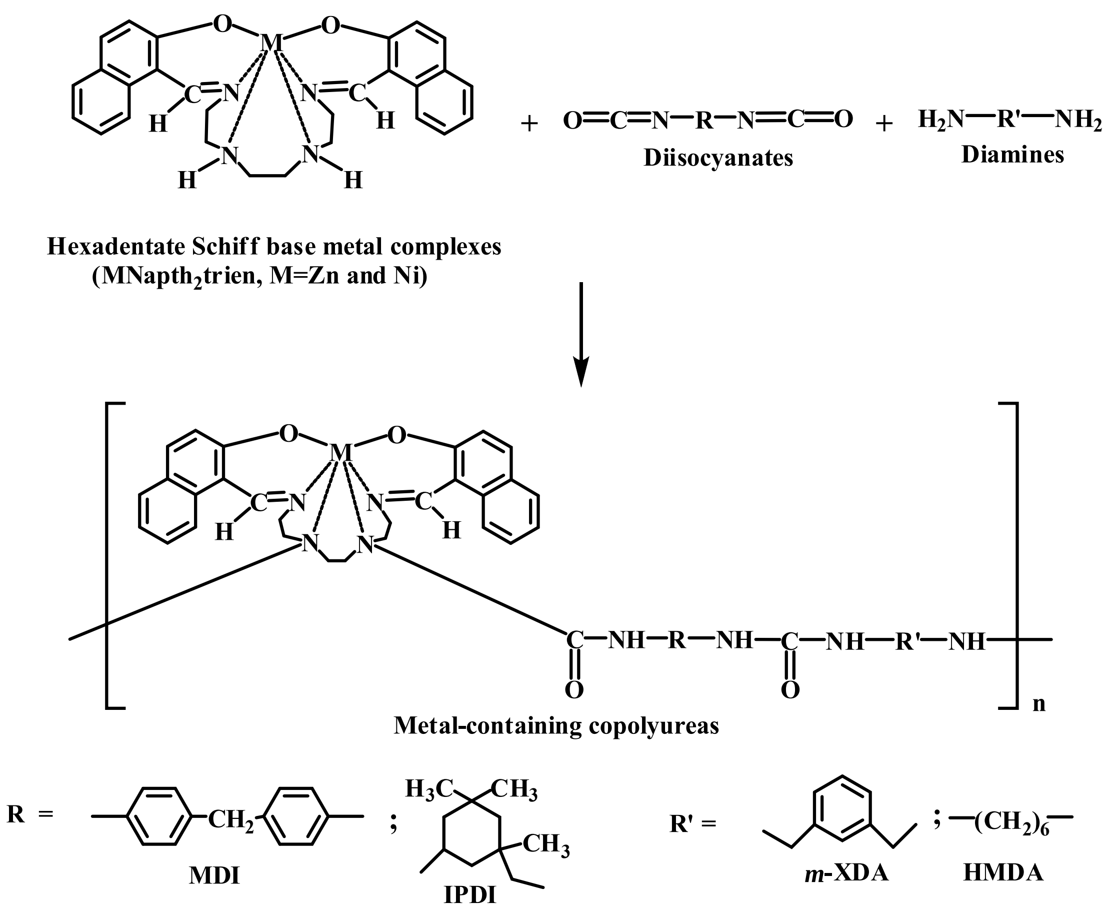

Scheme 3.4 Synthesis of metal-containing copolyureas

Table 3.2 Composition of starting materials in the preparation of metal-containing copolyureas based on ZnNapth$_2$trien

Polymer codes	Weight of ZnNapth$_2$trien (g)	Weights of composition (g)				Yield (%)
		MDI	IPDI	*m*-XDA	HMDA	
ZnNapth$_2$trien-MDI-*m*-XDA (0.5:2:1.5)	0.259	0.500	-	0.204	-	88
ZnNapth$_2$trien-MDI-*m*-XDA (1:2:1)	0.517	0.500	-	0.136	-	79
ZnNapth$_2$trien-MDI-*m*-XDA (1.5:2:0.5)	0.776	0.500	-	0.068	-	81
ZnNapth$_2$trien-IPDI-*m*-XDA (0.5:2:1.5)	0.259	-	0.444	0.204	-	70
ZnNapth$_2$trien-IPDI-*m*-XDA (1:2:1)	0.517	-	0.444	0.136	-	83
ZnNapth$_2$trien-IPDI-*m*-XDA (1.5:2:0.5)	0.776	-	0.444	0.068	-	79
ZnNapth$_2$trien-MDI-HMDA (0.5:2:1.5)	0.259	0.500	-	-	0.174	88
ZnNapth$_2$trien-MDI-HMDA (1:2:1)	0.517	0.500	-	-	0.116	55
ZnNapth$_2$trien-MDI-HMDA (1.5:2:0.5)	0.776	0.500	-	-	0.058	87
ZnNapth$_2$trien-IPDI-HMDA (0.5:2:1.5)	0.259	-	0.444	-	0.174	71
ZnNapth$_2$trien-IPDI-HMDA (1:2:1)	0.517	-	0.444	-	0.116	74
ZnNapth$_2$trien-IPDI-HMDA (1.5:2:0.5)	0.776	-	0.444	-	0.058	78

Table 3.3 Composition of starting materials in the preparation of metal-containing copolyureas based on NiNapth$_2$trien

Polymer codes	**Weight. Of NiNapth$_2$trien (g)**	**Weights of composition (g)**				**Yield (%)**
		MDI	**IPDI**	***m*-XDA**	**HMDA**	
NiNapth$_2$trien-MDI-*m*-XDA (0.5:2:1.5)	0.255	0.500	-	0.204	-	94
NiNapth$_2$trien-MDI-*m*-XDA (1:2:1)	0.511	0.500	-	0.136	-	87
NiNapth$_2$trien-MDI-*m*-XDA (1.5:2:0.5)	0.766	0.500	-	0.068	-	90
NiNapth$_2$trien-IPDI-*m*-XDA (0.5:2:1.5)	0.255	-	0.444	0.204	-	68
NiNapth$_2$trien-IPDI-*m*-XDA (1:2:1)	0.511	-	0.444	0.136	-	71
NiNapth$_2$trien-IPDI-*m*-XDA (1.5:2:0.5)	0.766	-	0.444	0.068	-	64
NiNapth$_2$trien-MDI-HMDA (0.5:2:1.5)	0.255	0.500	-	-	0.174	75
NiNapth$_2$trien-MDI-HMDA (1:2:1)	0.511	0.500	-	-	0.116	75
NiNapth$_2$trien-MDI-HMDA (1.5:2:0.5)	0.766	0.500	-	-	0.058	74
NiNapth$_2$trien-IPDI-HMDA (0.5:2:1.5)	0.255	-	0.444	-	0.174	63
NiNapth$_2$trien-IPDI-HMDA (1:2:1)	0.511	-	0.444	-	0.116	79
NiNapth$_2$trien-IPDI-HMDA (1.5:2:0.5)	0.766	-	0.444	-	0.058	74

Since the copolymers obtained from different mole ratios have similar IR spectra, therefore, only the IR data of copolymers obtained from mole ratio of 1:2:1 are shown as follows:

MDI-*m*-XDA (1:1): IR (KBr, cm^{-1}); 3316 (NH), 3027, 2914, 1653(C=O), 1598, 1547, 1512, 1409, 1309, 1230, 1107, 1044, 1017, 908, 818, 773, 699. ^{1}H NMR (400 MHz, DMSO-d_6, ppm); δ8.42-8.56 (m, N**H**), 7.19-7.36 (m, Ar-**H**), 7.12-7.18 (m, Ar-**H**), 6.96-7.06 (m, Ar-**H**), 6.52-6.61 (m, Ar-**H**), 4.19-4.34 (m, C$\mathbf{H}_2$), 3.70-3.79 (m, C$\mathbf{H}_2$).

MDI-HMDA (1:1): IR (KBr, cm^{-1}); 3319 (NH), 2926, 2855, 1648 (C=O), 1598, 1551, 1513, 1408, 1309, 1236, 1108, 1011, 816, 761, 652, 508. ^{1}H NMR (400 MHz, DMSO-d_6, ppm); δ 8.22-8.40 (m, N**H**), 7.23-7.32 (m, Ar-**H**), 6.98-7.06 (m, Ar-**H**), 6.05 (s, N**H**), 3.71-3.77 (m, C**H**$_2$), 3.02-3.03 (m, C**H**$_2$), 1.93-2.17(m, C**H**$_2$), 1.09-1.53(m, C**H**$_2$)

IPDI-*m*-XDA (1:1): IR (KBr, cm^{-1}); 3360 (NH), 2947, 2920, 1642(C=O), 1561, 1463, 1380, 1360, 1303, 1244, 1062, 829, 780, 700. ^{1}H NMR (400 MHz, DMSO-d_6, ppm); δ 7.18-7.30 (m, Ar-**H**), 7.03-7.13 (m, Ar-**H**), 6.14-6.42 (m, Ar-**H**), 5.96-6.13 (m, N**H**), 5.67-5.85 (m, N**H**), 4.03-4.29 (m, aliphatic-**H**), 3.72-3.77 (m, aliphatic-**H**), 3.39-3.60 (m, aliphatic-**H**), 2.67-2.83 (m, aliphatic-**H**), 1.38-1.58 (m, aliphatic-**H**), 1.01-1.11 (m, aliphatic-**H**), 0.65-0.99 (m, aliphatic-**H**).

IPDI-HMDA (1:1): IR (KBr, cm^{-1}); 3375 (NH), 2927, 2858, 1641(C=O), 1562, 1464, 1381, 1304, 1245, 1071, 892, 772. ^{1}H NMR (400 MHz, DMSO-d_6, ppm); δ 7.85-8.05(m, N**H**), 5.45-5.93 (m, N**H**), 3.57-3.76 (m, aliphatic-**H**), 2.88-3.08 (m, aliphatic-**H**), 2.66-2.82 (m, aliphatic-**H**), 2.10-2.24 (m, aliphatic-**H**), 1.15-1.60 (m, aliphatic-**H**), 0.70-1.09 (m, aliphatic-**H**).

ZnNapth$_2$trien-MDI-XDA (1:2:1): IR (KBr, cm^{-1}); 3348 (NH), 3027, 2923, 2848, 1660 (C=O), 1615(C=N), 1541, 1514, 1463, 1413, 1355, 1309, 1234, 1183, 1105, 1043, 1016, 966, 911, 828, 750. ^{1}H NMR (400 MHz, DMSO-d_6, ppm); δ 9.07-9.32 (m, C**H**=N), 8.36-8.55 (m, N**H**), 7.91-8.14 (m, Ar-**H**), 7.56-7.68 (m, Ar-**H**), 7.44-7.54 (m, Ar-**H**), 7.19-7.40 (m, Ar-**H**), 6.96-7.19 (m, Ar-**H**), 6.72-6.94 (m, Ar-**H**), 6.40-6.67 (m, Ar-**H**), 4.76-4.92 (m, N**H**), 4.58-4.76 (m, N**H**), 4.16-4.35 (m, C**H**$_2$), 3.50-3.82 (m, C**H**$_2$), 2.96-3.04 (m, C**H**$_2$), 2.83-2.94 (m, C**H**$_2$), 2.68-2.78 (m, C**H**$_2$), 2.52-2.56 (m, C**H**$_2$).

ZnNapth$_2$trien-MDI-HMDA (1:2:1): IR (KBr, cm^{-1}); 3334 (NH), 3043, 2926, 2856, 1656 (C=O), 1622(C=N), 1601, 1544, 1512, 1463, 1410, 1362, 1309, 1234, 1179, 1117, 1021, 973, 946, 918, 824, 751. ^{1}H NMR (400 MHz, DMSO-d_6, ppm); δ 9.04-9.39 (m, C**H**=N), 8.66-8.81 (m, N**H**), 8.45-8.55 (m, Ar-**H**), 8.24-8.37 (m, Ar-**H**), 7.98-8.14 (m, Ar-**H**), 7.74-7.80 (m, Ar-**H**), 7.66-7.72 (m, Ar-**H**), 7.57-7.66 (m, Ar-**H**), 7.48-7.57 (m, Ar-**H**), 7.43-7.48 (m, Ar-**H**), 7.20-7.40 (m, Ar-**H**), 6.96-7.20 (m, Ar-**H**), 6.77-6.86 (m, Ar-**H**), 6.68-6.72 (m, Ar-**H**), 6.58-6.64 (m, Ar-**H**), 6.44-6.49 (m, Ar-**H**), 6.02-6.12 (m, N**H**), 3.56-3.97 (m, C**H**$_2$), 2.96-3.18 (m, C**H**$_2$), 2.68-2.93 (m, C**H**$_2$), 2.00-2.16(m, C**H**$_2$), 1.15-1.50 (m, C**H**$_2$), 0.70-0.92 (m, C**H**$_2$).

ZnNapth$_2$trien-IPDI-*m*-XDA (1:2:1): IR (KBr, cm^{-1}); 3360 (NH), 2922, 2854, 1689 (C=O), 1630(C=N), 1551, 1460, 1397, 1355, 1304, 1246, 1149, 1037, 946, 861, 830, 750. ^{1}H NMR (400 MHz, DMSO-d_6, ppm); δ 9.26-9.36 (m, C**H**=N), 8.67-8.38 (m, Ar-**H**), 8.22-8.35 (m, Ar-**H**), 8.14-8.22 (m, Ar-**H**), 7.99-8.12 (m, Ar-**H**), 7.85-7.98 (m, Ar-**H**), 7.70-7.76 (m, Ar-**H**), 7.56-7.66 (m, Ar-**H**), 7.49-7.55 (m, Ar-**H**), 7.41-7.47 (m, Ar-**H**), 7.29-7.37 (m, Ar-**H**), 7.13-7.25 (m, Ar-**H**), 6.98-7.09 (m, Ar-**H**), 6.80-6.72 (m, Ar-**H**), 6.07-6.24 (m, N**H**), 5.37-5.97 (m, N**H**), 4.06-4.15 (m, aliphatic-**H**), 3.62-3.70 (m, aliphatic-**H**), 3.02-3.11 (m, aliphatic-**H**), 2.90-3.01 (m, aliphatic-**H**), 2.62-2.89 (m, aliphatic-**H**), 1.97-2.12 (m, aliphatic-**H**), 1.33-1.57 (m, aliphatic-**H**), 0.64-1.09 (m, aliphatic-**H**).

ZnNapth$_2$trien-IPDI-HMDA (1:2:1): IR (KBr, cm^{-1}); 3375 (NH), 2924, 2852, 1669 (C=O), 1618(C=N), 1550, 1461, 1435, 1393, 1357, 1313, 1245, 1187, 1127, 1034, 992, 966, 895, 864, 832, 751. ^{1}H NMR (400 MHz, DMSO-d_6, ppm); δ 9.14-9.38 (m, C**H**=N), 8.03-8.16 (m , Ar-**H**), 7.92-8.02 (m, Ar-**H**), 7.56-7.75 (m, Ar-**H**), 7.28-7.44 (m, Ar-**H**), 7.07-7.23 (m, Ar-**H**), 6.96-7.05 (m, Ar-**H**), 6.70-6.78 (m, Ar-**H**), 5.44-5.78 (m, N**H**), 3.58-3.77 (m, aliphatic-**H**), 2.87-3.06 (m, aliphatic-**H**), 2.62-2.82 (m, aliphatic-**H**), 2.04-2.19 (m, aliphatic-**H**), 1.17-1.29 (m, aliphatic-**H**), 0.73-1.00 (m, aliphatic-**H**).

NiNapth$_2$trien-MDI-*m*-XDA (1:2:1): IR (KBr, cm^{-1}); 3316 (NH), 3029, 2913, 2848, 1656 (C=O), 1607(C=N), 1544, 1512, 1443, 1409, 1358, 1308, 1227, 1117, 1074, 1016, 950, 911, 817, 755.

NiNapth$_2$trien-MDI-HMDA (1:2:1): IR (KBr, cm^{-1}); 3346 (NH), 3047, 2925, 2855, 1673 (C=O), 1614(C=N), 1543, 1513, 1455, 1436, 1410, 1358, 1311, 1234, 1187, 1140, 1021, 946, 860, 823, 751.

NiNapth$_2$trien-IPDI-*m*-XDA (1:2:1): IR (KBr, cm^{-1}); 3353 (NH), 2924, 2855, 1660 (C=O), 1635(C=N), 1599, 1509, 1458, 1439, 1412, 1360, 1311, 1229, 1174, 1116, 1054, 1015, 972, 826, 750.

NiNapth$_2$trien-IPDI-HMDA (1:2:1): IR (KBr, cm^{-1}); 3366 (NH), 2922, 2856, 1670 (C=O), 1622(C=N), 1548, 1459, 1389, 1358, 1306, 1243, 1194, 1141, 1066, 1031, 964, 867, 828, 750.

3.3.2.3 Synthesis of metal-containing poly(urethane-urea)s from $MNapth_2trien$, diisocyanates and dialcohols

Metal-containing poly(urethane-urea)s were synthesized from $MNapth_2trien$ (where M = Zn and Ni), diisocyanates and dialcohols. The diisocyanates used were 4,4′-diphenylmethane diisocyanate (MDI) and isophorone diisocyanate (IPDI) and dialcohols used were 2,2-bis(4-Hydroxyphenyl)propane (BPO) and 1,6-hexamethylenediol (HDO). The mole ratios of $MNapth_2trien$: diisocyanate : dialcohol employed were 0.5:2:1.5, 1:2:1 and 1.5:2:0.5. $MNapth_2trien$ and dialcohol were dissolved in 5 mL of dried DMSO in a 50 mL, two-necked round bottomed flask equipped with a nitrogen inlet. Then, diisocyanate was dissolved in DMSO (2 mL) and added to the solution. Dibutyltin dilaurate was used as a catalyst and the reaction was maintained at 90 °C for 36 hours. Eventually, the hot solution was poured into distilled water to precipitate the polymer. The polymer was separated by filtration, washed with distilled methanol several times and dried in vacuo for 24 hours. Zinc-containing copoly(urethane-urea)s were obtained as yellow powder in 73-95% yield and nickel-containing copoly(urethane-urea)s were obtained as light brown powder in 53-89% yield. The compositions of starting materials in the preparation of polymers are shown in Tables 3.4 and 3.5.

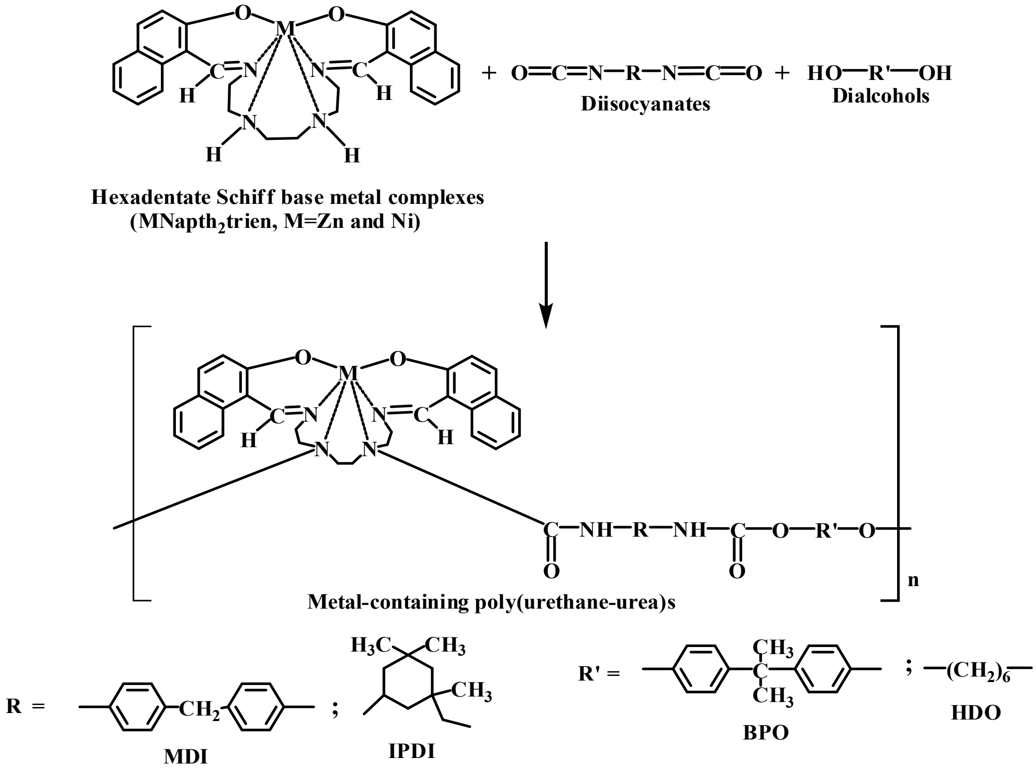

Scheme 3.5 Synthesis of metal-containing poly(urethane-urea)s

Table 3.4 Composition of starting materials in the preparation of metal-containing poly(urethane-urea)s based on ZnNapth$_2$trien

Polymer codes	**Weight of ZnNapth$_2$trien (g)**	**Weights of composition (g)**				**Yield (%)**
		MDI	**IPDI**	**BPA**	**HDO**	
ZnNapth$_2$trien-MDI-BPO (0.5:2:1.5)	0.259	0.500	-	0.342	-	89
ZnNapth$_2$trien-MDI-BPO (1:2:1)	0.517	0.500	-	0.228	-	73
ZnNapth$_2$trien-MDI-BPO (1.5:2:0.5)	0.776	0.500	-	0.114	-	86
ZnNapth$_2$trien-IPDI-BPO (0.5:2:1.5)	0.259	-	0.444	0.342	-	95
ZnNapth$_2$trien-IPDI-BPO (1:2:1)	0.517	-	0.444	0.228	-	79
ZnNapth$_2$trien-IPDI-BPO (1.5:2:0.5)	0.776	-	0.444	0.114	-	87
ZnNapth$_2$trien-MDI-HDO (0.5:2:1.5)	0.259	0.500	-	-	0.177	84
ZnNapth$_2$trien-MDI-HDO (1:2:1)	0.517	0.500	-	-	0.118	84
ZnNapth$_2$trien-MDI-HDO (1.5:2:0.5)	0.776	0.500	-	-	0.059	74
ZnNapth$_2$trien-IPDI-HDO (0.5:2:1.5)	0.259	-	0.444	-	0.177	95
ZnNapth$_2$trien-IPDI-HDO (1:2:1)	0.517	-	0.444	-	0.118	92
ZnNapth$_2$trien-IPDI-HDO (1.5:2:0.5)	0.776	-	0.444	-	0.059	74

Table 3.5 Composition of starting materials in the preparation of metal-containing poly(urethane-urea)s based on NiNapth$_2$trien

Polymer codes	**Weight of NiNapth$_2$trien (g)**	**Weights of composition (g)**				**Yield (%)**
		MDI	**IPDI**	**BPA**	**HDO**	
NiNapth$_2$trien-MDI-BPO (0.5:2:1.5)	0.255	0.500	-	0.342	-	77
NiNapth$_2$trien-MDI-BPO (1:2:1)	0.511	0.500	-	0.228	-	77
NiNapth$_2$trien-MDI-BPO (1.5:2:0.5)	0.766	0.500	-	0.114	-	89
NiNapth$_2$trien-IPDI-BPO (0.5:2:1.5)	0.255	-	0.444	0.342	-	84
NiNapth$_2$trien-IPDI-BPO (1:2:1)	0.511	-	0.444	0.228	-	81
NiNapth$_2$trien-IPDI-BPO (1.5:2:0.5)	0.766	-	0.444	0.114	-	80
NiNapth$_2$trien-MDI-HDO (0.5:2:1.5)	0.255	0.500	-	-	0.177	54
NiNapth$_2$trien-MDI-HDO (1:2:1)	0.511	0.500	-	-	0.118	53
NiNapth$_2$trien-MDI-HDO (1.5:2:0.5)	0.766	0.500	-	-	0.059	88
NiNapth$_2$trien-IPDI-HDO (0.5:2:1.5)	0.255	-	0.444	-	0.177	83
NiNapth$_2$trien-IPDI-HDO (1:2:1)	0.511	-	0.444	-	0.118	76
NiNapth$_2$trien-IPDI-HDO (1.5:2:0.5)	0.766	-	0.444	-	0.059	56

Since the copolymers obtained from different mole ratios have similar IR spectra, therefore, only the IR data of copolymers obtained from mole ratio of 1:2:1 are shown as follows:

MDI-BPO (1:1): IR (KBr, cm^{-1}); 3308 (NH), 2910, 2840, 1645 (C=O), 1597, 1545, 1511, 1410, 1308, 1234, 1108, 1011, 812, 649, 508. ^{1}H-NMR (400 MHz, DMSO-d_6, ppm); δ 8.53 (m, N**H**), 7.33-7.35 (m, Ar-**H**), 7.09-7.11 (m, Ar-**H**), 6.83-6.85 (m, Ar-**H**), 6.47-6.48 (m, Ar-**H**), 3.67-3.80 (m, C**H**$_2$) 1.18-1.33 (m, C**H**$_2$).

MDI-HDO (1:1): IR (KBr, cm^{-1}); 3323 (NH), 2930, 2851, 1706 (C=O), 1599, 1528, 1412, 1410, 1311, 1228, 1069, 816, 769, 508. ^{1}H-NMR (400 MHz, DMSO-d_6, ppm); δ 8.50 (m, N**H**), 7.32-7.33 (m, Ar-**H**), 7.05-7.07 (m, Ar-**H**), 4.03 (m, CH_2), 3.80 (m, CH_2), 1.20-1.59 (m, CH_2).

IPDI-BPO (1:1): IR (KBr, cm^{-1}); 3379(NH), 2953, 2921, 1647(C=O), 1556, 1466, 1383, 1366, 1306, 1239, 1148, 1065, 959, 926, 889, 869, 829, 769. ^{1}H-NMR (400 MHz, DMSO-d_6, ppm); δ 6.89-7.04 (m, Ar-**H**), 6.58-6.67 (m, Ar-**H**), 5.40-5.99 (m, N**H**), 3.57-3.77 (m, aliphatic-**H**), 2.68-2.83 (m, aliphatic-**H**), 1.37-1.63 (m, aliphatic-**H**), 0.61-1.30 (m, aliphatic-**H**).

IPDI-HDO (1:1): IR (KBr, cm^{-1}); 3370(NH), 2926, 2857, 1705(C=O), 1643, 1562, 1463, 1383, 1306, 1242, 1196, 1104, 1067, 865, 768, 722. ^{1}H-NMR (400 MHz, DMSO-d_6, ppm); δ 5.48-5.98 (m, N**H**), 4.26-4.43 (m, aliphatic-**H**), 3.83-4.07 (m, aliphatic-**H**), 3.57-3.78 (m, aliphatic-**H**), 2.60-2.87 (m, aliphatic-**H**), 2.21-2.30 (m, aliphatic-**H**), 1.34-1.65 (m, aliphatic-**H**), 0.63-1.03 (m, aliphatic-**H**).

ZnNapth$_2$trien-MDI-BPO (1:2:1): IR (KBr, cm^{-1}); 3334 (NH), 3035, 2920, 2852, 1667 (C=O), 1617 (C=N), 1591, 1541, 1510, 1459, 1432, 1411, 1354, 1307, 1233, 1175, 1117, 1020, 946, 829, 750. ^{1}H-NMR (400 MHz, DMSO-d_6, ppm); δ 9.09-9.30 (m, C**H**=N), 8.46-8.55 (m, N**H**), 7.92-8.14 (m, Ar-**H**), 7.56-7.78 (m, Ar-**H**), 7.46-7.54 (m, Ar-**H**), 7.24-7.44 (m, Ar-**H**), 7.18-7.24 (m, Ar-**H**), 7.00-7.14 (m, Ar-**H**), 6.76-6.94 (m, Ar-**H**), 6.60-6.74 (m, Ar-**H**), 6.42-6.52 (m, Ar-**H**), 4.72-4.89 (m, N**H**), 3.76-3.86 (m, CH_2), 3.42-3.74 (m, CH_2), 2.95-3.04 (m, CH_2), 2.87-2.94 (m, CH_2), 2.71-2.75 (m, CH_2), 2.53-2.55 (m, CH_2), 1.45-1.66 (m, CH_2), 1.11-1.28 (m, CH_2).

ZnNapth$_2$trien-MDI-HDO (1:2:1): IR (KBr, cm^{-1}); 3339 (NH), 3046, 2922, 2853, 1670 (C=O), 1619 (C=N), 1540, 1512, 1460, 1413, 1358, 1308, 1233, 1180, 1133, 1117, 1021, 958, 911, 861, 824, 749. ^{1}H-NMR (400 MHz, DMSO-d_6, ppm); δ 9.18-9.28 (m, C**H**=N), 8.45-8.59 (m, N**H**), 7.90-8.14 (m, Ar-**H**), 7.60-7.64 (m, Ar-**H**), 7.44-7.54 (m, Ar-**H**), 7.26-7.40 (m, Ar-**H**), 6.93-7.16 (m, Ar-**H**), 6.73-6.90 (m, Ar-**H**), 6.55-6.67 (m, Ar-**H**), 6.41-6.55 (m, Ar-**H**), 4.79-4.90 (m, N**H**), 4.28-4.37 (m, CH_2), 3.74-3.85 (m, CH_2), 3.61-3.72 (m, CH_2), 2.95-3.04 (m, CH_2), 2.86-2.91 (m, CH_2), 2.68-2.78 (m, CH_2), 1.34-1.46 (m, CH_2), 1.24-1.33 (m, CH_2), 1.10-1.24 (m, CH_2).

ZnNapth$_2$trien-IPDI-BPO (1:2:1): IR (KBr, cm^{-1}); 3365 (NH), 2921, 2855, 1669 (C=O), 1627 (C=N), 1550, 1510, 1461, 1393, 1359, 1308, 1241, 1183, 1141, 1113, 1027, 969, 952, 833, 755. ^{1}H-NMR (400 MHz, DMSO-d_6, ppm); δ 9.26-9.36 (m, C**H**=N), 7.99-8.12 (m, Ar-**H**), 7.54-7.73 (m, Ar-**H**), 7.18-7.49 (m, Ar-**H**), 7.02-7.18 (m, Ar-**H**), 6.90-7.01 (m, Ar-**H**), 6.77-6.87 (m, Ar-**H**), 6.56-6.65 (m, Ar-**H**), 5.37-5.96 (m, N**H**), 3.54-3.74 (m, aliphatic-**H**), 2.90-3.01 (m, aliphatic-**H**), 2.62-2.89 (m, aliphatic-**H**), 1.97-2.12 (m, aliphatic-**H**), 1.40-1.57 (m, aliphatic-**H**), 0.60-1.29 (m, aliphatic-**H**).

ZnNapth$_2$trien-IPDI-HDO (1:2:1): IR (KBr, cm^{-1}); 3376 (NH), 2923, 2860, 1669 (C=O), 1622 (C=N), 1545, 1462, 1435, 1416, 1392, 1358, 1305, 1245, 1186, 1139, 1034, 957, 863, 832, 750. ^{1}H-NMR (400 MHz, DMSO-d_6, ppm); δ 9.06-9.27 (m, C**H**=N), 8.16-8.26 (m, Ar-**H**), 7.88-8.12 (m, Ar-**H**), 7.42-7.75 (m, Ar-**H**), 7.20-7.35 (m, Ar-**H**), 6.91-7.15 (m, Ar-**H**), 6.65-6.80 (m, Ar-**H**), 5.37-5.94 (m, N**H**), 3.75-3.90 (m, aliphatic-**H**), 3.57-3.72 (m, aliphatic-**H**), 2.85-3.01 (m, aliphatic-**H**), 2.58-2.71 (m, aliphatic-**H**), 2.06-1.98 (m, aliphatic-**H**), 1.30-1.63 (m, aliphatic-**H**), 1.01-1.29 (m, aliphatic-**H**), 0.62-1.00 (m, aliphatic-**H**).

NiNapth$_2$trien-MDI-BPO (1:2:1): IR (KBr, cm^{-1}); 3414 (NH), 2924, 2856, 1684 (C=O), 1616 (C=N), 1541, 1512, 1463, 1436, 1410, 1355, 1311, 1235, 1183, 1144, 1090, 1021, 969, 824, 750.

NiNapth$_2$trien-MDI-HDO (1:2:1): IR (KBr, cm^{-1}); 3312 (NH), 2923, 2854, 1688 (C=O), 1618 (C=N), 1544, 1512, 1459, 1435, 1410, 1354, 1309, 1235, 1186, 1139, 1124, 1021, 976, 953, 855, 824, 750.

NiNapth$_2$trien-IPDI-BPO (1:2:1): IR (KBr, cm^{-1}); 3390 (NH), 2923, 2856, 1674 (C=O), 1623 (C=N), 1546, 1513, 1461, 1439, 1412, 1390, 1358, 1307, 1243, 1183, 1140, 1093, 1033, 953, 891, 831, 750.

NiNapth$_2$trien-IPDI-HDO (1:2:1): IR (KBr, cm^{-1}); 3375 (NH), 2925, 2856, 1681 (C=O), 1618 (C=N), 1551, 1460, 1427, 1412, 1389, 1361, 1309, 1245, 1187, 1140, 1035, 953, 895, 864, 826, 750.

3.3.2.4 Synthesis of metal-containing poly(urea-imide)s from MNapth$_2$trien, diisocyanates and dianhydrides

Poly(urea-imide)s were synthesized from MNapth$_2$trien (where M = Zn and Ni), diisocyanates and dianhydrides. The diisocyanates used were 4,4′-diphenylmethane diisocyanate (MDI) and isophorone diisocyanate (IPDI) and dianhydrides used were pyromellitic dianhydride (PMDA) and benzophenone-3,3′,4,4′-tetracarboxylic dianhydride (BTDA). The mole ratio of MNapth$_2$trien :

diisocyanate : dianhydride employed were 1:2:0.5 and 1:2:1 as shown in Tables 3.6-3.7. A solution of diisocyanate (2.0 mmol) in DMSO (5 mL) was added to the solution of $MNapth_2trien$ (1.0 mmol) in DMSO (2 mL) under nitrogen atmosphere at room temperature. Dibutyltin dilaurate (0.04 mL, 0.067 mmol) was then added. The reaction was heated at 90°C for 12 hours to give isocyanate terminated prepolymers. The reaction mixture was cooled to room temperature. Dianhydride (0.5 mmol; mole ratio 1:2:0.5, 1.0 mmol; mole ratio 1:2:1) in DMSO was added into the reaction, followed by stirring at room temperature for 30 min. It was then heated to 90°C and maintained for 2 hours. Carbon dioxide gas evolution was observed at this temperature. The temperature of the reaction was raised to 110°C and maintained for 24 hours. The solution was poured into methanol and the precipitated compound was filtered and washed several times with methanol and then dried under vacuum for 48 hours. The yields obtained for metal-containing poly(urea-imide)s were 52-92%.

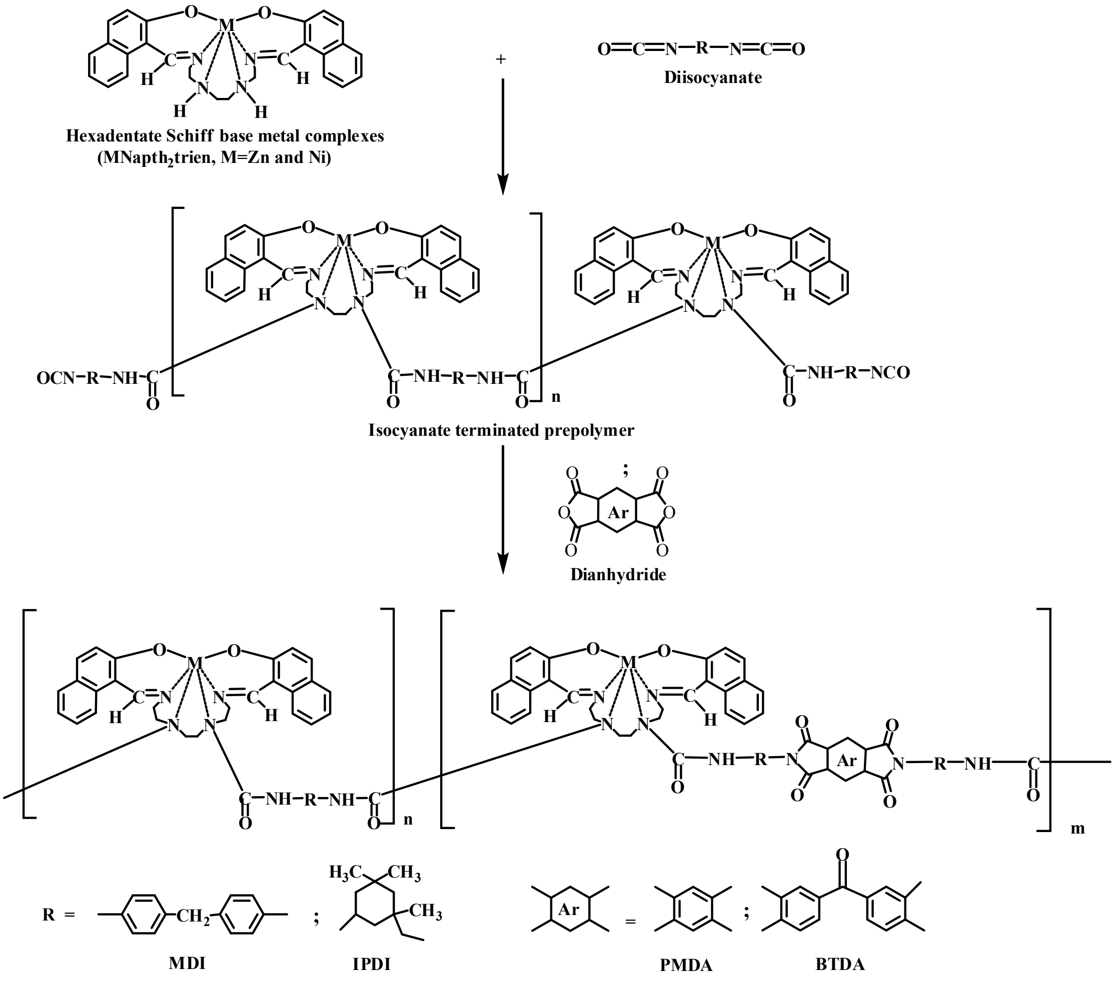

Scheme 3.6 Synthesis of metal-containing poly(urea-imide)s

Table 3.6 Composition of starting materials in the preparation of metal-containing poly(urea-imide)s based on ZnNapth$_2$trien

Polymer codes	**Weight of ZnNapth$_2$trien (g)**	**Weights of composition (g)**				**Yield (%)**
		MDI	**IPDI**	**PMDA**	**BTDA**	
ZnNapth$_2$trien-MDI-PMDA (1:2:0.5)	0.517	0.500	-	0.109	-	77
ZnNapth$_2$trien-MDI-PMDA (1:2:1)	0.517	0.500	-	0.218	-	72
ZnNapth$_2$trien-IPDI-PMDA(1:2:0.5)	0.517	-	0.444	0.109	-	89
ZnNapth$_2$trien-IPDI-PMDA (1:2:1)	0.517	-	0.444	0.218	-	90
ZnNapth$_2$trien-MDI-BTDA (1:2:0.5)	0.517	0.500	-	-	0.161	92
ZnNapth$_2$trien-MDI-BTDA (1:2:1)	0.517	0.500	-	-	0.322	89
ZnNapth$_2$trien-IPDI-BTDA (1:2:0.5)	0.517	-	0.444	-	0.161	66
ZnNapth$_2$trien-IPDI-BTDA (1:2:0.5)	0.517	-	0.444	-	0.322	54

Table 3.7 Composition of starting materials in the preparation of metal-containing poly(urea-imide)s based on NiNapth$_2$trien

Polymer codes	**Weight of NiNapth$_2$trien (g)**	**Weights of composition (g)**				**Yield (%)**
		MDI	**IPDI**	**PMDA**	**BTDA**	
NiNapth$_2$trien-MDI-PMDA (1:2:0.5)	0.511	0.500	-	0.109	-	87
NiNapth$_2$trien-MDI-PMDA (1:2:1)	0.511	0.500	-	0.218	-	86
NiNapth$_2$trien-IPDI-PMDA(1:2:0.5)	0.511	-	0.444	0.109	-	52
NiNapth$_2$trien-IPDI-PMDA (1:2:1)	0.511	-	0.444	0.218	-	89
NiNapth$_2$trien-MDI-BTDA (1:2:0.5)	0.511	0.500	-	-	0.161	68
NiNapth$_2$trien-MDI-BTDA (1:2:1)	0.511	0.500	-	-	0.322	80
NiNapth$_2$trien-IPDI-BTDA (1:2:0.5)	0.511	-	0.444	-	0.161	88
NiNapth$_2$trien-IPDI-BTDA (1:2:0.5)	0.511	-	0.444	-	0.322	84

Since the copolymers obtained from different mole ratios of MNapth$_2$trien : diisocyanate : dianhydride have similar IR and ^{1}H NMR spectra, therefore, only the IR and ^{1}H NMR data of copolymers obtained from mole ratio of 1:2:1 are shown as follows:

MDI-PMDA (1:1): IR (KBr, cm^{-1}); 3421, 3036, 3000, 1776 (C=O), 1724 (C=O), 1605, 1510, 1371, 1273, 1211, 1118, 1019, 948, 872, 805, 779, 723. ^{1}H NMR (400 MHz, DMSO-*d$_6$,* ppm); δ 8.27-8.37 (2H, m, Ar-**H**), 7.02-7.51 (8H, m, Ar-**H**), 2.10-2.30 (2H, m, C**H**$_2$).

MDI-BTDA (1:1): IR (KBr, cm^{-1}); 3476, 2925, 2855, 1778 (C=O), 1722 (C=O), 1667, 1601, 1512, 1419, 1376, 1289, 1243, 1213, 1165, 1096, 1017, 945, 861, 812, 753, 721. ^{1}H NMR (400 MHz, DMSO-*d$_6$,* ppm); δ 8.07-8.49 (4H, m, Ar-**H**), 7.84-8.01 (1H, m, Ar-**H**), 7.30-7.60 (4H, m, Ar-**H**), 6.94-7.28 (1H, m, Ar-**H**), 3.89-4.30 (2H, m, C**H**$_2$), 2.13-2.22 (2H, m, C**H**$_2$).

IPDI-PMDA (1:1): IR (KBr, cm^{-1}); 3465, 2954, 2921, 1771 (C=O), 1715 (C=O), 1556, 1463, 1429, 1346, 1250, 1150, 1096, 1029, 949, 915, 820, 785, 731. ^{1}H NMR (400 MHz, DMSO-*d$_6$,* ppm); δ 7.83-8.60 (2H, m, Ar-**H**), 4.18-4.52 (1H, m, aliphatic-H), 1.75-2.19 (2H, m, aliphatic-**H**), 0.48-1.71(14H, m, aliphatic-**H**).

IPDI-BTDA (1:1): IR (KBr, cm^{-1}); 3470, 2926, 2858, 1774 (C=O), 1716 (C=O), 1672, 1619, 1562, 1466, 1427, 1367, 1294, 1250, 1184, 1156, 1099, 1031, 953, 865, 779, 727. ^{1}H NMR (400 MHz, DMSO-*d$_6$,* ppm); δ 7.71-8.25 (6H, m, Ar-**H**), 1.83-2.35 (4H, m, aliphatic-**H**), 0.73-1.13(13H, m, aliphatic-**H**).

ZnNapth$_2$trien-MDI-PMDA (1:2:1): IR (KBr, cm^{-1}); 3422 (NH), 2924, 2854, 1773 (C=O), 1721 (C=O), 1617 (C=N), 1539, 1511, 1459, 1429, 1390, 1363, 1313, 1207, 1181, 1123, 1040, 1017, 974, 914, 825, 749. ^{1}H NMR (400 MHz, DMSO-*d$_6$,* ppm); δ 9.53-9.61 (m, C**H**=N), 8.36-8.61(m, N**H**), 7.81-7.90 (m, Ar-**H**), 7.67-7.80 (m, Ar-**H**), 7.44-7.58 (m, Ar-**H**), 7.21-7.40 (m, Ar-**H**), 7.09-7.15 (m, Ar-**H**), 6.89-6.98 (m, Ar-**H**), 6.83-6.89 (m, Ar-**H**), 6.72-6.83 (m, Ar-**H**), 6.35-6.50 (m, Ar-**H)**, 4.67-4.94 (m, N**H**), 3.82-3.93 (m, C**H**$_2$), 3.70-3.79 (m, C**H**$_2$), 3.58-3.66 (m, C**H**$_2$), 2.92-2.98 (m, C**H**$_2$), 2.62-2.73 (m, C**H**$_2$), 2.28-2.37 (m, C**H**$_2$).

ZnNapth$_2$trien-MDI-BTDA (1:2:1): IR (KBr, cm^{-1}); 3350 (NH), 2921, 2851, 1775 (C=O), 1716 (C=O), 1662, 1617 (C=N), 1539, 1511, 1463, 1387, 1304, 1239, 1184, 1118, 1096, 1021, 952, 828, 746, 724. ^{1}H NMR (400 MHz, DMSO-*d$_6$,* ppm); δ 9.51-9.64 (m, C**H**=N), 8.30-8.64 (m, N**H**), 7.64-8.30 (m, Ar-**H**), 7.90-8.25 (m, Ar-**H**), 7.80-7.89 (m, Ar-**H**), 7.61-7.77 (m, Ar-**H**), 7.44-7.57 (m, Ar-**H**), 7.22-7.41(m, Ar-**H**), 6.98-7.20 (m, Ar-**H**), 6.90-6.98 (m, Ar-**H**), 6.84-6.88 (m, Ar-**H**), 6.38-6.51 (m, Ar-**H**), 3.54-4.06 (m, C**H**$_2$), 3.20-3.27 (m, C**H**$_2$), 2.90-3.01 (m, C**H**$_2$), 2.54-2.60 (m, C**H**$_2$).

ZnNapth$_2$trien-IPDI-PMDA (1:2:1): IR (KBr, cm^{-1}); 3380 (NH), 2922, 2855, 1775 (C=O), 1716 (C=O), 1622 (C=N), 1546, 1461, 1430, 1391, 1296, 1245, 1187, 1139, 1096, 1023, 951, 838, 748, 726. ^{1}H NMR (400 MHz, DMSO-*d$_6$,* ppm); δ 9.01-9.30 (m, C**H**=N), 7.96-8.25 (m, Ar-**H**), 7.87-7.95 (m, Ar-**H**), 7.78-7.85 (m, Ar-**H**), 7.67-7.76 (m, Ar-**H**), 7.57-7.66 (m, Ar-**H**), 7.34-7.49 (m, Ar-**H**), 7.07-7.27 (m, Ar-**H**), 6.64-6.76 (m, Ar-**H**), 5.45-5.99 (m, N**H**), 3.80-4.02 (m, aliphatic-**H**), 2.61-3.03 (m, aliphatic-**H**), 2.27-2.35 (m, aliphatic-**H**), 1.66-1.85 (m, aliphatic-**H**), 1.27-1.66 (m, aliphatic-**H**), 0.71-1.27 (m, aliphatic-**H**).

ZnNapth$_2$trien-IPDI-BTDA (1:2:1): IR (KBr, cm^{-1}); 3405 (NH), 2925, 2860, 1775 (C=O), 1716 (C=O), 1625 (C=N), 1549, 1496, 1426, 1391, 1363, 1294, 1244, 1187, 1153, 1123, 1094, 1021, 952, 840, 725. ^{1}H NMR (400 MHz, DMSO-*d$_6$,* ppm) ; δ 9.02-9.60 (m, C**H**=N), 7.90-8.36 (m, Ar-**H**), 7.55-7.88 (m, Ar-**H**), 7.33-7.50 (m, Ar-**H**), 7.10-7.28 (m, Ar-**H**), 6.64-7.02 (m, Ar-**H**), 5.38-5.98 (m, N**H**), 3.83-4.19 (m, aliphatic-**H**), 3.57-3.83 (m, aliphatic-**H**), 3.44-3.57 (m, aliphatic-**H**), 2.97-3.01 (m, aliphatic-**H**), 2.60-2.88 (m, aliphatic-**H**), 1.30-1.82 (m, aliphatic-**H**), 0.55-1.27 (m, aliphatic-**H**).

NiNapth$_2$trien-MDI-PMDA (1:2:1): IR (KBr, cm^{-1}); 3380 (NH), 2924, 2855, 1772 (C=O), 1722 (C=O), 1617 (C=N), 1543, 1513, 1456, 1406, 1370, 1313, 1230, 1185, 1124, 1015, 962, 826, 749, 723.

NiNapth$_2$trien-MDI-BTDA (1:2:1): IR (KBr, cm^{-1}); 3365 (NH), 2923, 2848, 1775 (C=O), 1717 (C=O), 1670, 1607 (C=N), 1539, 1512, 1434, 1407, 1372, 1308, 1235, 1195, 1118, 1095, 1022, 953, 853, 826, 751, 723.

NiNapth$_2$trien-IPDI-PMDA (1:2:1): IR (KBr, cm^{-1}); 3410 (NH), 2925, 2855, 1766 (C=O), 1717 (C=O), 1622 (C=N), 1547, 1459, 1353, 1248, 1204, 1148, 1113, 1035, 970, 827, 747, 726.

NiNapth$_2$trien-IPDI-BTDA (1:2:1): IR (KBr, cm^{-1}); 3482 (NH), 2951, 2856, 1773 (C=O), 1713 (C=O), 1625 (C=N), 1547, 1456, 1436, 1387, 1364, 1299, 1247, 1198, 1155, 1125, 1102, 1038, 992, 965, 833, 746, 726.

3.3.2.5 Synthesis of metal-containing poly(urethane-urea-imide)s from MNapth$_2$trien, diisocyanates, PEG400 and dianhydrides

Poly(urethane-urea-imide)s were synthesized from MNapth$_2$trien (where M = Zn and Ni), diisocyanates, polyethylene glycol (PEG400) and dianhydrides. The diisocyanates used were 4,4′-diphenylmethane diisocyanate (MDI) and isophorone diisocyanate (IPDI) and dianhydride used were pyromellitic dianhydride (PMDA) and benzophenone-3,3′,4,4′-tetracarboxylic dianhydride (BTDA). The mole ratio of MNapth$_2$trien : diisocyanate/PEG400 : dianhydride employed 1:2:1. A solution of diisocyanate (2.0 mmol) in DMSO (5 mL) was added to the solution of PEG400 (1.0 mmol) in DMSO (2 mL) under nitrogen atmosphere at room temperature. Dibutyltin dilaurate (0.04 mL, 0.067 mmol) was then added. The reaction was heated at 90^{o}C for 30 min (MDI) or 40 min (IPDI) to give isocyanate terminated prepolymers. The amount of residue isocyanate was determined by titration with *n*-butylamine. MNapth$_2$trien (0.5 mmol) in DMSO was added into the reaction and stirring 30 min. The reaction mixture was cooled to room temperature. Dianhydride (0.5 mmol) in DMSO was added into the reaction, followed by stirring at room temperature for 30 min. It was then heated to 90^{o}C and maintained for 2 hours. Carbon dioxide gas evolution was observed at this temperature. The temperature of the reaction was raised to 110°C and maintained for 24 hours. The solution was poured into methanol and the precipitated compound was filtered and washed several times with methanol and then dried under vacuum for 48 hours. The yields obtained for metal-containing poly(urethane-urea-imide)s were 78-89%. The compositions of starting materials in the preparation of polymers are shown in Tables 3.8 and 3.9.

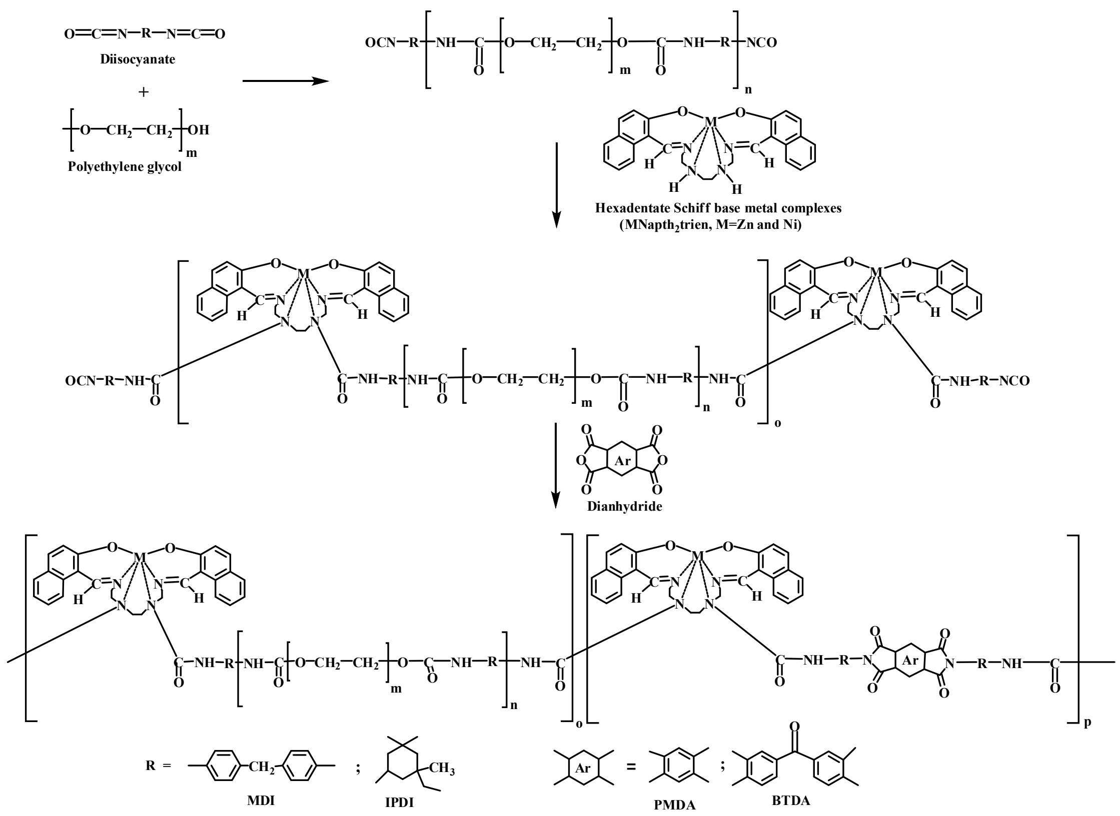

Scheme 3.7 Synthesis of metal-containing poly(urethane-urea-imide)s

Table 3.8 Composition of starting materials in the preparation of metal-containing poly(urethane-urea-imide)s based on ZnNapth$_2$trien

Polymer codes	Weight of ZnNapth$_2$trien (g)	Weights of composition (g)					Yield (%)
		MDI	IPDI	PEG 400	PMDA	BTDA	
ZnNapth$_2$trien-MDI/PEG400-PMDA	0.259	0.500	-	0.400	0.109	-	89
ZnNapth$_2$trien-IPDI/PEG400-PMDA	0.259	-	0.444	0.400	0.109	-	85
ZnNapth$_2$trien-MDI/PEG400-BTDA	0.259	0.500	-	0.400	-	0.161	84
ZnNapth$_2$trien-IPDI/PEG400-BTDA	0.259	-	0.444	0.400	-	0.161	78

Table 3.9 Composition of starting materials in the preparation of metal-containing poly(urethane-urea-imide)s based on NiNapth$_2$trien

Polymer codes	Weight of NiNapth$_2$trien (g)	Weights of composition (g)					Yield (%)
		MDI	IPDI	PEG 400	PMDA	BTDA	
NiNapth$_2$trien-MDI/PEG400-PMDA	0.255	0.500	-	0.400	0.109	-	85
NiNapth$_2$trien-IPDI/PEG400-PMDA	0.255	-	0.444	0.400	0.109	-	87
NiNapth$_2$trien-MDI/PEG400-BTDA	0.255	0.500	-	0.400	-	0.161	82
NiNapth$_2$trien-IPDI/PEG400-BTDA	0.255	-	0.444	0.400	-	0.161	80

IR data of copolymers are shown as follows:

ZnNapth$_2$trien-MDI/PEG400-PMDA : IR (KBr, cm^{-1}); 3350 (NH), 2875, 1772 (C=O), 1718 (C=O), 1662, 1606 (C=N), 1513, 1411, 1309, 1230, 1109, 947, 821, 759, 725.

ZnNapth$_2$trien-MDI/PEG400-BTDA: IR (KBr, cm^{-1}); 3352 (NH), 2875, 1774 (C=O), 1714 (C=O), 1660, 1617 (C=N), 1534, 1513, 1412, 1306, 1234, 1098, 949, 827, 759, 724.

NiNapth$_2$trien-MDI/PEG400-PMDA : IR (KBr, cm^{-1}); 3334 (NH), 2871, 1773 (C=O), 1722 (C=O), 1660, 1604 (C=N), 1534, 1514, 1458, 1411, 1365, 1311, 1227, 1074, 946, 822, 758, 725.

NiNapth$_2$trien-MDI/PEG400-BTDA: IR (KBr, cm^{-1}); 3359 (NH), 2873, 1775 (C=O), 1717 (C=O), 1660, 1605 (C=N), 1535, 1514, 1410, 1364, 1309, 1228, 1097, 948, 824, 755, 725.

ZnNapth$_2$trien-IPDI/PEG400-PMDA) : (KBr, cm^{-1}); 3392 (NH), 2947, 1772 (C=O), 1720 (C=O), 1634 (C=N), 1546, 1465, 1362, 1306, 1244, 1103, 949, 833, 750.

ZnNapth$_2$trien-IPDI/PEG400-BTDA: IR (KBr, cm^{-1}); 3389 (NH), 2902, 1774 (C=O), 1719 (C=O), 1633(C=N), 1549, 1463, 1360, 1301, 1244, 1103, 946, 837, 752, 726.

NiNapth$_2$trien-IPDI/PEG400-PMDA: IR (KBr, cm^{-1}); 3380 (NH), 2907, 1774 (C=O), 1720 (C=O), 1655, 1628 (C=N), 1551, 1462, 1385, 1360, 1246, 1102, 947, 832, 752.

NiNapth$_2$trien-IPDI/PEG400-BTDA: IR (KBr, cm^{-1}); 3376 (NH), 2908, 1774 (C=O), 1718 (C=O), 1663, 1625 (C=N), 1546, 1460, 1384, 1364, 1303, 1244, 1098, 948, 863, 832, 749, 725.

CHAPTER IV

RESULTS AND DISCUSSION

4.1 Synthesis of hexadentate Shiff base metal complexes

Hexadentate Schiff base metal complexes were synthesized following the synthetic route described in the literature [43]. The reaction between 2-hydroxy-1-naphthaldehyde and metal (II) acetate in methanol formed a template intermediate. Subsequently, the solution of triethylenetetramine was then added to obtain metal complexes (MNapth$_2$trien; M = Zn and Ni) as shown in Scheme 4.1

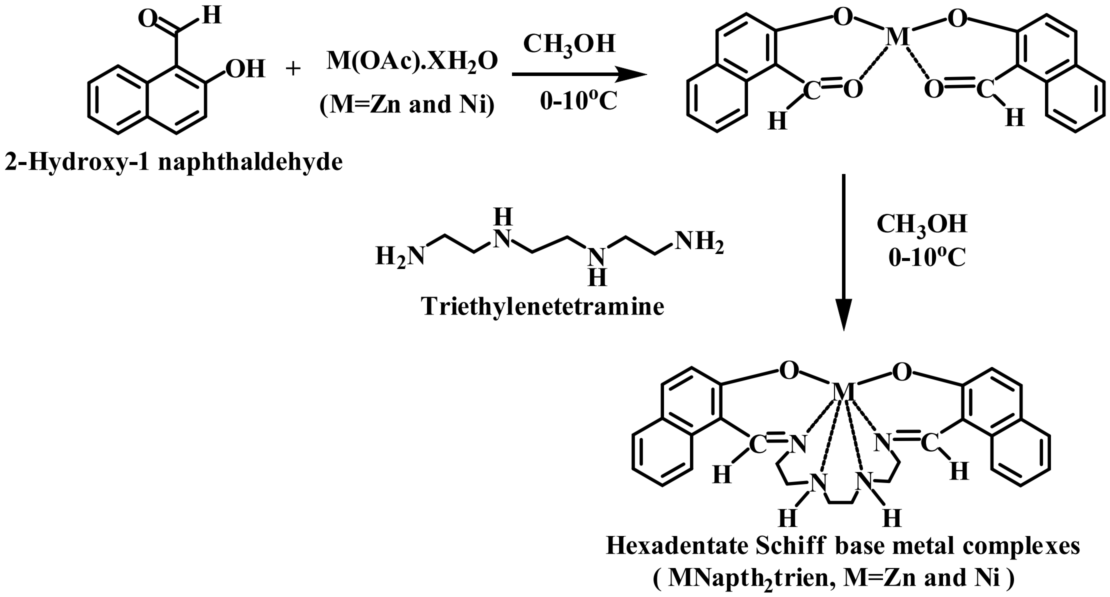

Scheme 4.1 Synthesis of hexadentate Shiff base metal complexes

ZnNapth$_2$trien and NiNapth$_2$trien metal complexes were obtained as yellow and brown solid, respectively. The metal complexes were soluble in toluene dichloromethane, chloroform, tetrahydrofuran, dimethyl formamide and dimethyl sulphoxide, and, partial soluble in methanol and acetonitrile, insoluble in hexane and water.

4.1.1 Characterization of hexadentate Shiff base metal complexes

4.1.1.1 IR spectroscopy of metal complexes

IR spectrum of ZnNapth$_2$trien exhibited absorption band of NH stretching at 3340 cm^{-1}, C=N stretching at 1619 cm^{-1} and aromatic C=C stretching at 1533 cm^{-1}. IR spectrum of NiNapth$_2$trien exhibited absorption band of NH stretching at 3438 cm^{-1}, C=N stretching at 1623 cm^{-1} and aromatic C=C stretching at 1533 cm^{-1}. Figure 4.1 shows IR spectra of metal complexes.

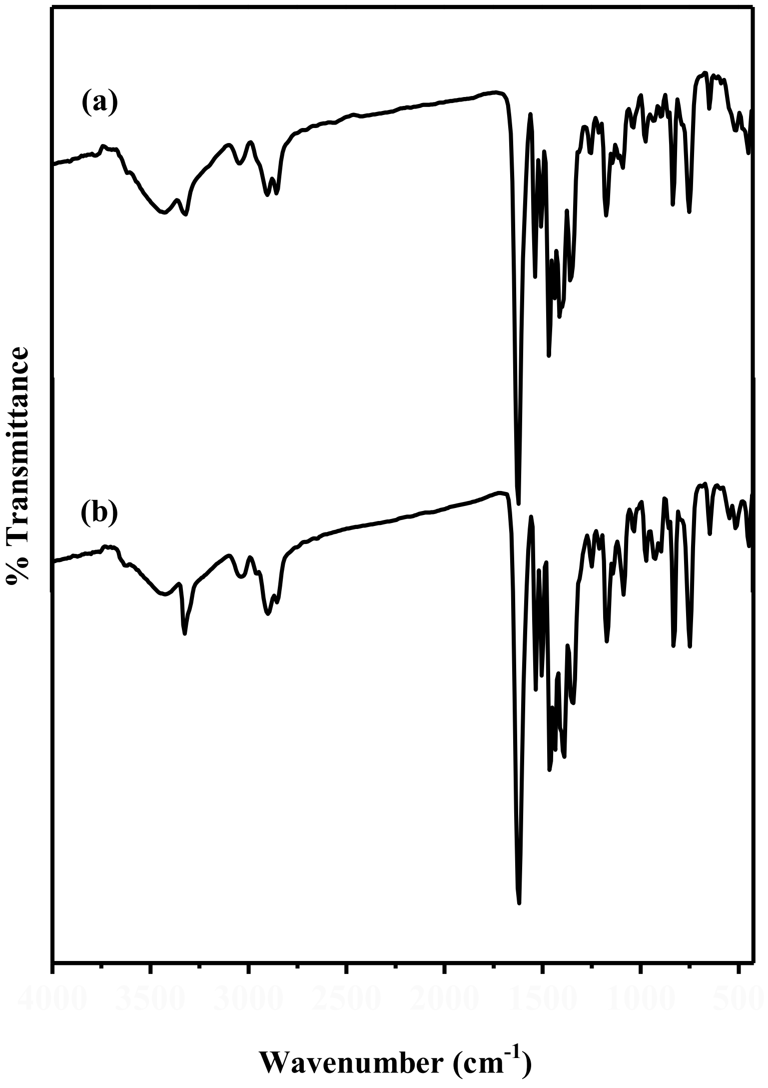

Figure 4.1 IR spectra of (a) ZnNapth$_2$trien; (b) NiNapth$_2$trien

4.1.1.2 ^{1}H NMR spectroscopy of ZnNapth$_2$trien

^{1}H and ^{13}C NMR spectra of ZnNapth$_2$trien are shown in Figure 4.2-4.3. The characteristic imine -CH=N- proton and carbon were appeared at 9.21 and 172.60 ppm, respectively. The aromatic protons and carbons were observed at 6.62-8.06 and 107.44-161.50 ppm, respectively. The peaks at 2.37-3.93 and 43.46-55.78 ppm were due to the methylene protons and carbons, respectively. The NMR spectra of NiNapth$_2$trien could not be obtained since the complex was 6-coordinated and therefore paramagnetic. Only 4-coordinated nickel complex with square planar geometry was diamagnetic and gave NMR signals.

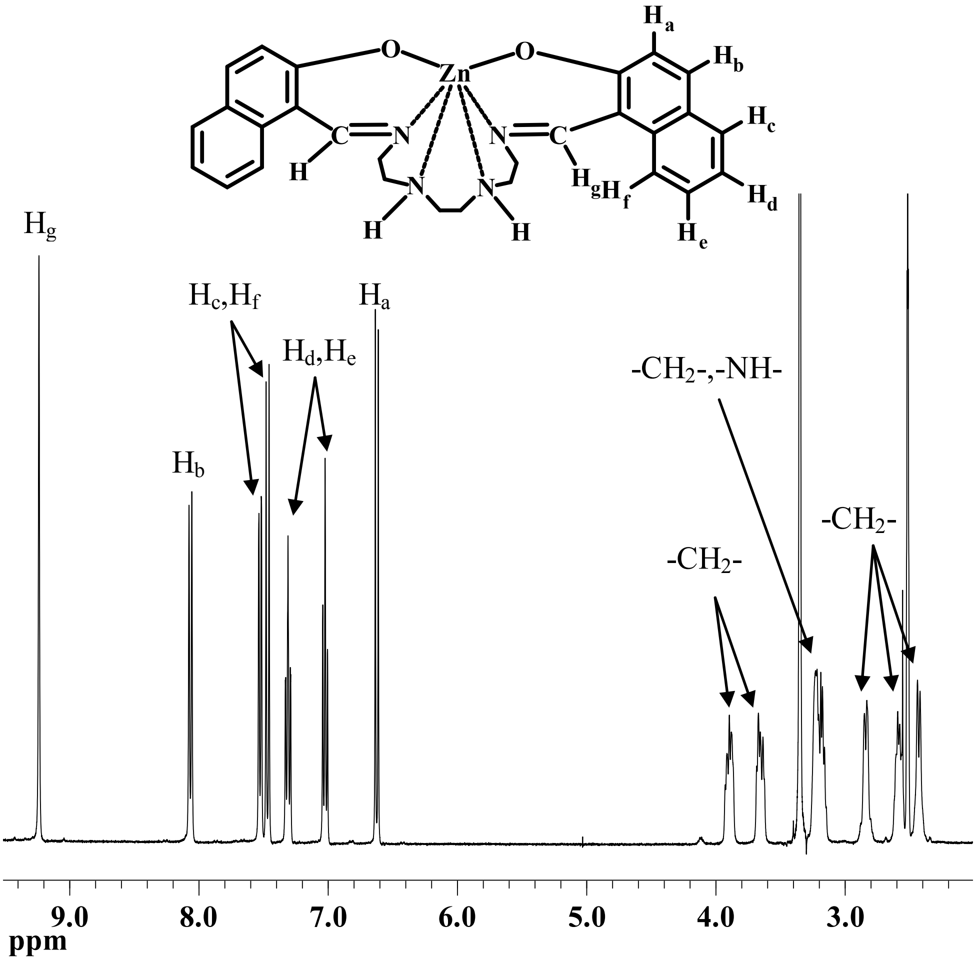

Figure 4.2 ^{1}H NMR spectrum of ZnNapth$_2$trien in DMSO-d_6

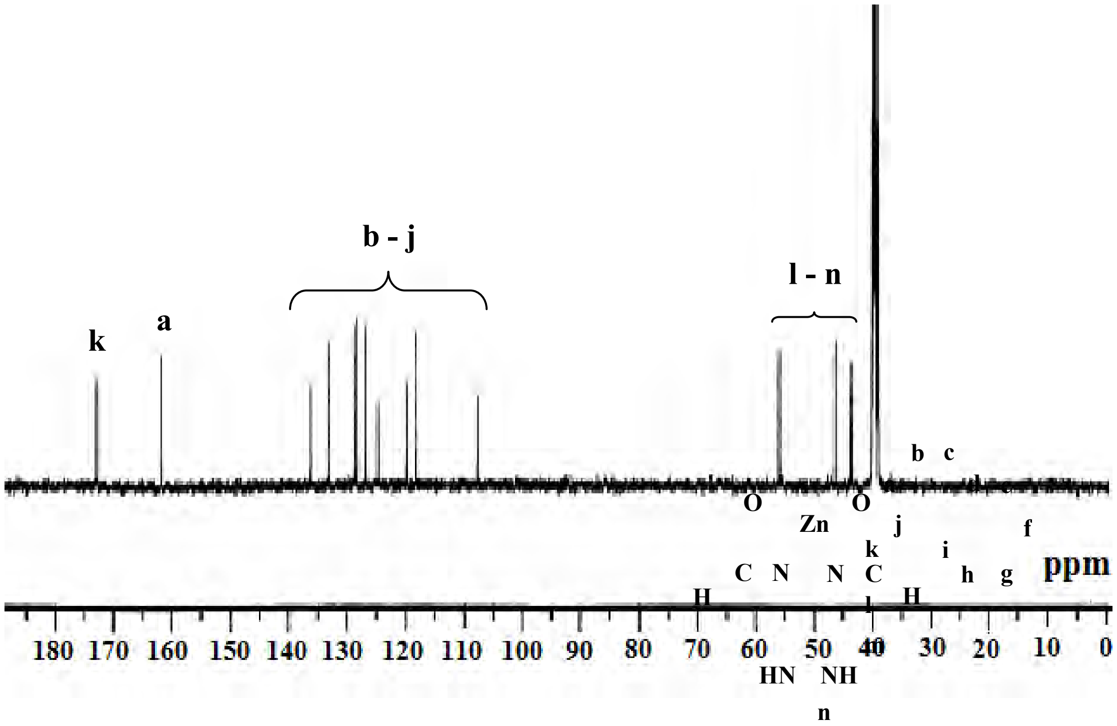

Figure 4.3 ^{13}C NMR spectrum of ZnNapth$_2$trien

4.1.1.3 Elemental analysis

Table 4.1 indicates the possible molecular formula and weight of zinc complexes. MS data of both zinc and nickel complexes give the corresponding molecular formula. Analytical data showed that the experimentally determined percentage values of carbon, hydrogen and nitrogen are within the calculated values.

Table 4.1 Analytical data of metal complexes

Metal complex	Formula	Analytical data found (calculated) (%)			*m/z*
		C	H	N	
ZnNapth$_2$trien	$C_{28}H_{28}N_4O_2Zn.1/2H_2O$	63.47 (63.81)	5.33 (5.55)	10.44 (10.63)	518.79
NiNapth$_2$trien	$C_{28}H_{28}N_4O_2Ni.1/2H_2O$	64.61 (64.64)	5.52 (5.63)	11.02 (10.77)	511.14

4.1.1.4 Thermogravimetric analysis

Thermal properties of zinc and nickel complexes were investigated using thermogravimetric analysis (TGA) as shown in Figure 4.4. Weight loss percentage and initial decomposition temperatures are given in Table 4.2. It was found that zinc and nickel complexes were stable up to 298 and 280°C, respectively.

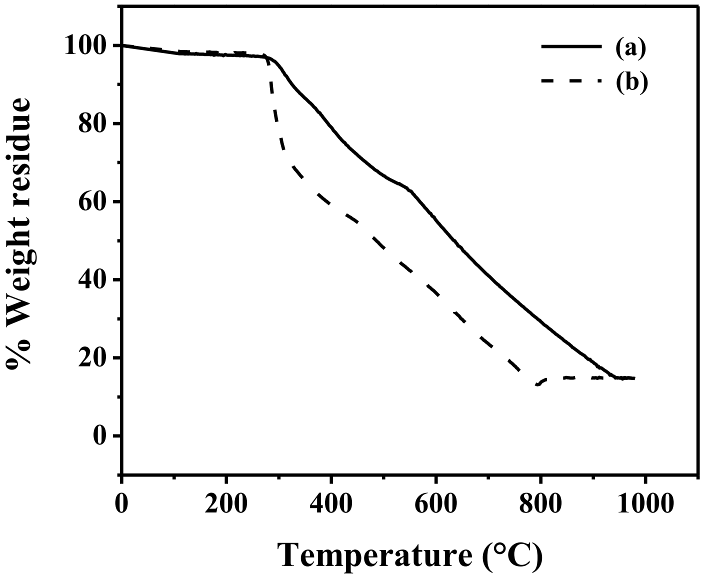

Figure 4.4 TGA thermograms of (a) $ZnNapth_2trien$; (b) $NiNapth_2trien$

Table 4.2 TGA data of $ZnNapth_2trien$ and $NiNapth_2trien$

Polymer	**IDT (°C)**	**Weight residue (%) at different temperature (°C)**						
		300	**400**	**500**	**600**	**700**	**800**	**900**
$ZnNapth_2trien$	298	95	79	67	55	41	29	19
$NiNapth_2trien$	280	79	59	48	37	24	14	15

The incorporation of metals into polymer can improve its final properties such as thermal stability. In this work, hexadentate Shiff base metal complexes which are stable at high temperature were used in the synthesis thermally stable metal-containing polymers.

4.2 Synthesis of metal-containing polyureas

4.2.1 Synthesis of metal-containing polyureas from the reaction between MNapth$_2$trien and diisocyanates

Polyureas were synthesized by reacting MNapth$_2$trien (where M = Zn and Ni) with diisocyanates (Scheme 4.2). The diisocyanate used were 4,4'-diphenylmethane diisocyanate (MDI) and isophorone diisocyanate (IPDI) to obtain the polymers containing aromatic and aliphatic parts, respectively. The reaction was carried out at the mole ratio of MNapth$_2$trien:diisocyanate as 1:1 in dried CH_2Cl_2 at 40 °C for 4 and 24 hours with DBTDL as a catalyst. Zinc- and nickel-containing polyureas were obtained as yellow and brown powder, respectively.

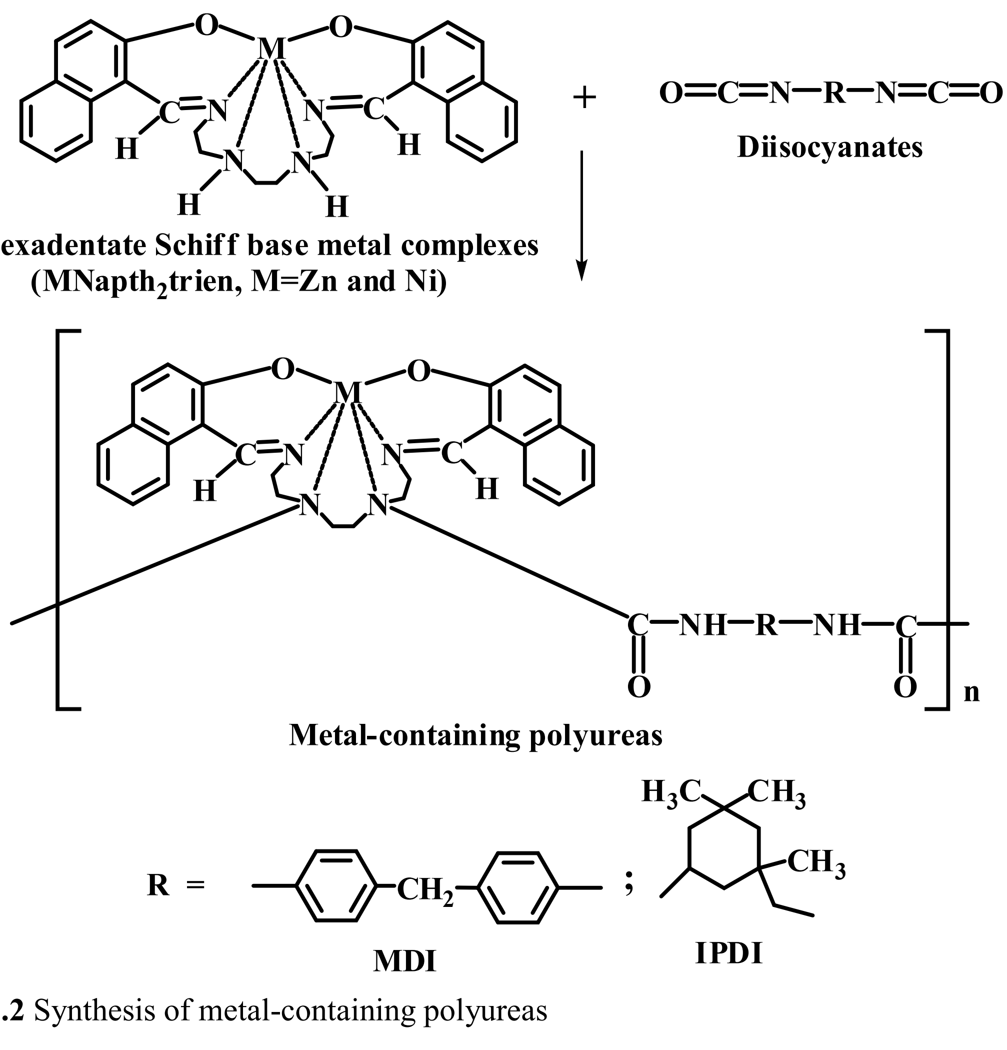

Scheme 4.2 Synthesis of metal-containing polyureas

Table 4.3 Synthesis data of polyureas

Polymers	**Weight of metal in polymer (%)**	**Yield (%)**	**External appearance**
ZnNapth$_2$trien:MDI	67.4	85	Yellow powder
NiNapth$_2$trien:MDI	67.1	82	Brown powder
ZnNapth$_2$trien:IPDI	69.9	65	Yellow powder
NiNapth$_2$trien:IPDI	69.7	53	Brown powder

The progress of reaction was followed by IR spectroscopy. The reaction progress could be observed by the disappearance of the strong –NCO absorption in diisocyanate at 2270 cm^{-1} and the appearance of a new –NCON- absorption band from the reaction of –NH group in metal complexes with –NCO group at 1680-1720 cm^{-1}. The possible polymerization mechanism was that the amino groups in MNapth$_2$trien underwent reaction with isocyanate groups to give urea linkages as shown in Scheme 4.3.

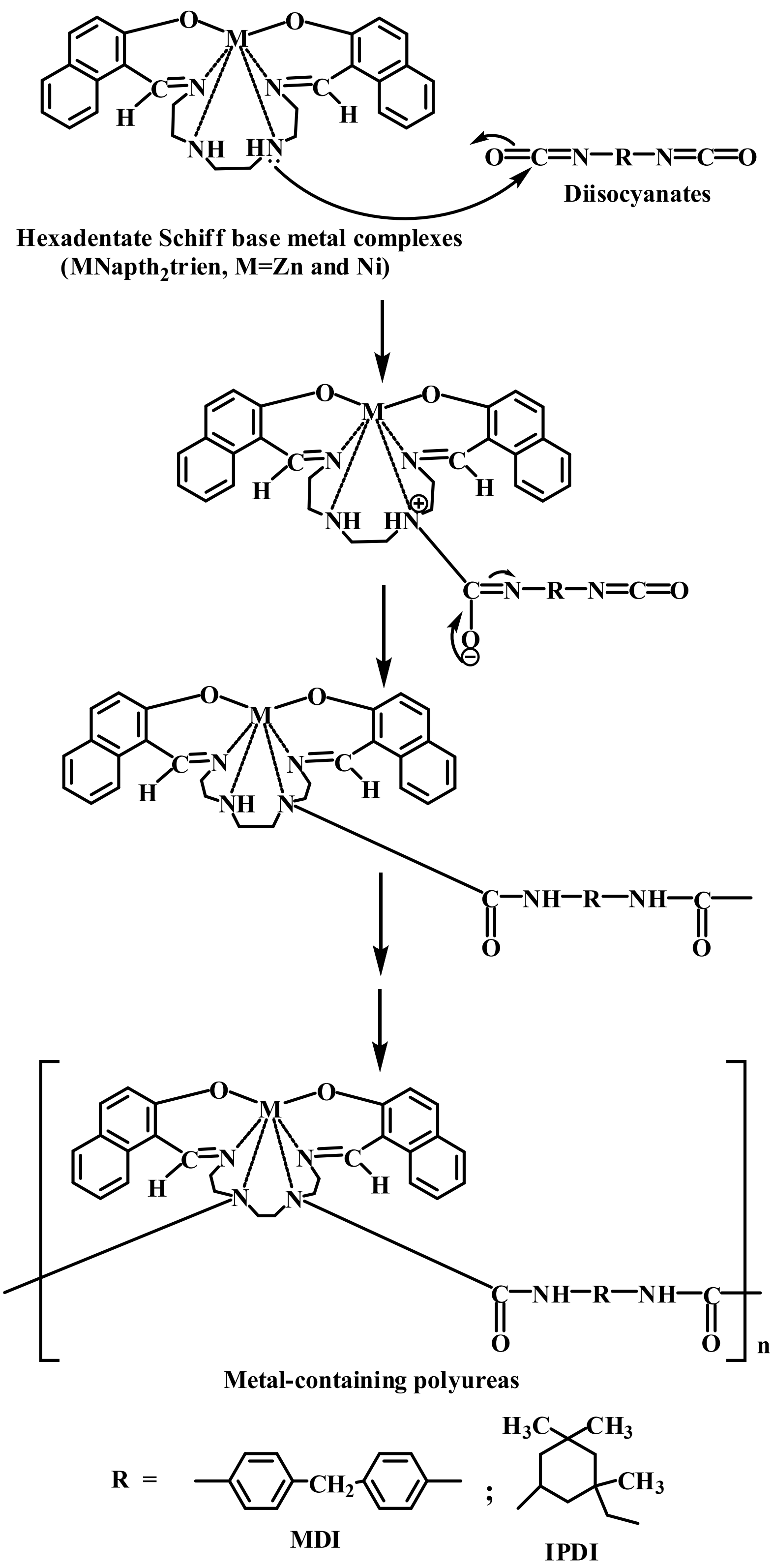

Scheme 4.3 Proposed mechanism of the reaction between MNapth$_2$trien and diisocyanates

It was found that MDI was more reactive towards MNapth$_2$trien than IPDI. IR spectra of the reaction between ZnNapth$_2$trien with MDI and IPDI are shown in figure 4.5 and 4.6, respectively. After heating the reaction mixtures for 4 hours (Figure 4.5) and 24 hours (Figure 4.6), new carbonyl (C=O) stretching vibration of –NCON- group at 1680 and 1720 cm^{-1}, respectively, were observed. The completeness of polymerization was determined by the disappearance of the NCO peak at 2270 cm^{-1} [44-45]

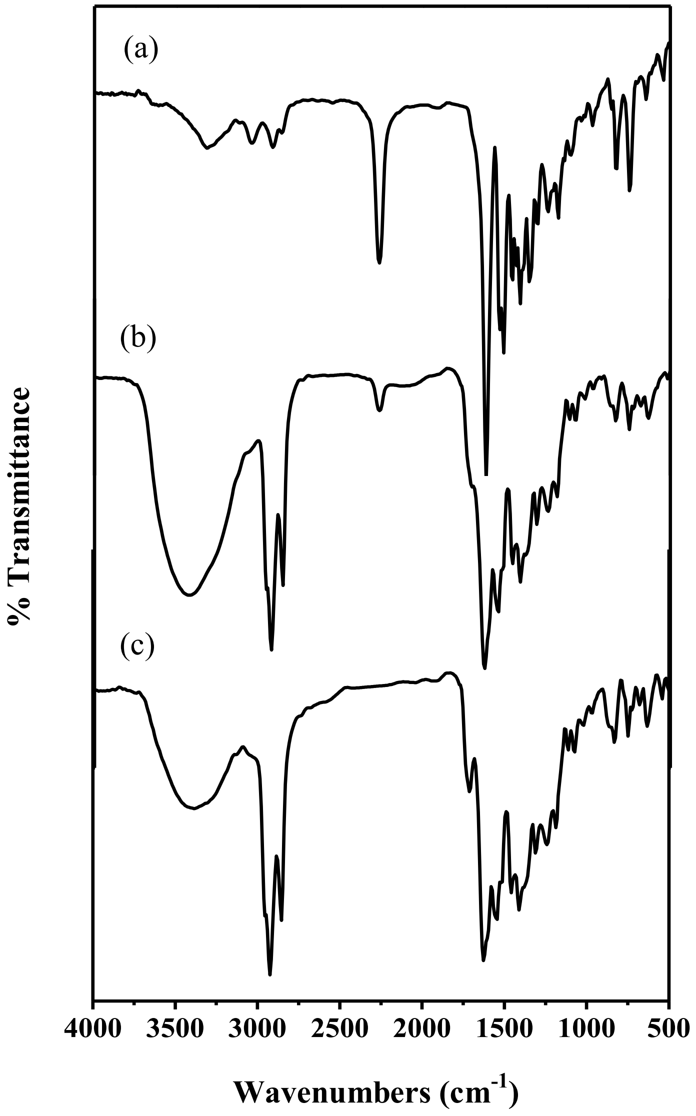

Figure 4.5 IR spectra of a reaction mixture of ZnNapth$_2$trien:MDI at a mole ratio of 1 : 1 in CH_2Cl_2 (a) before heating; (b) after heating at reflux for 3 h; (c) after heating at reflux for 4 h.

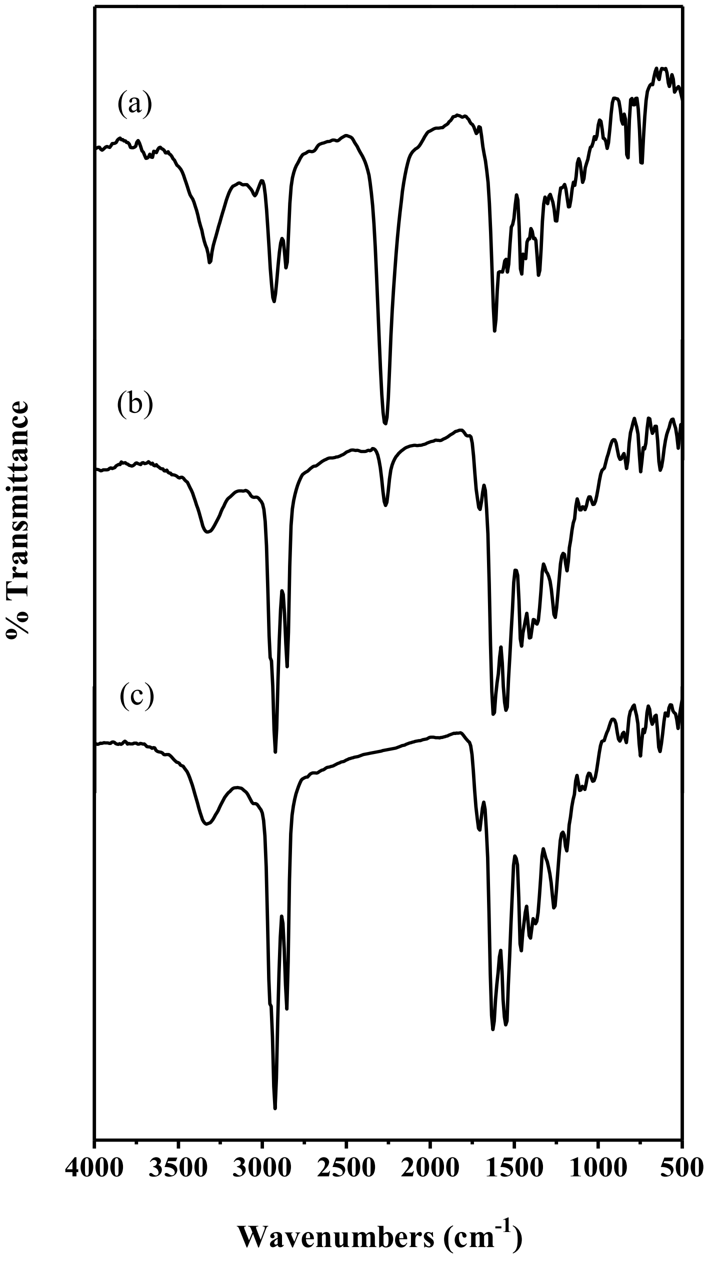

Figure 4.6 IR spectra of a reaction mixture of ZnNapth$_2$trien:IPDI at a mole ratio of 1 : 1 in CH_2Cl_2 (a) before heating; (b) after heating at reflux for 12 h; (c) after heating at reflux for 24 h.

4.2.2 Characterization of metal-containing polyureas

4.2.2.1 IR spectroscopy of metal-containing polyureas

IR spectra and data of metal-containing polyureas obtained from MNapth$_2$trien:diisocyanate at the mole ratio of 1:1 are shown in Figures 4.7 and Table 4.4, respectively.

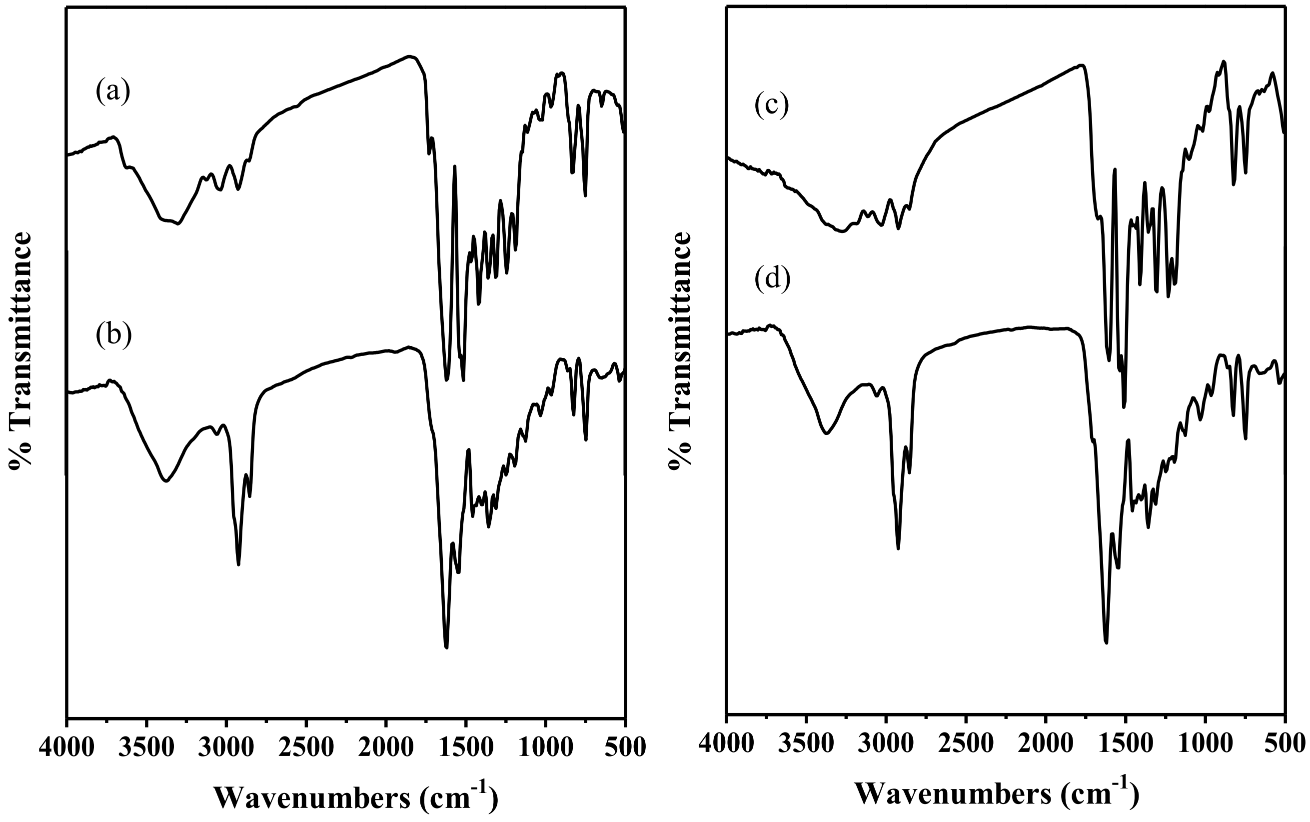

Figure 4.7 IR spectra of (a) ZnNapth$_2$trien-MDI; (b) ZnNapth$_2$trien-IPDI; (c) NiNapth$_2$trien-MDI; (d) NiNapth$_2$trien-IPDI

All zinc- and nickel-containing polyureas showed similar IR spectra. The important characteristic absorption bands were observed at 3360-3400 cm^{-1} (N-H stretching) and 1616-1623 cm^{-1} (C=N stretching). The carbonyl of urea appeared in the range of 1692-1720 cm^{-1} which was different from the typical urea C=O group normally appeared around 1660 cm^{-1}. The IR absorption of urea group in metal-containing polyureas was similar to that of amide group. This might be because one of urea nitrogen lone pair electron did not delocalize into the carbonyl part due to its coordination with metal atom. The carbonyl of –NCON- group could clearly be observed only in ZnNapth$_2$trien-MDI. Urea carbonyl in other polyureas appeared as a shoulder or broad peak due to the overlapping with –C=N- absorption.

Table 4.4 IR data of metal-containing polyureas

Metal-containing polyureas	**IR signals (cm^{-1})**
ZnNapth$_2$trien-MDI	3400 (NH), 3035, 2923, 1720 (C=O), 1616 (C=N), 1532, 1514, 1462, 1416, 1356, 1307, 1243, 1186, 965, 828, 749.
ZnNapth$_2$trien-IPDI	3360 (NH), 2941, 2923, 1692 (C=O), 1623 (C=N), 1543, 1463, 1434, 1394, 1358, 1304, 1245, 1189, 1040, 963, 831, 749.
NiNapth$_2$trien-MDI	3397 (NH), 3036, 2923, 1702 (C=O), 1618 (C=N), 1532, 1514, 1462, 1416, 1356, 1307, 1243, 1186, 1085, 972, 945, 892, 828, 749.
NiNapth$_2$trien-IPDI	3378 (NH), 2924, 2855, 1699 (C=O), 1623 (C=N), 1547, 1457, 1436, 1400, 1357, 1314, 1250, 1197, 1124, 1028, 961, 827, 750.

4.2.2.2 ^{1}H NMR spectroscopy of metal-containing polyureas

^{1}H NMR spectra of zinc-containing polyureas are recorded in DMSO-d_6 and their signals are presented in Table 4.5 Figure 4.8 and Figure A.3. ^{1}H NMR spectrum of ZnNapth$_2$trien-IPDI showed signals at 0.65-3.94 ppm which were assigned to the aliphatic parts of ZnNapth$_2$trien and IPDI. The signals in this region were difficult to observed due the large peaks of H_2O and DMSO. The urea NHs were observed at 5.34-5.98 ppm. The CH=N peaks were observed as multiplets at 9.08-9.31 ppm. The aromatic peaks of ZnNapth$_2$trien were found in ZnNapth$_2$trien-IPDI at 6.59-8.16 ppm, which were close to the region of aromatic protons observed in the ZnNapth$_2$trien complex at 6.62-8.06 ppm. However, all ^{1}H NMR signals of ZnNapth$_2$trien in ZnNapth$_2$trien-IPDI appeared as multiplets and there were more peaks than those observed in the ZnNapth$_2$trien complex. This might be due to the rigid structure of the polymer which causes these protons to be non-equivalent.

The ^{1}H NMR spectrum of ZnNapth$_2$trien-MDI was observed as shown in Figure 4.8. The -CH=N- signals were shown as multiplets at 9.09-9.28 ppm. The urea NHs were observed at 8.49-8.58 ppm. The aromatic protons of MDI and

ZnNapth$_2$trien were observed at 6.42-8.19 ppm. The peaks at 2.38-4.16 ppm were assigned to the methylene protons of ZnNapth$_2$trien and MDI.

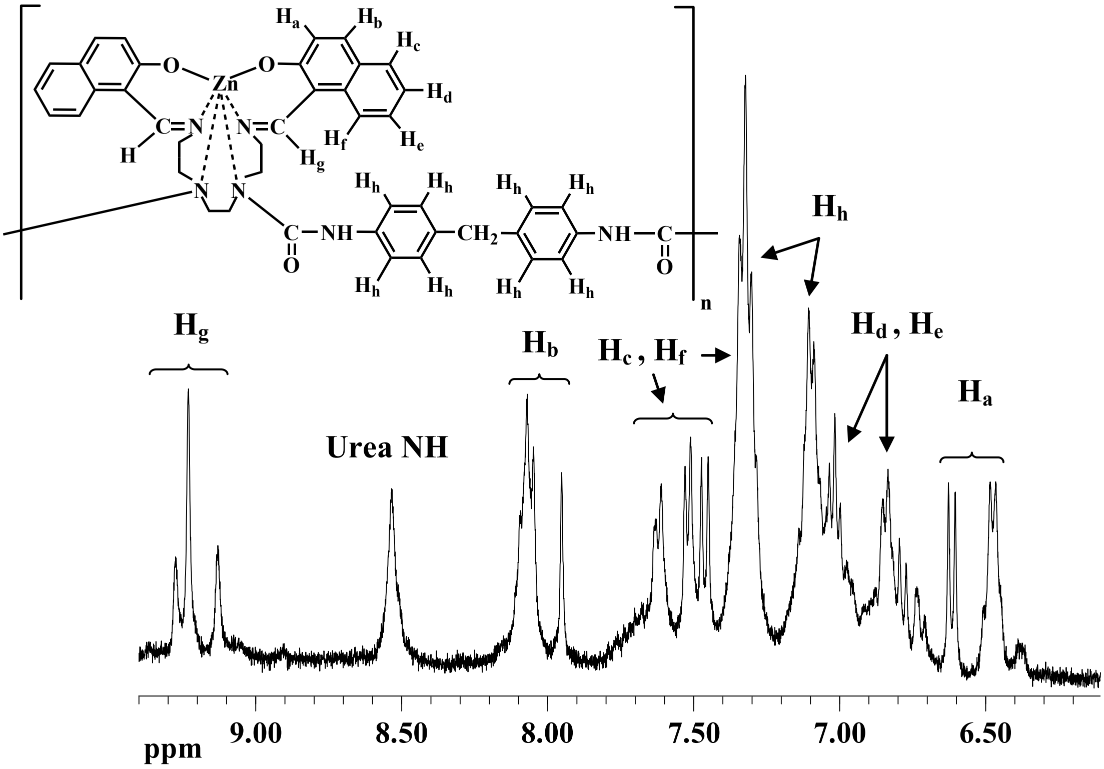

Figure 4.8 ^{1}H NMR data of ZnNapth$_2$trien-MDI in DMSO-d_6

Table 4.5 ^{1}H NMR data of zinc-containing polyureas

Metal-containing polyureas	**^{1}H NMR signals (ppm)**
ZnNapth$_2$trien-MDI	9.09-9.28 (m, CH=N), 8.49-8.58 (m, NH), 7.91-8.19 (m, Ar-H), 7.57-7.66 (m, Ar-H), 7.42-7.48 (m, Ar-H), 7.22-7.42 (m, Ar-H), 6.93-7.21 (m, Ar-H), 6.80-6.87 (m, Ar-H), 6.66-6.80 (m, Ar-H), 6.58-6.64 (m, Ar-H), 6.42-6.52 (m, Ar-H), 4.82-4.87 (m, NH), 3.96-4.16 (m, CH$_2$), 3.83-3.94 (m, CH$_2$), 3.73-2.81 (m, CH$_2$), 3.44-3.71 (m, CH$_2$), 3.10-3.25 (m, CH$_2$), 2.77-2.86 (m, CH$_2$), 2.69-2.75 (m, CH$_2$), 2.38-2.45 (m, CH$_2$).
ZnNapth$_2$trien-IPDI	9.08 - 9.31 (m, CH=N), 7.99 - 8.16 (m, Ar-H), 7.54-7.65 (m, Ar-H), 7.49-7.54 (m, Ar-H), 7.43-7.48 (m, Ar-H), 7.26-7.41 (m, Ar-H), 7.04-7.16 (m, Ar-H),6.98-7.04 (m, Ar-H), 6.70-6.79 (m, Ar-H), 6.59-6.64 (m, Ar-H), 5.34-5.98 (m, NH), 3.73-3.94 (m, aliphatic-H), 3.46-3.73 (m, aliphatic-H), 3.11-3.24 (m, aliphatic-H), 2.55-2.91 (m, aliphatic-H), 0.65-1.82 (m, aliphatic-H).

4.2.2.3 Elemental analysis

The chemical structure of metal-containing polyureas was confirmed by elemental analysis. Table 4.6 shows possible molecular formular of metal-containing polyureas. From the elemental analysis data, it was found that the percentage of carbon, hydrogen and nitrogen of ZnNapth$_2$trien-IPDI are in good agreement with the calculated values.

Table 4.6 Analytical data of polyureas

Metal complex	**Formula**	**Analytical data found (calculated) (%)**		
		C	**H**	**N**
ZnNapth$_2$trien-MDI	$C_{43}H_{38}N_6O_4Zn$	65.87 (67.23)	5.54 (4.99)	10.54 (10.94)
ZnNapth$_2$trien-IPDI	$C_{40}H_{46}N_6O_4Zn$	64.98 (64.90)	6.31 (6.26)	11.34 (11.35)
NiNapth$_2$trien-MDI	$C_{43}H_{38}N_6O_4Ni$	68.10 (67.82)	5.97 (5.03)	10.56 (11.04)
NiNapth$_2$trien-IPDI	$C_{40}H_{46}N_6O_4Ni$	63.57 (65.50)	8.30 (6.32)	12.14 (11.46)

4.2.2.4 Solubility of metal-containing polyureas

Solubility of metal-containing polyureas was tested in various polar and non-polar solvents. The maximum amount of each polymer that was able to dissolve in 1 mL of DMSO was determined as shown in Table 4.7. These polymers were soluble in polar solvents such as DMF and DMSO but insoluble in hexane, toluene, dichloromethane, chloroform, methanol, water, actonotrile and tetrahydrofuran. The polymers based on aliphatic diisocyanate showed higher solubility than the polymers based on aromatic diisocyanate might be due to the higher flexibility of the aliphatic part.

Table 4.7 Solubility of metal-containing polyureas

Polymers	DMF	DMSO	Maximum solubility (mg) in DMSO 1 (mL)
ZnNapth$_2$trien-MDI	+-	+-	3
ZnNapth$_2$trien-IPDI	+	+	47
NiNapth$_2$trien-MDI	+	+	10
NiNapth$_2$trien-IPDI	+	+	65

++ = Soluble at room temperature; + = soluble on heating; +- = partial soluble on heating; - = insoluble

4.2.2.5 Inherent viscosity of metal-containing polyureas

Viscosity of a polymer solution depends on concentration and size (i.e., molecular weight) of the dissolved polymer. By measuring the solution viscosity we should be able to get an idea about molecular weight. Viscosity techniques are very popular because they are experimentally simple. Inherent viscosity of all polyureas was measured at 40°C in DMSO as described in Appendix [B-1]. The viscosity data of polyureas are given in Table 4.8. It was found that both MDI- and IPDI-based polymers had low viscosities. The viscosity of ZnNapth$_2$trien-MDI could not be obtained since the polymer was not completely soluble in DMSO.

Table 4.8 Inherent viscosity of metal-containing polyureas

Polymers	η_{inh} **(dl g^{-1})**
ZnNapth$_2$trien-MDI	-
ZnNapth$_2$trien-IPDI	0.145
NiNapth$_2$trien-MDI	0.113
NiNapth$_2$trien-IPDI	0.169

4.2.2.6 Glass transition temperature

Glass transition temperature (T_g) of the metal-containing polyureas was determined by differential scanning calorimetry (DSC). T_gs could be observed for NiNapth$_2$trien-MDI and ZnNapth$_2$trien-IPDI at 149 and 147°C, respectively (Figures 4.9 and 4.10). Since the solubility of metal-containing polyureas in NMP were not good, brittle materials were obtained and their DMTA samples could not be prepared.

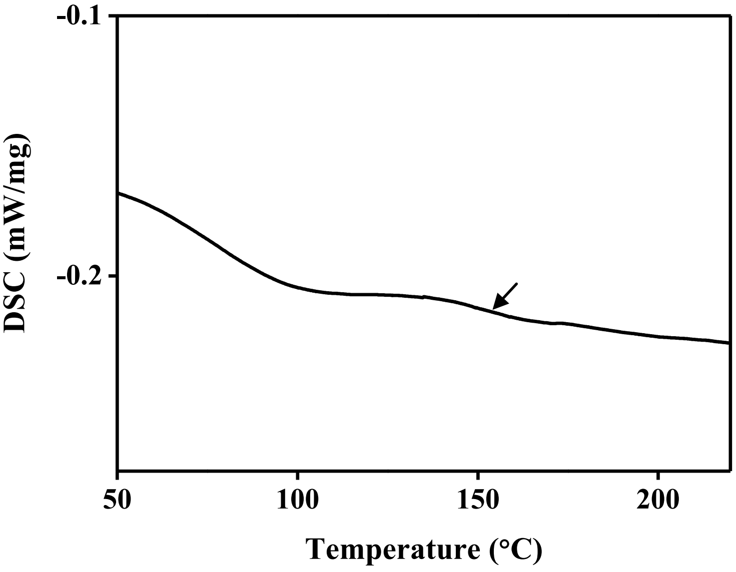

Figure 4.9 DSC thermogram of NiNapth$_2$trien-MDI

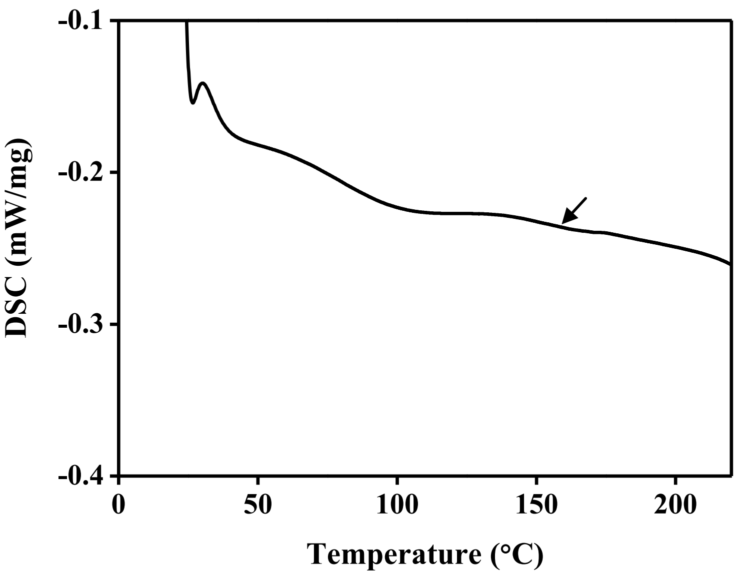

Figure 4.10 DSC thermogram of ZnNapth$_2$trien-IPDI

4.2.2.7 Thermogravimetric analysis

Thermal properties of metal-containing polyureas were investigated using thermogravimetric analysis (TGA). Thermal stability of the polymers was evaluated by the IDT value and weight of residue at different temperatures. For this work, IDT was identified as the temperature where 5 weight loss of the polymers occurs. For all polymers, the initial weight loss occuring in the temperature range 200-300°C was not much different, whereas weight loss in the range of 400-700°C could be observed. TGA results of metal-containing polyureas (Figure 4.11 and Table 4.9) showed that polymers based on MDI showed higher thermal stability than polymers based on IPDI. The residual weights at 600°C were in the range of 6-48%. Initial decomposition temperature (IDT) of the polymers was found to be in the range of 226-286°C. Zinc-containing polymers showed better thermal stability than nickel-containing polymers. Among all polyureas, ZnNapth$_2$trien-MDI was the most thermally stable polymers with IDT of 280ºC and char yield of 48% at 600ºC.

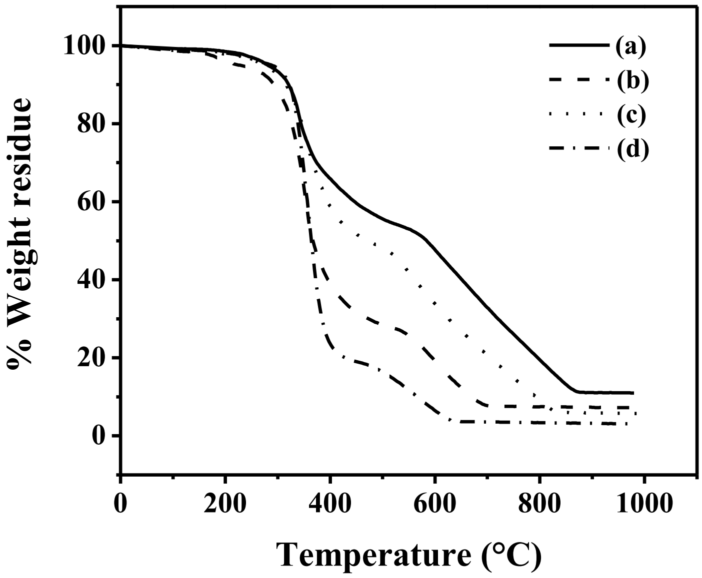

Figure 4.11 TGA thermogram of (a) ZnNapth$_2$trien-MDI; (b) ZnNapth$_2$trien-IPDI; (c) NiNapth$_2$trien-MDI; (d) NiNapth$_2$trien-IPDI

Table 4.9 TGA data of metal-containing polyureas

Polymer	**IDT (°C)**	**Weight residue (%) at different temperature (°C)**						
		300	**400**	**500**	**600**	**700**	**800**	**900**
ZnNapth$_2$trien-MDI	280	93	66	56	48	33	20	11
ZnNapth$_2$trien-IPDI	226	89	39	28	19	8	7	7
NiNapth$_2$trien-MDI	284	93	60	49	35	19	8	8
NiNapth$_2$trien-IPDI	286	94	24	16	6	4	3	3

4.2.2.8 X-ray diffraction

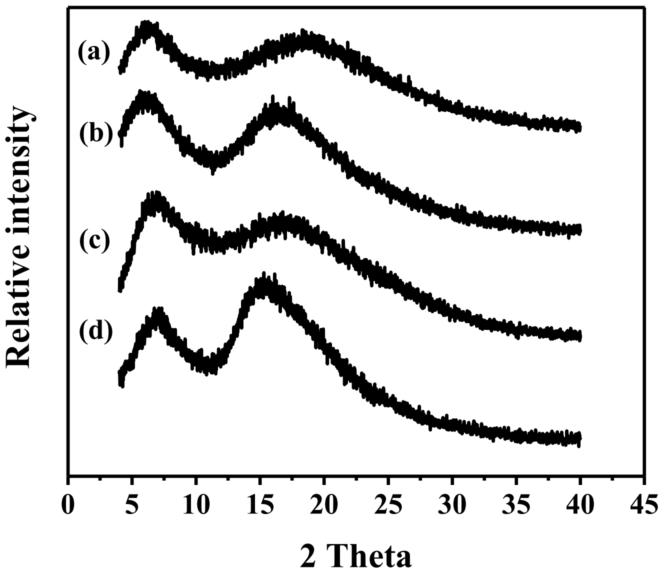

Figure 4.12 XRD patterns of (a) ZnNapth$_2$trien-MDI; (b) ZnNapth$_2$trien-IPDI; (c) NiNapth$_2$trien-MDI; (d) NiNapth$_2$trien-IPDI

Figure 4.12 shows the XRD patterns of metal-containing polyureas. The polymers did not show any sharp peak and therefore they were considered to be amorphous in nature. The amorphous of polymers was supported by the solubility test of polymers which showed that the metal-containing polymers were soluble in DMF and DMSO.

4.3 Synthesis of metal-containing copolyureas

4.3.1 Synthesis of metal-containing copolyureas from the reaction between MNapth$_2$trien, diisocyanates and diamines

Metal-containing copolyureas could be prepared by the reaction between MNapth$_2$trien, diisocyanates and diamines (Scheme 4.4). The reaction was carried out at the mole ratio of MNapth$_2$trien : diisocyanate : diamine as 0.5:2:1.5, 1:2:1 and 1.5:2:0.5 in dried DMSO with DBTDL as a catalyst. The diamines used were *m*-XDA and HMDA to obtain the polymers containing aromatic and aliphatic parts, respectively. Different amounts of MNapth$_2$trien and diamine were used to study their effects on the polymer properties. The reference polymers synthesized without metal complexes were also prepared by the reaction of diisocyanates with diamines.

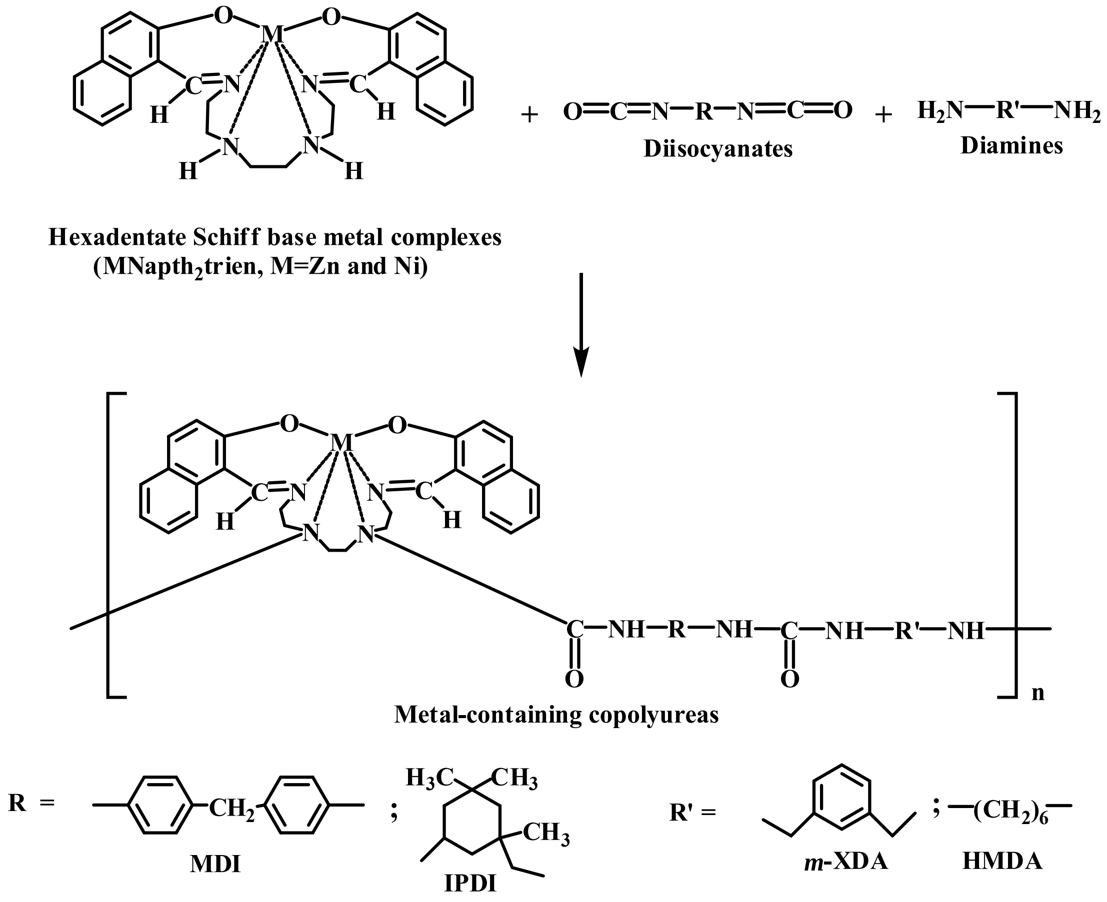

Scheme 4.4 Synthesis of metal-containing copolyureas from the reaction between MNapth$_2$trien, diisocyanates and diamines.

The possible polymerization mechanism was that the amino groups in MNapth$_2$trien and diamines underwent reaction with isocyanate groups in MDI and IPDI to give urea linkages (Scheme 4.5).

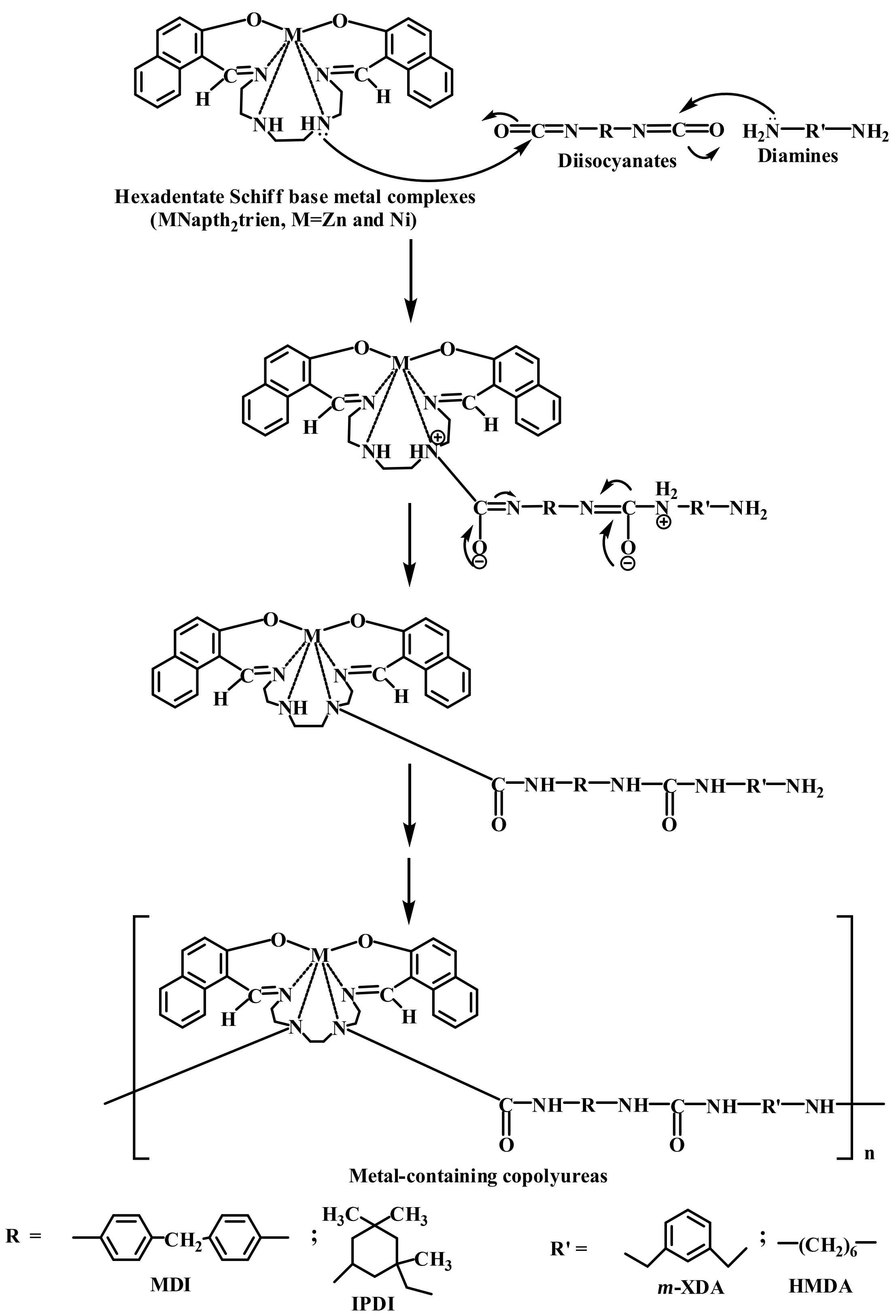

Scheme 4.5 Proposed mechanism of the reaction between MNapth$_2$trien, diisocyanates and diamines.

The yields of reference polymers and metal-containing copolyureas were found to be in the ranges of 57-90% and 55-94%, respectively (Table 4.10).

Table 4.10 Synthesis data of copolyureas

Polymers	**Weight of metal in polymer (%)**	**Yield (%)**	**External appearance**
MDI-*m*-XDA	-	90	Yellowish white powder
MDI-HMDA	-	73	Yellowish white powder
IPDI-*m*-XDA	-	78	Yellowish white powder
IPDI-HMDA	-	57	Yellowish white powder
ZnNapth$_2$trien-MDI-*m*-XDA (0.5:2:1.5)	26.7	88	Yellow powder
ZnNapth$_2$trien-MDI-*m*-XDA (1:2:1)	44.8	79	Yellow powder
ZnNapth$_2$trien-MDI-*m*-XDA (1.5:2:0.5)	57.7	81	Yellow powder
ZnNapth$_2$trien-MDI-HMDA (0.5:2:1.5)	27.8	88	Orange yellow powder
ZnNapth$_2$trien-MDI-HMDA (1:2:1)	45.6	55	Orange yellow powder
ZnNapth$_2$trien-MDI-HMDA (1.5:2:0.5)	58.2	87	Brown powder
NiNapth$_2$trien-MDI-*m*-XDA (0.5:2:1.5)	26.6	94	Brown powder
NiNapth$_2$trien-MDI-*m*-XDA (1:2:1)	44.6	87	Brown powder
NiNapth$_2$trien-MDI-*m*-XDA (1.5:2:0.5)	57.4	90	Brown powder
NiNapth$_2$trien-MDI-HMDA (0.5:2:1.5)	27.4	75	Brown powder
NiNapth$_2$trien-MDI-HMDA (1:2:1)	45.3	75	Brown powder
NiNapth$_2$trien-MDI-HMDA (1.5:2:0.5)	57.9	74	Brown powder
ZnNapth$_2$trien-IPDI-*m*-XDA (0.5:2:1.5)	28.6	70	Yellow powder
ZnNapth$_2$trien-IPDI-*m*-XDA (1:2:1)	47.1	83	Yellow powder
ZnNapth$_2$trien-IPDI-*m*-XDA (1.5:2:0.5)	60.2	79	Yellow powder
ZnNapth$_2$trien-IPDI-HMDA (0.5:2:1.5)	29.5	71	Orange yellow powder
ZnNapth$_2$trien-IPDI-HMDA (1:2:1)	48.0	74	Orange yellow powder
ZnNapth$_2$trien-IPDI-HMDA (1.5:2:0.5)	60.7	78	Brown powder
NiNapth$_2$trien-IPDI-*m*-XDA (0.5:2:1.5)	28.2	68	Brown powder
NiNapth$_2$trien-IPDI-*m*-XDA (1:2:1)	46.8	71	Brown powder
NiNapth$_2$trien-IPDI-*m*-XDA (1.5:2:0.5)	59.9	64	Brown powder
NiNapth$_2$trien-IPDI-HMDA (0.5:2:1.5)	29.2	63	Brown powder
NiNapth$_2$trien-IPDI-HMDA (1:2:1)	47.7	79	Brown powder
NiNapth$_2$trien-IPDI-HMDA (1.5:2:0.5)	60.4	74	Brown powder

4.3.2 Characterization of metal-containing copolyureas

4.3.2.1 IR spectroscopy of metal-containing copolyureas

IR spectra of zinc- and nickel-containing copolyureas showed C=N stretching bands between 1607-1635 cm^{-1}. The newly formed carbonyl of –NCON- groups were observed at 1656-1689 cm^{-1}, which were higher wavenumbers than the urea carbonyls of the reference polyureas synthesized without metal complexes. It was found that both zinc- and nickel- containing copolyureas obtained from different mole ratios showed similar IR spectra (Figure A.4-7). IR spectra and IR data of zinc- and nickel-containing copolyureas obtained from $MNapth_2trien$: diisocyanate : diamine at the mole ratio of 1:2:1 are shown in Figure 4.13 and Table 4.11, respectively.

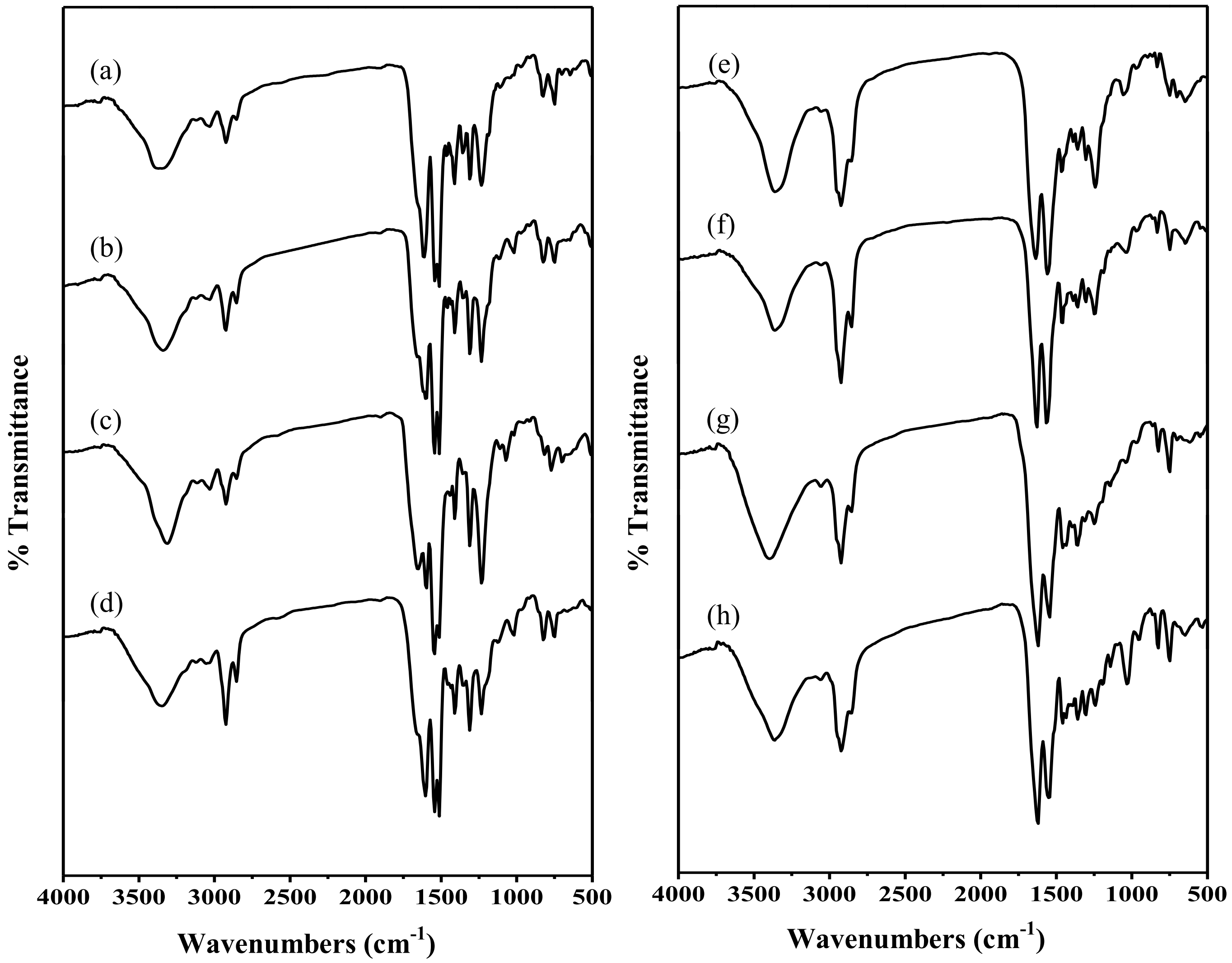

Figure 4.13 IR spectra of metal-containing copolyureas

(a) ZnNapth$_2$trien-MDI-*m*-XDA (b) ZnNapth$_2$trien-MDI-HMDA

(c) NiNapth$_2$trien-MDI-*m*-XDA (d) NiNapth$_2$trien-MDI-HMDA

(e) ZnNapth$_2$trien-IPDI-*m*-XDA (f) ZnNapth$_2$trien-IPDI-HMDA

(g) NiNapth$_2$trien-IPDI-*m*-XDA (h) NiNapth$_2$trien-IPDI-HMDA

Table 4.11 IR data of metal-containing copolyureas and reference polymers

Polymers	**IR signals (cm^{-1})**
MDI-*m*-XDA	3316 (NH), 3027, 2914, 1653 (C=O), 1598, 1547, 1512, 1409, 1309, 1230, 1107, 1044, 1017, 908, 818, 773, 699.
MDI-HMDA	3319 (NH), 2926, 2855, 1648 (C=O), 1598, 1551, 1513, 1408, 1309, 1236, 1108, 1011, 816, 761, 652, 508.
IPDI-*m*-XDA	3360 (NH), 2947, 2920, 1642 (C=O), 1561, 1463, 1380, 1360, 1303, 1244, 1062, 829, 780, 700.
IPDI-HMDA	3375 (NH), 2927, 2858, 1641 (C=O), 1562, 1464, 1381, 1304, 1245, 1071, 892, 772.
ZnNapth$_2$trien-MDI-*m*-XDA	3348 (NH), 3027, 2923, 2848, 1660 (C=O), 1615 (C=N), 1541, 1514, 1463, 1413, 1355, 1309, 1234, 1183, 1105, 1043, 1016, 966, 911, 828, 750.
ZnNapth$_2$trien-MDI-HMDA	3334 (NH), 3043, 2926, 2856, 1656 (C=O), 1622 (C=N), 1601, 1544, 1512, 1463, 1410, 1362, 1309, 1234, 1179, 1117, 1021, 973, 946, 918, 824, 751.
NiNapth$_2$trien-MDI-*m*-XDA	3316 (NH), 3029, 2913, 2848, 1656 (C=O), 1607 (C=N), 1544, 1512, 1443, 1409, 1358, 1308, 1227, 1117, 1074, 1016, 950, 911, 817, 755.
NiNapth$_2$trien-MDI-HMDA	3346 (NH), 3047, 2925, 2855, 1673 (C=O), 1614 (C=N), 1543, 1513, 1455, 1436, 1410, 1358, 1311, 1234, 1187, 1140, 1021, 946, 860, 823, 751.

Table 4.11 (continued)

Polymers	**IR signals (cm^{-1})**
ZnNapth$_2$trien-IPDI-*m*-XDA	3360 (NH), 2922, 2854, 1689 (C=O), 1630 (C=N), 1551, 1460, 1397, 1355, 1304, 1246, 1149, 1037, 946, 861, 830, 750.
ZnNapth$_2$trien-IPDI-HMDA	3375 (NH), 2924, 2852, 1669 (C=O), 1618 (C=N), 1550, 1461, 1435, 1393, 1357, 1313, 1245, 1187, 1127, 1034, 992, 966, 895, 864, 832, 751.
NiNapth$_2$trien-IPDI-*m*-XDA	3353 (NH), 2924, 2855, 1660 (C=O), 1635 (C=N), 1599, 1509, 1458, 1439, 1412, 1360, 1311, 1229, 1174, 1116, 1054, 1015, 972, 826, 750.
NiNapth$_2$trien-IPDI-HMDA	3366 (NH), 2922, 2856, 1670 (C=O), 1622 (C=N), 1548, 1459, 1389, 1358, 1306, 1243, 1194, 1141, 1066, 1031, 964, 867, 828, 750.

4.3.2.2 ^{1}H NMR spectroscopy of metal-containing copolyureas

^{1}H NMR spectra of metal-containing copolyureas showed signals for CH=N group at 9.04-9.39 ppm. Aromatic protons of metal complexes appeared as broad peaks and were observed at 6.40-8.55 ppm. NH protons attached to aromatic and methylene group showed absorption band in the range of 8.36-8.81 and 4.58-6.24 ppm, respectively. NMR spectra of copolyureas showed signals at 0.65-4.76 ppm which were assigned to the aliphatic parts of polymers. ^{1}H NMR data and spectra of zinc- and nickel-containing copolyureas obtained from MNapth$_2$trien : diisocyanate : diamine at the mole ratio of 1:2:1 are shown in Table 4.12 and Figures A.8-A.13, respectively. As an example, comparing between the ^{1}H NMR spectra of MDI-HMDA (Figures 4.14) and ZnNapth$_2$trien-MDI-HMDA (Figures 4.15), the aromatic region of MDI-HMDA spectrum contained aromatic protons of MDI while the spectrum of ZnNapth$_2$trien-MDI-HMDA showed aromatic protons of both MDI and ZnNapth$_2$trien.

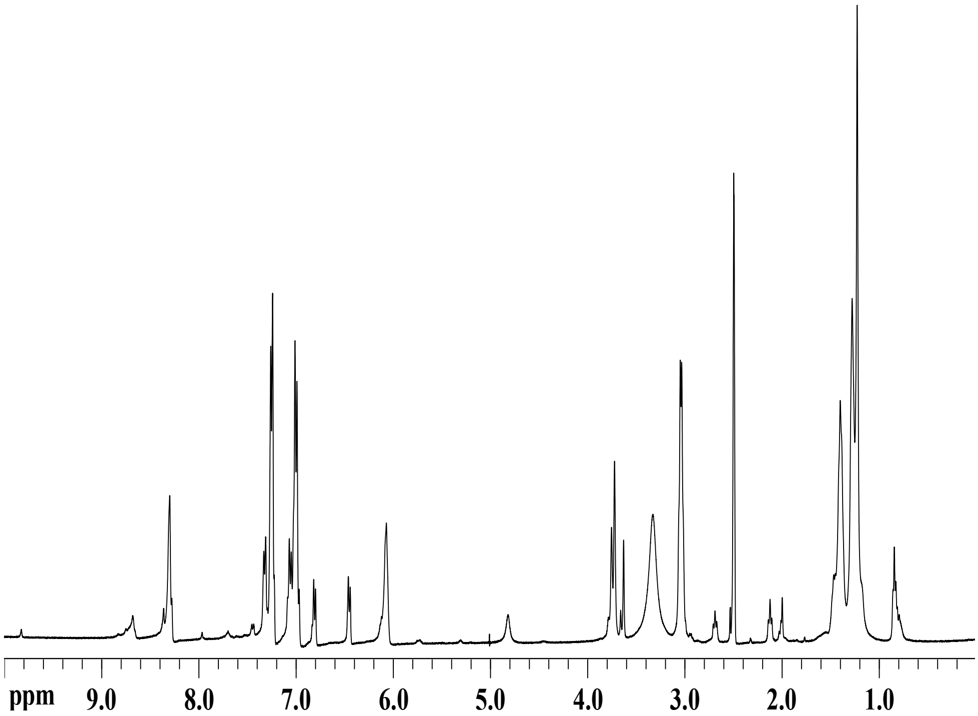

Figure 4.14 ^{1}H NMR spectrum of MDI-HMDA in DMSO-d_6

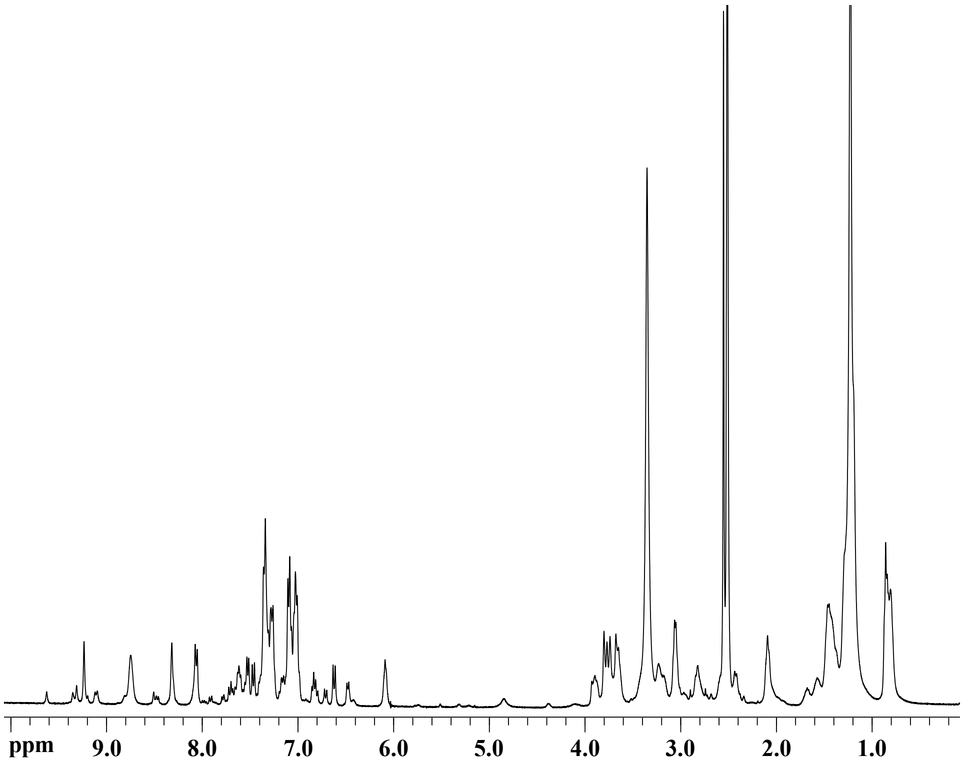

Figure 4.15 ^{1}H NMR spectrum of ZnNapth$_2$trien-MDI-HMDA in DMSO-d_6

Table 4.12 ^{1}H NMR data of zinc-containing copolyureas and reference polymers[a]

Polymers	C**H**=N	N**H**	Ar-**H**	Alkyl groups[b]
MDI-*m*-XDA	-	8.42-8.56	7.19-7.36, 7.12-7.18, 6.96-7.06 6.52-6.61	4.19-4.34, 3.70-3.79
MDI-HMDA	-	8.22-8.40, 6.05	7.23-7.32, 6.98-7.06	3.71-3.77, 3.02-3.03 1.93-2.17, 1.09-1.53
ZnNapth$_2$trien-MDI-*m*-XDA	9.07-9.32	8.36-8.55, 4.76-4.92, 4.58-4.76	7.91-8.14, 7.56-7.68 7.44-7.54, 7.19-7.40 6.96-7.19 6.72-6.94 6.40-6.67	4.16-4.35, 3.50-3.82, 2.96-3.04, 2.83-2.94, 2.68-2.78, 2.52-2.56
ZnNapth$_2$trien-MDI-HMDA	9.04-9.39	8.66-8.81, 6.02-6.12	8.45-8.55, 8.24-8.37, 7.98-8.14, 7.74-7.80, 7.66-7.72, 7.57-7.66, 7.48-7.57, 7.43-7.48, 7.20-7.40, 6.96-7.20, 6.77-6.86, 6.68-6.72, 6.58-6.64, 6.44-6.49,	3.56-3.97, 2.96-3.18, 2.68-2.93, 2.00-2.16, 1.15-1.50, 0.70-0.92
IPDI-HMDA	-	5.45-5.93, 7.85-8.05		3.57-3.76, 2.88-3.08, 2.66-2.82, 2.10-2.24, 1.15-1.60, 0.70-1.09
IPDI-*m*-XDA	-	5.96-6.13, 5.67-5.85	7.18-7.30,7.03-7.13, 6.14-6.42	4.03-4.29, 3.72-3.77, 3.39-3.60, 2.67-2.83, 1.38-1.58, 1.01-1.11, 0.65-0.99
ZnNapth$_2$trien-IPDI-*m*-XDA	9.26-9.36	8.67-8.38, 6.07-6.24, 5.37-5.97	8.22-8.35, 8.14-8.22, 7.99-8.12, 7.85-7.98, 7.70-7.76, 7.56-7.66, 7.49-7.55, 7.41-7.47, 7.29-7.37, 7.13-7.25, 6.98-7.09, 6.80-6.72,	4.06-4.15, 3.62-3.70, 3.02-3.11, 2.90-3.01, 2.62-2.89, 1.97-2.12, 1.33-1.57, 0.64-1.09
ZnNapth$_2$trien-IPDI-HMDA	9.14-9.38	5.44-5.78	8.03-8.16, 7.92-8.02, 7.56-7.75, 7.28-7.44, 7.07-7.23, 6.96-7.05, 6.70-6.78	3.58-3.77, 2.87-3.06, 2.62-2.82, 2.04-2.19, 1.17-1.29, 0.73-1.00

[a] all peaks are multiplets

[b] for MDI-based polymers, alkyl groups = -C$\mathbf{H}_2$;

for IPDI-based polymers, alkyl groups = C**H**, C$\mathbf{H}_2$ and C$\mathbf{H}_3$

4.3.2.3 Solubility of copolyureas

Solubility of all copolyureas was tested in various polar and non-polar solvents (Table 4.13). Metal-containing copolyureas were soluble in DMF and DMSO, partial soluble in tetrahydrofuran and acetonitrile, insoluble in hexane, toluene, dichloromethane, chloroform, methanol and water. The maximum amount of each polymer that was able to dissolve in 1 mL of DMSO was also determined.

The copolyureas showed great improvement in solubility when compared to that of metal-containing polyureas and reference polyureas synthesized without metal complexes. Most copolymers showed good solubility at the mole ratio of MNapth$_2$trien : diisocyanate : diamines = 1:2:1. MDI based copolymers showed better solubility than IPDI-based copolymers and *m*-XDA-based copolymers showed better solubility than HMDA-based copolymers. Solubility was greatly enhanced in the MDI and *m*-XDA series by the presence of bulky group. Incorporation of bulky group increased chain distance, free volume and decreased intermolecular interaction.

Table 4.13 Solubility of metal containing copolyureas and reference polymers

Polymers	**CH_3CN**	**THF**	**DMF**	**DMSO**	**Maximum solubility (mg) in 1 mL DMSO**
MDI-*m*-XDA	-	-	+-	+	5
ZnNapth$_2$trien-MDI-*m*-XDA (0.5:2:1.5)	-	-	++	++	216
ZnNapth$_2$trien-MDI-*m*-XDA (1:2:1)	-	-	++	++	429
ZnNapth$_2$trien-MDI-*m*-XDA (1.5:2:0.5)	-	-	++	++	496
NiNapth$_2$trien-MDI-*m*-XDA (0.5:2:1.5)	+-	+-	++	++	89
NiNapth$_2$trien-MDI-*m*-XDA (1:2:1)	+-	+-	++	++	183
NiNapth$_2$trien-MDI-*m*-XDA (1.5:2:0.5)	+-	+-	++	++	86
MDI-HMDA	-	-	+	+	30
ZnNapth$_2$trien-MDI-HMDA (0.5:2:1.5)	-	-	++	++	209
ZnNapth$_2$trien-MDI-HMDA (1:2:1)	-	-	++	++	187
ZnNapth$_2$trien-MDI-HMDA (1.5:2:0.5)	+-	+-	++	++	33
NiNapth$_2$trien-MDI-HMDA (0.5:2:1.5)	-	-	++	++	95
NiNapth$_2$trien-MDI-HMDA (1:2:1)	-	-	++	++	234
NiNapth$_2$trien-MDI-HMDA (1.5:2:0.5)	+-	+-	++	++	534
IPDI-*m*-XDA	-	-	+-	+	5
ZnNapth$_2$trien-IPDI-*m*-XDA (0.5:2:1.5)	-	-	+	++	570
ZnNapth$_2$trien-IPDI-*m*-XDA (1:2:1)	-	-	+	++	156
ZnNapth$_2$trien-IPDI-*m*-XDA (1.5:2:0.5)	-	-	+	++	151
NiNapth$_2$trien-IPDI-*m*-XDA (0.5:2:1.5)	-	-	+	++	96
NiNapth$_2$trien-IPDI-*m*-XDA (1:2:1)	-	-	+	++	268
NiNapth$_2$trien-IPDI-*m*-XDA (1.5:2:0.5)	-	-	+	++	272
IPDI-HMDA	-	-	+-	+	19
ZnNapth$_2$trien-IPDI-HMDA (0.5:2:1.5)	-	-	++	++	16
ZnNapth$_2$trien-IPDI-HMDA (1:2:1)	-	-	++	++	168
ZnNapth$_2$trien-IPDI-HMDA (1.5:2:0.5)	+-	+-	++	++	21
NiNapth$_2$trien-IPDI-HMDA (0.5:2:1.5)	-	-	++	++	15
NiNapth$_2$trien-IPDI-HMDA (1:2:1)	-	-	++	++	13
NiNapth$_2$trien-IPDI-HMDA (1.5:2:0.5)	+-	+-	++	++	56

++ = Soluble at room temperature; + = soluble on heating; +- = partial soluble on heating; - = insoluble

4.3.2.4 Inherent viscosity of copolyureas

Inherent viscosity of all copolyureas was measured at 40°C in DMSO as described in Appendix[B-1]. The viscosity data of all copolyureas are given in Table 4.14. Metal-containing copolyureas had viscosities in the range of 0.107-0.396 dl/g. Viscosity of metal-containing copolyureas was higher than that of reference copolyureas without metal complexes in both Zn and Ni series. This indicated that metal complexes did not dissociate in solvent.

Table 4.14 Inherent viscosity of metal-containing copolyureas and reference polymers

Polymers	**η_{inh} (dl g^{-1})**
MDI-*m*-XDA	0.172
MDI-HMDA	0.100
IPDI-*m*-XDA	0.202
IPDI-HMDA	0.188
ZnNapth$_2$trien-MDI-*m*-XDA (0.5:2:1.5)	0.396
ZnNapth$_2$trien-MDI-*m*-XDA (1:2:1)	0.190
ZnNapth$_2$trien-MDI-*m*-XDA (1.5:2:0.5)	0.107
ZnNapth$_2$trien-MDI-HMDA (0.5:2:1.5)	0.229
ZnNapth$_2$trien-MDI-HMDA (1:2:1)	0.350
ZnNapth$_2$trien-MDI-HMDA (1.5:2:0.5)	0.273
NiNapth$_2$trien-MDI-*m*-XDA (0.5:2:1.5)	0.206
NiNapth$_2$trien-MDI-*m*-XDA (1:2:1)	0.169
NiNapth$_2$trien-MDI-*m*-XDA (1.5:2:0.5)	0.237
NiNapth$_2$trien-MDI-HMDA (0.5:2:1.5)	0.212
NiNapth$_2$trien-MDI-HMDA (1:2:1)	0.282
NiNapth$_2$trien-MDI-HMDA (1.5:2:0.5)	0.256
ZnNapth$_2$trien-IPDI-*m*-XDA (0.5:2:1.5)	0.166
ZnNapth$_2$trien-IPDI-*m*-XDA (1:2:1)	0.211

Table 4.14 (continued)

Polymers	**η_{inh} (dl g^{-1})**
ZnNapth$_2$trien-IPDI-*m*-XDA (1.5:2:0.5)	0.155
ZnNapth$_2$trien-IPDI-HMDA (0.5:2:1.5)	0.302
ZnNapth$_2$trien-IPDI-HMDA (1:2:1)	0.315
ZnNapth$_2$trien-IPDI-HMDA (1.5:2:0.5)	0.258
NiNapth$_2$trien-IPDI-*m*-XDA (0.5:2:1.5)	0.271
NiNapth$_2$trien-IPDI-*m*-XDA (1:2:1)	0.250
NiNapth$_2$trien-IPDI-*m*-XDA (1.5:2:0.5)	0.194
NiNapth$_2$trien-IPDI-HMDA (0.5:2:1.5)	0.178
NiNapth$_2$trien-IPDI-HMDA (1:2:1)	0.195
NiNapth$_2$trien-IPDI-HMDA (1.5:2:0.5)	0.255

4.3.2.5 Thermogravimetric analysis

4.3.2.5.1 Metal-containing copolyureas based on *m*-XDA

Thermal stability of zinc- and nickel-containing copolyureas synthesized from *m*-XDA were analyzed from TGA thermograms under air atmosphere. TGA data and thermograms are shown in Table 4.15 and Figures 4.16-4.19, respectively.

From TGA thermograms of MDI-based zinc-containing polymers, IDTs (temperature at 5% weight loss) of ZnNapth$_2$trien-MDI-*m*-XDA were found in the range of 274-310°C. The IDTs of ZnNapth$_2$trien-MDI-*m*-XDA increased with increasing amount of *m*-XDA in the copolymers. The residual weights at 600°C was in the range of 39-43%. Reference polymer (MDI-*m*-XDA) showed higher thermal stability than metal-containing copolyureas. ZnNapth$_2$trien-MDI-*m*-XDA 0.5:2:1.5 showed higher IDT and slightly lower residual weight at 600°C than ZnNapth$_2$trien-MDI. For MDI-based nickel-containing copolyureas, the amount of *m*-XDA in the polymers did not show the effect on their IDTs when compared to ZnNapth$_2$trien-MDI-*m*-XDA. IDTs of NiNapth$_2$trien-MDI-*m*-XDA were found in the range of 272-317°C. NiNapth$_2$trien-MDI-*m*-XDA obtained at the mole ratios of 0.5:2:1.5 and 1.5:2.0.5 showed higher IDTs and residual weight at 600°C than NiNapth$_2$trien-MDI.

This might be NiNapth$_2$trien-MDI-*m*-XDA contained aromatic part of both MDI and *m*-XDA.

For IPDI-based polymers, IDTs of ZnNapth$_2$trien-IPDI-*m*-XDA was found in the range of 247-259°C. The IDT of ZnNapth$_2$trien-IPDI-*m*-XDA increased with increasing amount of *m*-XDA in the copolymers. The residual weight at 600°C was in the range of 27-39%. The residual weight at 600°C increased with increasing amount of metal complexes. Reference polymer (IPDI-*m*-XDA) showed higher IDT than copolyureas. This might be due to the fact that the metal catalyses the first stage decomposition and retards the further stages of decompositions, which is similar to Nanjundan's work [32]. Char yields of copolyureas were higher than those of IPDI-*m*-XDA and ZnNapth$_2$trien-IPDI. IDTs of NiNapth$_2$trien-IPDI-*m*-XDA were found in the range of 208-217°C. The residual weight at 600°C was in the range of 24-30%. The char yields of metal-containing copolyureas were comparable to that of NiNapth$_2$trien-IPDI and higher than that of reference polymer (IPDI-*m*-XDA).

Among all *m*-XDA-based copolyureas, NiNapth$_2$trien-MDI-*m*-XDA (0.5:2:1.5) was the most thermally stable polymer with IDT of 314°C and char yield at 600°C of 48%. This might be due to the presence of stiff ring of *m*-XDA in the polymer chain.

Table 4.15 TGA data of metal-containing copolyureas based on *m*-XDA

Polymer	**IDT (°C)**	**Weight residue (%) at different temperature (°C)**						
		300	**400**	**500**	**600**	**700**	**800**	**900**
MDI-*m*-XDA	303	95	69	61	54	42	29	15
ZnNapth$_2$trien-MDI	280	93	66	56	48	33	20	11
ZnNapth$_2$trien-MDI-*m*-XDA (0.5:2:1.5)	310	96	63	51	43	27	13	3
ZnNapth$_2$trien-MDI-*m*-XDA (1:2:1)	294	94	58	46	39	21	8	7
ZnNapth$_2$trien-MDI-*m*-XDA (1.5:2:0.5)	274	90	60	48	40	22	10	8
NiNapth$_2$trien-MDI	284	93	60	49	35	19	8	8
NiNapth$_2$trien-MDI-*m*-XDA (0.5:2:1.5)	314	97	67	58	48	29	13	2
NiNapth$_2$trien-MDI-*m*-XDA (1:2:1)	272	92	64	53	39	20	5	3
NiNapth$_2$trien-MDI-*m*-XDA (1.5:2:0.5)	317	97	66	60	47	32	20	9
IPDI-*m*-XDA	297	95	44	25	19	6	1	1
ZnNapth$_2$trien-IPDI	226	89	39	28	19	8	7	7
ZnNapth$_2$trien-IPDI-*m*-XDA (0.5:2:1.5)	259	83	45	36	27	15	12	12
ZnNapth$_2$trien-IPDI-*m*-XDA (1:2:1)	252	81	61	48	37	25	21	21
ZnNapth$_2$trien-IPDI-*m*-XDA (1.5:2:0.5)	247	86	62	47	39	23	10	8
NiNapth$_2$trien-IPDI	286	94	24	16	6	4	3	3
NiNapth$_2$trien-IPDI-*m*-XDA (0.5:2:1.5)	208	79	55	39	30	18	9	9
NiNapth$_2$trien-IPDI-*m*-XDA (1:2:1)	209	80	54	38	28	16	9	9
NiNapth$_2$trien-IPDI-*m*-XDA (1.5:2:0.5)	217	83	61	46	24	13	10	9

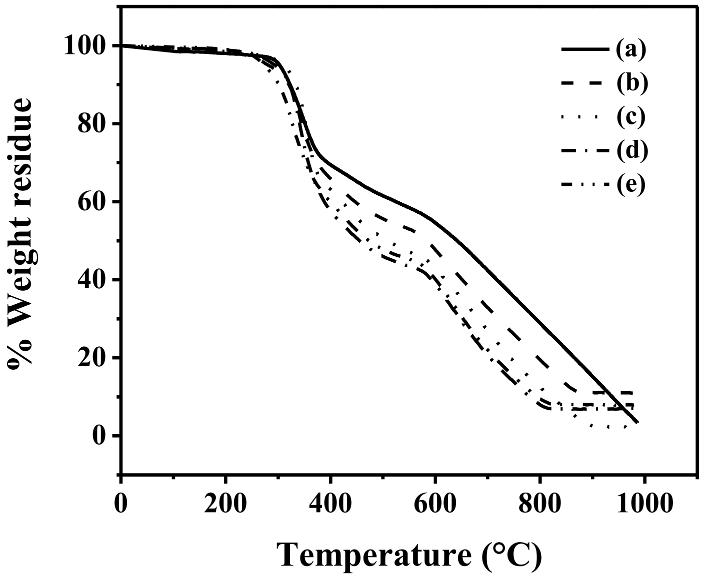

Figure 4.16 TGA thermograms of (a) MDI-*m*-XDA; (b) ZnNapth$_2$trien-MDI; (c) ZnNapth$_2$trien-MDI-*m*-XDA (0.5:2:1.5); (d) ZnNapth$_2$trien-MDI-*m*-XDA (1:2:1); (e) ZnNapth$_2$trien-MDI-*m*-XDA (1.5:2:0.5)

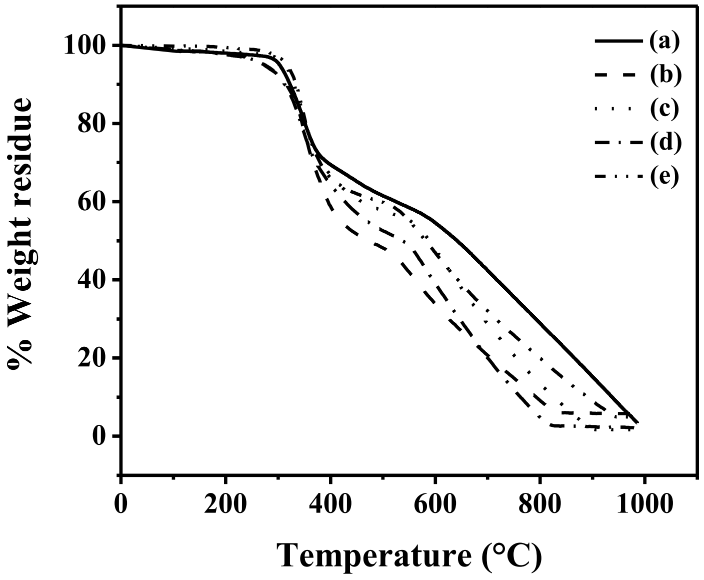

Figure 4.17 TGA thermograms of (a) MDI-*m*-XDA; (b) NiNapth$_2$trien-MDI; (c) NiNapth$_2$trien-MDI-*m*-XDA (0.5:2:1.5); (d) NiNapth$_2$trien-MDI-*m*-XDA (1:2:1); (e) NiNapth$_2$trien-MDI-*m*-XDA (1.5:2:0.5)

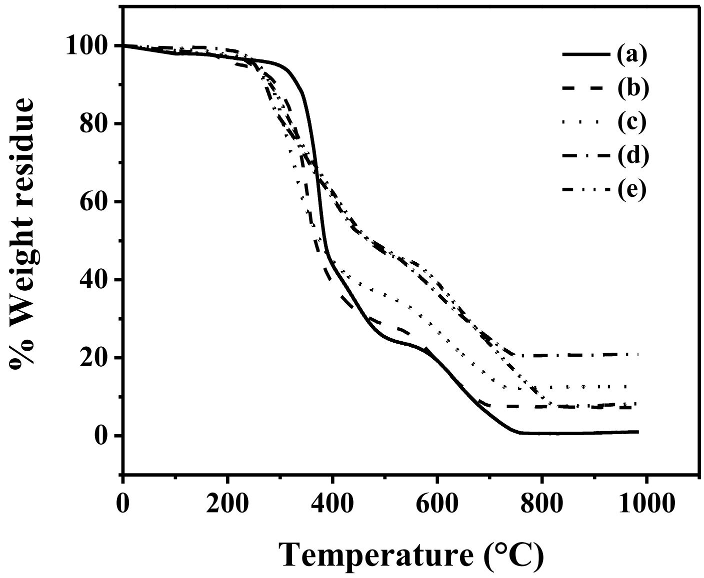

Figure 4.18 TGA thermograms of (a) IPDI-*m*-XDA; (b) ZnNapth$_2$trien-IPDI; (c) ZnNapth$_2$trien-IPDI-*m*-XDA (0.5:2:1.5); (d) ZnNapth$_2$trien-IPDI-*m*-XDA (1:2:1); (e) ZnNapth$_2$trien-IPDI-*m*-XDA (1.5:2:0.5)

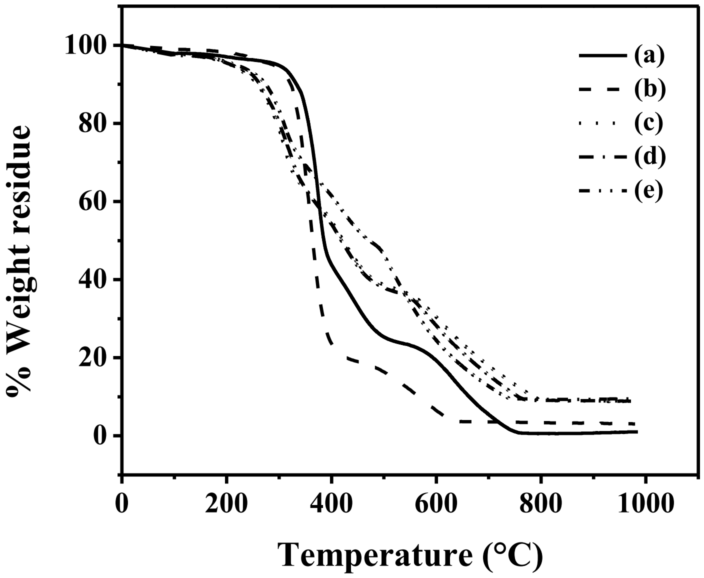

Figure 4.19 TGA thermograms of (a) IPDI-*m*-XDA; (b) NiNapth$_2$trien-IPDI; (c) NiNapth$_2$trien-IPDI-*m*-XDA (0.5:2:1.5); (d) NiNapth$_2$trien-IPDI-*m*-XDA (1:2:1); (e) NiNapth$_2$trien-IPDI-*m*-XDA (1.5:2:0.5)

4.3.2.5.2 Metal-containing copolyureas based on HMDA

TGA data and thermograms of zinc- and nickel-containing copolyureas synthesized from HMDA are shown in Table 4.16 and Figures 4.20-4.23, respectively.

For ZnNapth$_2$trien-MDI-HMDA, their IDTs were found in the range of 178-276°C. Their residual weights at 600°C were in the range of 26-42%. The residual weights at 600°C increased with increasing amount of complexes in the copolymers. Char yield of zinc-containing copolyureas was higher than reference polymer (MDI-HMDA). Both IDTs and char yields of ZnNapth$_2$trien-MDI-HMDA were lower than those of ZnNapth$_2$trien-MDI. For NiNapth$_2$trien-MDI-HMDA, their IDTs were found in the range of 184-252°C. Their residual weights at 600°C were in the range of 27-39%. NiNapth$_2$trien-MDI-HMDA showed lower IDTs than NiNapth$_2$trien-MDI and reference polymer (MDI- HMDA).

From TGA thermograms of ZnNapth$_2$trien-IPDI-HMDA, the amount of HMDA in the polymers did not have the effect on their IDTs and residue weight at 600°C. IDTs of ZnNapth$_2$trien-IPDI-HMDA were found in the range of 221-255°C. Their residual weights at 600°C were in the range of 16-23%. For NiNapth$_2$trien-IPDI-HMDA, their IDTs were found in the range of 180-261°C. Their residual weights at 600°C were in the range of 16-26%. The residual weight at 600°C increased with increasing amount of metal complexes in the copolymers.

HMDA-based copolyureas showed less thermal stability than *m*-XDA-based copolyureas. Among all HMDA-based copolyureas, the most thermally stable polymer was ZnNapth$_2$trien-MDI-HMDA (1:2:1) which had IDTs of 276°C and char yield at 600°C of 30%. The presence of metal in the polymer chain promoted the initial thermal decomposition. On the other hand, metal in the polymer increased the char yield of polymer.

Table 4.16 TGA data of metal-containing copolyureas based on HMDA

Polymer	IDT (°C)	Weight residue (%) at different temperature (°C)						
		300	400	500	600	700	800	900
MDI-HMDA	285	93	46	26	19	7	3	3
ZnNapth$_2$trien-MDI	280	93	66	56	48	33	20	11
ZnNapth$_2$trien-MDI-HMDA (0.5:2:1.5)	246	87	47	33	26	13	7	7
ZnNapth$_2$trien-MDI-HMDA (1:2:1)	276	91	48	38	30	17	7	7
ZnNapth$_2$trien-MDI-HMDA (1.5:2:0.5)	178	84	63	52	42	26	13	10
NiNapth$_2$trien-MDI	284	93	60	49	35	19	8	8
NiNapth$_2$trien-MDI-HMDA (0.5:2:1.5)	252	86	52	30	27	19	12	10
NiNapth$_2$trien-MDI-HMDA (1:2:1)	252	86	62	42	35	25	16	9
NiNapth$_2$trien-MDI-HMDA (1.5:2:0.5)	184	83	61	49	39	28	18	11
IPDI-HMDA	258	89	24	14	10	6	6	6
ZnNapth$_2$trien-IPDI	226	89	39	28	19	8	7	7
ZnNapth$_2$trien-IPDI-HMDA (0.5:2:1.5)	250	81	35	26	17	10	10	10
ZnNapth$_2$trien-IPDI-HMDA (1:2:1)	255	86	37	28	16	8	8	8
ZnNapth$_2$trien-IPDI-HMDA (1.5:2:0.5)	221	88	50	42	23	11	10	10
NiNapth$_2$trien-IPDI	286	94	24	16	6	4	3	3
NiNapth$_2$trien-IPDI-HMDA (0.5:2:1.5)	239	86	34	22	16	9	7	7
NiNapth$_2$trien-IPDI-HMDA (1:2:1)	261	85	43	32	22	12	9	9
NiNapth$_2$trien-IPDI-HMDA (1.5:2:0.5)	180	81	47	38	26	17	10	10

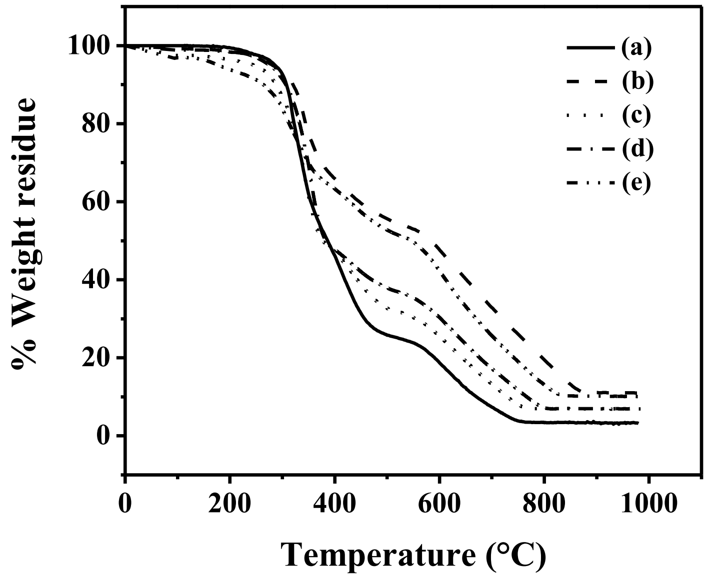

Figure 4.20 TGA thermograms of (a) MDI-HMDA; (b) ZnNapth$_2$trien-MDI; (c) ZnNapth$_2$trien-MDI-HMDA (0.5:2:1.5); (d) ZnNapth$_2$trien-MDI-HMDA (1:2:1); (e) ZnNapth$_2$trien-MDI-HMDA (1.5:2:0.5)

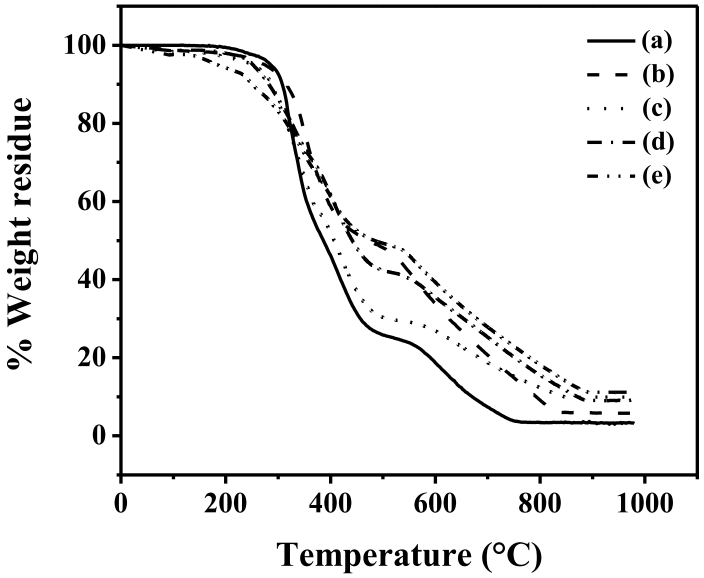

Figure 4.21 TGA thermograms of (a) MDI-HMDA; (b) NiNapth$_2$trien-MDI; (c) NiNapth$_2$trien-MDI-HMDA (0.5:2:1.5); (d) NiNapth$_2$trien-MDI-HMDA (1:2:1); (e) NiNapth$_2$trien-MDI-HMDA (1.5:2:0.5)

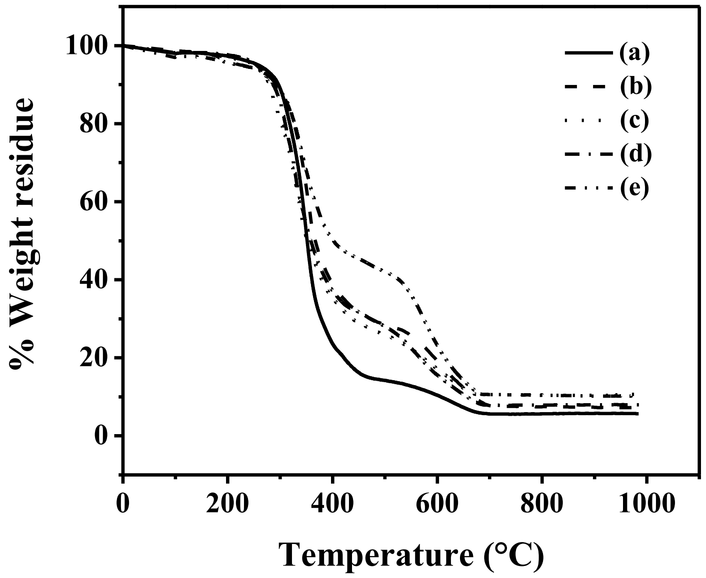

Figure 4.22 TGA thermograms of (a) IPDI-HMDA; (b) ZnNapth$_2$trien-IPDI; (c) ZnNapth$_2$trien-IPDI-HMDA (0.5:2:1.5); (d) ZnNapth$_2$trien-IPDI-HMDA (1:2:1); (e) ZnNapth$_2$trien-IPDI-HMDA (1.5:2:0.5)

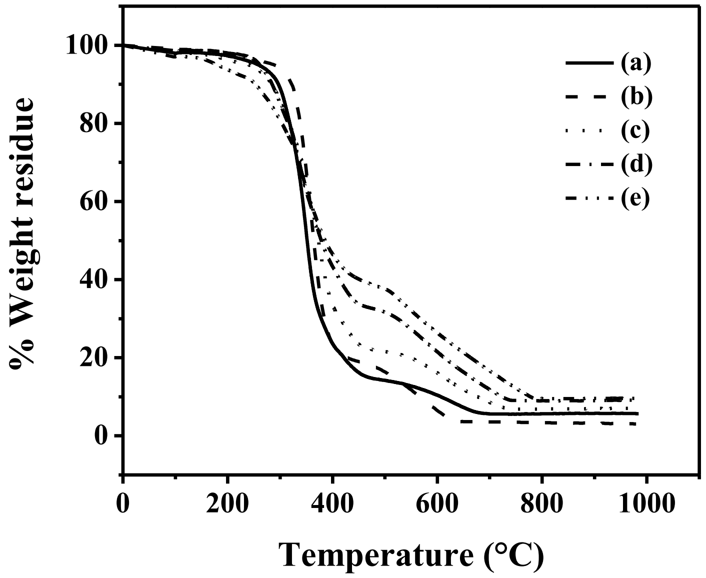

Figure 4.23 TGA thermograms of (a) IPDI-HMDA; (b) NiNapth$_2$trien-IPDI; (c) NiNapth$_2$trien-IPDI-HMDA (0.5:2:1.5); (d) NiNapth$_2$trien-IPDI-HMDA (1:2:1); (e) NiNapth$_2$trien-IPDI-HMDA (1.5:2:0.5)

4.3.2.6 X-ray diffraction

XRD patterns of MDI-HMDA showed some sharp peaks which indicate that the polymers contained crystalline part while zinc- and nickel-containing copolyureas based on MDI had board XRD peaks and therefore the polymers were amorphous (Figure 4.24). This XRD results corresponded with solubility results that the metal-containing copolyureas were soluble in DMF and DMSO.

XRD patterns of copolyureas based on IPDI showed that and IPDI-*m*-XDA are partially crystalline in nature as they showed some sharp peaks. Copolyureas based on IPDI do not show any sharp peaks which could be considered as amorphous in nature (Figure 4.25). This XRD results corresponded with solubility results that the metal-containing copolyureas were soluble in DMF and DMSO.

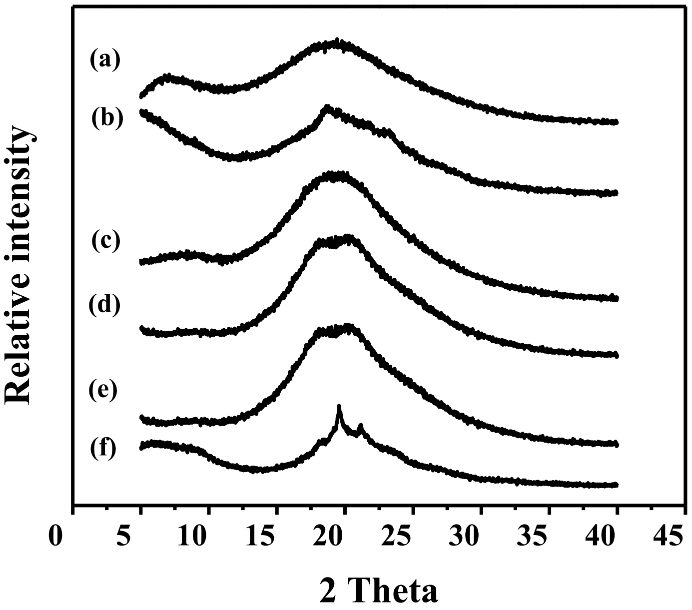

Figure 4.24 XRD patterns of (a) ZnNapth$_2$trien-MDI-*m*-XDA; (b) ZnNapth$_2$trien-MDI-HMDA; (c) NiNapth$_2$trien-MDI-*m*-XDA; (d) NiNapth$_2$trien-MDI-HMDA; (e) MDI-*m*-XDA (f) MDI-HMDA

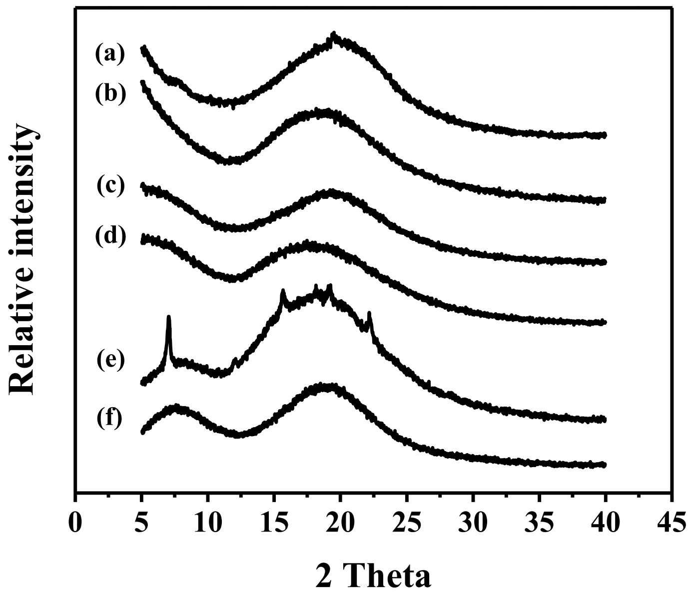

Figure 4.25 XRD patterns of (a) ZnNapth$_2$trien-IPDI-*m*-XDA; (b) ZnNapth$_2$trien-IPDI-HMDA; (c) NiNapth$_2$trien-IPDI-*m*-XDA; (d) NiNapth$_2$trien-IPDI-HMDA; (e) IPDI-*m*-XDA (f) IPDI-HMDA

4.4 Synthesis of metal-containing poly(urethane-urea)s

4.4.1 Synthesis of metal-containing poly(urethane-urea)s from the reaction between MNapth$_2$trien, diisocyanates and dialcohols

Metal-containing poly(urethane-urea)s could be prepared by the reaction between MNapth$_2$trien, diisocyanates and dialcohols (Scheme 4.6). The reaction was carried out at the mole ratio of MNapth$_2$trien : diisocyanate : dialcohol as 0.5:2:1.5, 1:2:1 and 1.5:2:0.5 in dried DMSO with DBTDL as a catalyst. The BPO and HDO dialcohols contained aromatic and aliphatic parts, respectively. Different amounts of MNapth$_2$trien and dialcohol were used to study effects on the polymer properties. The reference polymers without metal complexes were also prepared by the reaction of diisocyanates with dialcohols.

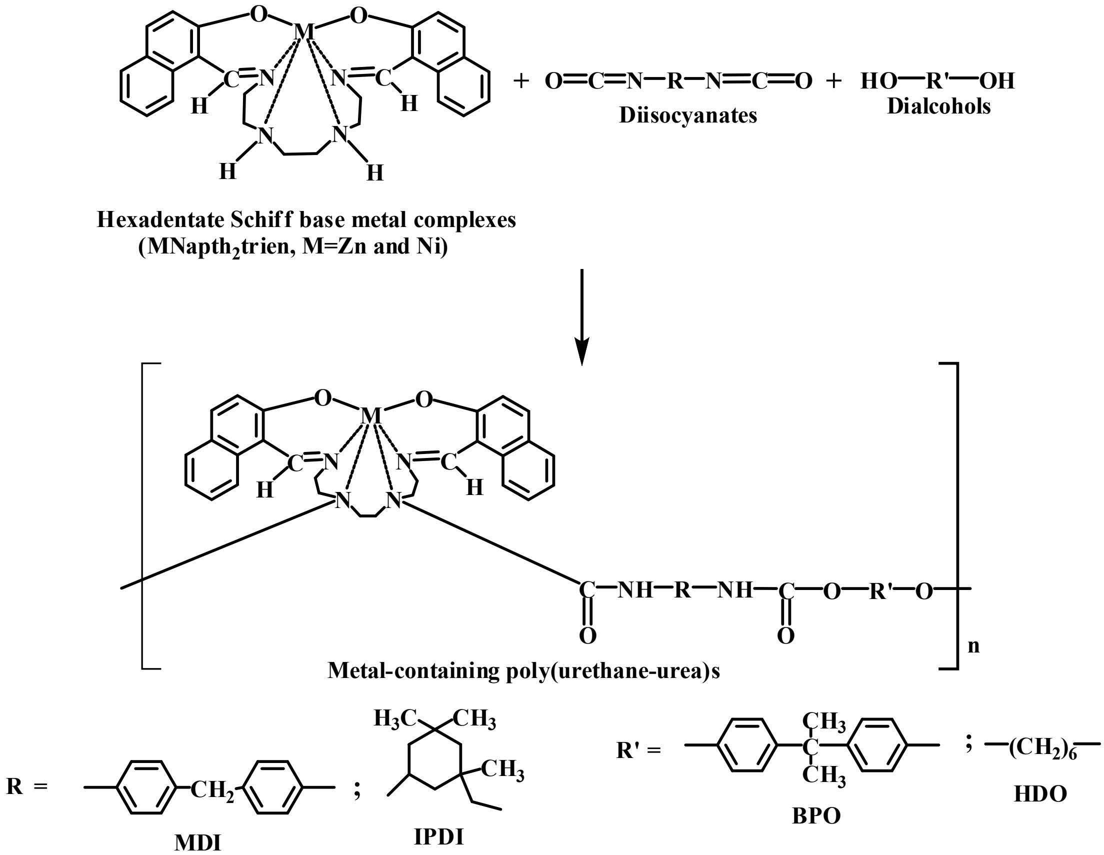

Scheme 4.6 Synthesis of metal-containing poly(urethane-urea)s from the reaction between MNapth$_2$trien, diisocyanates and dialcohols.

The possible polymerization mechanism was that the isocyanate groups in diisocyanate underwent reaction with amino groups in MNapth$_2$trien and hydroxyl groups in dialcohol to give urea and urethane linkages, respectively (Scheme 4.7).

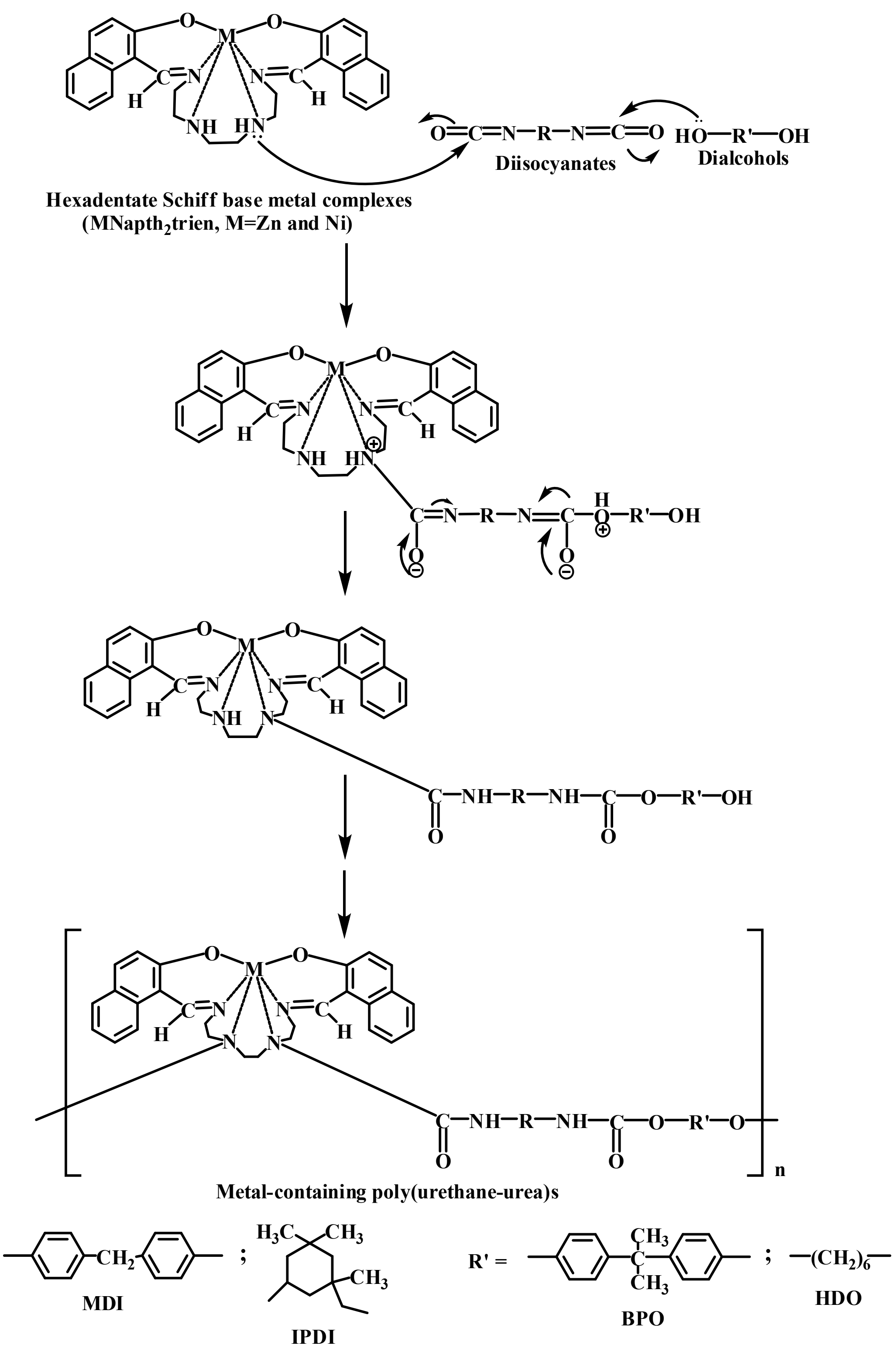

Scheme 4.7 Proposed mechanism of the reaction between MNapth$_2$trien, diisocyanates and dialcohols.

The yields of reference polymers and metal-containing poly(urethane-urea)s were found to be in the ranges 48-87% and 53-95%, respectively (Table 4.17).

Table 4.17 Synthesis data of poly(urethane-urea)s

Polymers	**Weight of metal in polymer (%)**	**Yield (%)**	**External appearance**
MDI-BPO	-	48	Yellowish white powder
MDI- HDO	-	76	Yellowish white powder
IPDI-BPO	-	77	Yellowish white powder
IPDI- HDO	-	87	Yellowish white powder
ZnNapth$_2$trien-MDI-BPO (0.5:2:1.5)	23.5	89	Red brown powder
ZnNapth$_2$trien-MDI-BPO (1:2:1)	41.5	73	Red brown powder
ZnNapth$_2$trien-MDI-BPO (1.5:2:0.5)	55.8	86	Red brown powder
ZnNapth$_2$trien-MDI- HDO (0.5:2:1.5)	27.7	84	Red brown powder
ZnNapth$_2$trien-MDI- HDO (1:2:1)	45.6	84	Brown powder
ZnNapth$_2$trien-MDI- HDO (1.5:2:0.5)	58.1	74	Brown powder
NiNapth$_2$trien-MDI-BPO (0.5:2:1.5)	23.2	77	Brown powder
NiNapth$_2$trien-MDI-BPO (1:2:1)	41.2	77	Brown powder
NiNapth$_2$trien-MDI-BPO (1.5:2:0.5)	55.5	89	Dark brown powder
NiNapth$_2$trien-MDI- HDO (0.5:2:1.5)	27.4	54	Brown powder
NiNapth$_2$trien-MDI- HDO (1:2:1)	45.3	53	Brown powder
NiNapth$_2$trien-MDI- HDO (1.5:2:0.5)	57.8	88	Dark brown powder
ZnNapth$_2$trien-IPDI-BPO (0.5:2:1.5)	27.8	95	Yellow brown powder
ZnNapth$_2$trien-IPDI-BPO (1:2:1)	43.5	79	Yellow brown powder
ZnNapth$_2$trien-IPDI-BPO (1.5:2:0.5)	58.2	87	Brown powder
ZnNapth$_2$trien-IPDI- HDO (0.5:2:1.5)	29.4	95	Yellow brown powder
ZnNapth$_2$trien-IPDI- HDO (1:2:1)	47.9	92	Yellow brown powder
ZnNapth$_2$trien-IPDI- HDO (1.5:2:0.5)	60.7	74	Brown powder
NiNapth$_2$trien-IPDI-BPO (0.5:2:1.5)	27.5	84	Brown powder
NiNapth$_2$trien-IPDI-BPO (1:2:1)	43.2	81	Brown powder
NiNapth$_2$trien-IPDI-BPO (1.5:2:0.5)	57.9	80	Dark brown powder
NiNapth$_2$trien-IPDI- HDO (0.5:2:1.5)	29.1	83	Brown powder
NiNapth$_2$trien-IPDI- HDO (1:2:1)	47.6	76	Brown powder
NiNapth$_2$trien-IPDI- HDO (1.5:2:0.5)	60.4	56	Dark brown powder

4.4.2 Characterization of metal-containing poly(urethane-urea)s

4.4.2.1 IR spectroscopy of metal-containing poly(urethane-urea)s

Zinc- and nickel-containing poly(urethane-urea)s showed N-H stretching signals at 3308-3414 cm^{-1}. The C-H stretching appeared between 2840-2953 cm^{-1} and the carbonyl (C=O) stretching of urethane and urea appeared as a shoulder at 1645-1706 cm^{-1} and the signal of urethane linkage overlapped with the urea linkage signal. The imine (C=N) absorption band was observed at 1616-1627 cm^{-1}. It was found that both zinc- and nickel- containing copolyureas obtained from different mole ratios show similar IR spectra (Figure A.14-17). IR spectra and data of metal-containing poly(urethane-urea)s obtained from $MNapth_2trien$: diisocyanates : dialcohols at the mole ratio of 1:2:1 are shown in Figure 4.26 and Table 4.18, respectively.

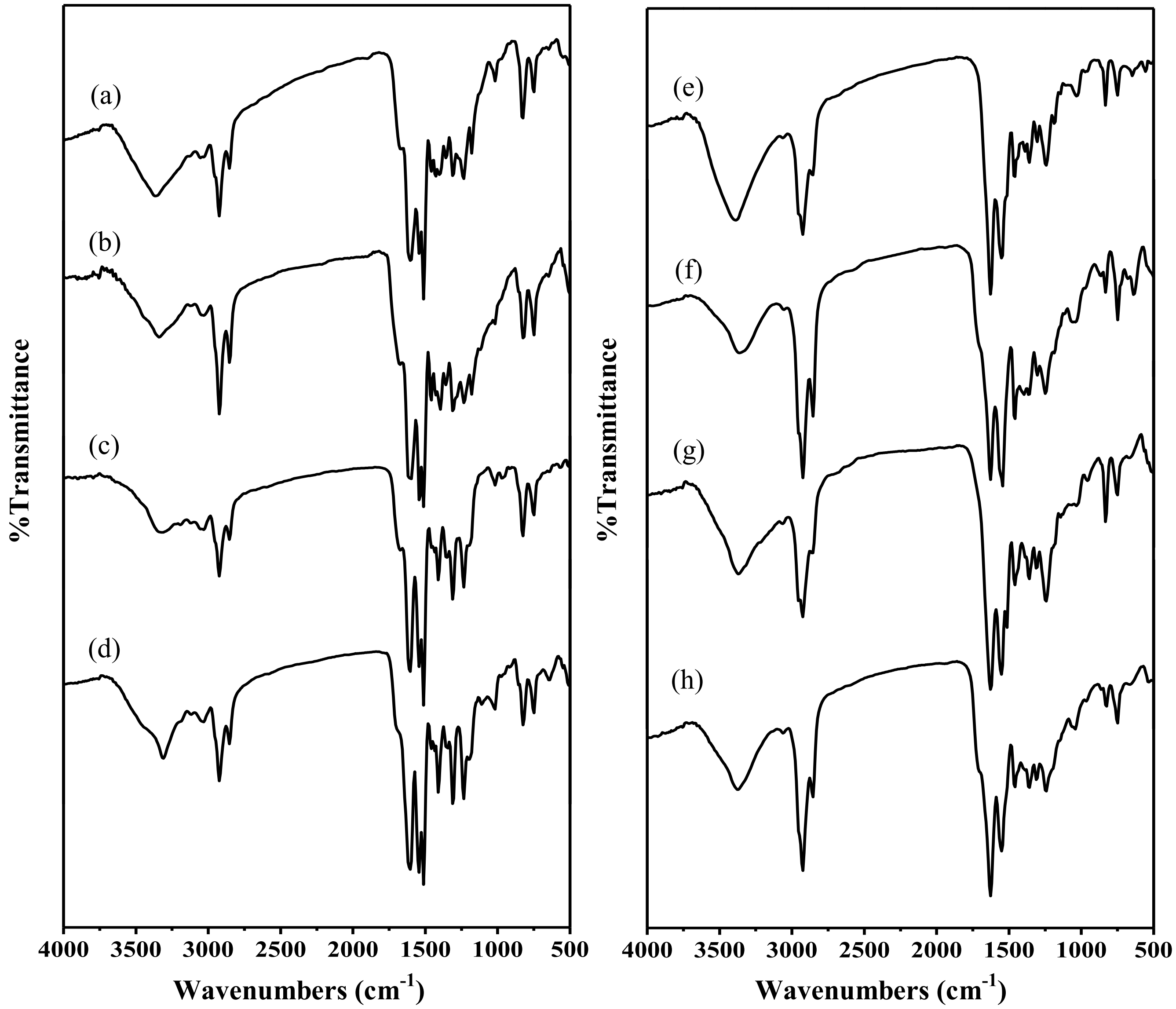

Figure 4.26 IR spectra of metal-containing poly(urethane-urea)s

(a) ZnNapth$_2$trien-MDI-BPO (1:2:1) (b) ZnNapth$_2$trien-MDI-HDO (1:2:1)

(c) NiNapth$_2$trien-MDI-BPO (1:2:1) (d) NiNapth$_2$trien-MDI- HDO (1:2:1)

(e) ZnNapth$_2$trien-IPDI-BPO (1:2:1) (f) ZnNapth$_2$trien-IPDI-HDO (1:2:1)

(g) NiNapth$_2$trien-IPDI-BPO (1:2:1) (h) NiNapth$_2$trien-IPDI-HDO (1:2:1)

Table 4.18 IR data of metal-containing poly(urethane-urea)s

Polymers	IR signals (cm^{-1})
MDI-BPO	3308 (NH), 2910, 2840, 1645 (C=O), 1597, 1545, 1511, 1410, 1308, 1234, 1108, 1011, 812, 649, 508.
MDI-HDO	3323 (NH), 2930, 2851, 1706 (C=O), 1599, 1528, 1412, 1410, 1311, 1228, 1069, 816, 769, 508.
IPDI-BPO	3379 (NH), 2953, 2921, 1647 (C=O), 1556, 1466, 1383, 1366, 1306, 1239, 1148, 1065, 959, 926, 889, 869, 829, 769.
IPDI-HDO	3370 (NH), 2926, 2857, 1705 (C=O), 1643, 1562, 1463, 1383, 1306, 1242, 1196, 1104, 1067, 865, 768, 722.
ZnNapth$_2$trien-MDI-BPO	3334 (NH), 3035, 2920, 2852, 1667 (C=O), 1617 (C=N), 1591, 1541, 1510, 1459, 1432, 1411, 1354, 1307, 1233, 1175, 1117, 1020, 946, 829, 750.
ZnNapth$_2$trien-MDI-HDO	3339 (NH), 3046, 2922, 2853, 1670 (C=O), 1619 (C=N), 1540, 1512, 1460, 1413, 1358, 1308, 1233, 1180, 1133, 1117, 1021, 958, 911, 861, 824, 749.
NiNapth$_2$trien-MDI-BPO	3414 (NH), 2924, 2856, 1684 (C=O), 1616 (C=N), 1541, 1512, 1463, 1436, 1410, 1355, 1311, 1235, 1183, 1144, 1090, 1021, 969, 824, 750.
NiNapth$_2$trien-MDI-HDO	3312 (NH), 2923, 2854, 1688 (C=O), 1618 (C=N), 1544, 1512, 1459, 1435, 1410, 1354, 1309, 1235, 1186, 1139, 1124, 1021, 976, 953, 855, 824, 750.
ZnNapth$_2$trien-IPDI- BPO	3365 (NH), 2921, 2855, 1669 (C=O), 1627 (C=N), 1550, 1510, 1461, 1393, 1359, 1308, 1241, 1183, 1141, 1113, 1027, 969, 952, 833, 755.

Table 4.18 (continued)

Polymers	**IR signals (cm^{-1})**
ZnNapth$_2$trien-IPDI-HDO	3376 (NH), 2923, 2860, 1669 (C=O), 1622 (C=N), 1545, 1462, 1435, 1416, 1392, 1358, 1305, 1245, 1186, 1139, 1034, 957, 863, 832, 750
NiNapth$_2$trien-IPDI-BPO	3390 (NH), 2923, 2856, 1674 (C=O), 1623 (C=N), 1546, 1513, 1461, 1439, 1412, 1390, 1358, 1307, 1243, 1183, 1140, 1093, 1033, 953, 891, 831, 750.
NiNapth$_2$trien-IPDI-HDO	3375 (NH), 2925, 2856, 1681 (C=O), 1618 (C=N), 1551, 1460, 1427, 1412, 1389, 1361, 1309, 1245, 1187, 1140, 1035, 953, 895, 864, 826, 750.

4.4.2.2 ^{1}H NMR spectroscopy of metal-containing poly(urethane-urea)s

^{1}H NMR spectra of zinc-containing poly(urethane-urea)s were recorded in DMSO-d_6. ^{1}H NMR data and spectra of poly(urethane-urea)s obtained from MNapth$_2$trien : diisocyanates : dialcohols at the mole ratio of 1:2:1 are presented in Table 4.19 and Figures 4.27-4.28, A.18-A.23. The ^{1}H NMR spectra of metal-containing poly(urethane-urea)s showed signals for the CH=N at 9.06-9.36 ppm. Aromatic proton of metal complexes appeared as broad peaks. The absorption of aromatic proton was observed at 6.41-8.26 ppm. NH protons of urea attached to aromatic and urethane group showed absorption band in the range of 8.45-8.59 ppm. NH protons of attached to methylene group appeared at 4.72-5.96 ppm. The signals at 0.62-4.37 ppm were assigned to -CH, -CH$_2$ and -CH$_3$ groups. As an example, ZnNapth$_2$trien-MDI-HDO (1:2:1) spectrum (Figure 4.28) showed peak at 9.18-9.28 ppm for CH=N and 8.45-8.59, 4.79-4.90 ppm for NH proton, respectively. As compared to the spectrum of MDI-HDO (Figure 4.27), where aromatic protons of MDI could be observed, the aromatic protons of ZnNapth$_2$trien and MDI in ZnNapth$_2$trien-MDI-HDO (1:2:1) were observed at 6.41-8.14 ppm. The signals at 1.10-4.90 ppm were assigned to alkyl groups.

Table 4.19 ^{1}H NMR data of zinc-containing poly(urethane-urea)s[a]

Polymers	C**H**=N	N**H**	Ar-**H**	Alkyl groups[b]
MDI-BPO	-	8.53	7.33-7.35, 7.09-7.11, 6.83-6.85, 6.47-6.48	3.67-3.80,1.18-1.33
MDI-HDO	-	8.50	7.32-7.33, 7.05-7.07	4.03, 3.80, 1.20-1.59
ZnNapth$_2$trien-MDI-BPO	9.09-9.30	8.46-8.55, 4.72-4.89	7.92-8.14, 7.56-7.78, 7.46-7.54, 7.24-7.44, 7.18-7.24, 7.00-7.14, 6.76-6.94, 6.60-6.74, 6.42-6.52	3.76-3.86, 3.42-3.74, 2.95-3.04, 2.87-2.94, 2.71-2.75, 2.53-2.55, 1.45-1.66, 1.11-1.28
ZnNapth$_2$trien-MDI-HDO	9.18-9.28	8.45-8.59, 4.79-4.90	7.90-8.14, 7.60-7.64, 7.44-7.54, 7.26-7.40, 6.93-7.16, 6.73-6.90, 6.55-6.67, 6.41-6.55,	4.28-4.37, 3.74-3.85, 3.61-3.72, 2.95-3.04, 2.86-2.91, 2.68-2.78, 1.34-1.46, 1.24-1.33, 1.10-1.24
IPDI-BPO		5.40-5.99	6.89-7.04, 6.58-6.67	3.57-3.77, 2.68-2.83, 1.37-1.63, 0.61-1.30
IPDI-HDO		5.48-5.98		4.26-4.43, 3.83-4.07, 3.57-3.78, 2.60-2.87, 2.21-2.30, 1.34-1.65, 0.63-1.03
ZnNapth$_2$trien-IPDI-BPO	9.26-9.36	5.37-5.96	7.99-8.12, 7.54-7.73, 7.18-7.49, 7.02-7.18, 6.90-7.01, 6.77-6.87, 6.56-6.65	3.55-3.74, , 2.90-3.01, 2.62-2.89, 1.97-2.12 1.40-1.57, 0.60-1.29
ZnNapth$_2$trien-IPDI-HDO	9.06-9.27	5.37-5.94	8.16-8.26, 7.88-8.12, 7.42-7.75, 7.20-7.35, 6.91-7.15, 6.65-6.80	3.75-3.90, 3.57-3.72 2.85-3.01, 2.58-2.71, 2.06-1.98, 1.30-1.63, 1.01-1.29, 0.62-1.00

[a] all peaks are multiplets

[b] for MDI-based polymers, alkyl groups = -C**H**$_2$;
for IPDI-based polymers, alkyl groups = C**H**, C**H**$_2$ and C**H**$_3$

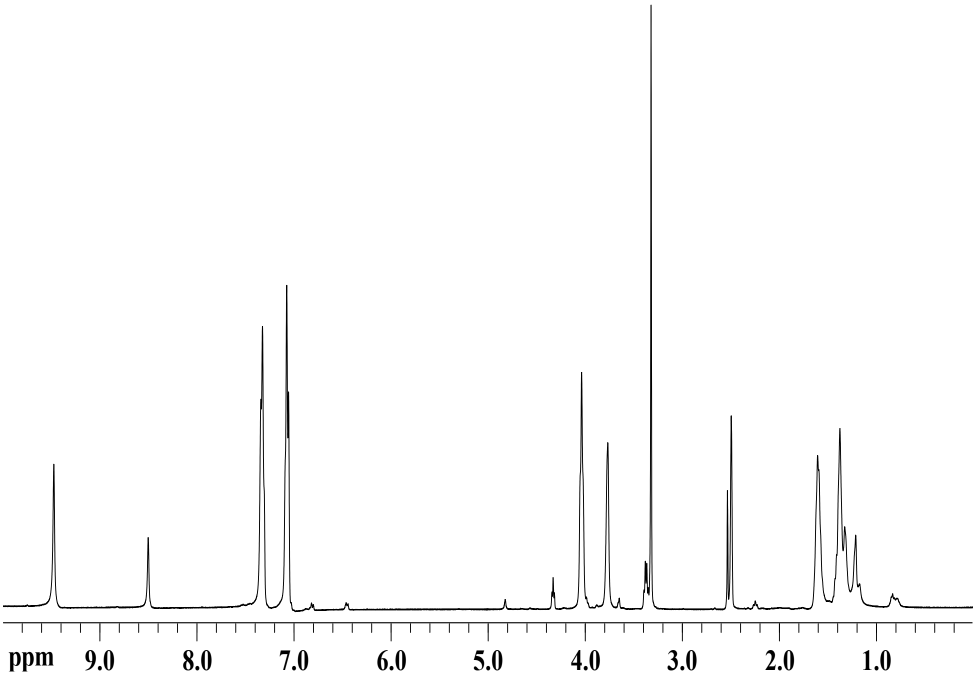

Figure 4.27 ^{1}H NMR spectrum of MDI-HDO in DMSO-d_6

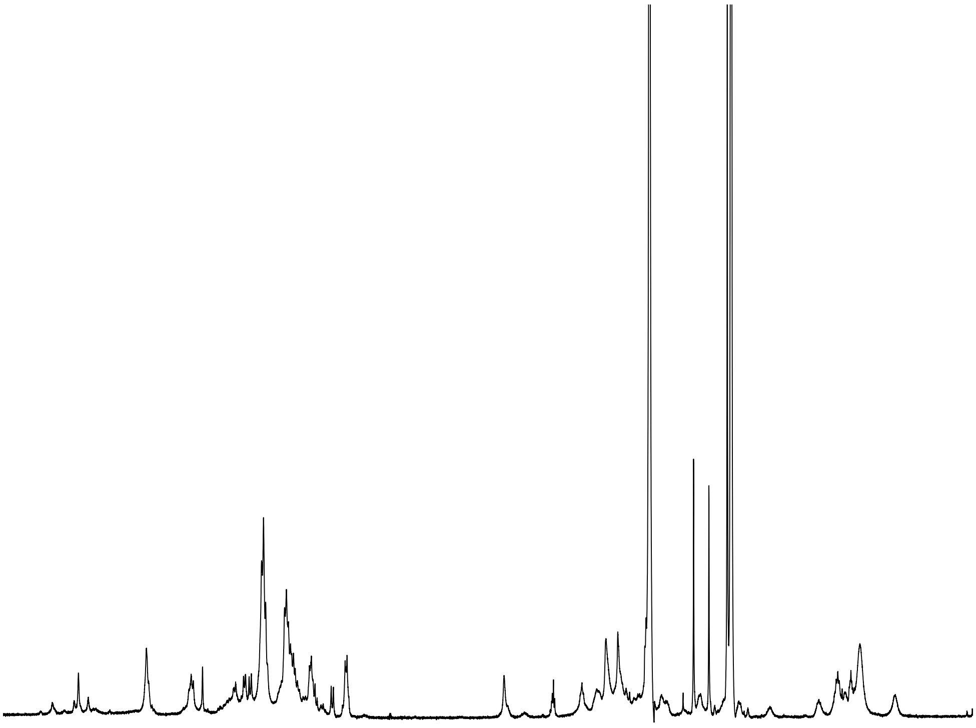

Figure 4.28 ^{1}H NMR spectrum of ZnNapth$_2$trien-MDI-HDO in DMSO-d_6

4.4.2.3 Solubility of poly(urethane-urea)s

Solubility of metal-containing poly(urethane-urea)s and reference polymers were tested in various polar and non-polar solvents (Table 4.20). The maximum amount of each polymer that was able to dissolve in 1 mL of DMSO was also determined. Metal-containing poly(urethane-urea)s were soluble DMF and DMSO, insoluble in hexane, toluene, dichloromethane, methanol, acetonitrile and water. Some of metal-containing poly(urethane-urea)s with good solubility such as ZnNapth$_2$trien-MDI-BPO and NiNapth$_2$trien-MDI-BPO were partial soluble in chloroform and tetrahydrofuran.

Poly(urethane-urea)s showed great improvement in solubility compared with that of metal-containing polyureas. This was because poly(urethane-urea)s contained less 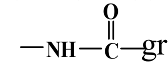 $-NH-\overset{O}{\overset{\|}{C}}-$ groups and therefore had less hydrogen bonding than polyurea. Many poly(urethane-urea)s had the solubility of >200 mg in 1 mL of DMSO. Most copolymers showed good solubility at the mole ratio of MNapth$_2$trien : diisocyanate : dialcohols = 0.5:2:1.5 and 1:2:1. Most MDI based copolymers had better solubility than IPDI-based copolymers. HDO-based polymers showed better solubility than BPO-based polymers.

Table 4.20 Solubility of metal-containing poly(urethane-urea)s based on MDI

Polymers	THF	DMF	DMSO	Maximum solubility (mg)/ DMSO 1 (mL)
MDI-BPO	-	+-	+	5
ZnNapth$_2$trien-MDI-BPO (0.5:2:1.5)	+-	+	++	118
ZnNapth$_2$trien-MDI-BPO (1:2:1)	+-	+	++	180
ZnNapth$_2$trien-MDI-BPO (1.5:2:0.5)	+-	+	++	138
NiNapth$_2$trien-MDI-BPO (0.5:2:1.5)	+-	+	+	11
NiNapth$_2$trien-MDI-BPO (1:2:1)	+-	+	++	210
NiNapth$_2$trien-MDI-BPO (1.5:2:0.5)	+-	+	++	93
MDI-HDO	-	++	++	90
ZnNapth$_2$trien-MDI-HDO (0.5:2:1.5)	-	++	++	275
ZnNapth$_2$trien-MDI-HDO (1:2:1)	+-	++	++	151

++ = Soluble at room temperature; **+** = soluble on heating; **+-** = partial soluble on heating; **-** = insoluble

Table 4.20 (continued**)**

Polymers	**THF**	**DMF**	**DMSO**	**Maximum solubility (mg)/ DMSO 1 (mL)**
ZnNapth$_2$trien-MDI-HDO (1.5:2:0.5)	-	++	+	43
NiNapth$_2$trien-MDI-HDO (0.5:2:1.5)	-	++	++	798
NiNapth$_2$trien-MDI-HDO (1:2:1)	+-	++	++	499
NiNapth$_2$trien-MDI-HDO (1.5:2:0.5)	-	++	++	348

++ = Soluble at room temperature; **+** = soluble on heating; **+-** = partial soluble on heating; **-** = insoluble

Table 4.21 Solubility of metal containing poly(urethane-urea)s based on IPDI

Polymers	**THF**	**DMF**	**DMSO**	**Maximum solubility (mg)/ DMSO 1 (mL)**
IPDI-BPO	-	-	+	5
ZnNapth$_2$trien-IPDI-BPO (0.5:2:1.5)	-	-	+	20
ZnNapth$_2$trien-IPDI-BPO (1:2:1)	-	-	+	45
ZnNapth$_2$trien-IPDI-BPO (1.5:2:0.5)	-	-	++	53
NiNapth$_2$trien-IPDI-BPO (0.5:2:1.5)	-	-	++	75
NiNapth$_2$trien-IPDI-BPO (1:2:1)	-	-	++	53
NiNapth$_2$trien-IPDI-BPO (1.5:2:0.5)	-	-	+	30
IPDI-HDO	-	++	+	48
ZnNapth$_2$trien-IPDI-HDO (0.5:2:1.5)	++	++	++	119
ZnNapth$_2$trien-IPDI-HDO (1:2:1)	++	++	++	97
ZnNapth$_2$trien-IPDI-HDO (1.5:2:0.5)	-	++	++	527
NiNapth$_2$trien-IPDI-HDO (0.5:2:1.5)	+	++	++	396
NiNapth$_2$trien-IPDI-HDO (1:2:1)	++	++	++	540
NiNapth$_2$trien-IPDI-HDO (1.5:2:0.5)	-	++	++	833

++ = Soluble at room temperature; **+** = soluble on heating; **+-** = partial soluble on heating; **-** = insoluble

4.4.2.4 Inherent viscosity of poly(urethane-urea)s

Inherent viscosity of all poly(urethane-urea)s was measured at 40°C in DMSO as described in Appendix[B-1]. Metal-containing poly(urethane-urea)s had viscosities in the range of 0.194-0.478 dl/g (Table 4.22). The viscosity of metal-containing poly(urethane-urea)s was higher than that of reference poly(urethane-urea)s without metal complexes in both Zn and Ni series.

Table 4.22 Inherent viscosity of metal-containing poly(urethane-urea)s

Polymers	**η_{inh} (dl g^{-1})**
MDI-BPO	0.116
MDI-HDO	0.139
IPDI-BPO	0.192
IPDI-HDO	0.180
ZnNapth$_2$trien-MDI-BPO (0.5:2:1.5)	0.218
ZnNapth$_2$trien-MDI-BPO (1:2:1)	0.227
ZnNapth$_2$trien-MDI-BPO (1.5:2:0.5)	0.478
ZnNapth$_2$trien-MDI-HDO (0.5:2:1.5)	0.265
ZnNapth$_2$trien-MDI-HDO (1:2:1)	0.241
ZnNapth$_2$trien-MDI-HDO (1.5:2:0.5)	0.209
NiNapth$_2$trien-MDI-BPO (0.5:2:1.5)	0.200
NiNapth$_2$trien-MDI-BPO (1:2:1)	0.235
NiNapth$_2$trien-MDI-BPO (1.5:2:0.5)	0.470
NiNapth$_2$trien-MDI-HDO (0.5:2:1.5)	0.203
NiNapth$_2$trien-MDI-HDO (1:2:1)	0.239
NiNapth$_2$trien-MDI-HDO (1.5:2:0.5)	0.222
ZnNapth$_2$trien-IPDI-BPO (0.5:2:1.5)	0.207
ZnNapth$_2$trien-IPDI-BPO (1:2:1)	0.293
ZnNapth$_2$trien-IPDI-BPO (1.5:2:0.5)	0.433
ZnNapth$_2$trien-IPDI-HDO (0.5:2:1.5)	0.194
ZnNapth$_2$trien-IPDI-HDO (1:2:1)	0.283

Table 4.22 (continued)

Polymers	η_{inh} **(dl g^{-1})**
ZnNapth$_2$trien-IPDI-HDO (1.5:2:0.5)	0.224
NiNapth$_2$trien-IPDI-BPO (0.5:2:1.5)	0.212
NiNapth$_2$trien-IPDI-BPO (1:2:1)	0.293
NiNapth$_2$trien-IPDI-BPO (1.5:2:0.5)	0.271
NiNapth$_2$trien-IPDI-HDO (0.5:2:1.5)	0.232
NiNapth$_2$trien-IPDI-HDO (1:2:1)	0.230
NiNapth$_2$trien-IPDI-HDO (1.5:2:0.5)	0.227

4.4.2.5 Thermogravimetric analysis

Thermal stability and degradation of metal-containing poly(urethane-urea)s were analyzed based on the TGA thermograms obtained under air atmosphere. TGA data and thermograms of the polymers are presented in Table 4.23-4.24 and Figures 4.29-4.36, respectively.

4.4.2.5.1 Metal-containing poly(urethane-urea)s based on BPO

IDTs of ZnNapth$_2$trien-MDI-BPO were found in the range of 181-242°C. Their residual weights at 600°C were in the range of 31-40%. The residual weight at 600°C increased with increasing amount of metal complexes. When compared to ZnNapth$_2$trien-MDI polyurea, addition of BPO decreased both IDTs and char yields at 600 °C of poly(urethane-urea)s. IDTs of NiNapth$_2$trien-MDI-BPO were found in the range of 192-246°C. Their residual weights at 600°C were in the range of 36-53%. When compared to NiNapth$_2$trien-MDI polyurea, addition of BPO increased char yields at 600 °C but decreased IDTs of poly(urethane-urea)s

IDTs of ZnNapth$_2$trien-IPDI-BPO were found in the range of 160-223°C. Their residual weights at 600°C were in the range of 16-28%. IDTs of ZnNapth$_2$trien-IPDI-BPO increased with increasing amount of BPO in poly(urethane-urea)s. The residual weight at 600°C increased with increasing amount of metal complexes. IDTs of NiNapth$_2$trien-IPDI-BPO were found in the range of 168-242°C. The residual weights at 600°C were in the range of 14-21%. For all nickel-containing copolymers, addition of dialcohols in the polymerization results in the increase in char yields at 600 °C but IDTs were decreased. The residual weights at 600°C increased with increasing amount of metal complexes. Char yields of $\mathrm{NiNapth_2trien}$-IPDI-BPO were higher than that of the reference polymer (IPDI-BPO).

From Figure 4.30, $\mathrm{NiNapth_2trien}$-MDI-BPO (0.5:2:1.5) showed the highest thermal stability because of the rigid aromatic ring in MDI and BPO. Phenyl and naphthyl rings had planar structures and could thus be easily packed which increased the chain-to-chain interaction.

Table 4.23 TGA data of metal-containing poly(urethane-urea)s based on BPO

Polymer	**IDT (°C)**	**Weight residue (%) at different temperature (°C)**						
		300	**400**	**500**	**600**	**700**	**800**	**900**
MDI-BPO	253	85	58	39	28	10	6	6
ZnNapth$_2$trien-MDI	280	93	66	56	48	33	20	11
ZnNapth$_2$trien- MDI-BPO (0.5:2:1.5)	211	80	55	39	31	17	6	5
ZnNapth$_2$trien- MDI-BPO (1:2:1)	242	85	62	46	39	28	17	8
ZnNapth$_2$trien- MDI-BPO (1.5:2:0.5)	181	81	63	50	40	22	11	11
NiNapth$_2$trien-MDI	284	93	60	49	35	19	8	8
NiNapth$_2$trien- MDI-BPO (0.5:2:1.5)	219	80	70	62	53	43	34	24
NiNapth$_2$trien- MDI-BPO (1:2:1)	246	87	61	45	38	28	20	12
NiNapth$_2$trien- MDI-BPO (1.5:2:0.5)	192	82	60	44	36	25	16	10
IPDI-BPO	290	95	14	8	3	1	1	1
ZnNapth$_2$trien-IPDI	226	89	39	28	19	8	7	7
ZnNapth$_2$trien- IPDI-BPO (0.5:2:1.5)	223	78	34	23	16	7	7	6
ZnNapth$_2$trien- IPDI-BPO (1:2:1)	203	80	39	31	19	9	7	7
ZnNapth$_2$trien- IPDI-BPO (1.5:2:0.5)	160	79	49	41	28	15	10	10
NiNapth$_2$trien-IPDI	286	94	24	16	6	4	3	3
NiNapth$_2$trien- IPDI-BPO (0.5:2:1.5)	228	89	31	23	14	6	5	5
NiNapth$_2$trien- IPDI-BPO (1:2:1)	242	84	40	31	19	11	6	6
NiNapth$_2$trien- IPDI-BPO (1.5:2:0.5)	168	82	43	33	21	12	8	8

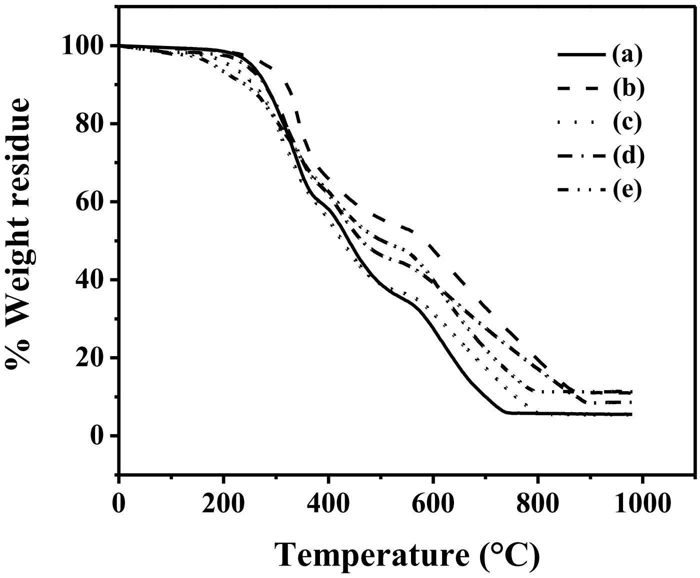

Figure 4.29 TGA thermograms of (a) MDI-BPO; (b) $ZnNapth_2trien$-MDI; (c) $ZnNapth_2trien$-MDI-BPO (0.5:2:1.5); (d) $ZnNapth_2trien$-MDI-BPO (1:2:1); (e) $ZnNapth_2trien$-MDI-BPO (1.5:2:0.5)

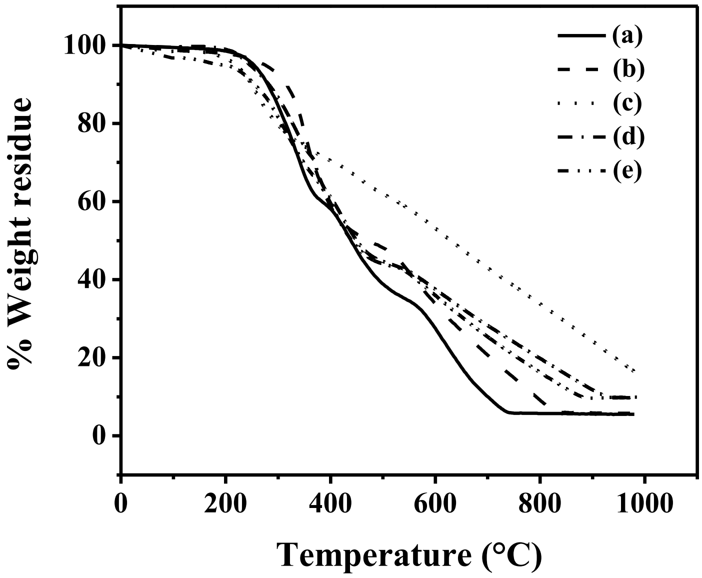

Figure 4.30 TGA thermograms of (a) MDI-BPO; (b) $NiNapth_2trien$-MDI; (c) $NiNapth_2trien$-MDI-BPO (0.5:2:1.5); (d) $NiNapth_2trien$-MDI-BPO (1:2:1); (e) $NiNapth_2trien$-MDI-BPO (1.5:2:0.5)

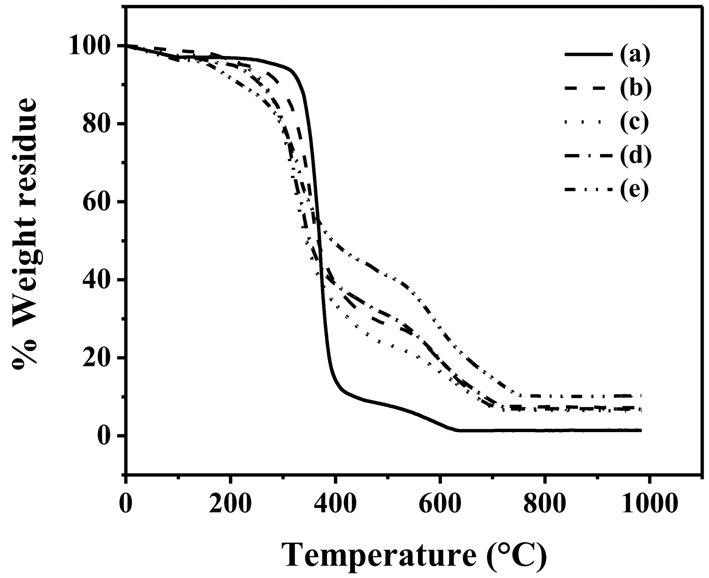

Figure 4.31 TGA thermograms of (a) IPDI-BPO; (b) ZnNapth$_2$trien-IPDI; (c) ZnNapth$_2$trien-IPDI-BPO (0.5:2:1.5); (d) ZnNapth$_2$trien-IPDI-BPO (1:2:1); (e) ZnNapth$_2$trien-IPDI-BPO (1.5:2:0.5)

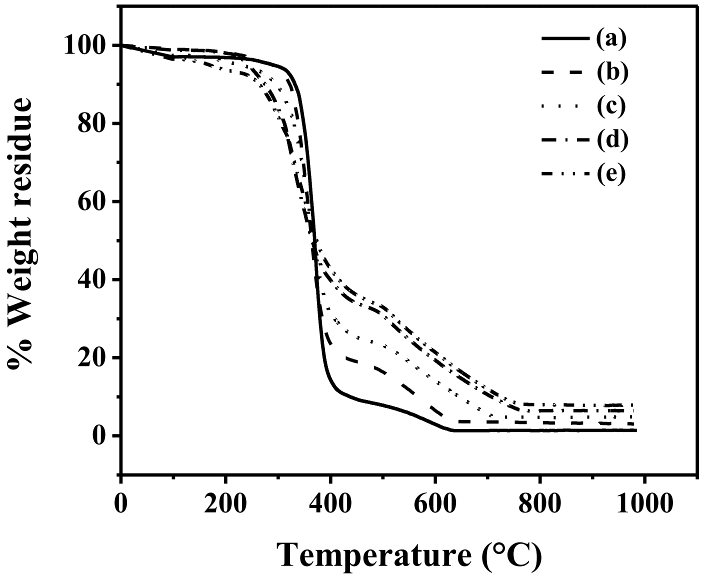

Figure 4.32 TGA thermograms of (a) IPDI-BPO; (b) NiNapth$_2$trien-IPDI; (c) NiNapth$_2$trien-IPDI-BPO (0.5:2:1.5); (d) NiNapth$_2$trien-IPDI-BPO (1:2:1); (e) NiNapth$_2$trien-IPDI-BPO (1.5:2:0.5)

4.4.2.5.2 Metal-containing poly(urethane-urea)s based on HDO

IDTs of ZnNapth$_2$trien-MDI-HDO and NiNapth$_2$trien-MDI-HDO were found in the range of 170-234 and 171-259°C, respectively The residual weights at 600°C of ZnNapth$_2$trien-MDI-HDO and NiNapth$_2$trien-MDI-HDO were in the range of 32-43 and 29-42%, respectively. The residual weights at 600°C increased with increasing amount of metal complexes. The char yields of both ZnNapth$_2$trien-MDI-HDO and NiNapth$_2$trien-MDI-HDO were higher than that of the reference polymer (MDI-HDO).

IDTs of ZnNapth$_2$trien-IPDI-HDO and NiNapth$_2$trien-IPDI-HDO were found in the range of 167-256 and 226-255°C, respectively. The residual weights at 600°C of ZnNapth$_2$trien-IPDI-HDO and NiNapth$_2$trien-IPDI-HDO were in the range of 15-31 and 14-25%, respectively. IDT of NiNapth$_2$trien-IPDI-HDO increased with increasing amount of BPO in poly(urethane-urea)s. The residual weights at 600°C increased with increasing amount of metal complexes. The char yield of metal-containing poly(urethane-urea)s was higher than reference polymer (IPDI-HDO).

Table 4.24 TGA data of metal-containing poly(urethane-urea)s based on HDO

Polymer	**IDT (°C)**	**Weight residue (%) at different temperature (°C)**						
		300	**400**	**500**	**600**	**700**	**800**	**900**
MDI-HDO	270	81	52	28	18	5	3	3
ZnNapth$_2$trien-MDI	280	93	66	56	48	33	20	11
ZnNapth$_2$trien-MDI-HDO (0.5:2:1.5)	226	78	57	39	32	20	8	7
ZnNapth$_2$trien-MDI-HDO (1:2:1)	234	86	67	45	38	25	13	10
ZnNapth$_2$trien-MDI-HDO (1.5:2:0.5)	170	82	64	52	43	26	13	12
NiNapth$_2$trien-MDI	284	93	60	49	35	19	8	8
NiNapth$_2$trien-MDI-HDO (0.5:2:1.5)	220	80	53	36	29	17	8	5
NiNapth$_2$trien-MDI-HDO (1:2:1)	259	86	65	40	35	24	17	10
NiNapth$_2$trien-MDI-HDO (1.5:2:0.5)	171	81	62	53	42	28	16	9
IPDI-HDO	241	81	33	17	11	9	9	9
ZnNapth$_2$trien-IPDI	226	89	39	28	19	8	7	7
ZnNapth$_2$trien- IPDI-HDO (0.5:2:1.5)	238	80	30	24	15	7	7	7
ZnNapth$_2$trien- IPDI-HDO (1:2:1)	256	81	48	30	23	14	14	14
ZnNapth$_2$trien- IPDI-HDO (1.5:2:0.5)	167	84	49	41	31	18	10	10
NiNapth$_2$trien-IPDI	286	94	24	16	6	4	3	3
NiNapth$_2$trien- IPDI-HDO (0.5:2:1.5)	255	83	31	24	14	7	6	6
NiNapth$_2$trien- IPDI-HDO (1:2:1)	240	81	39	30	20	11	6	6
NiNapth$_2$trien- IPDI-HDO (1.5:2:0.5)	226	80	42	34	25	18	11	10

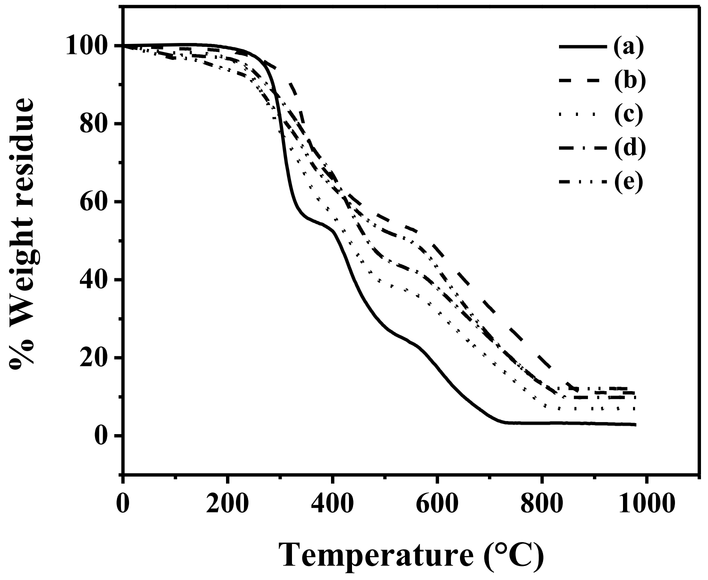

Figure 4.33 TGA thermograms of (a) MDI-HDO; (b) $ZnNapth_2trien$-MDI; (c) $ZnNapth_2trien$-MDI-HDO (0.5:2:1.5); (d) $ZnNapth_2trien$-MDI-HDO (1:2:1); (e) $ZnNapth_2trien$-MDI-HDO (1.5:2:0.5)

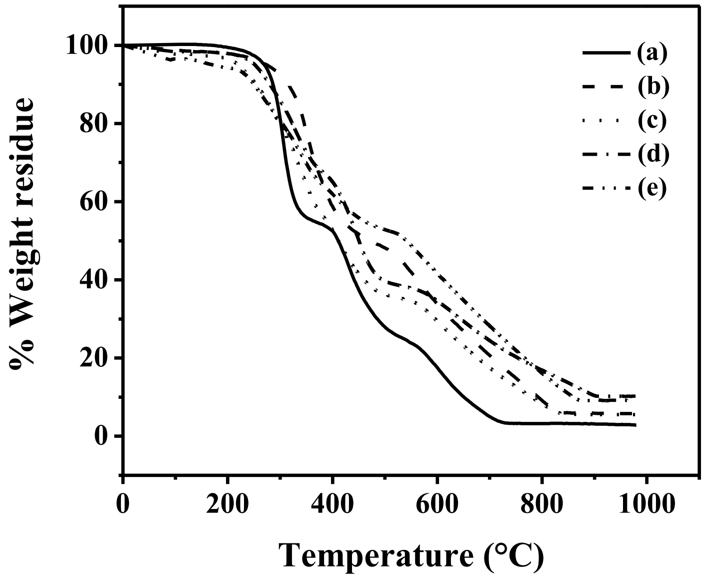

Figure 4.34 TGA thermograms of (a) MDI-HDO; (b) $NiNapth_2trien$-MDI; (c) $NiNapth_2trien$-MDI-HDO (0.5:2:1.5); (d) $NiNapth_2trien$-MDI-HDO (1:2:1); (e) $NiNapth_2trien$-MDI-HDO (1.5:2:0.5)

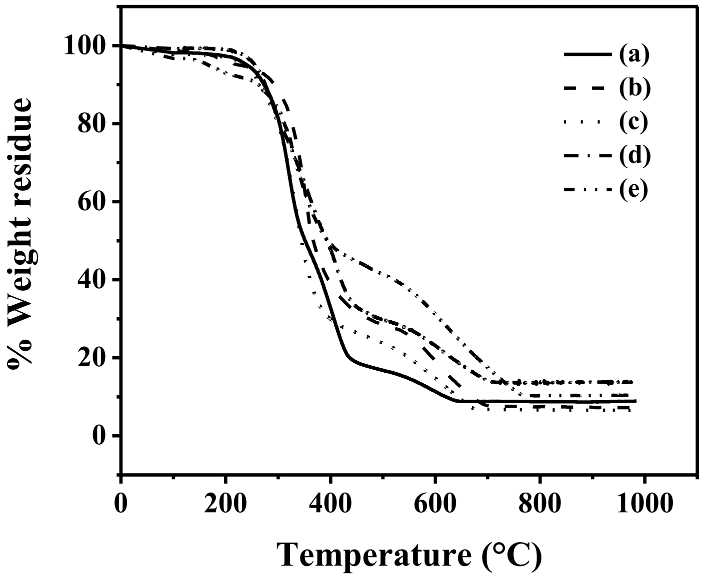

Figure 4.35 TGA thermograms of (a) IPDI-HDO; (b) ZnNapth$_2$trien-IPDI; (c) ZnNapth$_2$trien-IPDI-HDO (0.5:2:1.5); (d) ZnNapth$_2$trien-IPDI-HDO (1:2:1); (e) ZnNapth$_2$trien-IPDI-HDO (1.5:2:0.5)

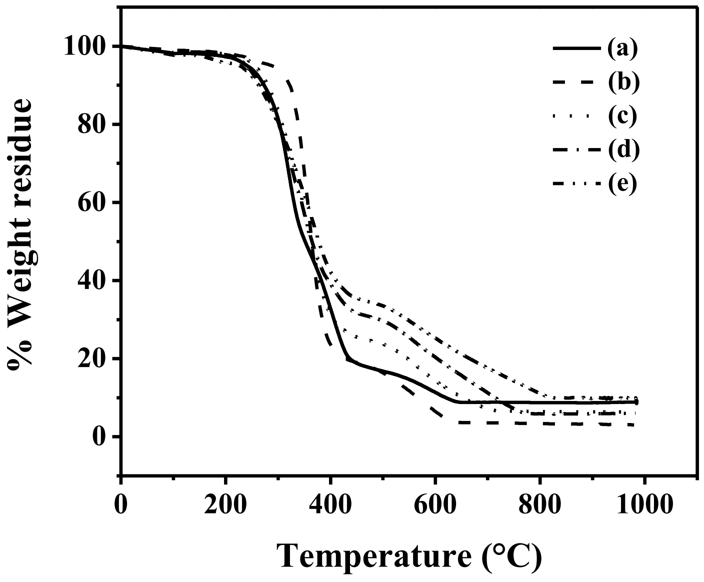

Figure 4.36 TGA thermograms of (a) IPDI-HDO; (b) NiNapth$_2$trien-IPDI; (c) NiNapth$_2$trien-IPDI-HDO (0.5:2:1.5); (d) NiNapth$_2$trien-IPDI-HDO (1:2:1); (e) NiNapth$_2$trien-IPDI-HDO (1.5:2:0.5)

4.4.2.6 X-ray diffraction

The XRD patterns of MDI-BPO and MDI-HDO showed some sharp peaks which indicated that the polymers contained crystalline part while zinc- and nickel-containing poly(urethane-urea)s based on MDI had board XRD peaks and therefore the polymers were amorphous (Figure 4.37). This XRD results corresponded with solubility resulted that the metal-containing poly(urethane-urea)s were soluble in DMF and DMSO.

The XRD patterns of poly(urethane-urea)s based on IPDI (Figure 4.38) showed that poly(urethane-urea)s based on IPDI did not show any sharp peaks which could be considered as amorphous in nature. This XRD results corresponded with solubility resulted that the metal-containing poly(urethane-urea)s were soluble in DMF and DMSO.

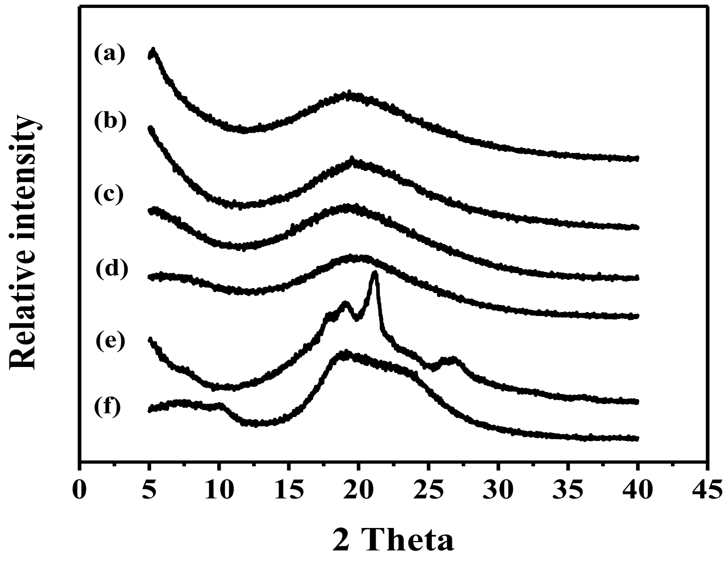

Figure 4.37 XRD patterns of (a) $ZnNapth_2trien$-MDI-BPO; (b) $ZnNapth_2trien$-MDI-HDO; (c) $NiNapth_2trien$-MDI-BPO; (d) $NiNapth_2trien$-MDI-HDO; (e) MDI-BPO (f) MDI-HDO

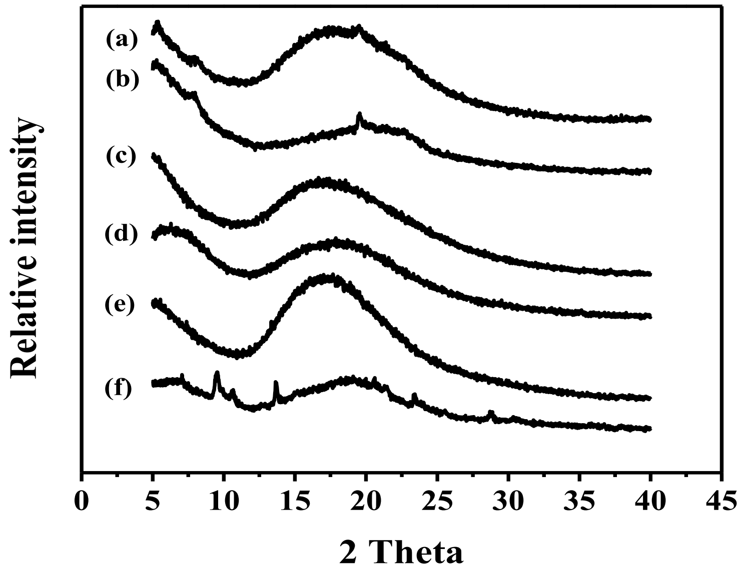

Figure 4.38 XRD patterns of (a) ZnNapth$_2$trien-IPDI-BPO; (b) ZnNapth$_2$trien-IPDI-HDO; (c) NiNapth$_2$trien-IPDI-BPO; (d) NiNapth$_2$trien-IPDI-HDO; (e) IPDI-BPO (f) IPDI-HDO

4.5 Synthesis of metal-containing poly(urea-imide)s

4.5.1 Synthesis of metal-containing poly(urea-imide)s from the reaction between MNapth$_2$trien, diisocyanates and dianhydride

Metal-containing poly(urea-imide)s were synthesized in two steps. In the first step, polyaddition of MNapth$_2$trien (M = Zn and Ni) to 4,4′-diphenylmethane diisocyanate (MDI) or isophorone diisocyanate (IPDI) gave isocyanate terminated prepolymers (Scheme 4.8).

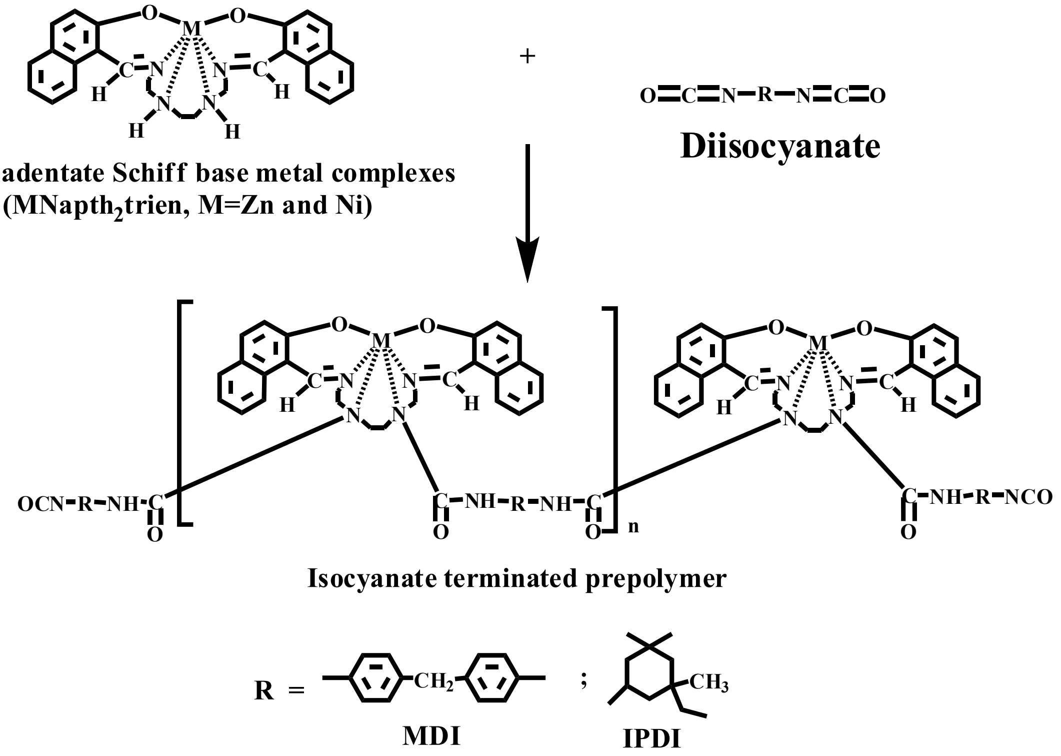

Scheme 4.8 Synthesis of isocyanate terminated prepolymers

In the second step, the prepolymers were then reacted with pyromellitic dianhydride (PMDA) or benzophenone-3,3′,4,4′-tetracarboxylic dianhydride (BTDA). Isocyanate groups in the prepolymers underwent reaction with anhydride groups to give imide groups as shown in Scheme 4.9. The reaction was carried out at the moles ratio of MNapth$_2$trien : diisocyanate : dianhydride as 1:2:0.5 and 1:2:1 in dried DMF. The yield of zinc containing poly(urea-imide)s was in the range of 54-92%. The yield of nickel-containing poly(urea-imide)s was in the range of 52-89%. (Table 4.25).

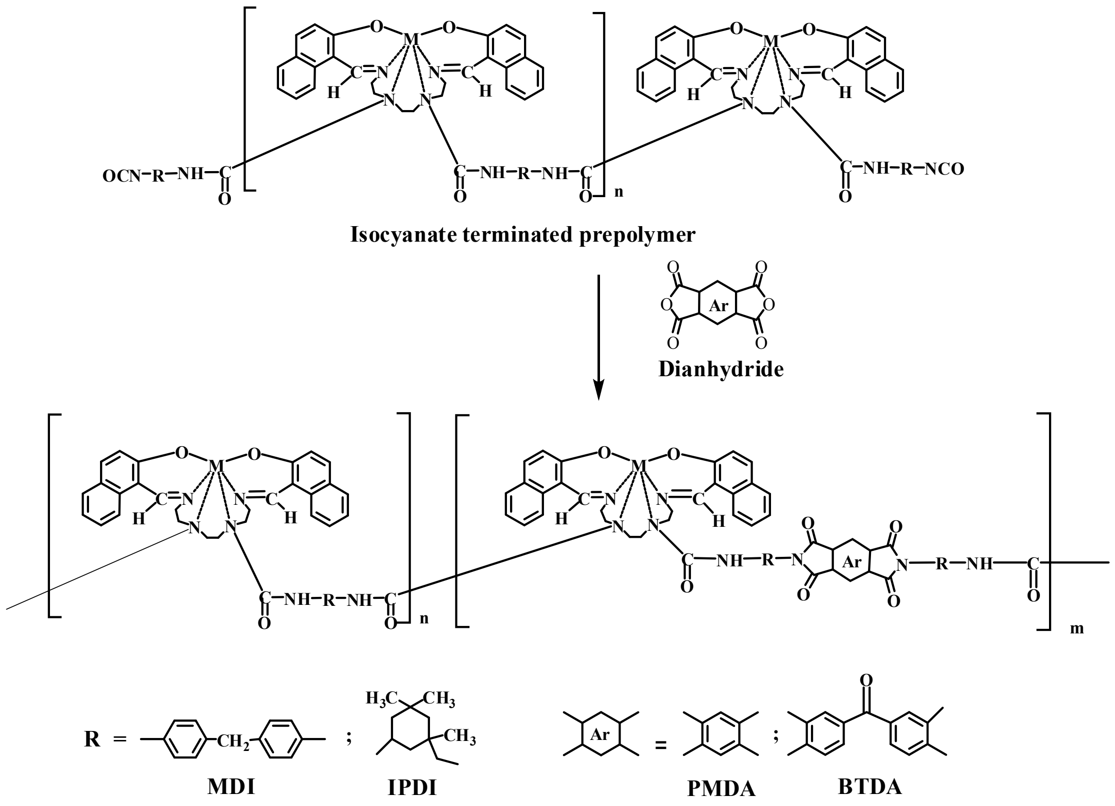

Scheme 4.9 Synthesis of metal-containing poly(urea-imide)s

Table 4.25 Synthesis data of poly(urea-imide)s

Polymers	**Weight of metal in polymer (%)**	**Yield (%)**	**External appearance**
MDI-PMDA (1:1)	-	95	Yellowish white powder
MDI-BTDA (1:1)	-	92	Yellowish white powder
IPDI-PMDA (1:1)	-	93	Yellowish white powder
IPDI-BTDA (1:1)	-	92	Yellowish white powder
ZnNapth$_2$trien-MDI-PMDA (1:2:0.5)	49.5	77	Yellow powder
ZnNapth$_2$trien-MDI-PMDA (1:2:1)	41.9	72	Yellow powder
ZnNapth$_2$trien-MDI-BTDA (1:2:0.5)	43.9	92	Orange yellow powder
ZnNapth$_2$trien-MDI-BTDA (1:2:1)	38.6	89	Brown yellow powder
NiNapth$_2$trien-MDI-PMDA (1:2:0.5)	45.6	87	Brown yellow powder
NiNapth$_2$trien-MDI-PMDA (1:2:1)	41.6	86	Dark brown powder
NiNapth$_2$trien-MDI-BTDA (1:2:0.5)	43.6	68	Brown yellow powder
NiNapth$_2$trien-MDI-BTDA (1:2:1)	38.3	80	Brown powder
ZnNapth$_2$trien-IPDI-PMDA (1:2:0.5)	48.3	89	Yellow powder
ZnNapth$_2$trien-IPDI-PMDA (1:2:1)	43.9	90	Yellow powder
ZnNapth$_2$trien-IPDI-BTDA (1:2:0.5)	46.2	66	Orange yellow powder
ZnNapth$_2$trien-IPDI-BTDA (1:2:1)	40.3	54	Orange yellow powder
NiNapth$_2$trien-IPDI-PMDA (1:2:0.5)	48.0	52	Brown powder
NiNapth$_2$trien-IPDI-PMDA (1:2:1)	43.6	89	Dark brown powder
NiNapth$_2$trien-IPDI-BTDA (1:2:0.5)	45.8	88	Brown powder
NiNapth$_2$trien-IPDI-BTDA (1:2:1)	40.0	84	Dark brown powder

In the first step, the possible polymerization mechanism was that the metal complexes underwent reaction with isocyanate groups in MDI or IPDI to give urea linkages (Scheme 4.10).

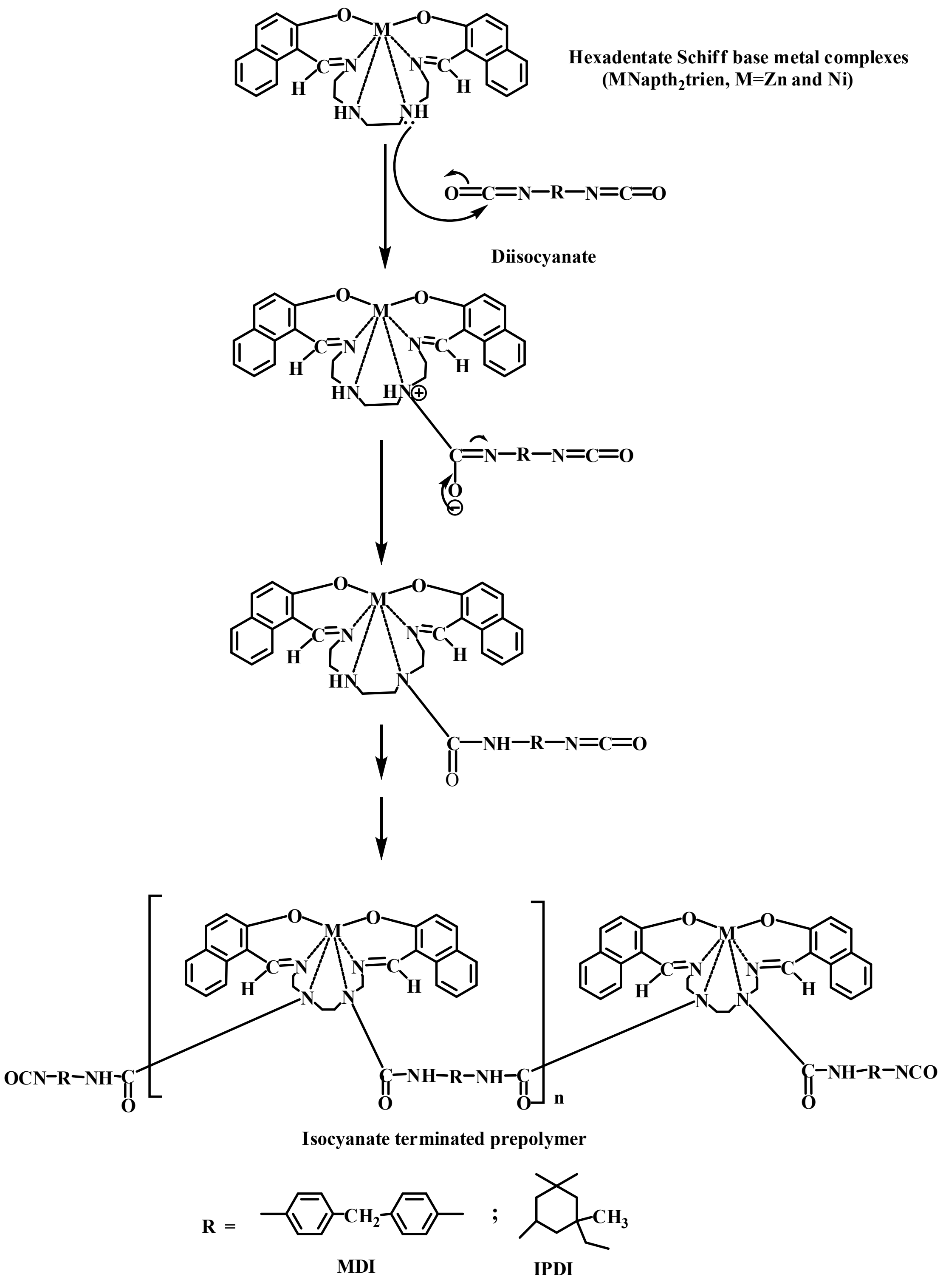

Scheme 4.10 Possible mechanism of the reaction between MNapth$_2$trien and diisocyanates

In the second step, the possible mechanism was the addition of isocyanate groups to dianhydride groups to give 7-membered ring intermediate followed by decarboxylation to give imide groups (Scheme 4.11). It was found that in the first step (Scheme 4.10), MDI showed higher reactivity towards isocyanate group in MNapth$_2$trien than IPDI [46]. The electron-withdrawing group attached to the NCO moiety will increase the positive charge on the carbon atom, thereby increasing the reactivity of the isocyanate towards nucleophilic attack. Conversely, electron-donating groups will reduce the reactivity of the NCO group. In the second step(Scheme 4.11), PMDA was more reactive toward isocyanate groups in the prepolymers than BTDA. The reason for the relatively high reactivity of PMDA was the electronic environment of the anhydride groups. This might be because BTDA has a carbonyl group that withdraws electrons from both aromatic rings. Therefore, the dianhydride groups of BTDA have less electrons than those of PMDA. In this reaction, dianhydrides and diisocyanates served as nucleophile and electrophile, respectively. BTDA has an electron-withdrawing carbonyl group between two aromatic rings. This causes the dianhydride groups in BTDA to have less electrons than those in PMDA. Therefore, PMDA was better nucleophile towards diisocyanate than BTDA.

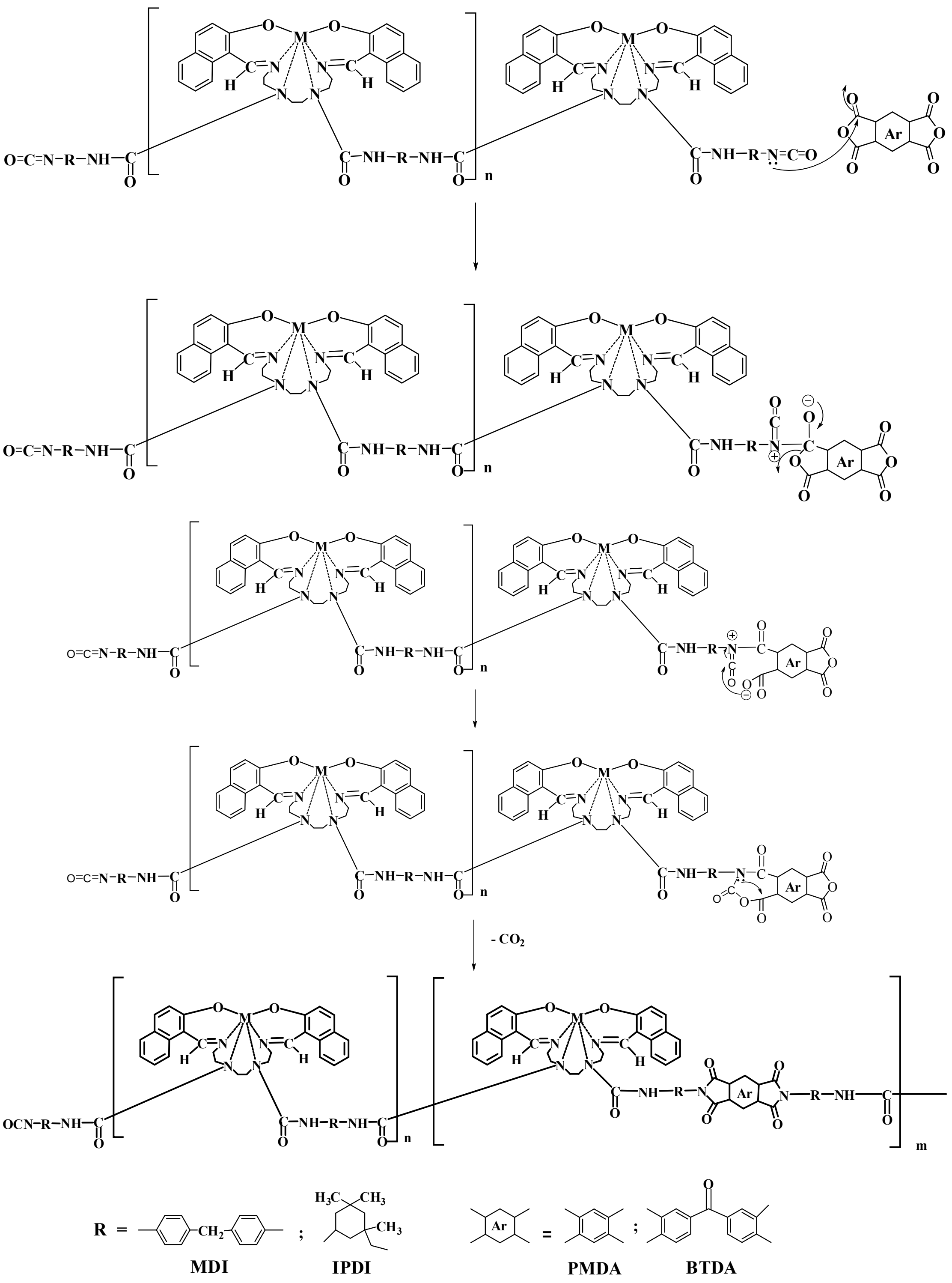

Scheme 4.11 Proposed mechanism of the reaction between isocyanate terminated prepolymers and dianhydrides

4.5.2 Characterization of metal-containing poly(urea-imide)s

4.5.2.1 IR spectroscopy of metal-containing poly(urea-imide)s

The FTIR spectra of metal-containing poly(urea-imide)s obtained from MNapth$_2$trien : diisocyanate : dianhydride at the mole ratio of 1:2:1 and 1:2:0.5 are shown in Figure 4.39 and Figure A.24, respectively.

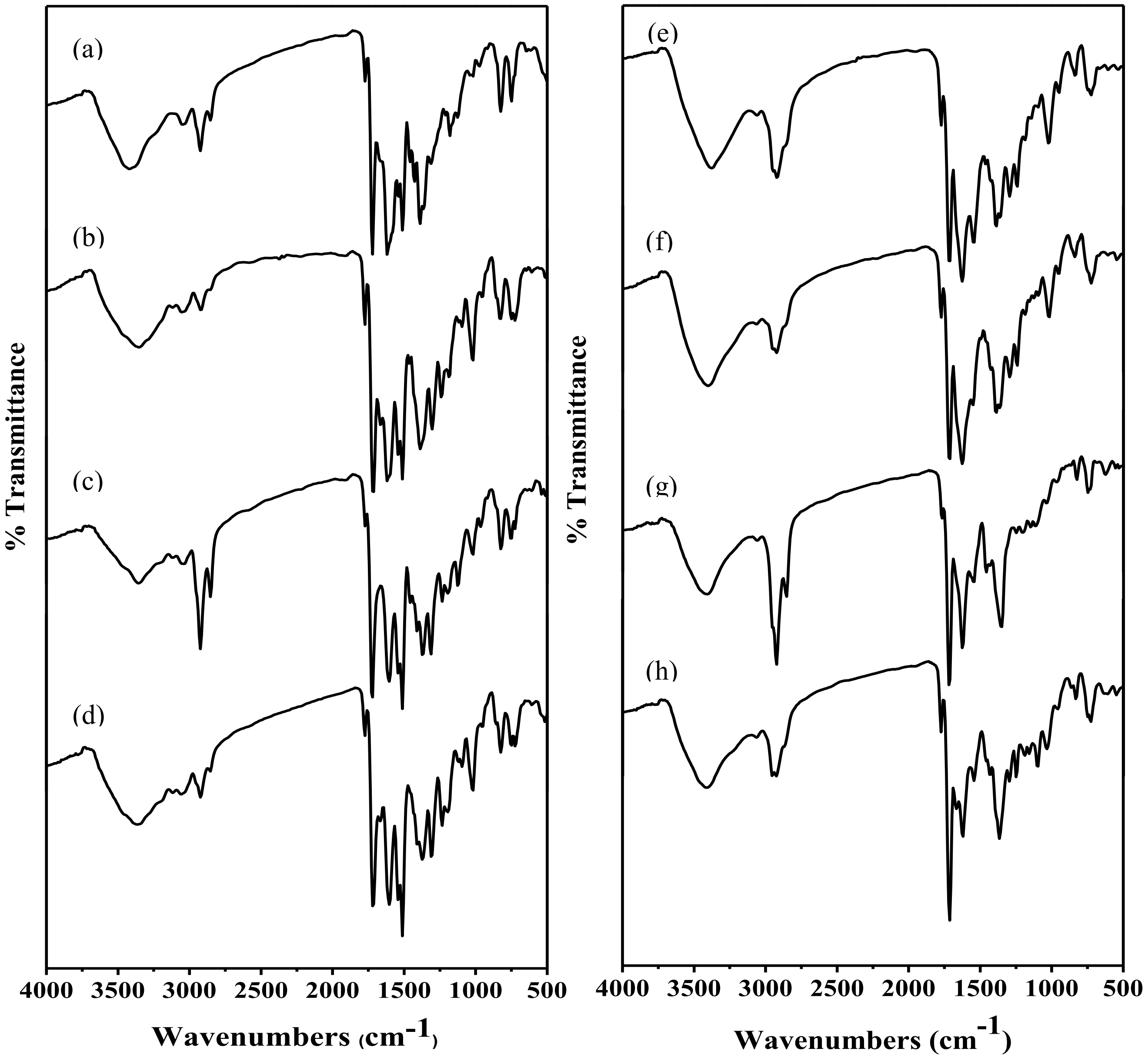

Figure 4.39 IR spectra of metal-containing poly(urea-imide)s

(a) ZnNapth$_2$trien-MDI-PMDA (1:2:1) (b) ZnNapth$_2$trien-MDI-BTDA (1:2:1)

(c) NiNapth$_2$trien-MDI-PMDA (1:2:1) (d) NiNapth$_2$trien-MDI-BTDA (1:2:1)

(e) ZnNapth$_2$trien-IPDI-PMDA (1:2:1) (f) ZnNapth$_2$trien-IPDI-BTDA (1:2:1)

(g) NiNapth$_2$trien-IPDI-PMDA (1:2:1) (h) NiNapth$_2$trien-IPDI-BTDA (1:2:1)

All metal-containing poly(urea-imide)s had similar IR spectra. The important characteristic absorption bands are 3350-3482 cm^{-1} that could be attributed to N-H stretching. The absorption bands at 2848-2951 cm^{-1} were due to C-H stretching. The absorptions at 1766-1775 and 1713-1722 cm^{-1} were assigned to asymmetric and symmetric C=O stretching vibration of imide ring. There were no signs of anhydride carbonyl band at 1870 and 1725cm^{-1} (asymmetric and symmetric stretching), which indicate the complete reaction of anhydride groups with isocyanate functional groups and formation of imide structures.IR data of metal-containing poly(urea-imide)s are shown in Table 4.26.

Table 4.26 IR data of metal-containing poly(urea-imide)s

Metal-containing poly(urea-imide)s	**IR signals (cm^{-1})**
MDI-PMDA	3421, 3036, 3000, 1776 (C=O), 1724 (C=O), 1605, 1510, 1371, 1273, 1211, 1118, 1019, 948, 872, 805, 779, 723.
MDI-BTDA	3476, 2925, 2855, 1778 (C=O), 1722 (C=O), 1667, 1601, 1512, 1419, 1376, 1289, 1243, 1213, 1165, 1096, 1017, 945, 861, 812, 753, 721.
IPDI-PMDA	3465, 2954, 2921, 1771 (C=O), 1715 (C=O), 1556, 1463, 1429, 1346, 1250, 1150, 1096, 1029, 949, 915, 820, 785, 731.
IPDI-BTDA	3470, 2926, 2858, 1774 (C=O), 1716 (C=O), 1672, 1619, 1562, 1466, 1427, 1367, 1294, 1250, 1184, 1156, 1099, 1031, 953, 865, 779, 727.
ZnNapth$_2$trien-MDI-PMDA	3422 (NH), 2924, 2854, 1773 (C=O), 1721 (C=O), 1617 (C=N), 1539, 1511, 1459, 1429, 1390, 1363, 1313, 1207, 1181, 1123, 1040, 1017, 974, 914, 825, 749.
ZnNapth$_2$trien-MDI-BTDA	3350 (NH), 2921, 2851, 1775 (C=O), 1716 (C=O), 1662, 1617 (C=N), 1539, 1511, 1463, 1387, 1304, 1239, 1184, 1118, 1096, 1021, 952, 828, 746, 724.

Table 4.26 (continued)

Metal-containing poly(urea-imide)s	**IR signals (cm^{-1})**
ZnNapth2trien-IPDI-PMDA	3380 (NH), 2922, 2855, 1775 (C=O), 1716 (C=O), 1622 (C=N), 1546, 1461, 1430, 1391, 1296, 1245, 1187, 1139, 1096, 1023, 951, 838, 748, 726.
ZnNapth$_2$trien-IPDI-BTDA	3405 (NH), 2925, 2860, 1775 (C=O), 1716 (C=O), 1625 (C=N), 1549, 1496, 1426, 1391, 1363, 1294, 1244, 1187, 1153, 1123, 1094, 1021, 952, 840, 725.
NiNapth$_2$trien-MDI-PMDA	3380 (NH), 2924, 2855, 1772 (C=O), 1722 (C=O), 1617 (C=N), 1543, 1513, 1456, 1406, 1370, 1313, 1230, 1185, 1124, 1015, 962, 826, 749, 723.
NiNapth$_2$trien-MDI-BTDA	3365 (NH), 2923, 2848, 1775 (C=O), 1717 (C=O), 1670, 1607 (C=N), 1539, 1512, 1434, 1407, 1372, 1308, 1235, 1195, 1118, 1095, 1022, 953, 853, 826, 751, 723.
NiNapth$_2$trien-IPDI-PMDA	3410 (NH), 2925, 2855, 1766 (C=O), 1717 (C=O), 1622 (C=N), 1547, 1459, 1353, 1248, 1204, 1148, 1113, 1035, 970, 827, 747, 726.
NiNapth$_2$trien-IPDI-BTDA	3482 (NH), 2951, 2856, 1773 (C=O), 1713 (C=O), 1625 (C=N), 1547, 1456, 1436, 1387, 1364, 1299, 1247, 1198, 1155, 1125, 1102, 1038, 992, 965, 833, 746, 726.

4.5.2.2 ^{1}H NMR spectroscopy of metal-containing poly(urea-imide)s

^{1}H NMR spectra of zinc-containing poly(urea-imide)s are recorded in DMSO-d_6 and their characteristic signals are presented in Table 4.27 and Figures A.25-A.32. ^{1}H NMR spectra of poly(urea-imide)s based on IPDI showed signals at 0.55-4.19 ppm which were assigned to the aliphatic parts of ZnNapth$_2$trien and IPDI. The urea NHs were observed at 5.38-5.99 ppm. The CH=N peaks were observed at 9.01-9.60 ppm. The aromatic peaks of ZnNapth$_2$trien and dianhydrides were found at 6.64-8.36 ppm. For the poly(urea-imide)s based on MDI, their ^{1}H NMR showed -CH=N- signals at 9.51-9.64 ppm. The urea NHs were observed at 8.30-8.64 ppm. The aromatic protons were observed at 6.35-8.30 ppm. The peaks at 2.28-4.06 ppm were assigned to the methylene protons of ZnNapth$_2$trien and MDI. All ^{1}H NMR signals appeared as multiplets.

Table 4.27 ^{1}H NMR data of zinc-containing poly(urea-imide)s and reference polymers[a]

Polymers	C**H**=N	N**H**	Ar-**H**	Alkyl groups[b]
MDI-PMDA	-	-	8.27-8.37 (2H), 7.02-7.51 (8H),	2.10-2.30 (2H)
MDI-BTDA	-	-	8.07-8.49 (4H), 7.84-8.01 (1H), 7.30-7.60 (4H), 6.94-7.28 (1H)	3.89-4.30 (2H)
IPDI-PMDA	-	-	7.83-8.60 (2H)	4.18-4.52 (1H), 1.75-2.19 (2H), 0.48-1.71(14H)
IPDI-BTDA	-	-	7.71-8.25 (6H)	1.83-2.35 (4H), 0.73-1.13 (13H)
ZnNapth$_2$trien-MDI-PMDA	9.53-9.61	8.36-8.61, 4.67-4.94	7.81-7.90, 7.67-7.80, 7.44-7.58, 7.21-7.40, 7.09-7.15, 6.89-6.98, 6.83-6.89, 6.72-6.83, 6.35-6.50	3.82-3.93, 3.70-3.79, 3.58-3.66, 2.92-2.98, 2.62-2.73, 2.28-2.37
ZnNapth$_2$trien-MDI-BTDA	9.51-9.64	8.30-8.64	7.64-8.30, 7.90-8.25, 7.80-7.89, 7.61-7.77, 7.44-7.57, 7.22-7.41, 6.98-7.20, 6.90-6.98, 6.84-6.88, 6.38-6.51	3.54-4.06, 3.20-3.27, 2.90-3.01, 2.54-2.60
ZnNapth$_2$trien-IPDI-PMDA	9.01-9.30	5.45-5.99	7.96-8.25, 7.87-7.95, 7.78-7.85, 7.67-7.76, 7.57-7.66, 7.34-7.49, 7.07-7.27, 6.64-6.76	3.80-4.02, 2.61-3.03, 2.27-2.35, 1.66-1.85, 1.27-1.66, 0.71-1.27
ZnNapth$_2$trien-IPDI-BTDA	9.02-9.60	5.38-5.98	7.90-8.36, 7.55-7.88, 7.33-7.50, 7.10-7.28, 6.64-7.02	3.83-4.19, 3.57-3.83, 3.44-3.57, 2.97-3.01, 2.60-2.88, 1.30-1.82, 0.55-1.27

[a] all peaks are multiplets

[b] for MDI-based polymers, alkyl groups = -C**H**$_2$;

for IPDI-based polymers, alkyl groups = C**H**, C**H**$_2$ and C**H**$_3$

4.5.2.3 Solubility of poly(urea-imide)s

Solubility of metal-containing poly(urea-imide)s was tested in various polar and non-polar solvents (Table 4.28-4.29). Metal-containing poly(urea-imide)s were soluble in polar solvents such as DMF and DMSO but insoluble in hexane, toluene, dichloromethane, chloroform, methanol, acetonitrile and water. The polymer obtained from metal complexes with good solubility such as ZnNapth$_2$trien-MDI-BTDA, NiNapth$_2$trien-MDI-BTDA, NiNapth$_2$trien-IPDI-PMDA were soluble in THF. The maximum amount of each polymer that was able to dissolve in 1 mL of DMSO was also determined.

Table 4.28 Solubility of metal containing poly(urea-imide)s based on MDI

Polymers	**THF**	**DMF**	**DMSO**	**Maximum solubility (mg)/ DMSO 1 (mL)**
MDI-PMDA	-	-	-	2
ZnNapth$_2$trien-MDI-PMDA (1:2:0.5)	-	++	++	128
ZnNapth$_2$trien-MDI-PMDA (1:2:1)	-	+	+	132
NiNapth$_2$trien-MDI-PMDA (1:2:0.5)	-	+	++	85
NiNapth$_2$trien-MDI-PMDA (1:2:1)	-	+	+	151
MDI-BTDA	-	-	-	2
ZnNapth$_2$trien-MDI-BTDA (1:2:0.5)	+-	++	++	32
ZnNapth$_2$trien-MDI-BTDA (1:2:1)	+-	+	+	45
NiNapth$_2$trien-MDI-BTDA (1:2:0.5)	+-	++	++	162
NiNapth$_2$trien-MDI-BTDA (1:2:1)	+-	++	++	145

++ = Soluble at room temperature; **+** = soluble on heating; **+-** = partial soluble on heating; **-** = insoluble

Table 4.29 Solubility of metal containing poly(urea-imide)s based on IPDI

Polymers	THF	DMF	DMSO	Maximum solubility (mg)/ DMSO 1 (mL)
IPDI-PMDA	++	++	++	42
ZnNapth$_2$trien-IPDI-PMDA (1:2:0.5)	-	++	++	25
ZnNapth$_2$trien-IPDI-PMDA (1:2:1)	-	+	+	55
NiNapth$_2$trien-IPDI-PMDA (1:2:0.5)	++	++	++	137
NiNapth$_2$trien-IPDI-PMDA (1:2:1)	-	++	+	58
IPDI-BTDA	+	+	+	15
ZnNapth$_2$trien-IPDI-BTDA (1:2:0.5)	+-	++	++	33
ZnNapth$_2$trien-IPDI-BTDA (1:2:1)	-	+	+	24
NiNapth$_2$trien-IPDI-BTDA (1:2:0.5)	+-	++	++	145
NiNapth$_2$trien-IPDI-BTDA (1:2:1)	-	++	++	262

++ = Soluble at room temperature; **+** = soluble on heating; **+-** = partial soluble on heating; **-** = insoluble

4.5.2.4 Inherent viscosity of poly(urea-imide)s

Inherent viscosity of all poly(urea-imide)s was measured at 40°C in DMSO as described in Appendix[B-1]. The viscosity data of poly(urea-imide)s and Shore D hardness are given in Table 4.30. Metal-containing poly(urea-imide)s obtained from MNapth$_2$trien : diisocyanate : dianhydride at the mole ratio of 1:2:0.5 has lower viscosities than those obtained at the mole ratio of 1:2:1. Inherent viscosity of the poly(urea-imide)s was found to be in the range between 0.181-0.736 dl/g for zinc-containing polymers and 0.210-0.687 dl/g for nickel-containing polymers. Shore D hardness were performed using a Zwick 3100 durometer. Hardness value of NiNapth$_2$trien-MDI-PMDA (1:2:1), NiNapth$_2$trien-IPDI-PMDA (1:2:1) were 92 and 94, respectively. Both of them were hard materials. For NiNapth$_2$trien-MDI-BTDA (1:2:1), brittle material was obtained since its solubility in NMP was not good, and therefore NiNapth$_2$trien-MDI-BTDA showed low hardness value of 34. For the other polymers, brittle materials were obtained.

Table 4.30 Inherent viscosity and shore D hardness of poly(urea-imide)s

Polymers	**η_{inh} (dl g^{-1})**	**Shore D hardness**
MDI-PMDA (1:1)	-	-
MDI-BTDA (1:1)	-	-
IPDI-PMDA (1:1)	0.251	-
IPDI-BTDA (1:1)	0.273	-
ZnNapth$_2$trien-MDI-PMDA (1:2:0.5)	0.188	-
ZnNapth$_2$trien-MDI-PMDA (1:2:1)	0.736	-
ZnNapth$_2$trien-MDI-BTDA (1:2:0.5)	0.260	-
ZnNapth$_2$trien-MDI-BTDA (1:2:1)	0.355	-
NiNapth$_2$trien-MDI-PMDA (1:2:0.5)	0.228	-
NiNapth$_2$trien-MDI-PMDA (1:2:1)	0.663	92
NiNapth$_2$trien-MDI-BTDA (1:2:0.5)	0.299	-
NiNapth$_2$trien-MDI-BTDA (1:2:1)	0.349	34
ZnNapth$_2$trien-IPDI-PMDA (1:2:0.5)	0.181	-
ZnNapth$_2$trien-IPDI-PMDA (1:2:1)	0.527	-
ZnNapth$_2$trien-IPDI-BTDA (1:2:0.5)	0.274	-
ZnNapth$_2$trien-IPDI-BTDA (1:2:1)	0.307	-
NiNapth$_2$trien-IPDI-PMDA (1:2:0.5)	0.210	-
NiNapth$_2$trien-IPDI-PMDA (1:2:1)	0.687	94
NiNapth$_2$trien-IPDI-BTDA (1:2:0.5)	0.289	-
NiNapth$_2$trien-IPDI-BTDA (1:2:1)	0.322	-

4.5.2.5 Glass transition temperature

Glass transition temperature (T_g) of the poly(urea-imide)s was first determined by differential scanning calorimetry (DSC). T_gs of most polymers could not be clearly observed. T_gs could be obtained for two polymers, ZnNapth$_2$trien-MDI-PMDA (1 : 2 : 0.5) and ZnNapth$_2$trien-MDI-BTDA (1 : 2 : 0.5).

Therefore, T_gs of the other polymers were determined from the maximum point of tan δ peak using dynamic mechanical thermal analysis (DMTA). DMTA samples were prepared by solution-cast and using NMP as a solvent. Brittle materials were obtained from zinc-containing poly(urea-imide)s since their solubility in NMP was not good, and therefore their DMTA samples could not be prepared.

Nickel-containing poly(urea-imide)s prepared at the mole ratio of MNapth$_2$trien : diisocyanate : dianhydride = 1 : 2 : 0.5 were also brittle polymers. DMTA samples were obtained only from nickel-containing poly(urea-imide)s prepared at the mole ratio of MNapth$_2$trien : diisocyanate : dianhydride = 1 : 2 : 1. T_gs of NiNapth$_2$trien-MDI-PMDA (1 : 2 : 1), NiNapth$_2$trien-MDI-BTDA (1 : 2 : 1) and NiNapth$_2$trien-IPDI-PMDA (1 : 2 : 1) were observed at 115, 89 and 110°C, respectively. PMDA-based polymers were harder material than BTDA-based polymers. NiNapth$_2$trien-IPDI-BTDA was brittle material and its DMTA sample could not be obtained. T_gs of nickel-containing poly(urea-imide)s were lower than that of their corresponding polyurea. NiNapth$_2$trien-MDI-PMDA showed slightly higher T_g than NiNapth$_2$trien-IPDI-PMDA. Figure 4.40 shows DMTA thermogram of NiNapth$_2$trien-MDI-PMDA (1:2:1).

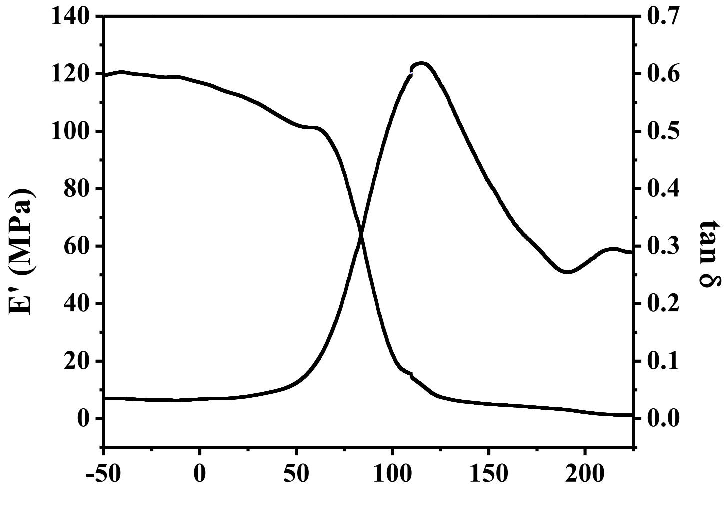

Figure 4.40 DMTA thermogram of NiNapth$_2$trien-MDI-PMDA

4.5.2.6 Thermogravimetric analysis

TGA results of polymers are present in Figures 4.41-4.45 and Tables 4.31-4.32. IDTs of reference polymers were found in the range of 225-290°C. Their residual weight at 600°C were in the range of 25-68%. Reference polymer based on MDI showed higher thermal stability than reference polymer based on IPDI. IDTs of zinc-containing poly(urea-imide)s based on MDI and IPDI were found in the range of 209-270 and 207-246°C, respectively. The residual weights at 600°C of MDI- and IPDI-based polymers were in the range of 44-58 and 26-37%, respectively. IDTs of nickel-containing poly(urea-imide)s based on MDI and IPDI were found in the range of 208-243 and 229-245°C, respectively. The residual weights at 600°C of MDI- and IPDI-based polymers were in the range of 54-68 and 33-46%, respectively.

TGA results (Table 4.31-4.32) showed that the IDTs of zinc- and nickel-containing poly(urea-imide)s were lower than those of the metal-containing polyureas synthesized without PMDA and BTDA. This was because the MNapth$_2$trien contents in polyureas were higher than those in poly(urea-imide)s. Metal-containing polyureas contained MNapth$_2$trien in the range of 67.1-69.7 wt%, while the MNapth$_2$trien amount presents in metal-containing poly(urea-imide)s was in the range of 38.3-48.3 wt%. Most poly(urea-imide)s showed the decrease in IDTs when the wt% of MNapth$_2$trien in the polymers was decreased.

TGA results showed that all metal-containing poly(urea-imide)s had higher char yields at 600°C than the metal-containing polyureas synthesized without PMDA and BTDA, namely ZnNapth$_2$trien-MDI, NiNapth$_2$trien-MDI, ZnNapth$_2$trien-IPDI and NiNapth$_2$trien-IPDI. This was due to the introduction of imide groups into the polymer backbone. When comparing to their corresponding polyureas, addition of PMDA and BTDA in the synthesis of nickel-containing poly(urea-imide)s results in better improvement in char yields than in the case of zinc-containing poly(urea-imide)s. Comparing to the reference polyimides synthesized from diisocyanates and dianhydrides, the char yields at 600°C of ZnNapth$_2$trien-MDI-PMDA and NiNapth$_2$trien-MDI-PMDA were lower than that of MDI-PMDA. Poly(urea-imide)s based on MDI-BTDA and IPDI-BTDA had comparable char yields to their corresponding reference polyimides.

For most of MDI-based poly(urea-imide)s, TGA results of ZnNapth$_2$trien-MDI-PMDA, NiNapth$_2$trien-MDI-PMDA and NiNapth$_2$trien-MDI-BTDA showed that the variable amount of PMDA and BTDA in zinc- and nickel-containing poly(urea-imide)s do not affect their char yields at 600°C. Except for ZnNapth$_2$trien-MDI-BTDA (1 : 2 : 0.5), which had less char yield than ZnNapth$_2$trien-MDI-BTDA (1 : 2 : 1). TGA results of most IPDI-based poly(urea-imide)s, namely ZnNapth$_2$trien-IPDI-PMDA, NiNapth$_2$trien-IPDI-PMDA and NiNapth$_2$trien-IPDI-BTDA showed that their char yields at 600°C increase with increasing amount of PMDA and BTDA in the copolymers. Except for ZnNapth$_2$trien-IPDI-BTDA, which the polymers obtained from different amount of BTDA had the same char yield.

The IDTs of zinc- and nickel-containing poly(urea-imide)s were in the range of 207-270 and 207-245°C, respectively, which were lower than those of the metal-containing polyureas synthesized without PMDA and BTDA. Most poly(urea-imide)s showed the decrease in IDT when the amount of imide group in the polymer was increased. Among all poly(urea-imide)s, ZnNapth$_2$trien-MDI-PMDA (1 : 2 : 0.5) was the most thermally stable polymer with the highest IDT and char yield of 270°C and 58%, respectively.

Table 4.31 TGA data of metal-containing poly(urea-imide)s based on PMDA

Polymer	**IDT (°C)**	**Weight residue (%) at different temperature (°C)**						
		300	**400**	**500**	**600**	**700**	**800**	**900**
MDI-PMDA	225	91	87	83	68	49	38	28
ZnNapth$_2$trien-MDI-PMDA (1:2:0.5)	270	93	81	69	58	45	33	21
ZnNapth$_2$trien-MDI-PMDA (1:2:1)	232	88	77	69	58	46	34	24
NiNapth$_2$trien-MDI-PMDA (1:2:0.5)	234	85	74	62	54	44	34	25
NiNapth$_2$trien-MDI-PMDA (1:2:1)	222	89	81	68	54	42	32	21
IPDI-PMDA	258	83	62	45	25	17	17	17
ZnNapth$_2$trien-IPDI-PMDA (1:2:0.5)	244	91	80	46	26	9	5	5
ZnNapth$_2$trien-IPDI-PMDA (1:2:1)	217	86	66	51	37	23	10	7
NiNapth$_2$trien-IPDI-PMDA (1:2:0.5)	229	78	58	44	36	27	18	14
NiNapth$_2$trien-IPDI-PMDA (1:2:1)	245	84	68	54	43	33	23	14

Table 4.32 TGA data of metal-containing poly(urea-imide)s based on BTDA

Polymer	**IDT (°C)**	**Weight residue (%) at different temperature (°C)**						
		300	**400**	**500**	**600**	**700**	**800**	**900**
MDI-BTDA	255	89	75	66	52	42	33	24
ZnNapth$_2$trien-MDI-BTDA (1:2:0.5)	255	89	74	53	44	29	18	11
ZnNapth$_2$trien-MDI-BTDA (1:2:1)	209	88	81	71	58	45	33	21
NiNapth$_2$trien-MDI-BTDA (1:2:0.5)	243	87	79	68	56	45	34	24
NiNapth$_2$trien-MDI-BTDA (1:2:1)	208	85	79	72	60	48	37	25
IPDI-BTDA	290	94	81	49	37	20	9	8
ZnNapth$_2$trien-IPDI-BTDA (1:2:0.5)	246	84	58	43	34	21	10	8
ZnNapth$_2$trien-IPDI-BTDA (1:2:1)	207	87	67	49	35	24	14	10
NiNapth$_2$trien-IPDI-BTDA (1:2:0.5)	240	80	61	47	33	17	11	11
NiNapth$_2$trien-IPDI-BTDA (1:2:1)	235	90	73	59	46	35	25	15

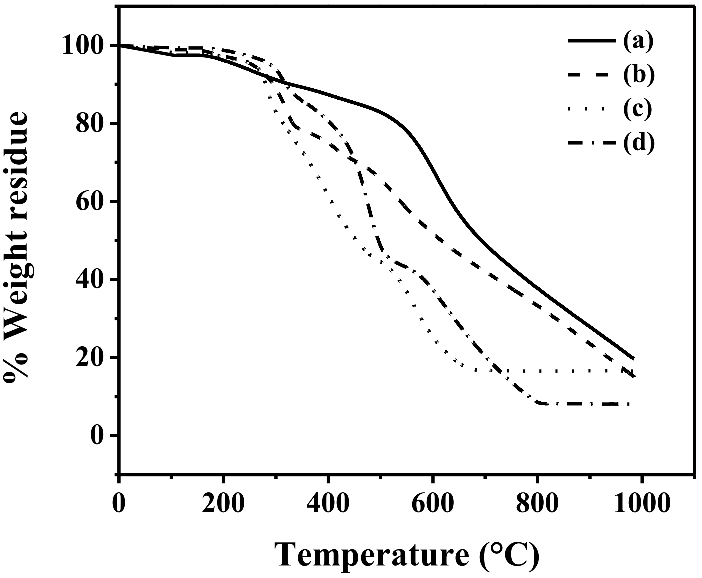

Figure 4.41 TGA thermograms of (a) MDI-PMDA; (b) MDI-BTDA; (c) IPDI-PMDA; (d) IPDI-BTDA

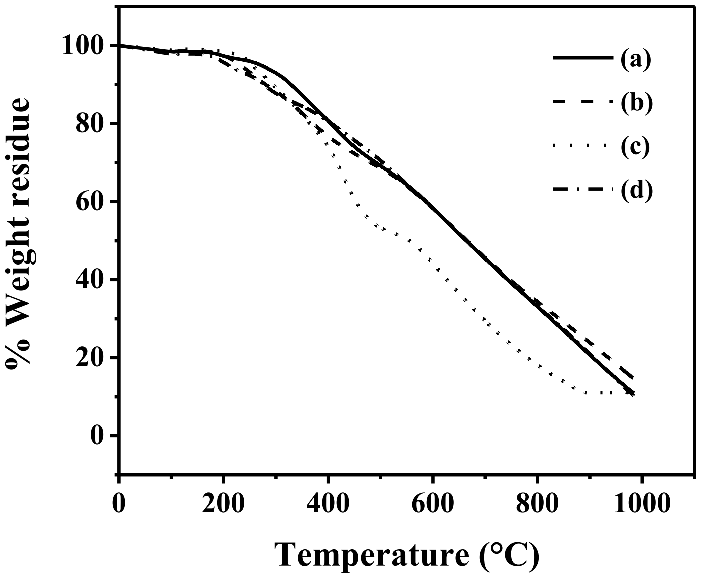

Figure 4.42 TGA thermograms of (a) ZnNapth$_2$trien-MDI-PMDA (1:2:0.5); (b) ZnNapth$_2$trien-MDI-PMDA (1:2:1); (c) ZnNapth$_2$trien-MDI-BTDA (1:2:0.5); (d) ZnNapth$_2$trien-MDI-BTDA (1:2:1)

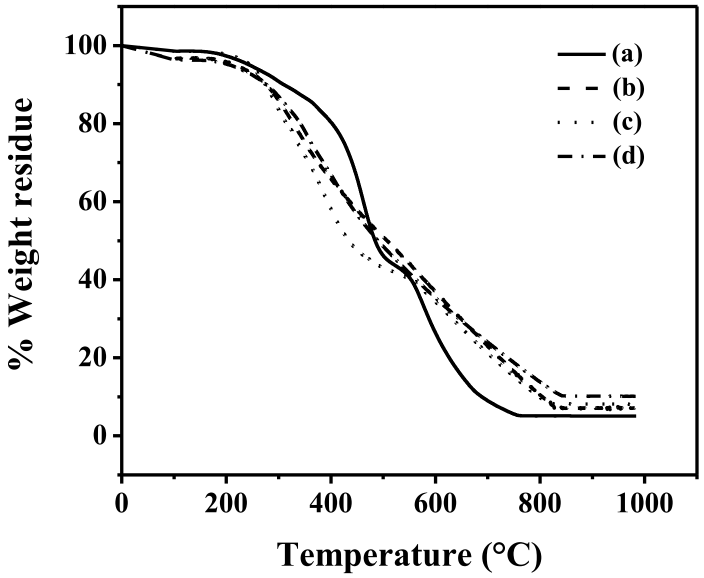

Figure 4.43 TGA thermograms of (a) ZnNapth$_2$trien-IPDI-PMDA (1:2:0.5); (b) ZnNapth$_2$trien-IPDI-PMDA (1:2:1); (c) ZnNapth$_2$trien-IPDI-BTDA (1:2:0.5); (d) ZnNapth$_2$trien-IPDI-BTDA (1:2:1)

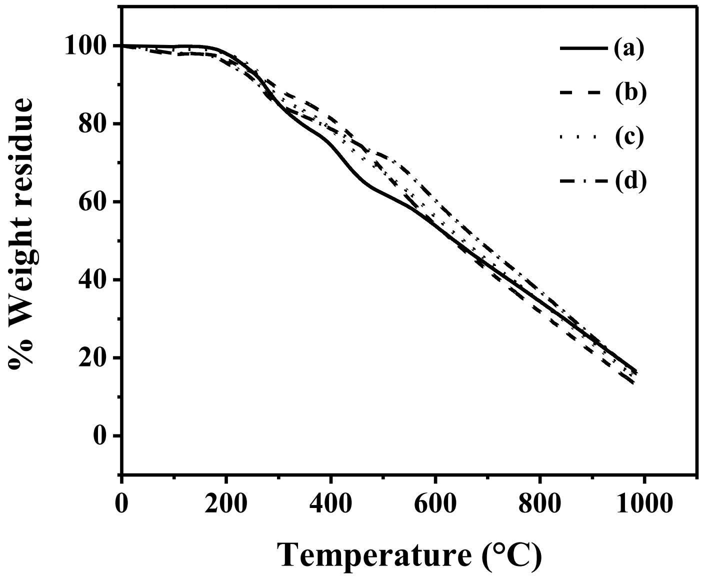

Figure 4.44 TGA thermograms of (a) NiNapth$_2$trien-MDI-PMDA (1:2:0.5); (b) NiNapth$_2$trien-MDI-PMDA (1:2:1); (c) NiNapth$_2$trien-MDI-BTDA (1:2:0.5); (d) NiNapth$_2$trien-MDI-BTDA (1:2:1)

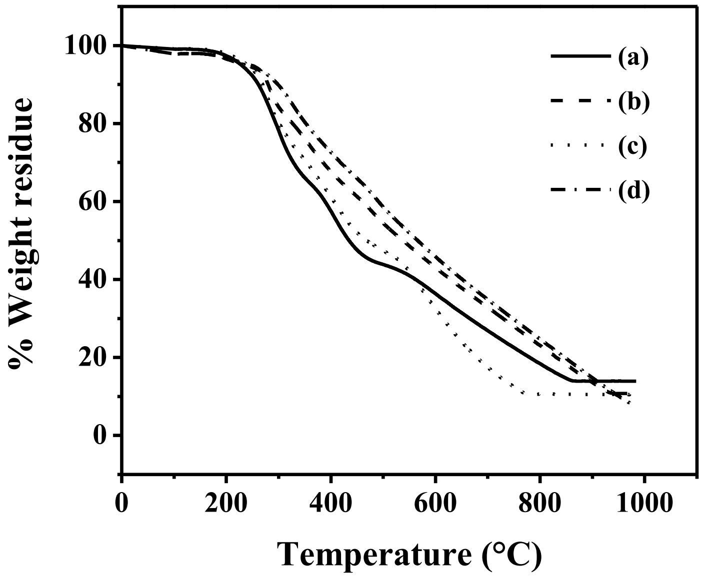

Figure 4.45 TGA thermograms of (a) NiNapth$_2$trien-IPDI-PMDA (1:2:0.5); (b) NiNapth$_2$trien-IPDI-PMDA (1:2:1); (c) NiNapth$_2$trien-IPDI-BTDA (1:2:0.5); (d) NiNapth$_2$trien-IPDI-BTDA (1:2:1)

4.5.2.7 X-ray diffraction

The XRD patterns of MDI-PMDA and MDI-BTDA showed sharp peaks which indicates that the polymers contained crystalline part while zinc- and nickel-containing poly(urea-imide)s based on MDI had board XRD peaks and therefore the polymers were amorphous (Figure 4.46). This XRD results corresponded with solubility results that the metal-containing poly(urea-imide)s were soluble in DMSO.

The XRD patterns of reference polymer and metal-containing poly(urea-imide)s based on IPDI had board XRD peaks and therefore the polymers were amorphous (Figure 4.47). This XRD results corresponded with solubility results that the polymers were soluble in DMSO.

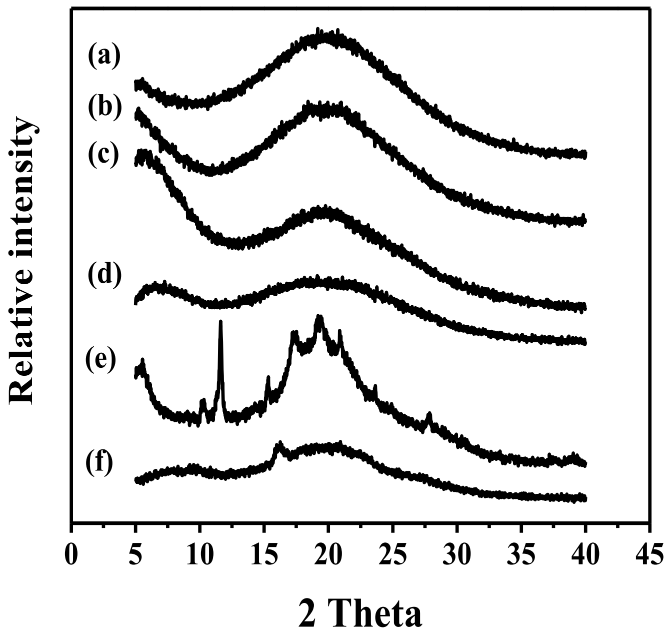

Figure 4.46 XRD patterns of (a) ZnNapth$_2$trien-MDI-PMDA; (b) ZnNapth$_2$trien-MDI-BTDA; (c) NiNapth$_2$trien-MDI-PMDA; (d) NiNapth$_2$trien-MDI-BTDA; (e) MDI-PMDA; (f) MDI-BTDA

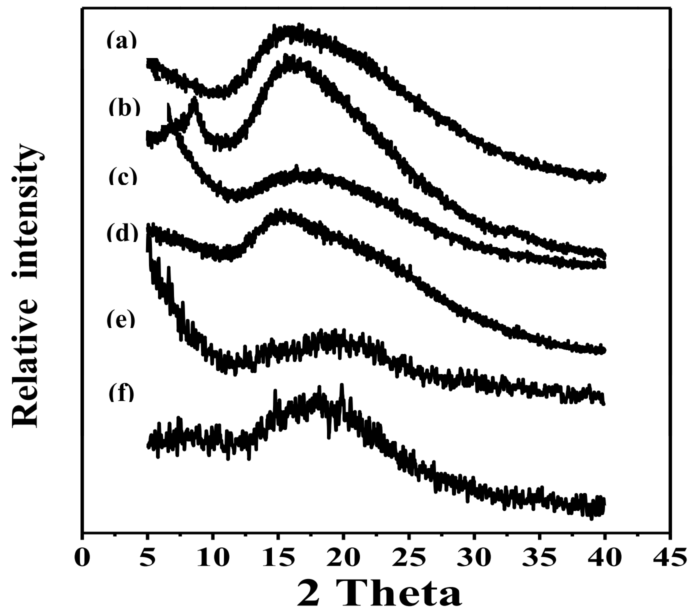

Figure 4.47 XRD patterns of (a) ZnNapth$_2$trien-IPDI-PMDA; (b) ZnNapth$_2$trien-IPDI-BTDA; (c) NiNapth$_2$trien-IPDI-PMDA; (d) NiNapth$_2$trien-IPDI-BTDA; (e) IPDI-PMDA; (f) IPDI-BTDA

4.6 Synthesis of metal-containing poly(urethane-urea-imide)s

4.6.1 Synthesis of metal-containing poly(urethane-urea-imide)s from the reaction between MNapth$_2$trien, diisocyanates, PEG400 and dianhydrides

Metal-containing poly(urethane-urea-imide)s were synthesized by the reaction between MNapth$_2$trien (M = Zn and Ni), polyethylene glycol (PEG400), diisocyanates amd dianhydrides (Scheme 4.12).

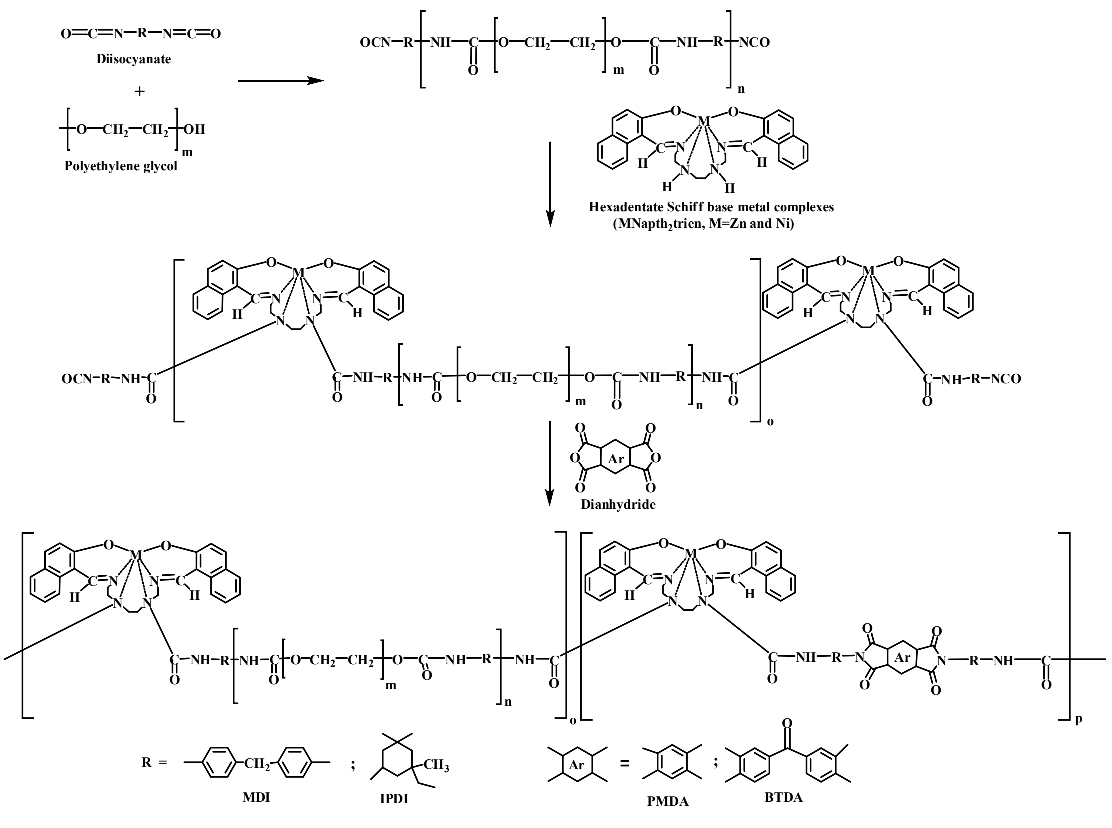

Scheme 4.12 Synthesis of metal-containing poly(urethane-urea-imide)s

The yield of zinc containing poly(urethane-urea-imide)s was in the range of 78-89%. The yield of nickel-containing poly(urethane-urea-imide)s was in the range of 80-87%. (Table 4.33). The possible polymerization mechanism is that the hydroxyl groups in PEG 400 undergo reaction with isocyanate groups in diisocyanate at mole ratio 1:2 to give urethane linkages, followed by the residue of isocyanate groups in diisocyanate were reacted with amino group of MNapth$_2$trien to give urea linkages (Scheme 4.13). It was found that order of reactivity MDI higher than IPDI. The reference polymers without metal complexes were also prepared by the reaction of diisocyanates and dianhydrides.

.

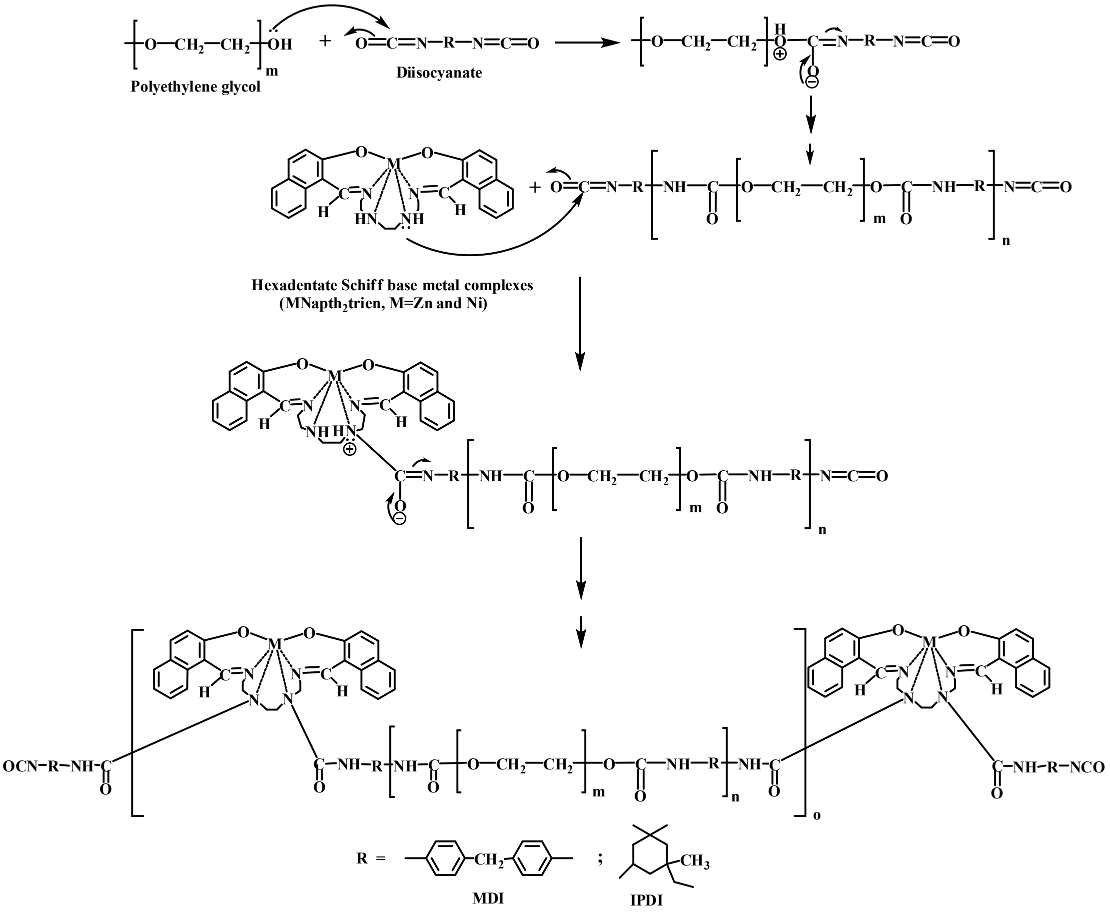

Scheme 4.13 Proposed mechanism of the reaction between MNapth$_2$trien, PEG400 and diisocyanates.

Next step was the reaction of diisocyanates with dianhydrides to give imide group (Scheme 4.14).

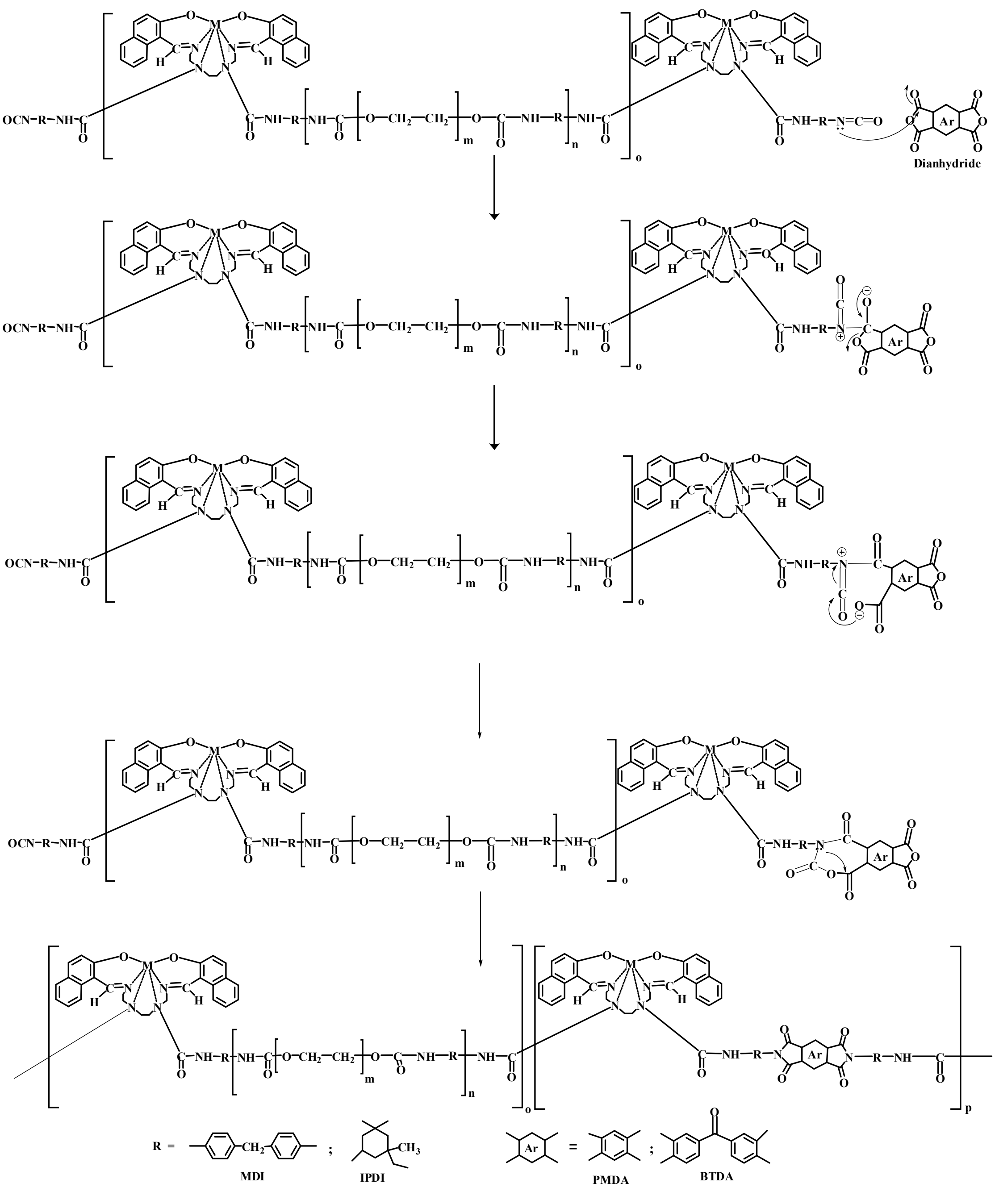

Scheme 4.14 Proposed mechanism of the reaction between isocyanate terminated prepolymers and dianhydrides

Table 4.33 Synthesis data of metal-containing poly(urethane-urea-imide)s

Polymers	**Weight of metal in polymer (%)**	**Yield (%)**	**External appearance**
ZnNapth$_2$trien-MDI/PEG400-PMDA	20.4	89	Red brown powder
ZnNapth$_2$trien-MDI/PEG400-BTDA	19.6	84	Red brown powder
NiNapth$_2$trien-MDI/PEG400-PMDA	20.2	85	Dark brown powder
NiNapth$_2$trien-MDI/PEG400-BTDA	19.4	82	Dark brown powder
ZnNapth$_2$trien-IPDI/PEG400-PMDA	21.4	85	Red brown powder
ZnNapth$_2$trien-IPDI/PEG400-BTDA	20.5	78	Red brown powder
NiNapth$_2$trien-IPDI/PEG400-PMDA	21.1	87	Dark brown powder
NiNapth$_2$trien-IPDI/PEG400-BTDA	20.3	80	Dark brown powder

4.6.2 Characterization of metal-containing poly(urethane-urea-imide)s

4.6.2.1 IR spectroscopy of metal-containing poly(urethane-urea-imide)s

The FTIR spectra of All metal-containing poly(urethane-urea-imide)s obtained from MNapth$_2$trien : diisocyanate/PEG400 : dianhydride at the mole ratio of 1:2:1 are showed in Figures 4.48.

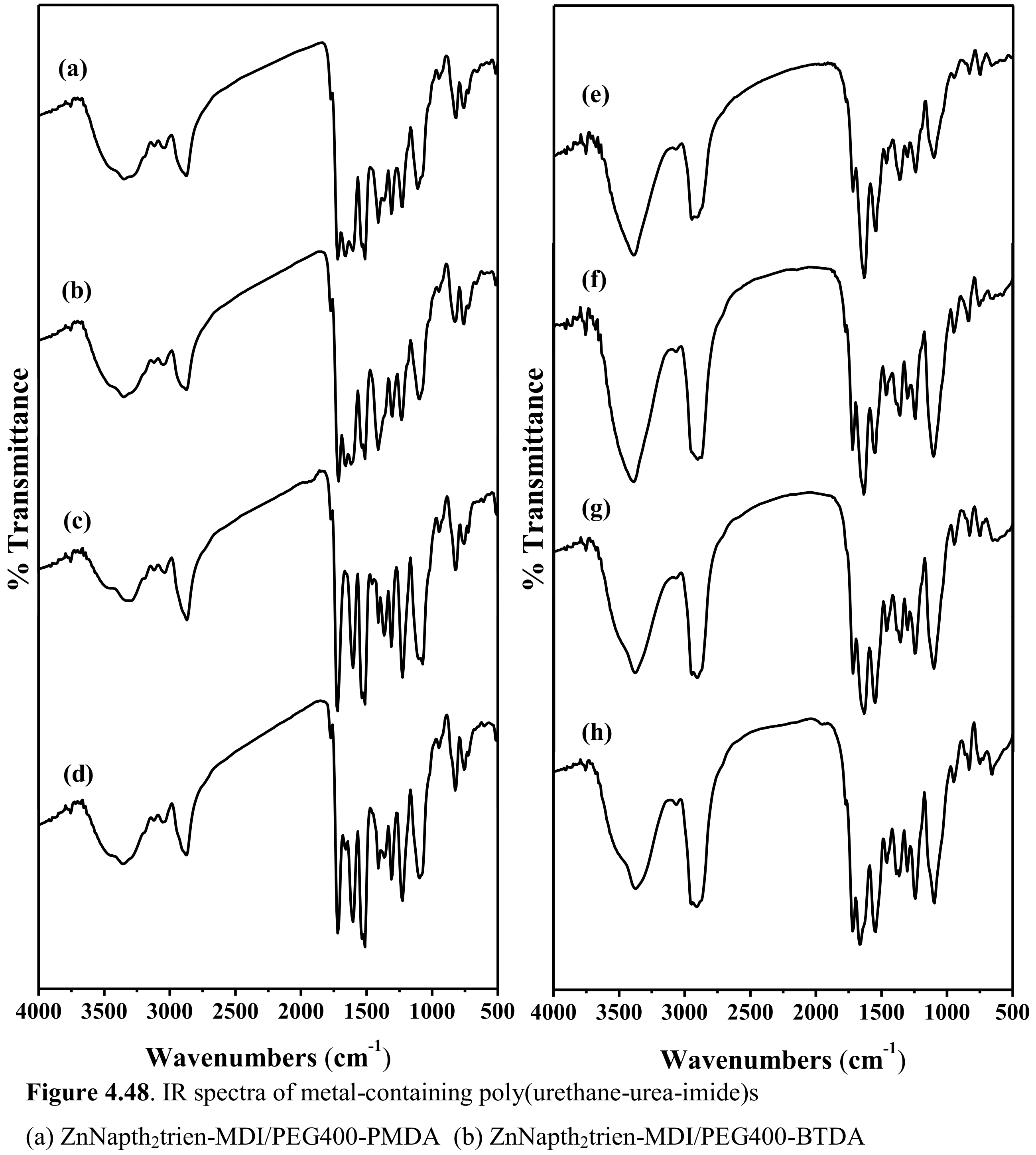

Figure 4.48. IR spectra of metal-containing poly(urethane-urea-imide)s

(a) ZnNapth$_2$trien-MDI/PEG400-PMDA (b) ZnNapth$_2$trien-MDI/PEG400-BTDA

(c) NiNapth$_2$trien-MDI/PEG400-PMDA (d) NiNapth$_2$trien-MDI/PEG400-BTDA

(e) ZnNapth$_2$trien-IPDI/PEG400-PMDA (f) ZnNapth$_2$trien-IPDI/PEG400-BTDA

(g) NiNapth$_2$trien-IPDI/PEG400-PMDA (h) NiNapth$_2$trien-IPDI/PEG400-BTDA

All metal-containing poly(urethane-urea-imide)s had similar IR spectra. The important characteristic absorption bands are 3334-3392 cm^{-1} that could be attributed to N-H stretching. The absorption bands at 2871-2947 cm^{-1} were due to C-H stretching. The absorptions at 1766-1775 and 1714-1722 cm^{-1} were assigned to asymmetric and symmetric C=O stretching vibration of imide ring. IR data of metal-containing poly(urethane-urea-imide)s are showed in Table 4.34.

Table 4.34 IR data of metal-containing poly(urethane-urea-imide)s

metal-containing poly(urethane-urea-imide)s	**IR signals (cm^{-1})**
ZnNapth$_2$trien-MDI/PEG400-PMDA	3350 (NH), 2875, 1772 (C=O), 1718 (C=O), 1662, 1606 (C=N), 1513, 1411, 1309, 1230, 1109, 947, 821, 759, 725.
ZnNapth$_2$trien-MDI/PEG400-BTDA	3352 (NH), 2875, 1774 (C=O), 1714 (C=O), 1660, 1617 (C=N), 1534, 1513, 1412, 1306, 1234, 1098, 949, 827, 759, 724.
NiNapth$_2$trien-MDI/PEG400-PMDA	3334 (NH), 2871, 1773 (C=O), 1722 (C=O), 1660, 1604 (C=N), 1534, 1514, 1458, 1411, 1365, 1311, 1227, 1074, 946, 822, 758, 725.
NiNapth$_2$trien-MDI/PEG400-BTDA	3359 (NH), 2873, 1775 (C=O), 1717 (C=O), 1660, 1605 (C=N), 1535, 1514, 1410, 1364, 1309, 1228, 1097, 948, 824, 755, 725.
ZnNapth$_2$trien-IPDI/PEG400-PMDA	3392 (NH), 2947, 1772 (C=O), 1720 (C=O), 1634 (C=N), 1546, 1465, 1362, 1306, 1244, 1103, 949, 833, 750.
ZnNapth$_2$trien-IPDI/PEG400-BTDA	3389 (NH), 2902, 1774 (C=O), 1719 (C=O), 1633(C=N), 1549, 1463, 1360, 1301, 1244, 1103, 946, 837, 752, 726.
NiNapth$_2$trien-IPDI/PEG400-PMDA	3380 (NH), 2907, 1774 (C=O), 1720 (C=O), 1655, 1628 (C=N), 1551, 1462, 1385, 1360, 1246, 1102, 947, 832, 752.
NiNapth$_2$trien-IPDI/PEG400-BTDA	3376 (NH), 2908, 1774 (C=O), 1718 (C=O), 1663, 1625 (C=N), 1546, 1460, 1384, 1364, 1303, 1244, 1098, 948, 863, 832, 749, 725.

4.6.2.2 Solubility of metal-containing poly(urethane-urea-imide)s

Solubility of metal-containing poly(urethane-urea-imide)s was tested in various polar and non-polar solvents (Table 4.35). Metal-containing poly(urethane-urea-imide)s were soluble in polar solvents such as DMF and DMSO but insoluble in hexane, toluene , dichloromethane, chloroform, methanol, actonitrile, water. The polymer obtained from metal complexes with good solubility such as ZnNapth$_2$trien-MDI-BTDA, NiNapth$_2$trien-MDI-BTDA, NiNapth$_2$trien-IPDI-PMDA were soluble in THF.

Table 4.35 Solubility of metal containing poly(urethane-urea-imide)s

Polymers	**DMF**	**DMSO**	**Maximum solubility (mg)/ DMSO 1 (mL)**
ZnNapth$_2$trien-MDI/PEG400-PMDA (1:2:1)	+-	+	392
ZnNapth$_2$trien-MDI/PEG400-BTDA (1:2:1)	+-	+	408
NiNapth$_2$trien-MDI/PEG400-PMDA (1:2:1)	+-	+	512
NiNapth$_2$trien-MDI/PEG400-BTDA (1:2:1)	+-	+	577
ZnNapth$_2$trien-IPDI/PEG400-PMDA (1:2:1)	+	++	427
ZnNapth$_2$trien-IPDI/PEG400-BTDA (1:2:1)	+	++	525
NiNapth$_2$trien-IPDI/PEG400-PMDA (1:2:1)	+	++	471
NiNapth$_2$trien-IPDI/PEG400-BTDA (1:2:1)	+	++	720

++ = Soluble at room temperature; **+** = soluble on heating; **+-** = partial soluble on heating; **-** = insoluble

4.6.2.3 Inherent viscosity of poly(urethane-urea-imide)s

Inherent viscosity of all poly(urethane-urea-imide)s was measured at 40°C in DMSO as described in Appendix[B-1]. The viscosity data of poly(urethane-urea-imide)s are given in Table 4.36. Inherent viscosity of the poly(urethane-urea-imide)s was found to be in the range between 0.184-0.204 dl/g for zinc-containing polymers and 0.192-0.210 dl/g for nickel-containing polymers.

The used of PEG 400 as a chain extender improved the solubility and processing characteristics of the copolymer. Poly(urethane-urea-imide)s samples could be prepared by solution cast in a mold. NiNapth$_2$trien-MDI/PEG400-PMDA and NiNapth$_2$trien-MDI/PEG400-BTDA had hardness value greater than 100. ZnNapth$_2$trien-MDI/PEG400-BTDA also had a high value. Hardness of the other polymers were observed in the range of 53-84. NiNapth$_2$trien-based polymers were harder material than ZnNapth$_2$trien-based polymers.

Table 4.36 Inherent viscosity and shore D hardness of poly(urethane-urea-imide)s

Polymers	η_{inh} (dl g^{-1})	**Shore D hardness**
ZnNapth$_2$trien-MDI/PEG400-PMDA	0.204	66
ZnNapth$_2$trien-MDI/PEG400-BTDA	0.203	94
NiNapth$_2$trien-MDI/PEG400-PMDA	0.206	>100
NiNapth$_2$trien-MDI/PEG400-BTDA	0.210	>100
ZnNapth$_2$trien-IPDI/PEG400-PMDA	0.186	56
ZnNapth$_2$trien-IPDI/PEG400-BTDA	0.184	53
NiNapth$_2$trien-IPDI/PEG400-PMDA	0.192	84
NiNapth$_2$trien-IPDI/PEG400-BTDA	0.192	70

Inherent viscosity of the poly(urethane-urea-imide)s is found to be in the range between 0.184-0.206 dl/g. Metal-containing poly(urethane-urea-imide)s contain MNapth$_2$trien in the range of 19.4- 21.4 wt%.

4.6.2.4 Glass transition temperature

Glass transition temperature (T_g) of the poly(urethane-urea-imide)s was determined by from the maximum point of tanδ peak using dynamic mechanical thermal analysis (DMTA) as shown in Table 4.37. DMTA samples were prepared by solution-cast and using NMP as a solvent. Brittle materials were obtained from ZnNapth$_2$trien-MDI/PEG400-PMDA (1:2:1) since their solubility in NMP was not good, and therefore their DMTA samples showed low T$_g$. MDI-based polymers were harder material than IPDI-based polymers. T$_g$s of nickel-containing poly(urethane-urea-imide)s were lower than that of their corresponding polyurea. NiNapth$_2$trien-MDI/PEG400-PMDA showed highest T$_g$. Figures 4.49 shows DMTA thermogram of NiNapth$_2$trien-MDI/PEG400-PMDA (1:2:1).

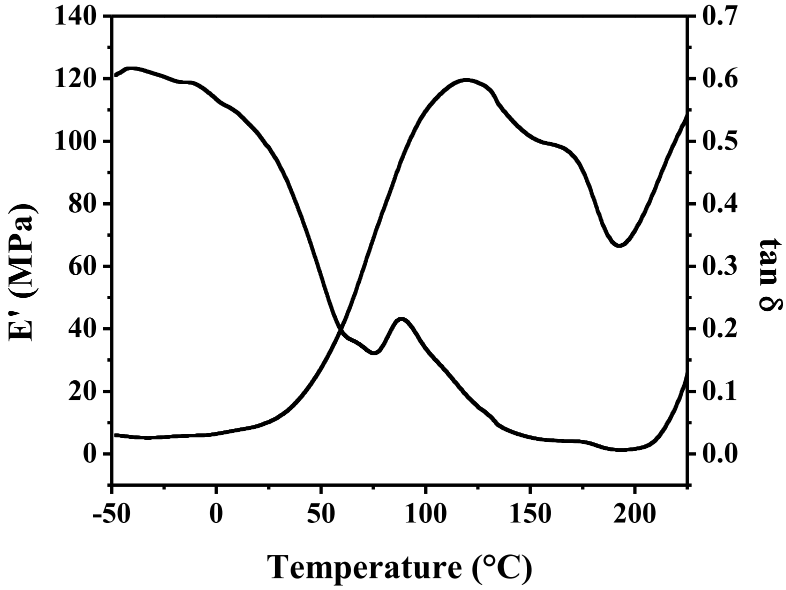

Figure 4.49 DMTA thermogram of NiNapth$_2$trien-MDI/PEG400-PMDA

Table 4.37 Glass transition temperature of the poly(urethane-urea-imide)s

Polymers	**T$_g$ (°C)**
ZnNapth$_2$trien-MDI/PEG400-PMDA (1:2:1)	44
ZnNapth$_2$trien-MDI/PEG400-BTDA (1:2:1)	74
NiNapth$_2$trien-MDI/PEG400-PMDA (1:2:1)	119
NiNapth$_2$trien-MDI/PEG400-BTDA (1:2:1)	86
ZnNapth$_2$trien-IPDI/PEG400-PMDA (1:2:1)	81
ZnNapth$_2$trien-IPDI/PEG400-BTDA (1:2:1)	115
NiNapth$_2$trien-IPDI/PEG400-PMDA (1:2:1)	98
NiNapth$_2$trien-IPDI/PEG400-BTDA (1:2:1)	96

4.6.2.5 Thermogravimetric analysis

TGA results of poly(urethane-urea-imide)s were present in Figures 4.50-4.51 and Table 4.38. The temperature at 5% weight loss (IDTs) of poly(urethane-urea-imide)s based on MDI was found in the range of 163-297°C. The residual weights at 600°C were in the range of 31-51%. poly(urethane-urea-imide)s based on MDI-BTDA showed higher thermal stability than poly(urethane-urea-imide)s based on MDI-PMDA. The temperature at 5% weight loss (IDT) of poly(urethane-urea-imide)s based on IPDI was found in the range of 196-237°C. The residual weights at 600°C were in the range of 20-29%. TGA results (Table 4.38) showed that the char yield at 600°C of metal-containing poly(urethane-urea-imide)s were lower than those of the metal-containing poly(urea-imide)s. This was because the flexible parts in poly(urethane-urea-imide)s were higher than those in poly(urea-imide)s. Most poly(urethane-urea-imide)s showed IDTs lower than poly(urea-imide)s. Except for NiNapth$_2$trien-MDI/PEG400-PMDA and NiNapth$_2$trien-MDI/PEG400-BTDA, which had IDTs at 297 and 292°C, respectively, which were higher than those of the metal-containing poly(urea-imide)s.

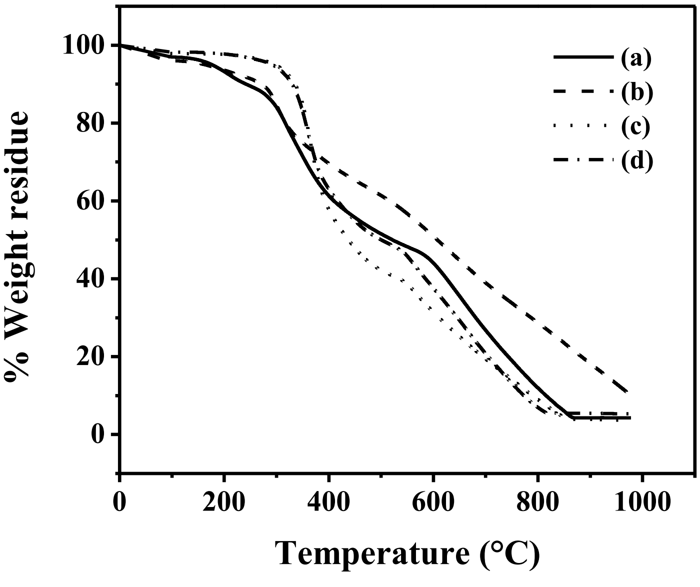

Figure 4.50 TGA thermograms of (a) ZnNapth$_2$trien-MDI/PEG400-PMDA (1:2:1) (b) ZnNapth$_2$trien-MDI/PEG400-BTDA (1:2:1) (c) NiNapth$_2$trien-MDI/PEG400-PMDA (1:2:1) (d) NiNapth$_2$trien-MDI/PEG400-BTDA (1:2:1)

Table 4.38 TGA data of zinc-containing poly(urethane-urea-imide)s

Polymer	IDT (°C)	Weight residue (%) at different temperature (°C)						
		300	400	500	600	700	800	900
ZnNapth$_2$trien-MDI/PEG400-PMDA	176	84	61	52	44	27	12	4
NiNapth$_2$trien-MDI/PEG400-PMDA	297	95	58	42	31	19	9	4
ZnNapth$_2$trien-MDI/PEG400-BTDA	163	85	70	61	51	39	29	18
NiNapth$_2$trien-MDI/PEG400-BTDA	292	94	63	50	38	21	7	5
ZnNapth$_2$trien-IPDI/PEG400-PMDA	211	88	44	33	22	9	4	4
NiNapth$_2$trien-IPDI/PEG400-PMDA	196	90	45	34	22	12	11	11
ZnNapth$_2$trien-IPDI/PEG400-BTDA	237	88	46	37	29	17	8	8
NiNapth$_2$trien-IPDI/PEG400-BTDA	204	90	41	30	20	12	10	10

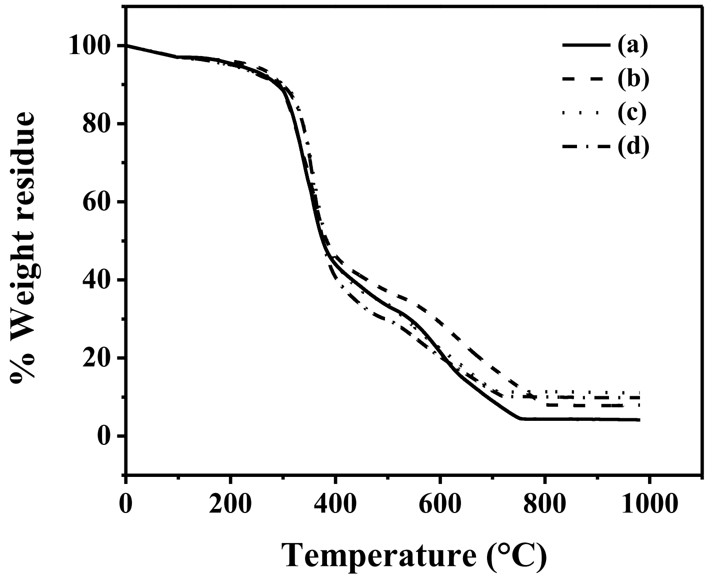

Figure 4.51 TGA thermograms of (a) ZnNapth$_2$trien-IPDI/PEG400-PMDA (1:2:1) (b) ZnNapth$_2$trien-IPDI/PEG400-BTDA (1:2:1) (c) NiNapth$_2$trien-IPDI/PEG400-PMDA (1:2:1) (d) NiNapth$_2$trien-IPDI/PEG400-BTDA (1:2:1)

Among all poly(urethane-urea-imide)s, NiNapth$_2$trien-MDI/PEG400-BTDA (1:2:1) was the most thermally stable polymers with IDT of 292°C and char yield at 600°C of 38%.

CHAPTER V

CONCLUSION AND SUGGESTION FOR FUTURE WORK

5.1 Conclusion

Two hexadentate Schiff base metal complexes, ZnNapth$_2$trien and NiNapth$_2$trien, were synthesized and used in the synthesis of metal-containing polyureas, metal-containing copolyureas, metal-containing poly(urethane-urea)s, metal-containing poly(urea-imide)s and metal-containing poly(urethane-urea-imide)s. All polymers were soluble in DMF and DMSO. Solubility of metal-containing polymer was improved when comparing to those of reference polymer synthesized without metal complexes.

Metal-containing polyureas showed residual weight at 600°C and IDTs in the range of 6-48% and 226-286°C, respectively. Among all polyureas, ZnNapth$_2$trien-MDI was the most thermally stable polymers with IDT of 280ºC and char yield of 48% at 600ºC.

Metal-containing copolyureas and poly(urethane-urea)s showed residual weight at 600°C in the range of 16-48% and 14-53%. IDTs of the polymers based on diamines and dialcohols were in the range of 178-317 and 160-259°C, respectively. Among all copolyureas and poly(urethane-urea)s, NiNapth$_2$trien-MDI-*m*-XDA was the most thermally stable polymer with IDT of 317°C and char yield of 48% at 600°C.

Metal-containing poly(urea-imide)s showed residual weight at 600°C and IDTs in the range of 26-60% and 207-270°C, respectively. Among all poly(urea-imide)s, ZnNapth$_2$trien-MDI-PMDA was the most thermally stable poly(urea-imide) with IDT of 270ºC and char yield of 58% at 600ºC. The introduction of imide groups increased thermal stability of polymers.

Metal-containing poly(urethane-urea-imide)s showed residual weight at 600°C and IDTs in the range of 20-51% and 163-297°C, respectively. In comparison to polyimides, these polymers exhibited improved thermal stability as well as good processibility and flexibility.

Metal-containing poly(urea-imide)s had higher thermal stability than the other polymers, which was due to the higher rigidity and thermal stability of imide units. Although metal-containing poly(urea-imide)s were the most thermally stable polymers, they were brittle materials and their solubility in organic solvents was not good. Other types of metal-containing polymers, namely copolyureas, poly(urethane-urea)s and poly(urethane-urea-imide)s, showed better solubility in organic solvents. These resulted indicated that these polymers exhibited good solubility and processability. However, their thermal stability were less than those of poly(urea-imide)s.

5.2 Suggestions for future work

Since metal-containing poly(urethane-urea-imide)s showed good thermal stability and processibility, metal-containing poly(urethane-urea-imide)s were synthesized from the reaction between $MNapth_2trien$, diisocyanates, PEG400 and dianhydrides. The suggestion for future work is to synthesize these copolymers by use of different polyethers with different structures and molecular weights. Variable mole ratios of starting materials could also be employed. This should improve mechanical properties, processing characteristics and flexibility of polymer.

REFERENCES

[1] Stevens, M.P.; Polymer Chemistry, an Introduction. Oxford University Press. 1999.

[2] Jiang, B. and Jones, W. Synthesis and Characterization of a conjugated polymer of poly(phylenevinylene) containing a metalloporphyrin incorporated into the polymer backbone Macromolecule 30 (1997) : 5575-5581.

[3] Simionescu, C.I.; Catanescu, O.; Grigoras, M.; Colotin, G.; Dobreanu, A. and Hurduc, N. Synthesis and Characterization of some aliphatic-aromatic poly(Schiff base)s. Eur. Polym. J. 37 (2001) : 2213-2216.

[4] Layer R.W. The chemistry of imines. Chem. Rev. 63(1963) : 489-510.

[5] Senthilkumar, N.; Raghavan, A. and Sultan Nasar, A. Novel-metal-containing polyurethane elastomers prepared using tetradentate Schiff base metal complexes. Macromol. Chem. Phys. 206 (2005): 2490-2500.

[6] Jayakumar, R.; Rajkumar, M.; Nagendran, R. and Nanjundan, S. Studies on metal containing polyurethanes based on divalent metal salts of mono(hydroxyethoxyethyl)phthalate. J. Macromol. Sci Pure. Appl. Chem. A. 38 (2001): 869-888.

[7] Jayakumar, R,; Nanjundan, S. and Prabaharan, M. Developments in metal-containing polyurethanes, copolyurethanes and polyurethane ionomers. J. Macromol. Sci. Polym. Rev. C. 45 (2005): 231-261.

[8] Jayakumar, R.; Nanjundan, S. and Prabaharan, M. Metal-containing polyurethanes, poly(urethane-urea)s and poly(urethane-ether)s. React. Funct. Polym. Rev. 66 (2006): 299-314.

[9] Kojio, K.; Fukumaru, T. and Furukawa, M. Highly softened polyurethane elastomer synthesized with novel 1,2-Bis(isocyanate)ethoxyethane. Macromolecules 37 (2004) :3287-3291.

[10] Furukawa, M.; Mitsui, Y.; Fukumaru, T. and Kojio, K. Microphase-separated structure and mechanical properties of novel polyurethane elastomers prepared with ether based diisocyanate. Polymer 46 (2005) : 10817-10822.

[11] Miyamoto, M.; Takashima, Y. and Kimura, Y. Preparation of novel thermally stable polyurea by cationic ring-opening isomerization polymerization of polycyclic pseudourea. Macromolecules 31 (1998) : 6822-6827.

[12] Rogulska, M.; Podkoscielny, W.; Kultys, A.; Pikus, S. and Pozdzik, E. Studies on thermoplastic polyurethanes based on new diphenylethane-derivative diols. I. Synthesis and Characterization of nonsegmented polyurethanes from HDI and MDI. Eur. Polym. J. 42 (2006): 1786-1797.

[13] Mallakpour S.and Zandi, H. Step-growth polymerization of 4-(1-naphthyl)1,2,4-triazolidine-3,5-dione with diisocyanates. Polym. Bulletin. 57 (2006) : 611-621.

[14] Azzam, A.R.; Mohamed, K.S.; Tol, R.; Everaert, V.; Reynaers, H. and Goderis, B. Synthesis and thermo-mechanical characterization of high performance polyurethane elastomer based on heterocyclic and aromatic diamine chain extenders. Polym. Degrad. Stabil. 92 (2007) :1316-1325.

[15] Jayakumar, R.; Lee, Y. S.; Rajkumar, M. and Nanjundan, S. Synthesis, characterization and antibacterial activity of metal-containing polyurethanes. J. Appl. Polym. Sci. 91 (2004): 288-295.

[16] Nanjundan, S. and Prasath, R.A. Synthesis and characterization of metal-containing polyurethanes and polyurethane-ureas. Eur. Polym. J. 35 (1999) : 1939-1948.

[17] Yeganeh, H.; Barikani, M. and Khodabad, F.N. Synthesis and properties of novel thermoplastic poly(urethane-imide)s. Eur. Polym. J. 36 (2000) : 2207-2211.

[18] Deligoz, H.; Yalcınyuva, T. and Ozgumus, S. A novel type of Si-containing poly(urethane-imide)s: synthesis, characterization and electrical properties. Eur. Polym. J. 41 (2005) :771-781.

[19] Radhakrishnan, G.; Gnanarajan, T.P.; Iyer, N.P. and Nasar, A.S. Preparation and properties of poly(urethane-imide)s derived from amine-blocked polyurethane prepolymer and pyromellitic dianhydride. Eur. Polym. J. 38 (2002) : 487-495.

[20] Takeichi, T.; Zuo, M. and Xiang, Q. "Preparation and properties of novel poly(urethane-imide)s" Polymer 39 (1998) : 6683-6689.

[21] Takeichi, T. and Zuo, M. Preparation and characterization of poly(urethane–imide) films prepared from reactive polyimide and polyurethane prepolymer. Polymer 40 (1999) : 5153-5160.

[22] Takeichi, T.; Ujiie, K. and Inoue, K. High performance poly(urethane-imide) prepared by introducing imide blocks into the polyurethane backbone. Polymer 46 (2005) : 11225-11231.

[23] Dyson R.W. Specialty Polymers. USA: Chapman and Hall, 1987.

[24] Yuki Y.; Lin J.-K.; Kunisada H. and Kondo S. Synthesis and characterization of new aromatic polyamides, polyimides, and polyureas containing 1,3,5,-triazine rings. J.Appl. Polm. Sci. 40 (1990) : 2113-2122.

[25] Mallakpour S. and Raheno H. Synthesis and characterization of new polyureas based on 4-(4 aminophenyl)urazole and various diisocyanates. J. Appl. Polm. Sci. 89 (2003) : 2692-2700.

[26] Radhakrishnan, G. and Rajalingam, P. Synthesis and characterization of metal-containing polyurethane-ureas. Polymer 33 (1992) : 2214-2216.

[27] Chantarasiri, N.; Sutivisedsak, N. and Pouyuan, C. Thermally stable metal-containing epoxy polymers from a epoxy resin-Shiff base metal complex-maleic anhydride system. Eur. Polym. J. 37(10) (2001) : 2031-2038.

[28] Matsuda, H. and Takechi, S. Syntheses and properties of halato-telechelic polyurethane-ureas from divalent metal salts of *p*-aminobenzoic acid, diamine, dialkylene glycols, and diisocyanate. J. Polym. Sci. A. 29 (1991) : 83-91.

[29] Wang X.; Qui W.; Zeng W.; Zhang X.; Li C.; Lu L.; Yang X. and Sanctuary, B.C. Preparation and characterization of polyureas from divalent metal (Ba, Sr, Pb, Zn) salts of sulfanilic acid. J. Appl. Polm. Sci. 49 (1993) : 405-415.

[30] Nanjundan, S.; Prasath, R. A. and Vijayanand, P. S. Studies on polyurethanes and polyurethane-ureas derived from divalent metal salts of mono(hydroxyl)hexolate. Polym. Int. 49 (2002) : 1464-1472.

[31] Jayakumar, R.; Prasart, R. A.; Radhakrishnan. and Nanjundan, S. Studies on zinc-containing polyurethanes and polyurethane-ureas. J. Macromol. Sci Pure. Appl. Chem. A. 39 (2002): 853-877.

[32] Jayakumar, R. and Nanjundan, S. Calcium-containing poly(urethane-urea)s: synthesis, spectral, and thermal studies. J. Polym. Sci,A. 42 (2003) : 1809-1819.

[33] Nanjundan, S.; Lee, Y. S. and Jaryakumar, R. Synthesis and Characterization of Calcium-containing poly(urethane-urea)s. J. Polym. Sci. 90 (2003) : 3488-3496.

[34] Nanjundan, S.; Lee, Y. S. and Jaryakumar, R. Studies on metal-containing copolyurethanes. React. Funct. Polym. 55 (2003): 267-276.

[35] Jayakumar, R. and Nanjundan, S. Studies on metal-containing co-polyurethanes base on mono(hydroxyethoxyethyl)phthalate. J. Macromol. Sci. Pure. Appl. Chem. A. 43 (2006): 945-954

[36] Wang, X.; Yang, Y.; Zhi, Z.; Yang, X. and Lu, L. Synthesis and characterization of novel polyurea-imides. Eur. Polym. J. 34 (1998) : 1893-1897.

[37] Imai, Y.; Park, K.H.; Tani T. and Kakimoto M. Synthesis and characterization of new soluble aromatic poly(ureaimide)s from *N,N'*-dimethyl-*N,N'*-bis(aminophenyl)ureas and aromatic tetracarboxylic dianhydrides. Macromol. Chem. Phys.199 (1998) **:** 457–461.

[38] Wang, H.H., and Wu, S.P. Synthesis of aromatic poly(urea-imide) with heterocyclic side-chain structure. J. Appl. Polm. Sci. 74 (1999) : 1719-1730.

[39] Wang, H.H. and Wu, S.P. Synthesis of aromatic poly(urea-imide) with hetero-cyclic side chain structure. Des. Monomers Polym. 5 (2002) : 297-315.

[40] Yeganeh, H. and Shamekhi, M.A. Poly(urethane-imide-imide), a new generation of thermoplastic polyurethane elastomers with enhanced thermal stability. Polymer 45 (2004), 359-365.

[41] Chantarasiri, N.; Chulamanee, C.; Mananunsap, T. and Muangsin N. Thermally stable metal-containing polyureas from hexadentate Schiff base metal complexes and diisocyanates. Polym. Degrad. Stabil. 86(3) (2004) : 505-513.

[42] Chantarasiri, N.; Damrongkosit, T.; Jangwong, W.; Sridaeng, D. and Suebphan, R. Synthesis, characterization and thermal properties of metal-containing polyurethane-ureas from hexadentate Schiff base metal complexes. Eur. Polym. J. 40 (2004): 1867-1874.

[43] Chantarasiri, N., Tuntulani, T. and Chanma, N. Application of hexadentate Schiff base metal complexes as Crosslinking agents for diglycidyl ether of bisphenol A. Eur. Polym. J. 36 (5) (2000) : 889-895.

[44] Raghavan, A., Senthilkumar, N.; Nasar, A.S. Novel Metal-Containing Polyurethane Elastomers Prepared Using Tetradentate Schiff Base Metal Complexes. Macromol. Chem. Phys. 206 (2005) : 2490–2500.

[45] Hong, K., Park, S. Preparation of polyurea microcapsules with different composition ratios: structures and thermal properties. Materials Sci. and Eng A. 272 (1999) 418–421.

[46] Arnold, R. G., Nelson, J. A., and Verbanc, J. J. Recent Advances In Isocyanate Chemistry Chem. Rev. 57 (1) (1957) : 47-76.

APPENDICES

APPENDIX A

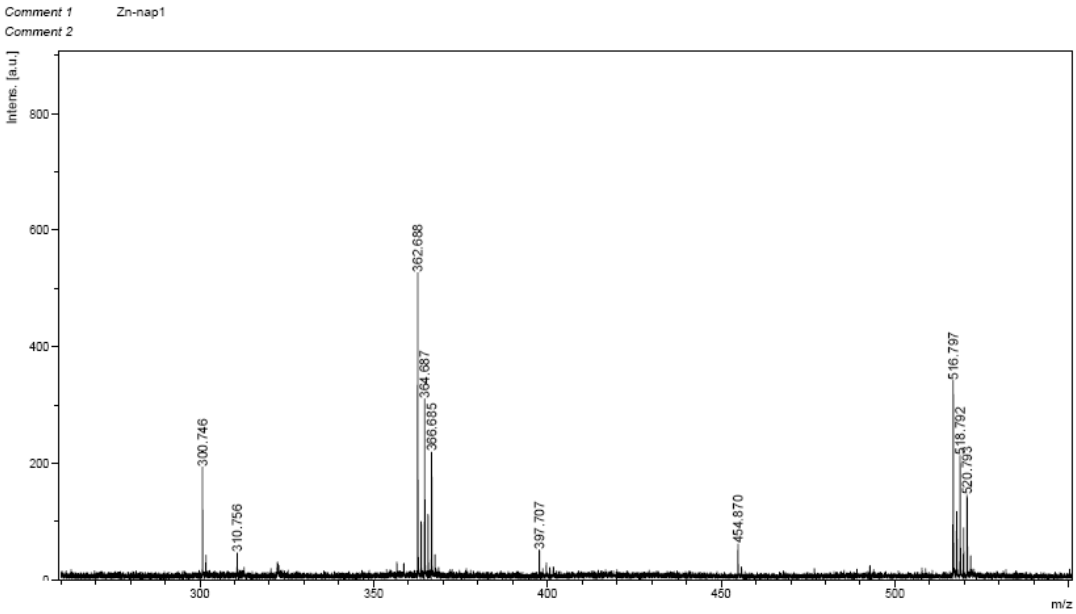

Figure A.1 Mass spectra of $ZnNapth_2trien$

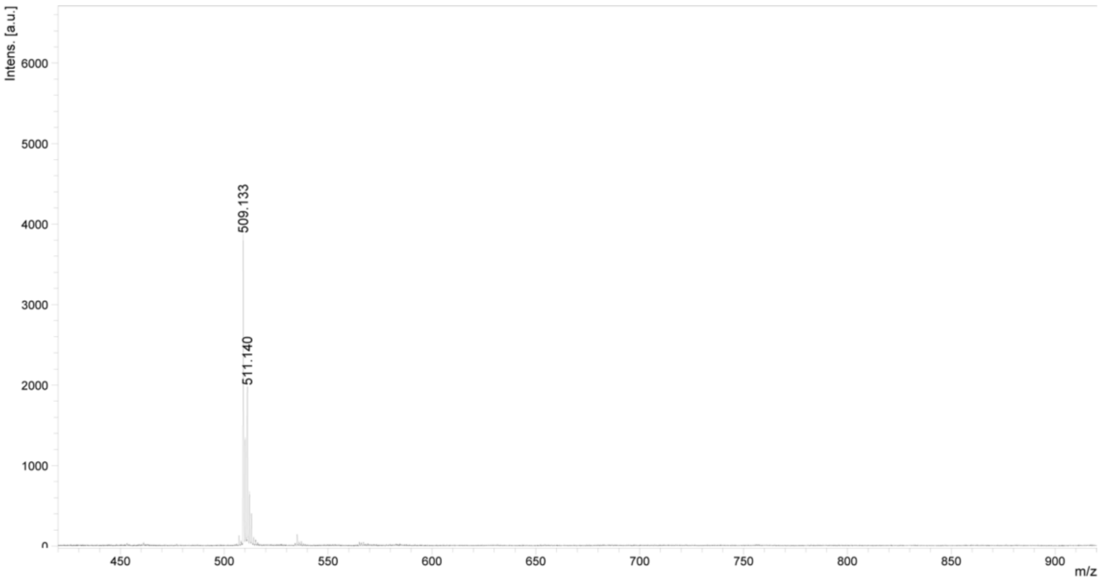

Figure A.2 Mass spectra of $NiNapth_2trien$

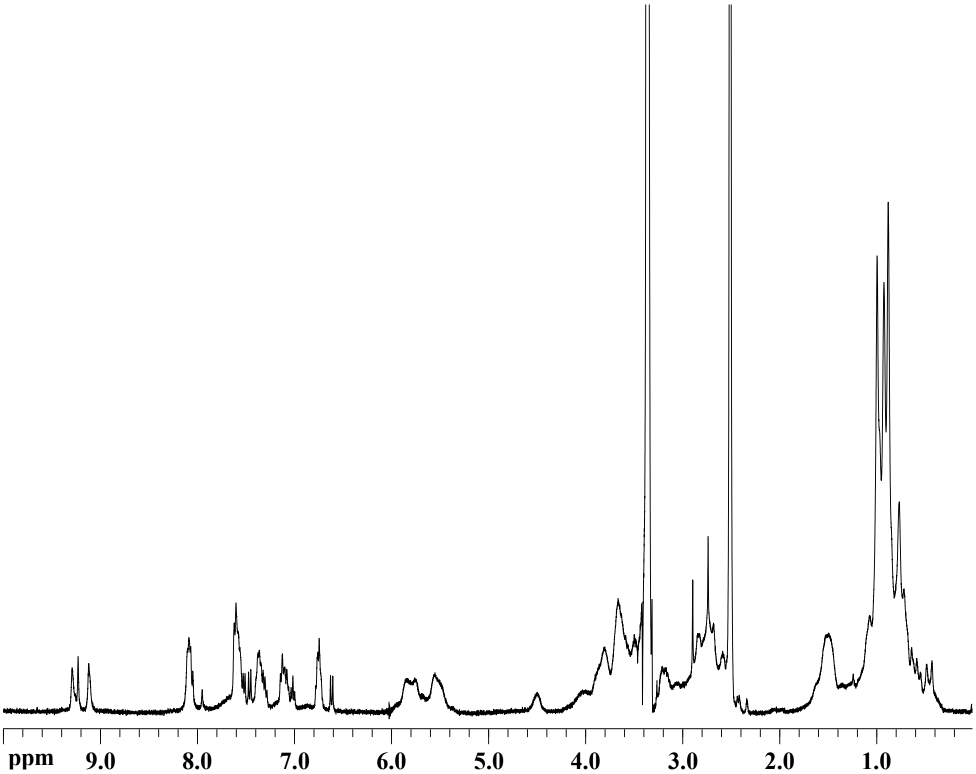

Figure A.3 ^{1}H NMR spectrum of ZnNapth$_2$trien-IPDI in DMSO-d_6

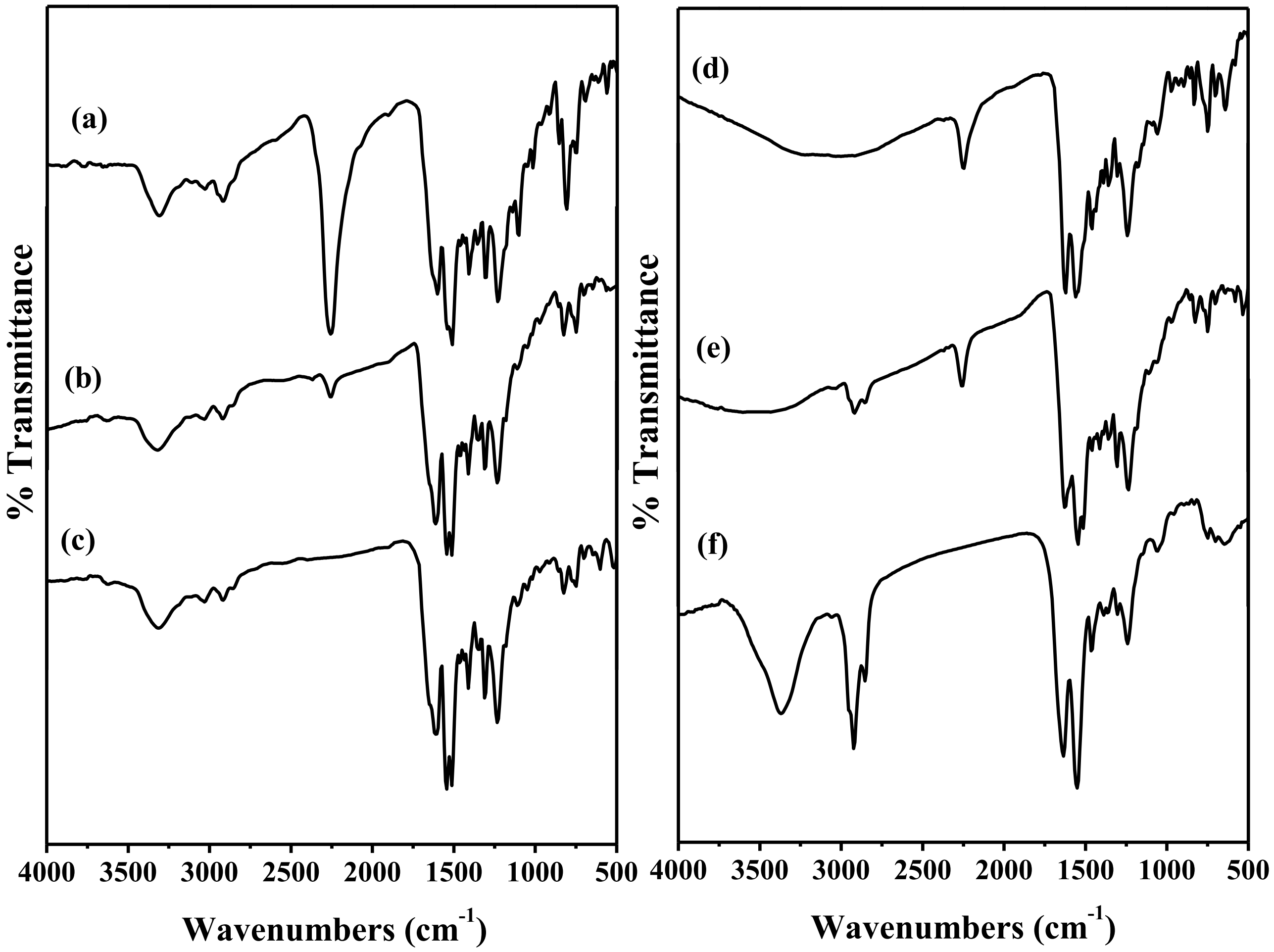

Figure A.4 IR spectra of metal-containing copolyureas based on *m*-XDA

(a) ZnNapth$_2$trien-MDI-*m*-XDA (before heating)

(b) ZnNapth$_2$trien-MDI-*m*-XDA (after heating at reflux for 2 h)

(c) ZnNapth$_2$trien-MDI-*m*-XDA (after heating at reflux for 4 h)

(d) ZnNapth$_2$trien-IPDI-*m*-XDA (before heating)

(e) ZnNapth$_2$trien-IPDI-*m*-XDA (after heating at reflux for 12 h)

(f) ZnNapth$_2$trien-IPDI-*m*-XDA (after heating at reflux for 24 h)

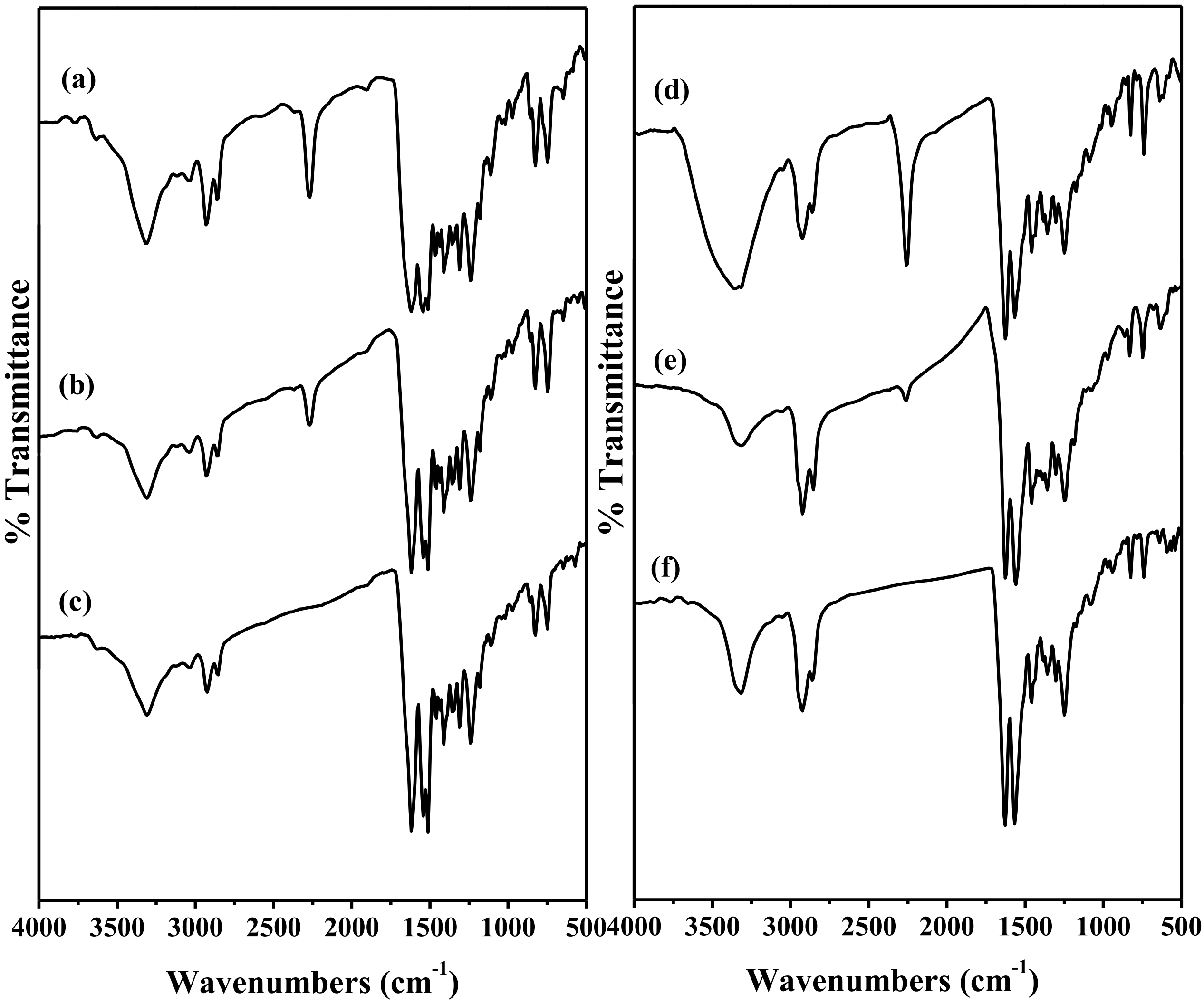

Figure A.5 IR spectra of metal-containing copolyureas based on HMDA

(a) ZnNapth$_2$trien-MDI-HMDA (before heating)

(b) ZnNapth$_2$trien-MDI-HMDA (after heating at reflux for 2 h)

(c) ZnNapth$_2$trien-MDI-HMDA (after heating at reflux for 4 h)

(d) ZnNapth$_2$trien-IPDI-HMDA (before heating)

(e) ZnNapth$_2$trien-IPDI-HMDA (after heating at reflux for 12 h)

(f) ZnNapth$_2$trien-IPDI-MDA (after heating at reflux for 24 h)

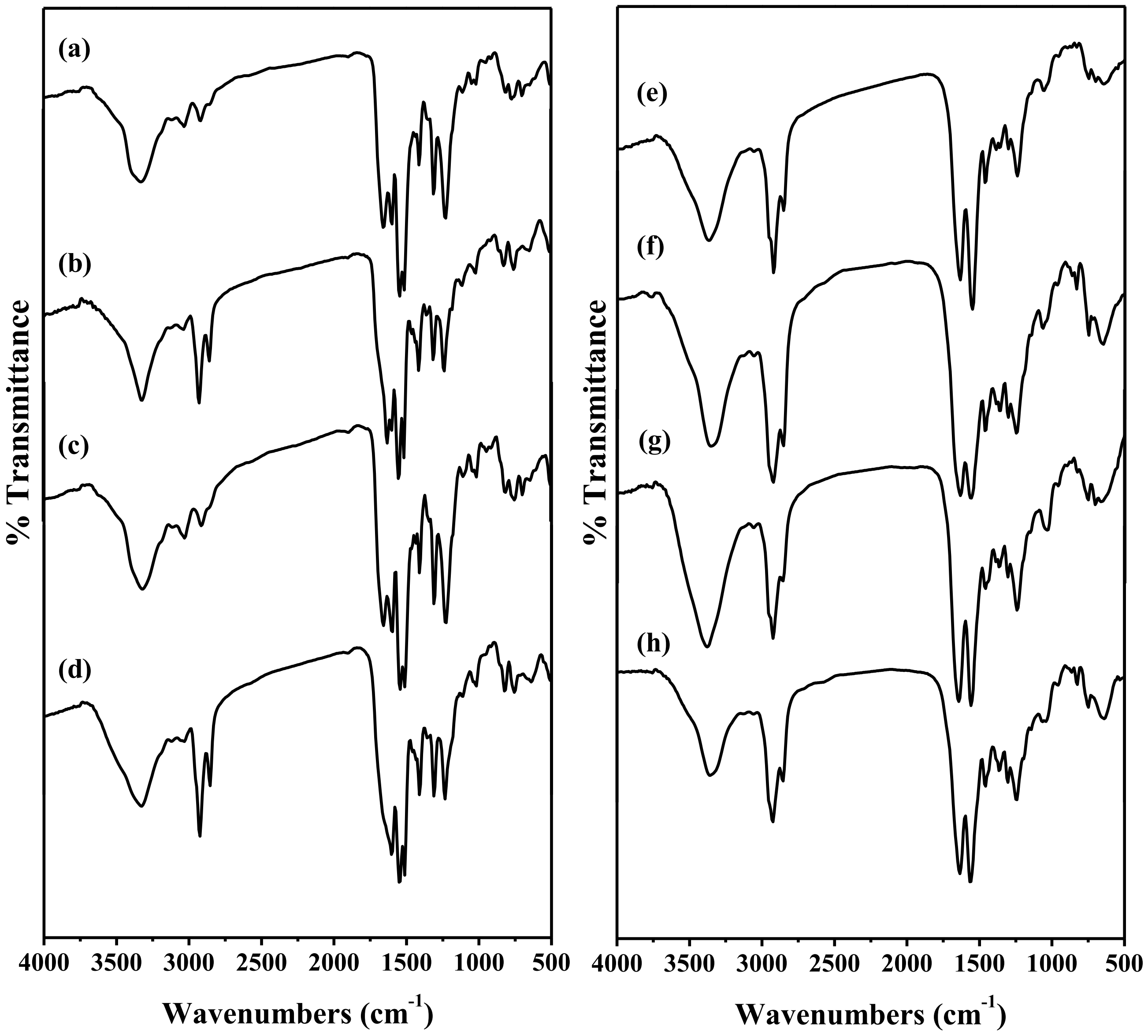

Figure A.6 IR spectra of metal-containing copolyureas

(a) ZnNapth$_2$trien-MDI-*m*-XDA (0.5:2:1.5)

(b) ZnNapth$_2$trien-MDI-HMDA (0.5:2:1.5)

(c) NiNapth$_2$trien-MDI-*m*-XDA (0.5:2:1.5)

(d) NiNapth$_2$trien-MDI-HMDA (0.5:2:1.5)

(e) ZnNapth$_2$trien-IPDI-*m*-XDA (0.5:2:1.5)

(f) ZnNapth$_2$trien-IPDI-HMDA (0.5:2:1.5)

(g) NiNapth$_2$trien-IPDI-*m*-XDA (0.5:2:1.5)

(h) NiNapth$_2$trien-IPDI-HMDA (0.5:2:1.5)

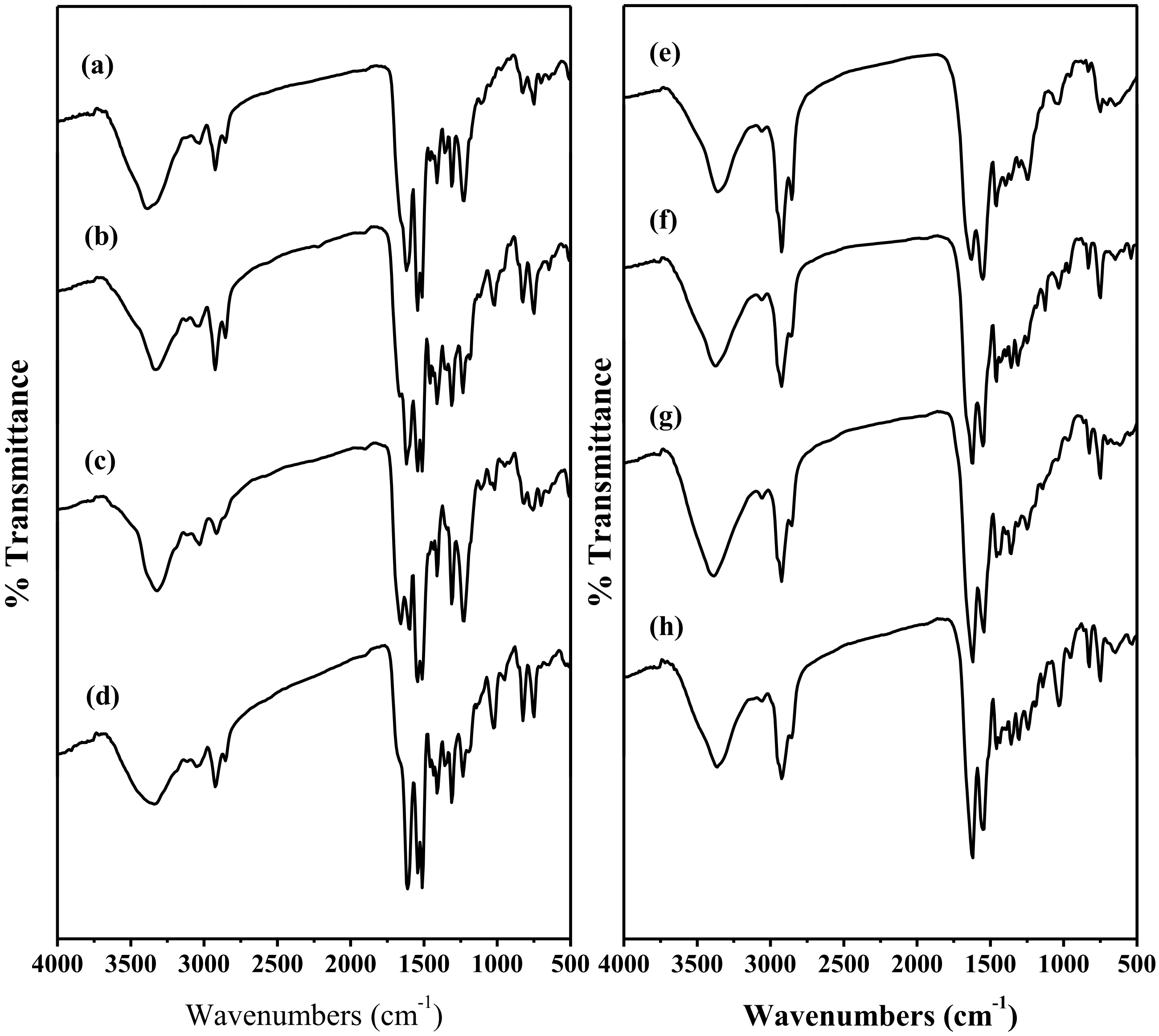

Figure A.7 IR spectra of metal-containing copolyureas

(a) ZnNapth$_2$trien-MDI-*m*-XDA (1.5:2:0.5)

(b) ZnNapth$_2$trien-MDI-HMDA (1.5:2:0.5)

(c) NiNapth$_2$trien-MDI-*m*-XDA (1.5:2:0.5)

(d) NiNapth$_2$trien-MDI-HMDA (1.5:2:0.5)

(e) ZnNapth$_2$trien-IPDI-*m*-XDA (1.5:2:0.5)

(f) ZnNapth$_2$trien-IPDI-HMDA (1.5:2:0.5)

(g) NiNapth$_2$trien-IPDI-*m*-XDA (1.5:2:0.5)

(h) NiNapth$_2$trien-IPDI-HMDA (1.5:2:0.5)

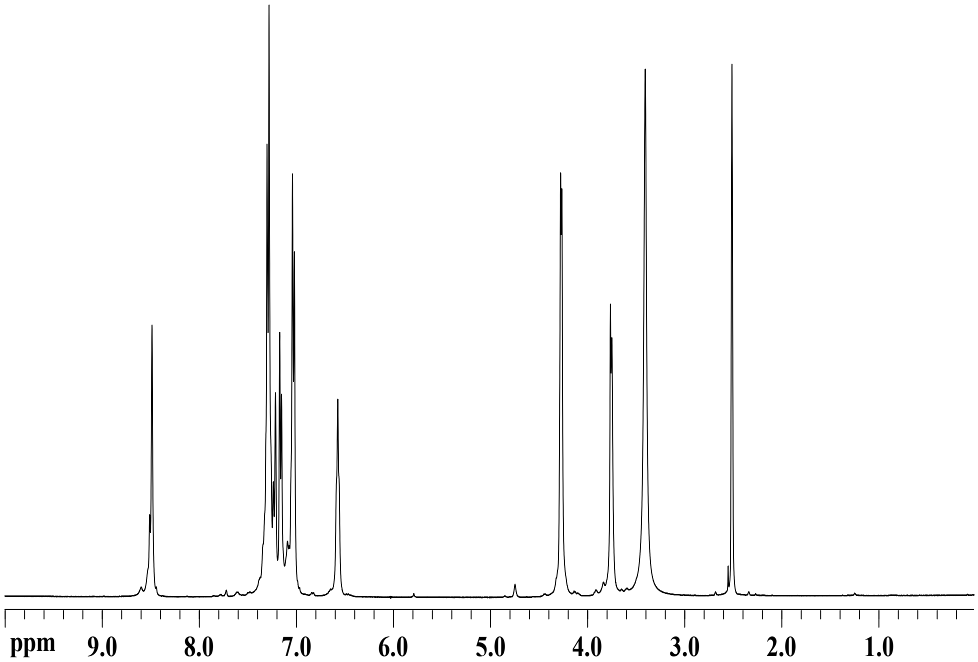

Figure A.8 ^{1}H NMR spectrum of MDI-*m*-XDA in DMSO-d_6

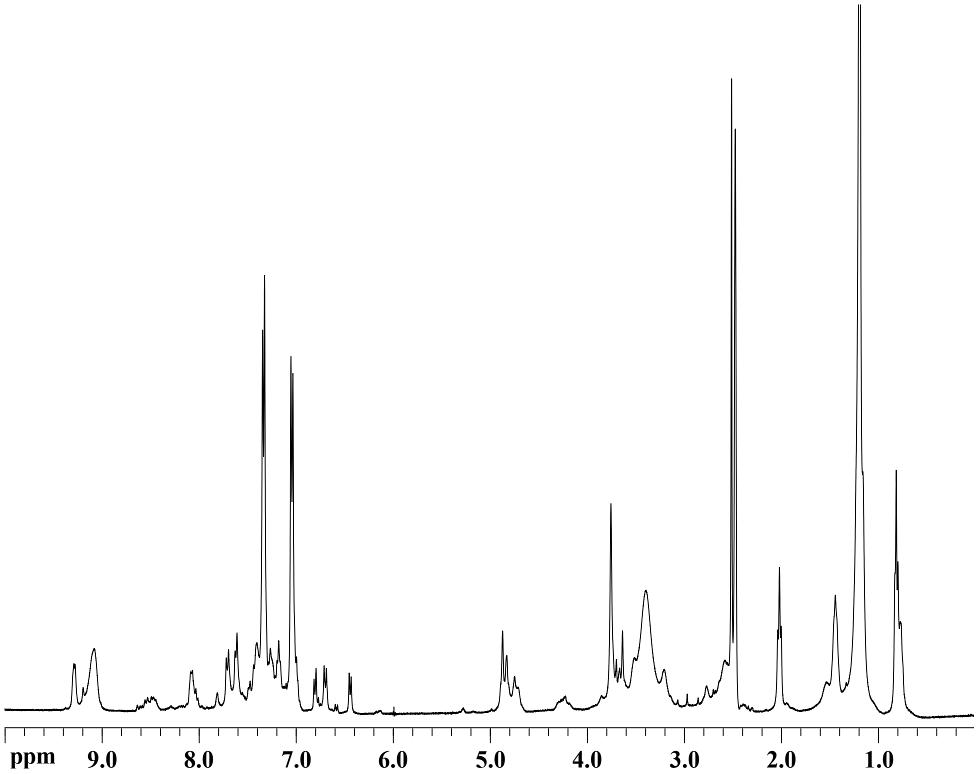

Figure A.9 ^{1}H NMR spectrum of ZnNapth$_2$trien-MDI-*m*-XDA in DMSO-d_6

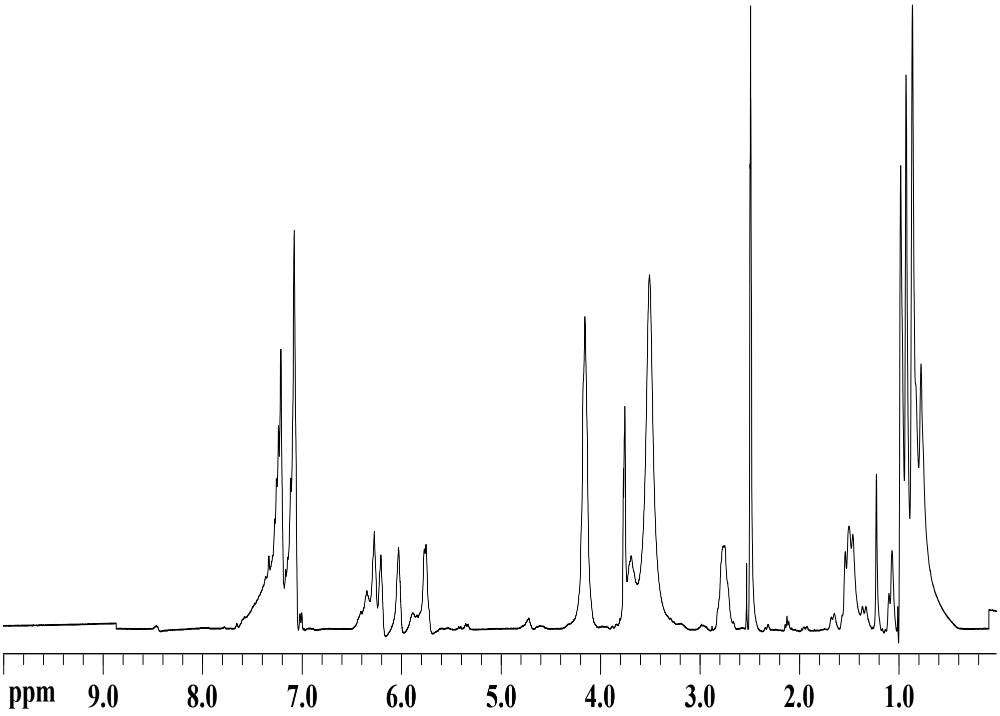

Figure A.10 ^{1}H NMR spectrum of IPDI-*m*-XDA in DMSO-d_6

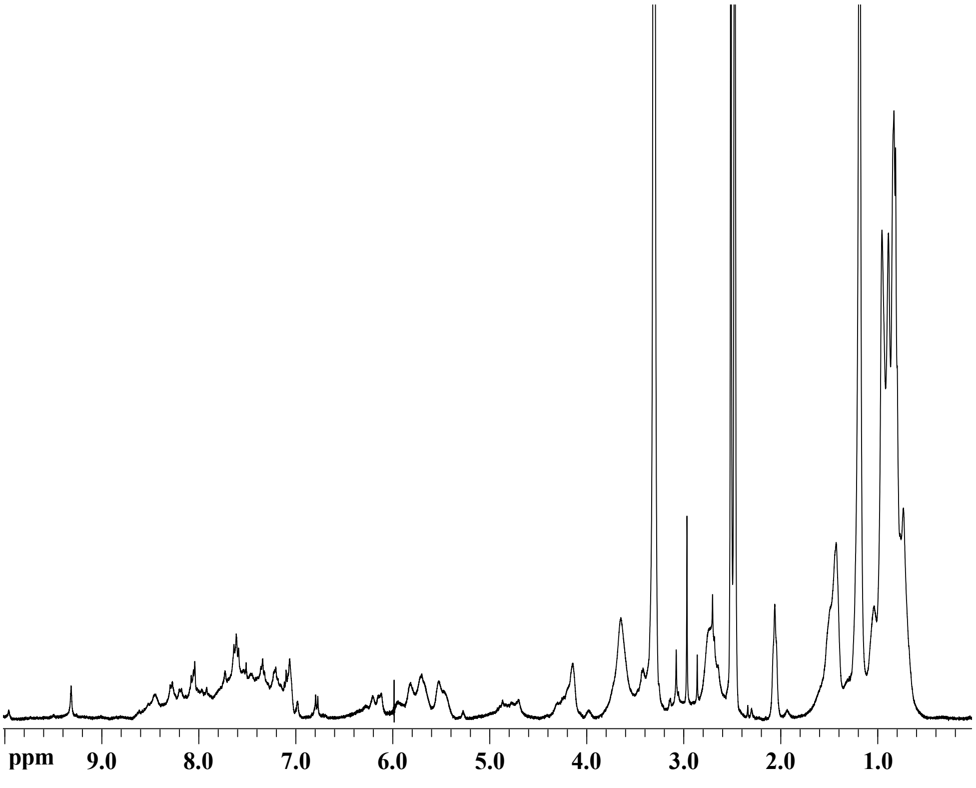

Figure A.11 ^{1}H NMR spectrum of ZnNapth$_2$trien- IPDI- *m*-XDA in DMSO-d_6

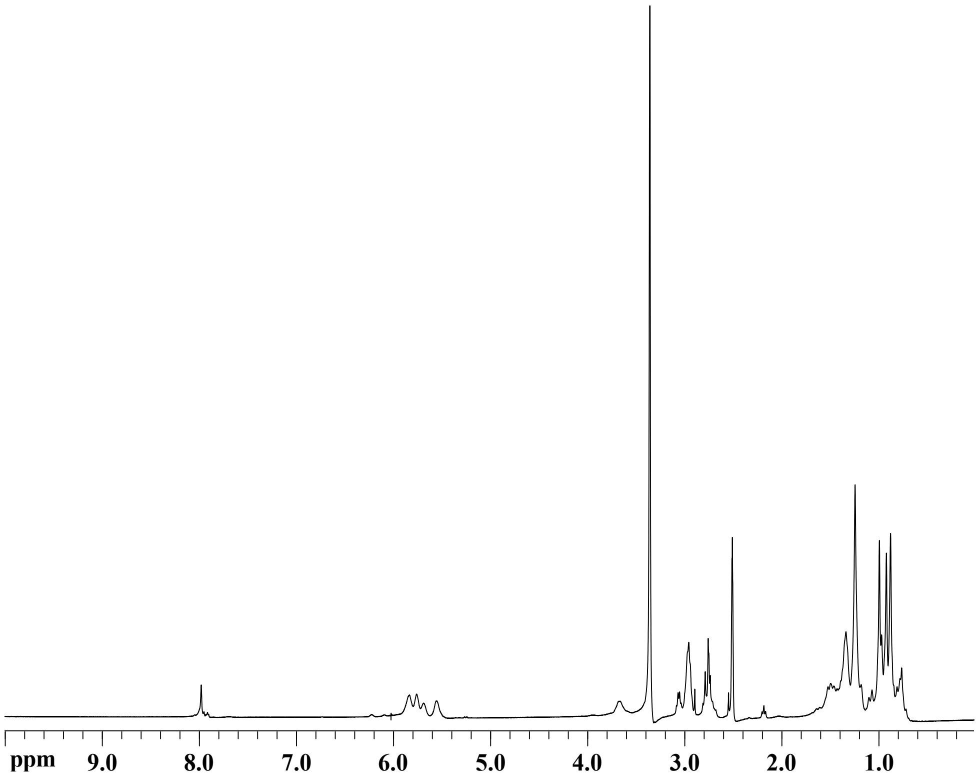

Figure A.12 ^{1}H NMR spectrum of IPDI-HMDA in DMSO-d_6

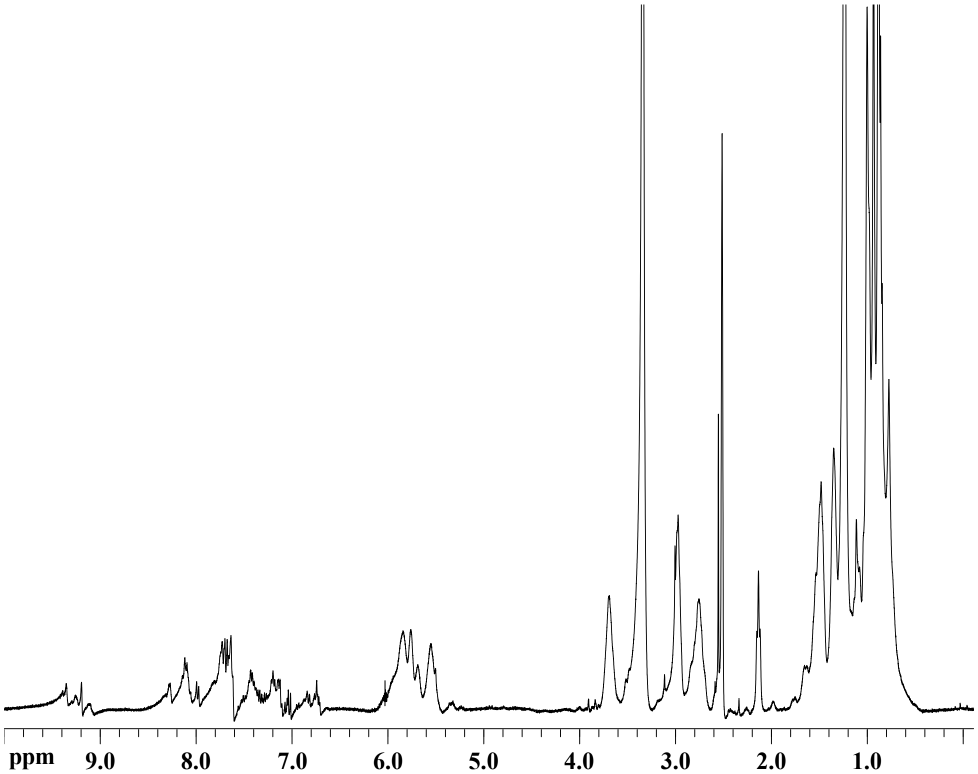

Figure A.13 ^{1}H NMR spectrum of ZnNapth$_2$trien-IPDI-HMDA in DMSO-d_6

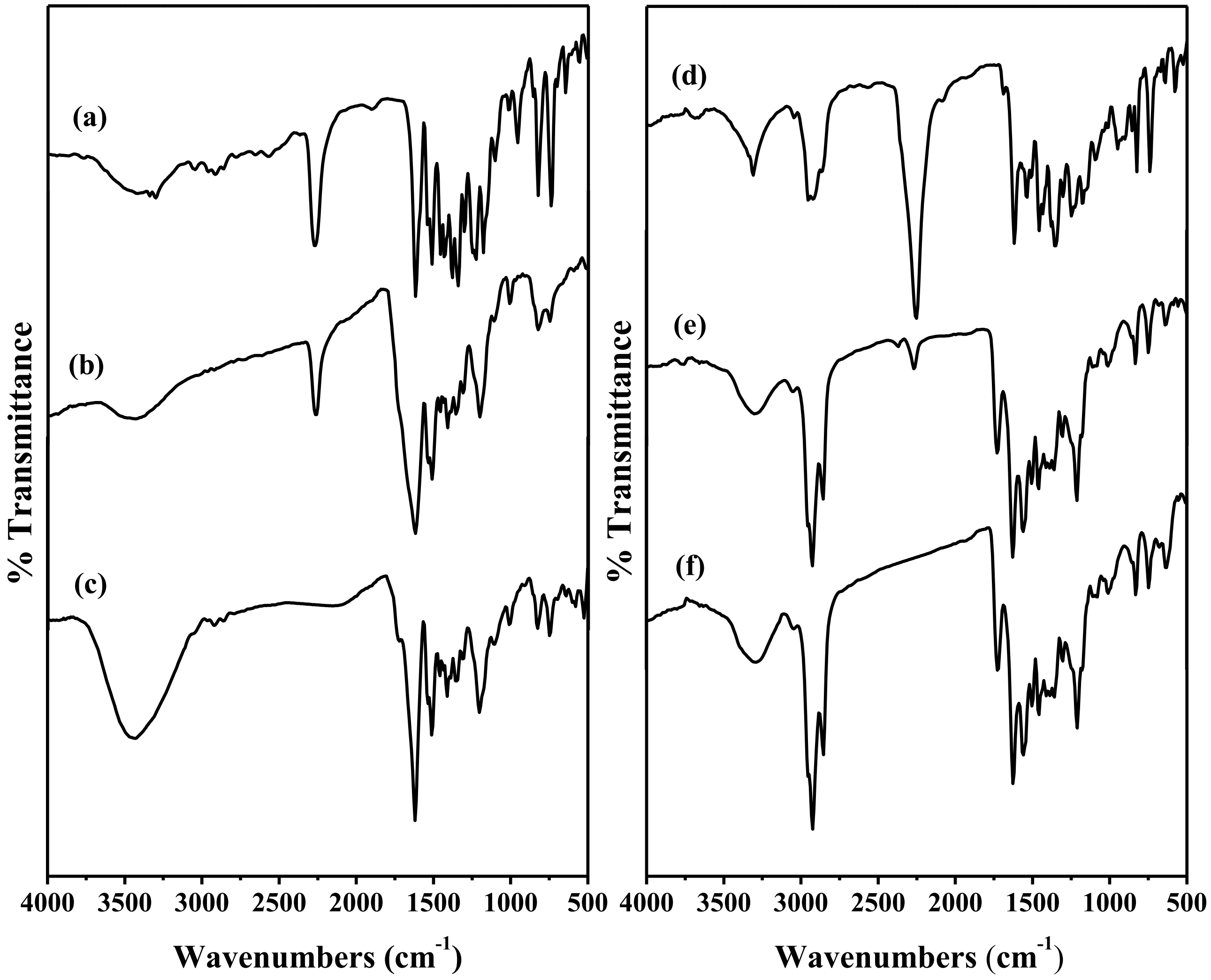

Figure A.14 IR spectra of metal-containing poly(urethane-urea)s based on BPO

(a) ZnNapth$_2$trien-MDI-BPO (before heating)

(b) ZnNapth$_2$trien-MDI-BPO (after heating at reflux for 2 h)

(c) ZnNapth$_2$trien-MDI-BPO (after heating at reflux for 4 h)

(d) ZnNapth$_2$trien-IPDI-BPO (before heating)

(e) ZnNapth$_2$trien-IPDI-BPO (after heating at reflux for 12 h)

(f) ZnNapth$_2$trien-IPDI-BPO (after heating at reflux for 36 h)

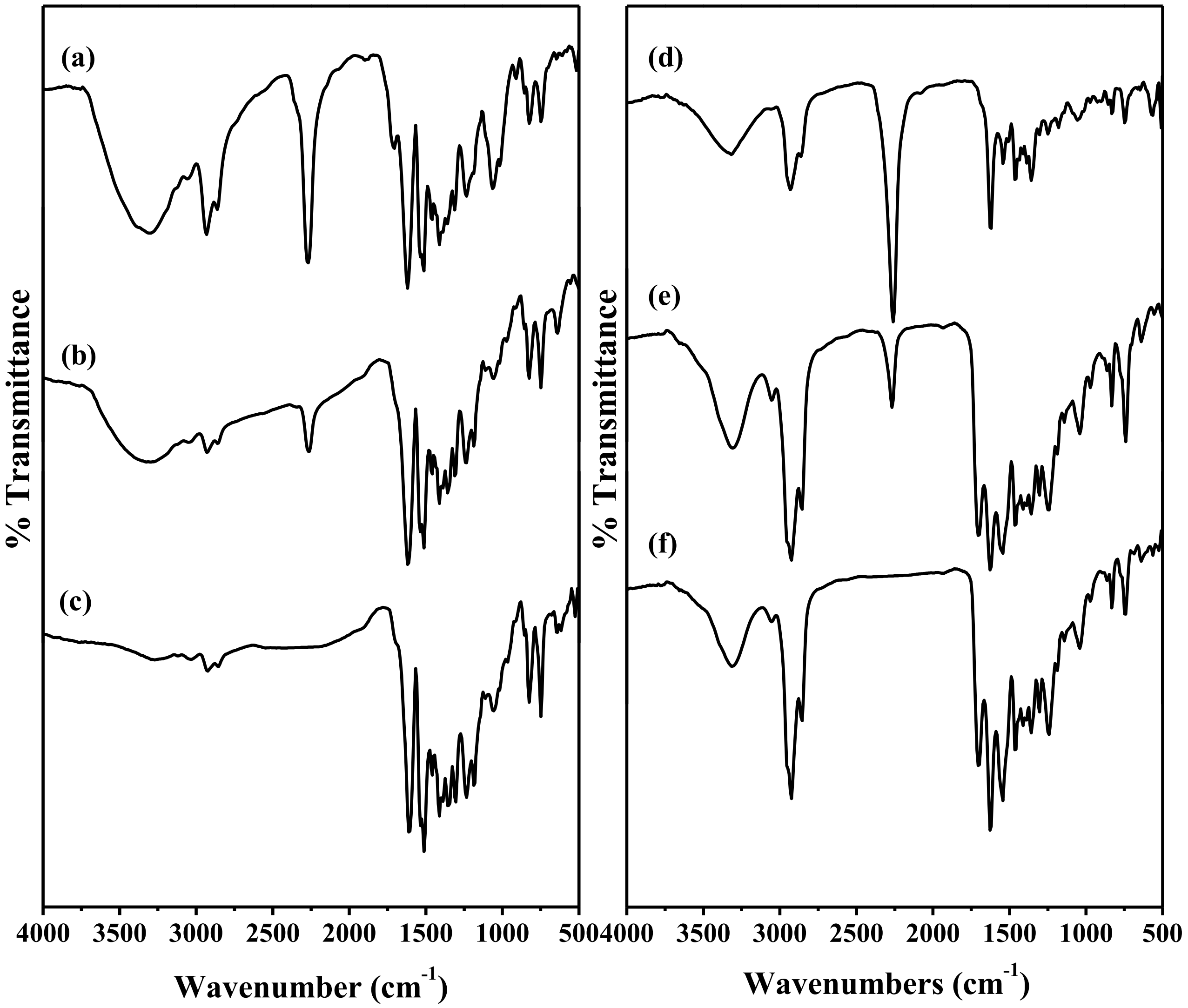

Figure A.15 IR spectra of metal-containing poly(urethane-urea)s based on HDO

(a) ZnNapth$_2$trien-MDI-HDO (before heating)

(b) ZnNapth$_2$trien-MDI-HDO (after heating at reflux for 2 h)

(c) ZnNapth$_2$trien-MDI-HDO (after heating at reflux for 4 h)

(d) ZnNapth$_2$trien-IPDI- HDO (before heating)

(e) ZnNapth$_2$trien-IPDI-HDO (after heating at reflux for 12 h)

(f) ZnNapth$_2$trien-IPDI-HDO (after heating at reflux for 36 h)

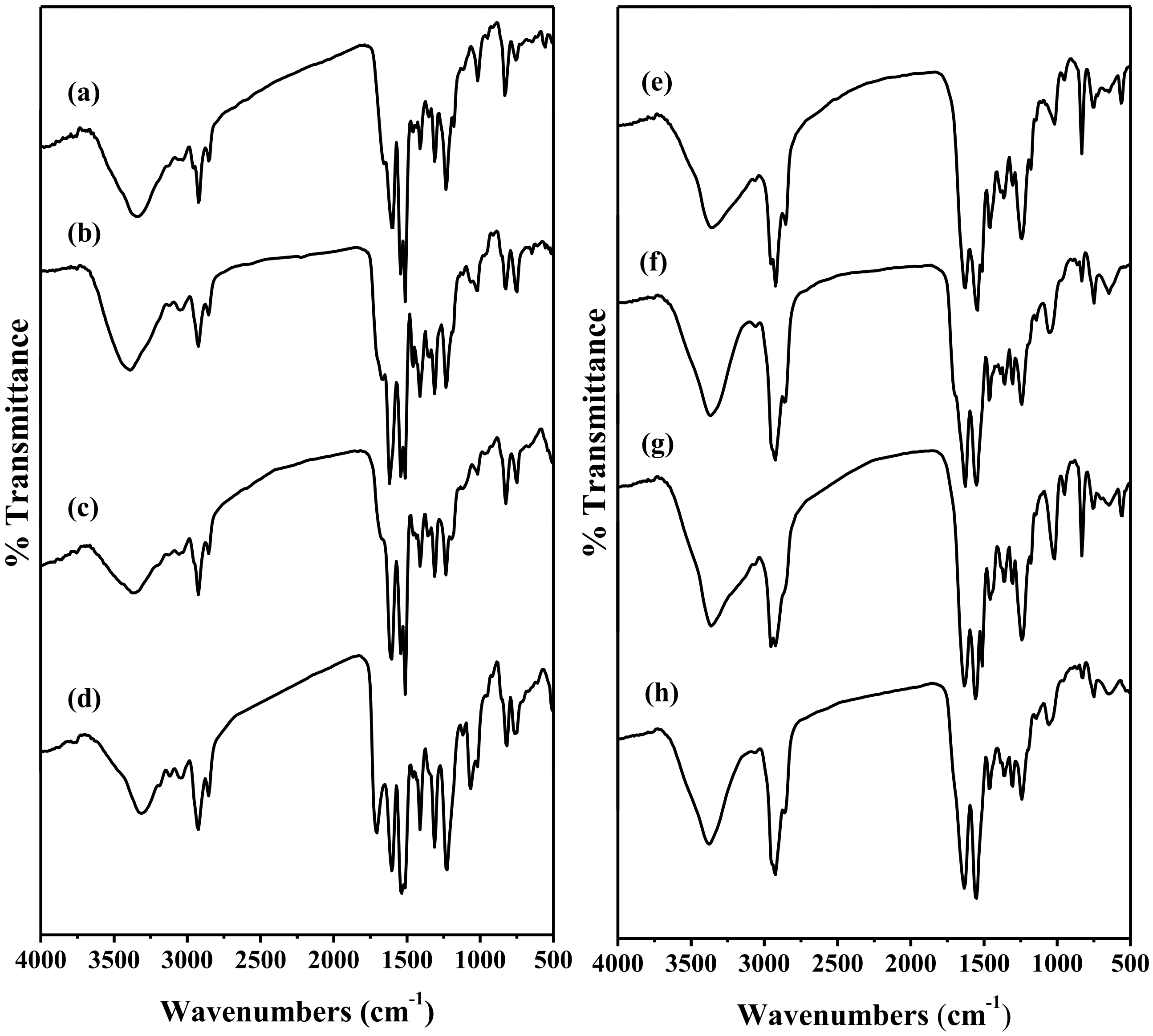

Figure A.16 IR spectra of metal-containing poly(urethane-urea)s

(a) ZnNapth$_2$trien-MDI-BPO (0.5:2:1.5) (b) ZnNapth$_2$trien-MDI-HDO (0.5:2:1.5)

(c) NiNapth$_2$trien-MDI-BPO (0.5:2:1.5) (d) NiNapth$_2$trien-MDI-HDO (0.5:2:1.5)

(e) ZnNapth$_2$trien-IPDI-BPO (0.5:2:1.5) (f) ZnNapth$_2$trien-IPDI-HDO (0.5:2:1.5)

(g) NiNapth$_2$trien-IPDI-BPO (0.5:2:1.5) (h) NiNapth$_2$trien-IPDI- HDO (0.5:2:1.5)

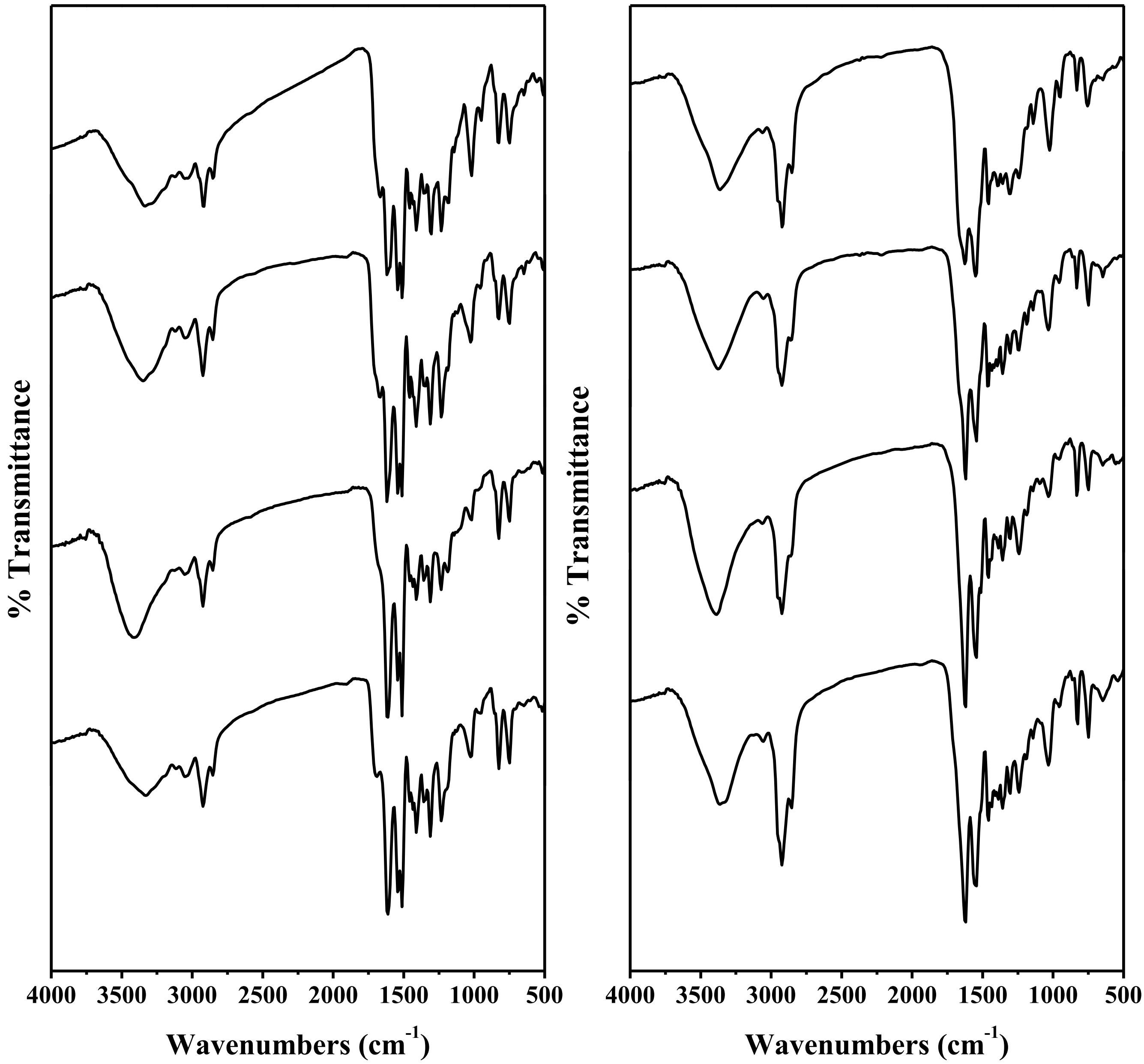

Figure A.17 IR spectra of metal-containing poly(urethane-urea)s

(a) ZnNapth$_2$trien-MDI-BPO (1.5:2:0.5)	(b) ZnNapth$_2$trien-MDI-HDO (1.5:2:0.5)
(c) NiNapth$_2$trien-MDI-BPO (1.5:2:0.5)	(d) NiNapth$_2$trien-MDI-HDO (1.5:2:0.5)
(e) ZnNapth$_2$trien-IPDI-BPO (1.5:2:0.5)	(f) ZnNapth$_2$trien-IPDI-HDO (1.5:2:0.5)
(g) NiNapth$_2$trien-IPDI-BPO (1.5:2:0.5)	(h) NiNapth$_2$trien-IPDI-HDO (1.5:2:0.5)

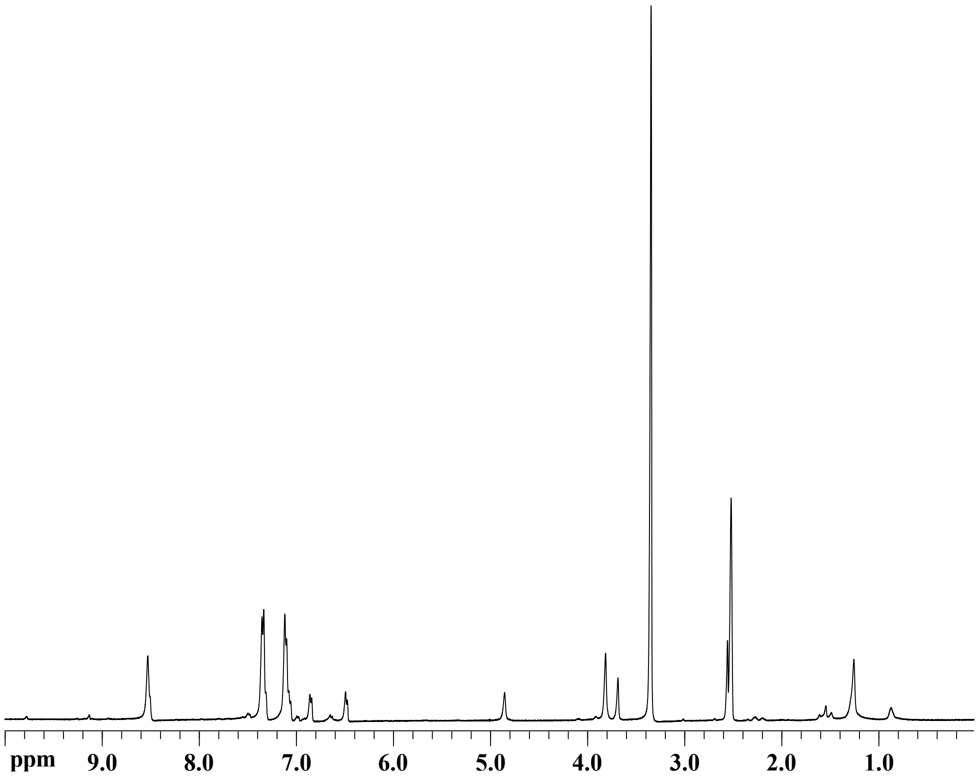

Figure A.18 ^{1}H NMR spectrum of MDI-BPO in DMSO-d_6

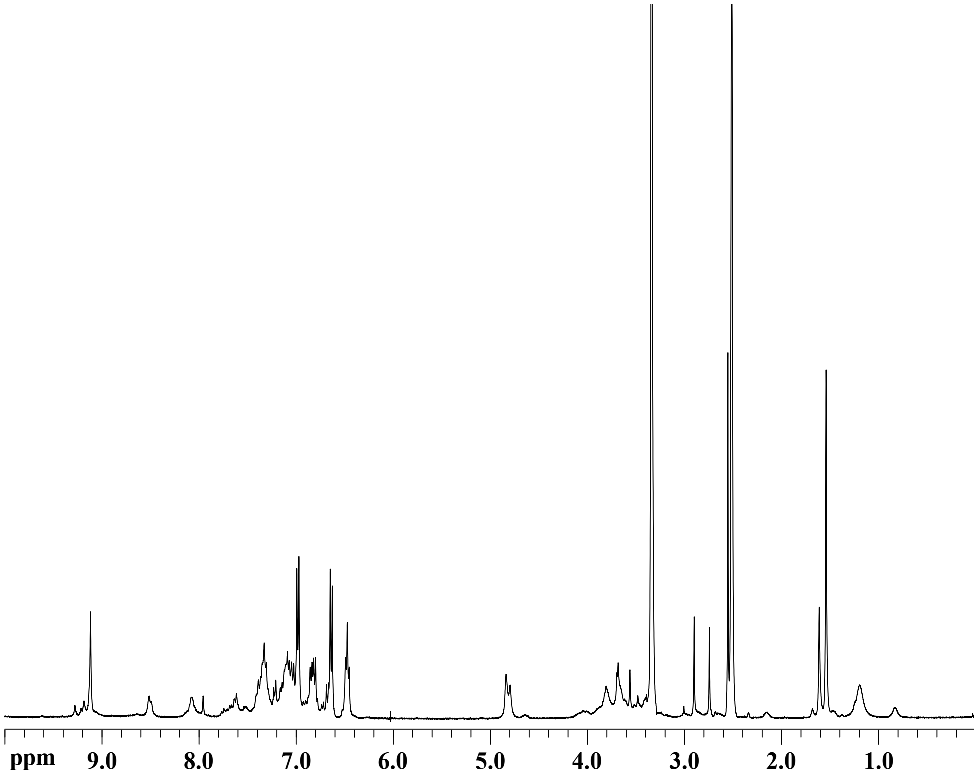

Figure A.19 ^{1}H NMR spectrum of ZnNapth$_2$trien-MDI-BPO in DMSO-d_6

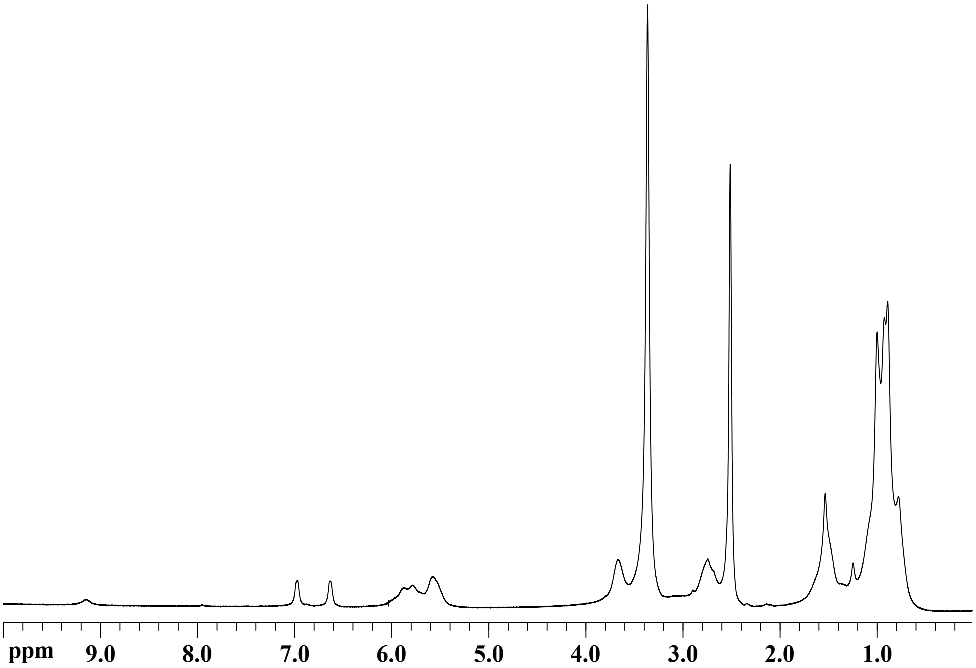

Figure A.20 ^{1}H NMR spectrum of IPDI-BPO in DMSO-d_6

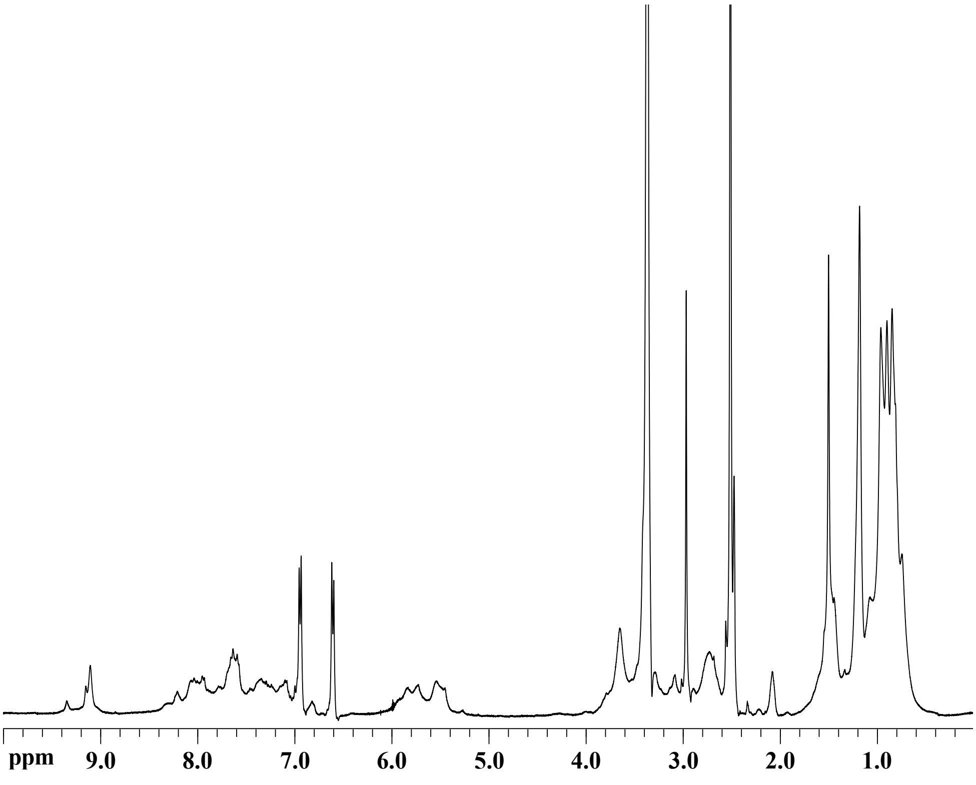

Figure A.21 ^{1}H NMR spectrum of ZnNapth$_2$trien-IPDI-BPO in DMSO-d_6

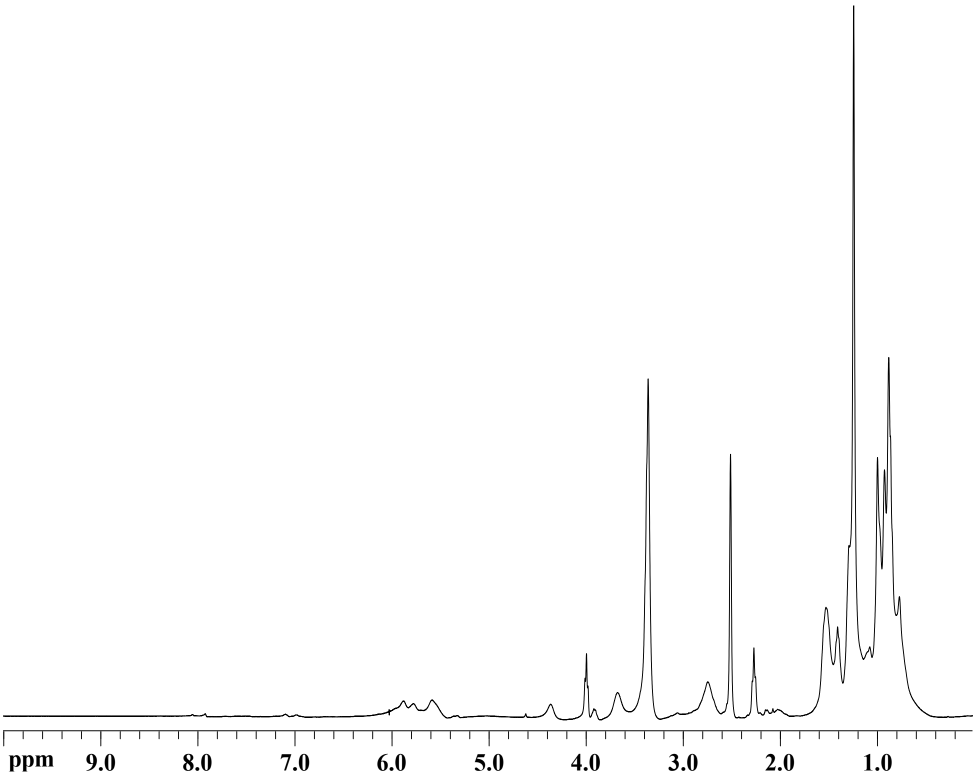

Figure A.22 ^{1}H NMR spectrum of IPDI-HDO in DMSO-d_6

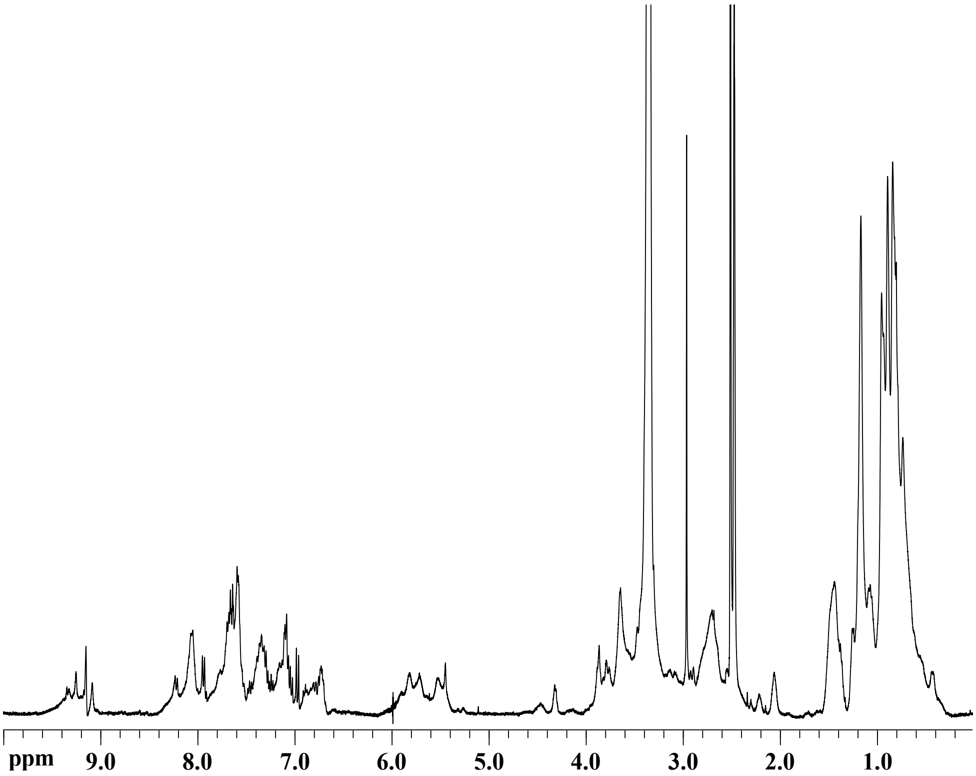

Figure A.23 ^{1}H NMR spectrum of ZnNapth$_2$trien-IPDI-HDO in DMSO-d_6

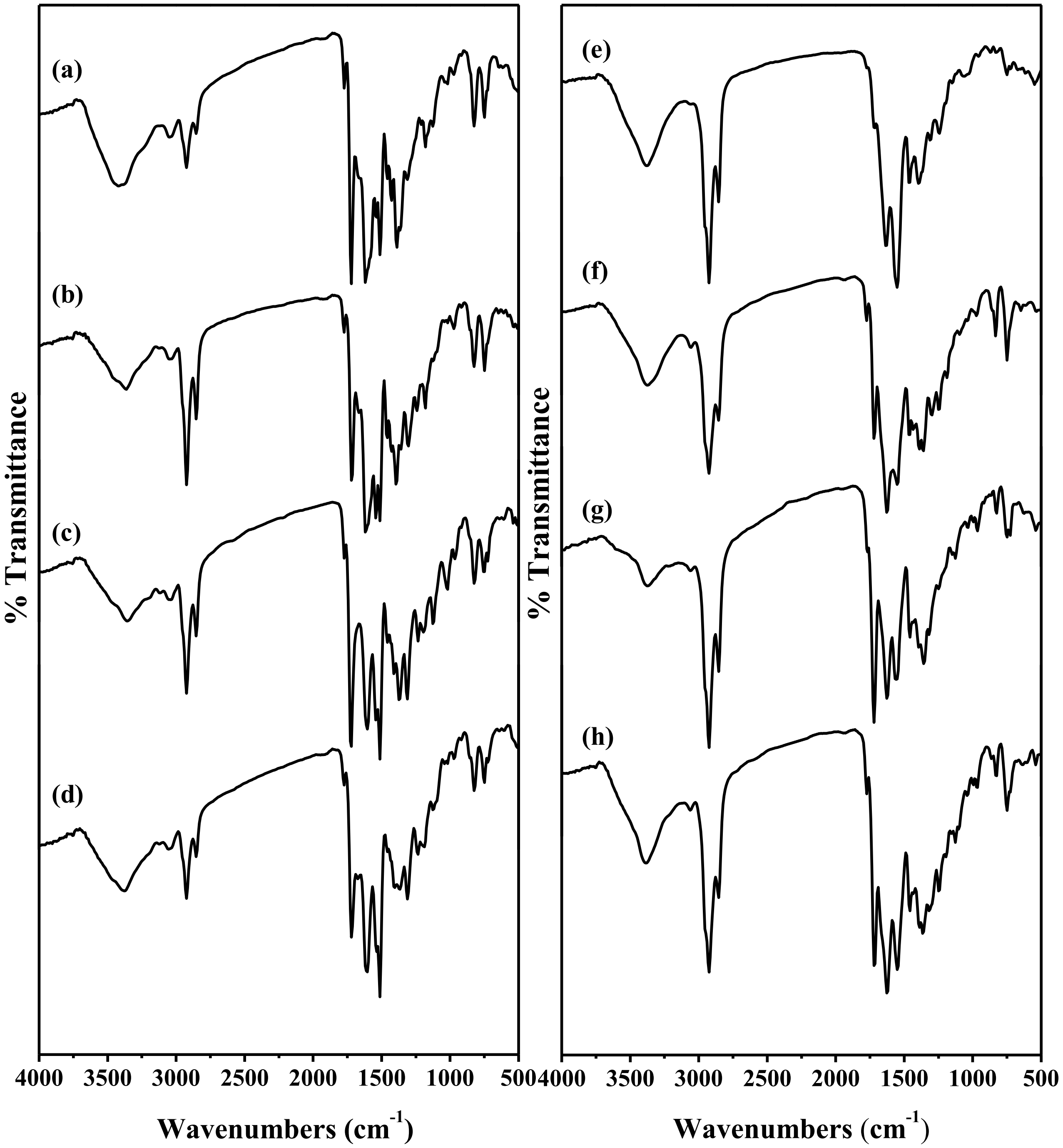

Figure A.24 IR spectra of metal-containing poly(urea-imide)s

(a) ZnNapth$_2$trien-MDI-PMDA (1:2:0.5) (b) ZnNapth$_2$trien-MDI-BTDA (1:2: 0.5)

(c) NiNapth$_2$trien-MDI-PMDA (1:2: 0.5) (d) NiNapth$_2$trien-MDI-BTDA (1:2: 0.5)

(e) ZnNapth$_2$trien-IPDI-PMDA (1:2: 0.5) (f) ZnNapth$_2$trien-IPDI-BTDA (1:2: 0.5)

(g) NiNapth$_2$trien-IPDI-PMDA (1:2: 0.5) (h) NiNapth$_2$trien-IPDI-BTDA (1:2: 0.5)

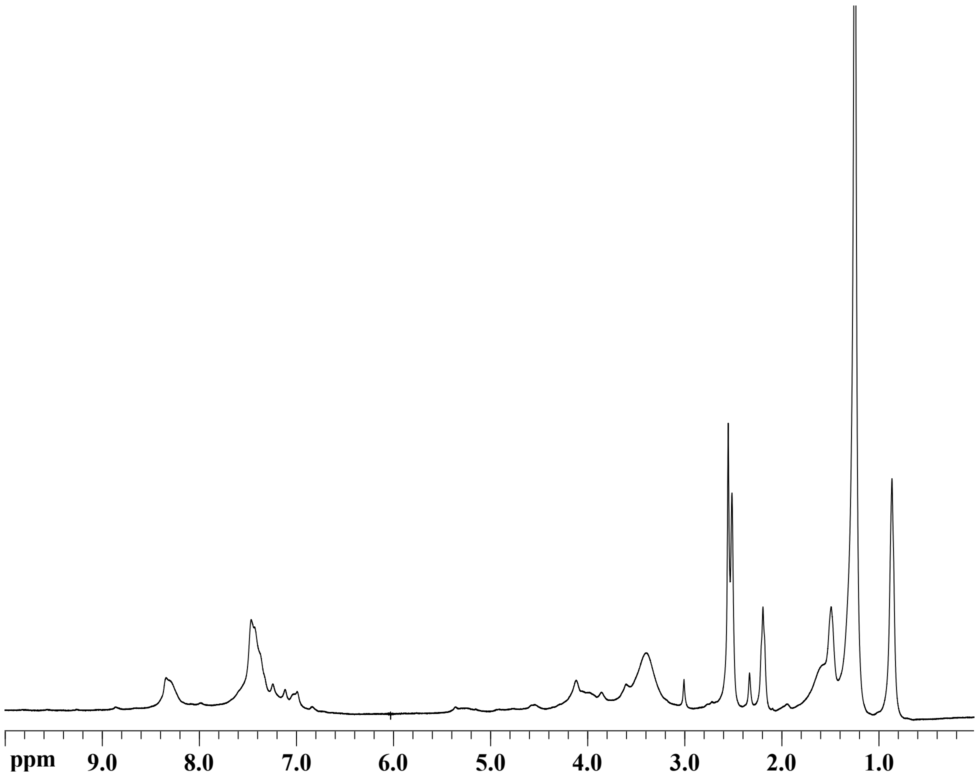

Figure A.25 ^{1}H NMR spectrum of MDI-PMDA in DMSO-d_6

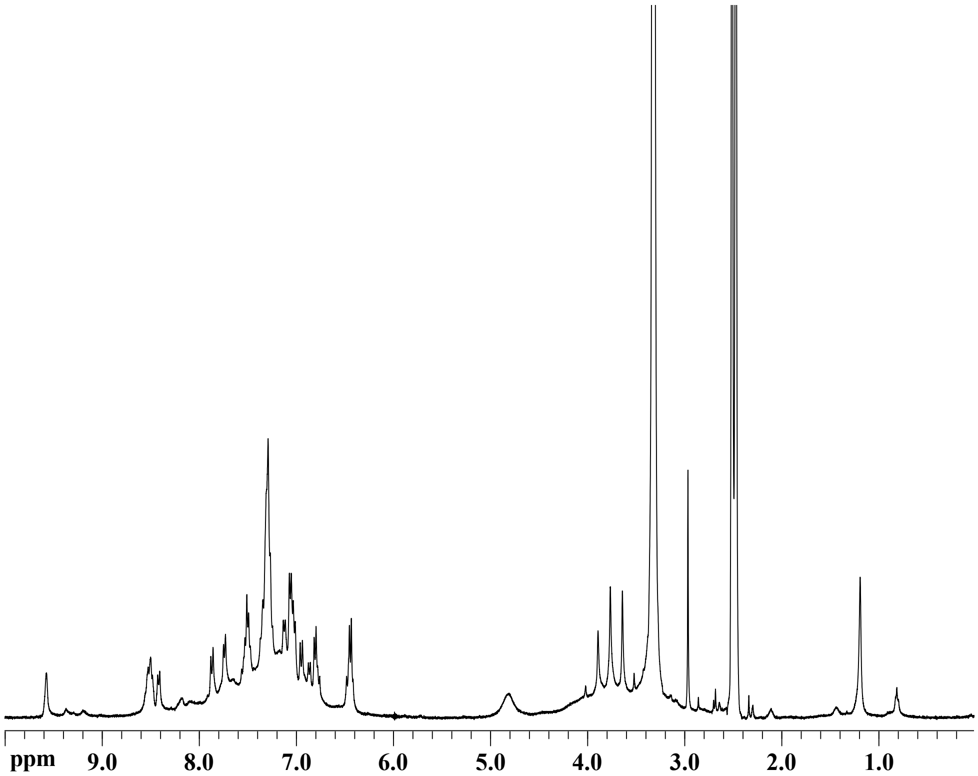

Figure A.26 ^{1}H NMR spectrum of ZnNapth$_2$trien-MDI-PMDA in DMSO-d_6

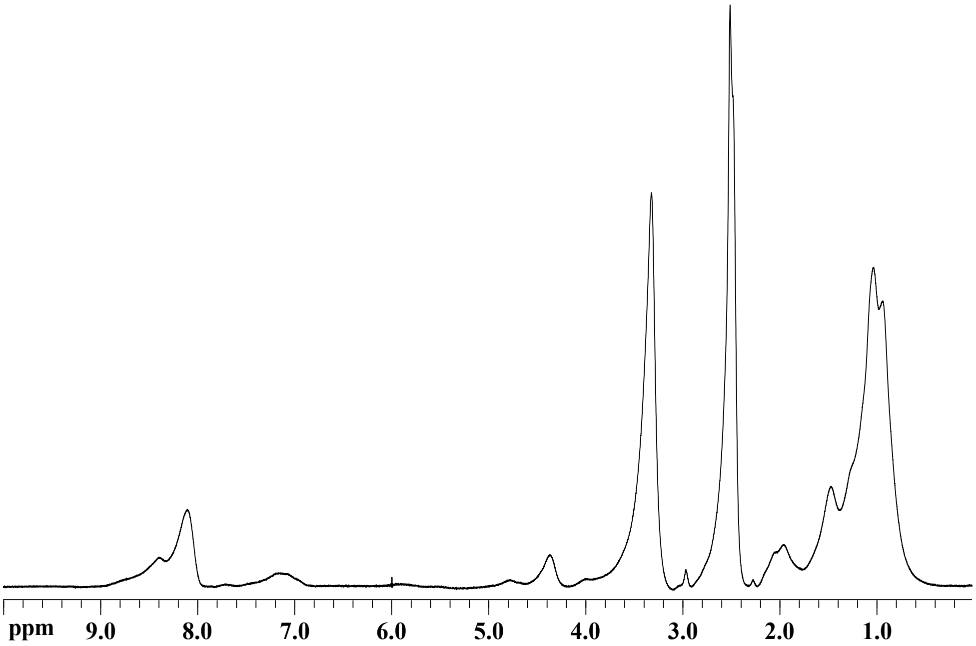

Figure A.27 ^{1}H NMR spectrum of IPDI-PMDA in DMSO-*d*$_6$

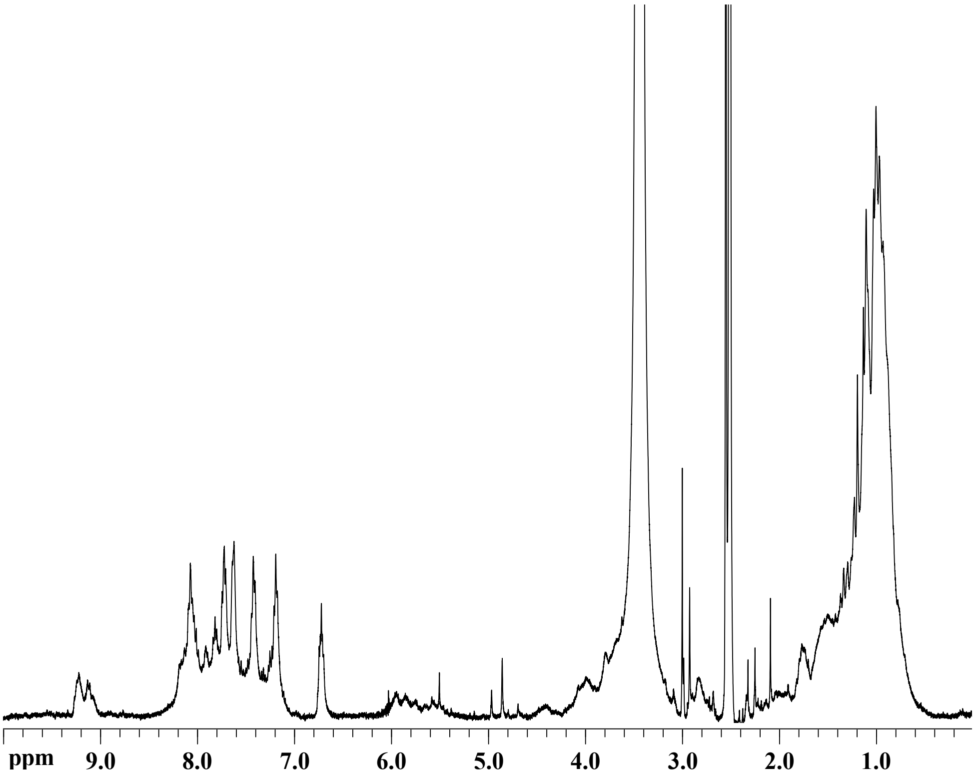

Figure A.28 ^{1}H NMR spectrum of ZnNapth$_2$trien-IPDI-PMDA in DMSO-*d*$_6$

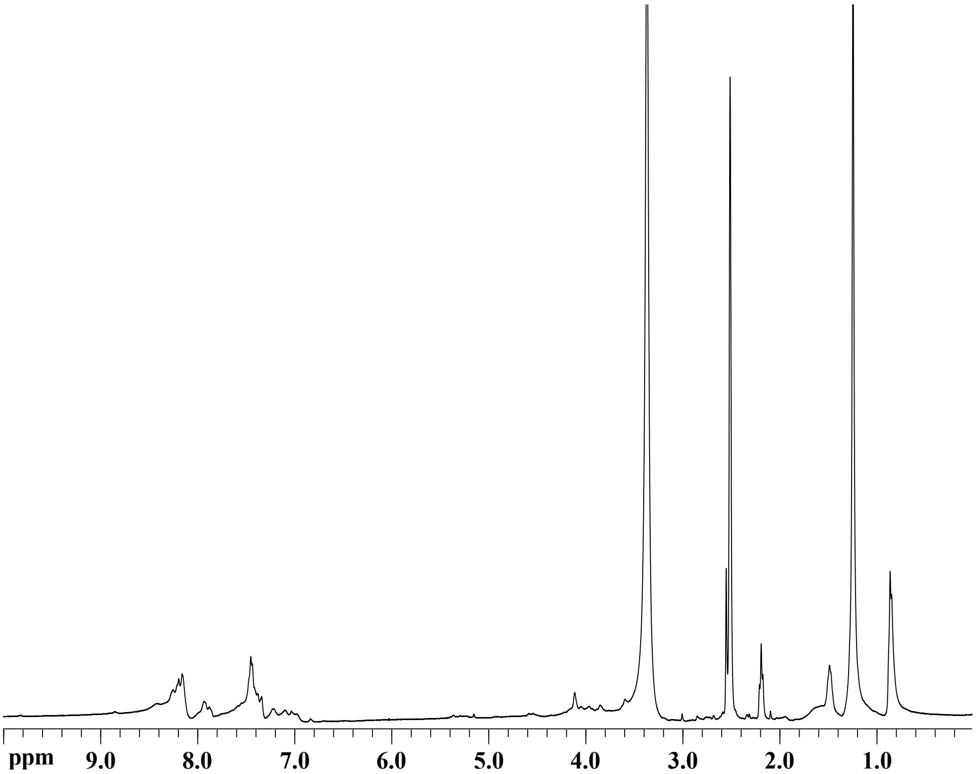

Figure A.29 ^{1}H NMR spectrum of MDI-BTDA in DMSO-d_6

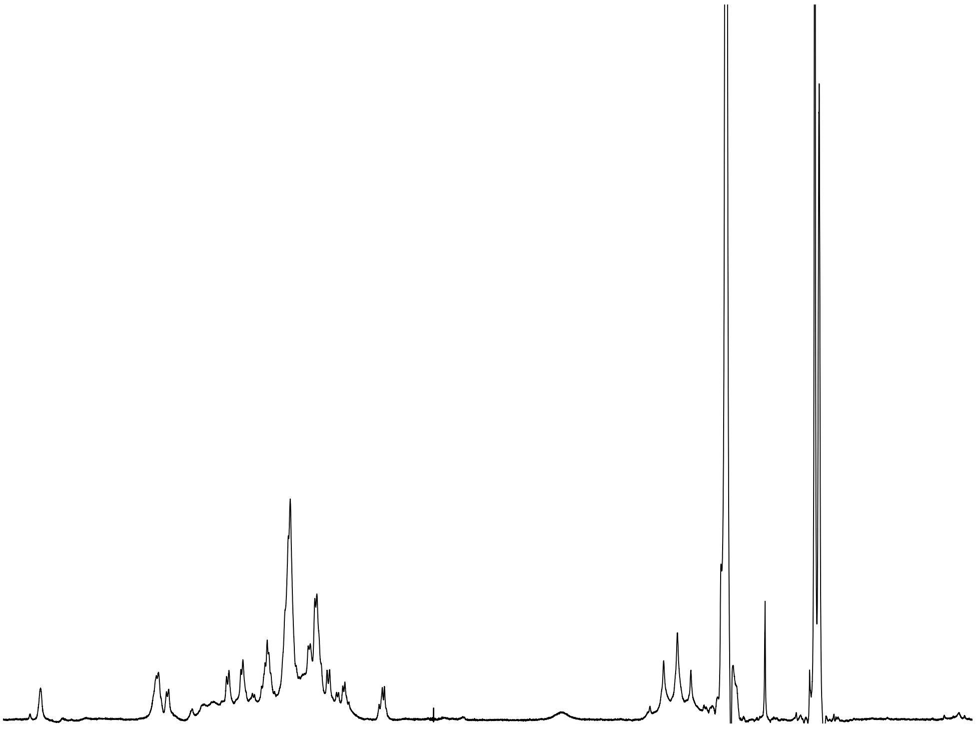

Figure A.30 ^{1}H NMR spectrum of ZnNapth$_2$trien-MDI-BTDA in DMSO-d_6

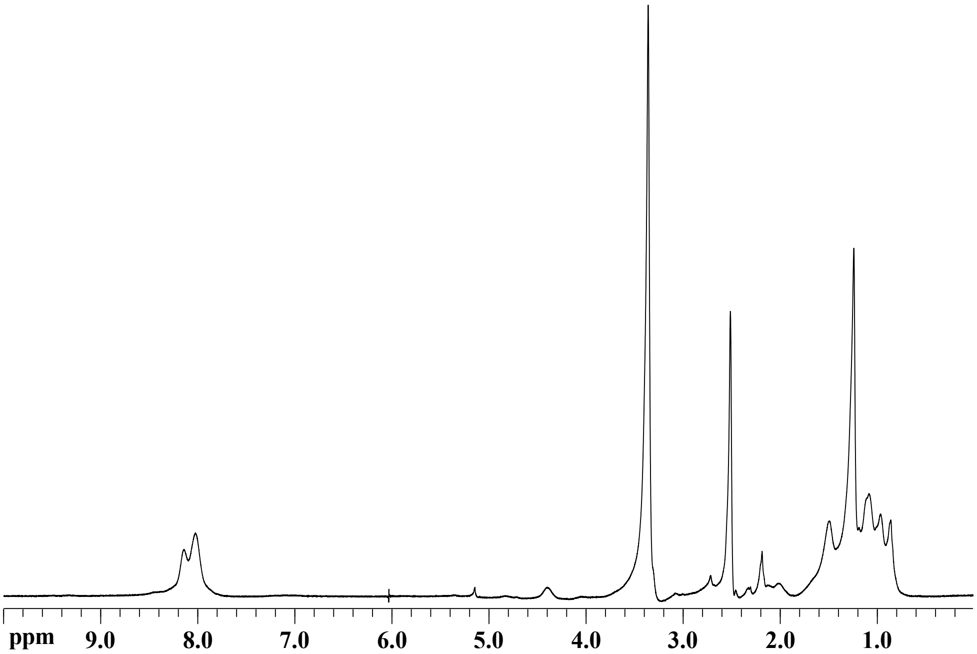

Figure A.31 ^{1}H NMR spectrum of IPDI-BTDA in DMSO-d_6

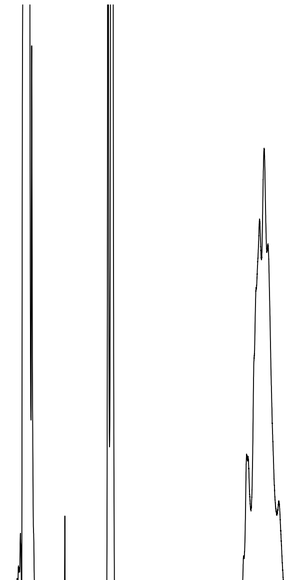

Figure A.32 ^{1}H NMR spectrum of ZnNapth$_2$trien-IPDI-BTDA in DMSO-d_6

APPENDIX B

B-1 DETERMINATION OF INHERENT VISCOSITY

Inherent viscosity [η_{inh}] ASTM D2270: Inherent viscosity is calculated from the dilute solution (1% or less) relative viscosity of the polymer. The inherent viscosity is calculated as:

The relative viscosity is given by:

$$\eta_{rel} = \frac{\text{solution flow time (t), sec}}{\text{solvent flow time } (t_0)\text{, sec}}$$

The inherent viscosity is calculated as:

$$\eta_{inh} = \frac{\eta_{rel}}{C}$$

where

C = concentration of the polymer in grams per 100 ml of solvent; usually, C = 0.5 g/100 mL

$\ln\eta_{rel}$ = natural logarithm of the relative viscosity of the dilute polymer solution

K = 0.01431, t_0 = 98.97 sec, Kt_0 = 1.4163 sec

Relative viscosity can be taken as the ratio of the flow times of a polymer solution and the pure solvent in the same viscometer and at the same temperature. Relative viscosity values generally are used for calculating the intrinsic or inherent viscosity of a polymer. The solvent to be used will depend on the polymer solubility. In general, the solvent should completely dissolve the sample in less than 30 minutes. It is desirable that the polymer be dissolved at room temperature although, heating is permissible if no degradation occurs. Select the viscometer through which the solvent will flow in not less than 100 seconds and not more than 200 seconds.

VITA

Name : Duangruthai Sridaeng

Born : October 3rd, 1977

Education :

2000	B.Sc. (Chemistry), Srinakharinwirot University, Bangkok, Thailand.
2003	M.Sc. (Petrochemistry and Polymer Science), Chulalongkorn University, Bangkok, Thailand.
2008	Ph.D. (Petrochemistry) Chulalongkorn University, Bangkok, Thailand.